UNIVERSITY OF SOUTHAMPTON

FACULTY OF NATURAL & ENVIRONMENTAL SCIENCE

Ocean and Earth Sciences

Plasticity & Adaptations of the Coral-Zooxanthellae Symbiosis:

Responses to Nutrient Availability & Insight into Inherent Thermal Tolerance

by

Sabrina Laura Rosset

Thesis for the degree of Doctor of Philosophy

2016

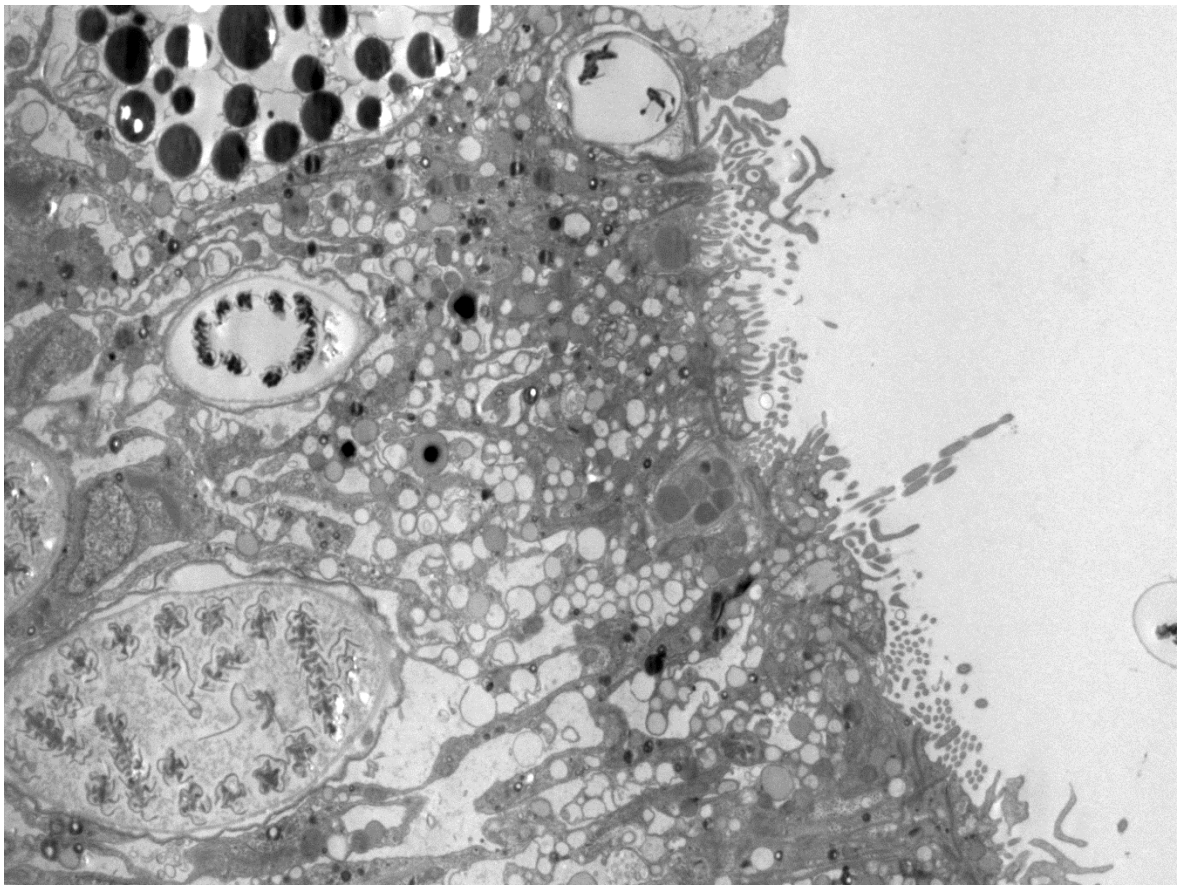

The world is full of wonders, but they become more wonderful, not less wonderful when science looks at them.

Sir David Atternborough

UNIVERSITY OF SOUTHAMPTON

ABSTRACT

FACULTY OF NATURAL AND ENVIRONMENTAL SCIENCES

Thesis for the degree of Doctor of Philosophy

PLASTICITY & ADAPTATIONS OF THE CORAL-ZOOXANTHELLAE SYMBIOSIS: RESPONSES TO NUTRIENT AVAILABILITY & INSIGHT INTO INHERENT THERMAL TOLERANCE

By Sabrina Laura Rosset

Sustaining an environment which conveys a high resilience to reef corals is critical in order to mitigate the immediate threat of climate change to reef ecosystems. The nutrient environment plays a significant role in sustaining the stability of the coral-zooxanthellae symbiosis, making anthropogenic nutrient pollution as well as the climate change driven nutrient impoverishment of oceanic waters pressing threats to coral reef persistence. Yet, many aspects of coral nutrient biology remain poorly understood, impeding science driven management strategies. This thesis aimed to advance our knowledge on how different nutrient environments affect the functioning of the coral-algal symbiosis by teasing apart the interacting effects of two principal nutrient sources (dissolved inorganic nutrient uptake and heterotrophic feeding), as well as of the two essential nutrients, nitrogen and phosphorus, both in dissolved inorganic and particulate organic forms. This was achieved through long-term exposure (up to 1.5 years) of the *Euphyllia paradivisa*-clade C1 *Symbiodinium* association to replete (+N+P), limited (-N-P), or imbalanced (+N-P/-N+P) dissolved inorganic nutrient availabilities in combination with targeted host feeding with balanced or nitrogen enriched prey items. Thereby, this work stood apart from past investigations by yielding definitive phenotypes representative of different nutrient availabilities. Moreover, the importance of food quality when considering the benefit of heterotrophy to reef corals had previously been overlooked. Findings suggest that heterotrophy provides a greater benefit to the coral host than to the symbiont and is unable to compensate for diminished dissolved inorganic nutrient availability, demonstrating a significantly greater dependence of the symbiosis to the latter nutrient source. A balanced N/P ratio, both in dissolved inorganic and particulate organic form, was shown to be essential for the stability of the symbiosis and for the nutritional benefit provided by heterotrophy. Particularly nitrogen enrichment resulted in severe nutrient stress and compromised thermal stress resilience, implying a vital reliance on a continued supply of phosphorus and emphasising the necessity of managing nitrogen pollution and monitoring N/P ratios. Zooxanthellae ultrastructural biomarkers established in this thesis (cell size, lipid body, starch granule and uric acid crystal accumulation, accumulation body fragmentation) hold potential for the aid in the identification of, and discrimination between different forms of nutrient stress in reef corals. Yet, ultimately corals need to adapt to warmer oceans. Diverse *Symbiodinium* genotypes convey varied thermal tolerance to their coral host. Yet, the mechanisms underpinning their thermal sensitivity remain largely elusive. The second aim of this thesis was to examine the role played by the algal membrane composition. The intact polar lipid biochemistry of a thermally-sensitive (clade C) and -tolerant (clade D) type were characterised by HPLC-ESI tandem mass spectrometry. Distinctions in chloroplast membrane composition could be related to differential inherent thermal tolerance. Moreover, vast differences in the lipid biochemistry of extraplastidic membranes were identified, exemplifying unprecedented metabolic differences among *Symbiodinium* clades. Biochemical markers of a thermally tolerant phenotype (MGDG/DGDG ratio, glycolipid saturation) could advance our understanding and projections of the potential of reef corals to acclimate and adapt to future climate change scenarios.

LIST OF CONTENTS

List of Tables

List of Figures

List of Appendices

List of Abbreviations

ANOVA	Analysis of variance
ATP	Adenosine triphosphate
C	Carbon
Cer PE	Ceramide Phosphatidylethanolamine
BLAST	Basic local alignment search tool
DGCC	Diacylglyceryl carboxyhydroxymethylcholine
DGDG	Digalactosyldiacylglycerol
DGTA	Diacylglyceryl hydroxymethyl trimethyl-b- alanine
DGTS	Diacylglyceryl trimethyl homoserine
DIN	Dissolved inorganic nutrients
DNA	Deoxyribonucleic acid
DON	Dissolved organic nutrients
ENSO	El Niño Southern Oscillation
ER	Endoplasmic reticulum
ESI	Electrospray ionisation
FA	Fatty acid
IPCC	Intergovernmental panel on climate change
ITS2	Internal transcribed spacer 2
LB	Lipid body
MGDG	Monogalactosyldiacylglycerol
MS/MS	Tandem mass spectrometry
N	Nitrogen
NADPH	Nicotinamide adenine dinucleotide phosphate
NL	Neutral loss scan
P	Precursor scan
P	Phosphorus
PC	Phosphatidylcholine
PCR	Polymerase chain reaction

PE	Phosphatidylethanolamine
PG	Phosphatidylglycerol
PI	Phosphatidylinositol
POM	Particulate organic matter
PS	Phosphatidylserine
PSII	Photosystem II
PUFA	Polyunsaturated fatty acid
RFI	Relative fluorescence intensity
ROS	Reactive oxygen species
S.D.	Standard deviation
SQDG	Sulfoquinovosyldiacylglycerol
TAG	Triacylglycerol
TEM	Transmission electron microscopy
TGDG	Trigalactosyldiacylglycerol
UA	Uric acid

DECLARATION OF AUTHORSHIP

I, Sabrina Laura Rosset declare that this thesis and the work presented in it are my own and have been generated by me as the result of my own original research.

Plasticity and adaptations of the coral-zooxanthellae symbiosis: Responses to nutrient availability & insight into inherent thermal tolerance

I confirm that:

1. This work was done wholly or mainly while in candidature for a research degree at this University;
2. Where any part of this thesis has previously been submitted for a degree or any other qualification at this University or any other institution, this has been clearly stated;
3. Where I have consulted the published work of others, this is always clearly attributed;
4. Where I have quoted from the work of others, the source is always given. With the exception of such quotations, this thesis is entirely my own work;
5. I have acknowledged all main sources of help;
6. Where the thesis is based on work done by myself jointly with others, I have made clear exactly what was done by others and what I have contributed myself;
7. Part of this work has been published as:

   Rosset S, D'Angelo C, Wiedenmann J (2015) Ultrastructural biomarkers in symbiotic algae reflect the availability of dissolved inorganic nutrients and particulate food to the reef coral holobiont. Frontiers in Marine Science, 2:1-10

Signed: .....

Date: .....

Acknowledgements

I would like to thank Jörg and Cecilia dearly for being my supervisors and excellent mentors. I have learnt so much from them during the course of my PhD. I am very grateful that they provided me with the freedom and opportunity of exploring different research questions which allowed me to learn a range of skills and gain broad insight into coral research.

My panel chair Alex Poulton always provided helpful feedback towards the progression of my PhD for which I am very grateful.

I am thankful to my two examiners Dr Christian Wild and Prof Eric Achterberg for a stimulating discussion and for providing comments and suggestions that strengthened this thesis.

I would also like to thank Anthony Postle, Alan Hunt, Grielof Koster and Joost Brandsma from the mass spectrometry unit at Southampton General Hospital. They provided excellent training and contributed significantly towards the method development for *Symbiodinium* polar lipid analysis. Particularly Grielof was extremely patient and I really appreciated his keen mind when it came to the interpretation of mass spectra.

I am also very grateful to the members of the biomedical imaging unit at Southampton General Hospital for their training and assistance in transmission electron microscopy. Anton Page and Lizzy Angus were always extremely enthusiastic and helpful which made working there a pleasure.

Thanks to Ben, Adam and Elena from the Coral Reef Laboratory. Having such amazing colleagues provided a very encouraging work environment. Ben taught me a lot of molecular skills. Adam is a great aquarist and always had time for some *Euphyllia* photography. Working together was very rewarding. I would also like to thank Luke for being a very enthusiastic MSc student. His efforts contributed towards the work presented in this thesis.

Finishing my thesis would not have been as easy without the support of friends who always had time for tea breaks and reassuring conversations. Thank you, Despo, Giang, Glaucia and Ming. I also need to thank Gav for always being supportive and encouraging me to pursue my goals. Finally, I am very grateful for the support of my family.

Chapter 1: Introduction

1.1. Background

Scleractinian corals are the foundation of coral reefs, a spectacular ecosystem that supports a vast biodiversity. The high productivity that coral reefs provide in a nutrient poor environment make them crucial for this marine ecosystem as well as for the people that depend on it. This productivity is attributed to their symbiosis with dinoflagellates of the genus *Symbiodinium*, termed zooxanthellae (Muscatine and Porter, 1977). Through their calcification they build the reef itself, providing habitat for other reef organisms (Bellwood and Hughes, 2001). Additionally, their turnover of inorganic and organic matter makes them responsible for key biogeochemical processes which drive the productivity of the reef ecosystem (Wild et al., 2011). It is estimated that approximately 30 million people depend directly on coral reefs for their livelihoods and for the land they inhabit (Wilkinson, 2008). Reefs are of high economic value providing sources of income through tourism, fishing, and the discovery of natural products to be used in drug discovery (Brander et al., 2006; Leal et al., 2012; Moberg and Folke, 1999). Additionally they provide coastal protection from storms, flooding and erosion. Coral reefs are globally threatened by a range of anthropogenic stressors, most notably by climate change which is causing increased warming and acidification of the oceans (Hoegh-Guldberg et al., 2007). Indeed, coral reefs are considered to be the ecosystem that is most sensitive to global climate change (Riegl et al., 2009). Furthermore, local pressures including nutrient pollution, sedimentation, over-fishing and more frequent incidence of disease and predator outbreaks are contributing to increasing rates of coral decline (Hughes et al., 2003). Critically, local pressures such as nutrient enrichment can act synergistically to increasing sea surface temperatures, thus decreasing the resilience of corals to climate change (D'Angelo and Wiedenmann, 2014). It is estimated that 20% of coral reefs have been lost globally and that a further 15% are under immediate threat of being lost within the next 10-20 years (Wilkinson, 2008). The important ecosystem services provided by coral reefs are therefore in peril of becoming extinct.

1.1.1. A photosynthetic endosymbiosis

Shallow-water coastal ecosystems are dominated by invertebrates in symbiosis with dinoflagellate microalgae. Scleractinian corals occur as a colony of many coral polyps which secrete a calcium carbonate skeleton. Most reef-building corals rely on the symbiosis with the dinoflagellates of the genus *Symbiodinium*, referred to as zooxanthellae (Muscatine and Porter, 1977). A symbiosis is defined as the interaction of two different organisms living in close physical association, constituting a mutually beneficial relationship.

The zooxanthellae are mostly located within the endodermal cells that line the gastrovascular cavity of the scleractinian host (Figure 2.1), enclosed in vacuoles called symbiosomes which are from phagosomal origin. Thus, the outer symbiosome membrane is host-derived. This outer membrane is part of a multilayer complex of which the remaining membranes are symbiont derived (Wakefield et al., 2000). This symbiosis is based on metabolic synergy: the integration of metabolic activities through efficient exchange of photosynthates and metabolites between the coral host and the algal symbionts. Indeed, the symbiotic state initiates a significant increase in the expression of proteins involved in inorganic carbon transport, lipid storage and transport, nitrogen transport and cycling, and intracellular trafficking (Oakley et al., 2015). According to the nitrogen conservation hypothesis, the preferential use of autotrophically derived carbon for host respiration allows for the conservation of nitrogen by reducing rates of protein catabolism by the host (Rees and Ellard, 1989; Wang and Douglas, 1998). However, the fundamental understanding of the functioning of the coral-zooxanthellae symbiosis remains limited.

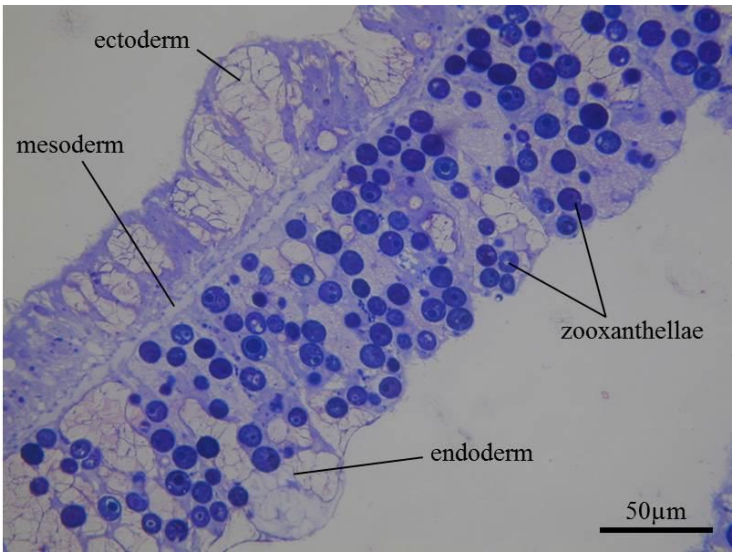

Figure 1.1| Section of a tentacle of the reef coral *Euphyllia paradivisa* depicting the zooxanthellae harboured within the endodermal cell layer (x400 magnification).

1.1.1.1. Carbon fixation

Photosynthetic carbon fixation necessitates a high concentration of carbon dioxide (CO_2) within the vicinity of the algal symbionts, requiring the uptake and transport of inorganic carbon for the sea water to the symbiosome. The inorganic carbon required for photosynthesis can be derived from the sea water in the form of bicarbonate (HCO_3^-), and from host respiration in the form of carbon dioxide (CO_2). Carbonic anhydrase, the enzyme that catalyses the interconversion of HCO_3^- and CO_2, was detected in cnidarians, and its role in assimilating inorganic carbon for photosynthesis is evidenced by a 29-fold increase of carbonic anhydrase activity in zooxanthellate compared to azooxanthellate corals (Weis et al., 1989). It is suggested that H+-ATP secretes H+ from the ectodermal cells into the seawater, promoting the formation of carbonic acid, which membrane-bound carbonic anhydrase then dehydrates into CO_2 (Furla et al., 2000). CO_2 can passively diffuse into cnidarian cells where it is trapped by hydration to HCO_3^- by cytosolic carbonic anhydrase. It is not understood how this HCO_3^- is transported to the zooxanthellae. Most likely an active inorganic carbon uptake system is involved, as well as intracellular carbon concentrating mechanisms (Davy et al., 2012). CO_2 is fixed by the Calvin cycle, involving a form II Rubisco (Rowan et al., 1996). Rates of carbon fixation follow a diurnal cycle, with highest rates occurring in the afternoon.

1.1.1.2. Translocation of photosynthetic products

Balanced growth of marine organisms is typically dependent on a set nutrient ratio of C:N:P 116:16:1, which is known as the Redfield ratio (Redfield, 1958). Yet, it is thought that the zooxanthellae are in a general state of limitation of the essential plant nutrients, nitrogen and phosphorus, *in hospite*. This nutrient limitation underpins the functioning of the symbiosis since it results in a chemical imbalance of the zooxanthellae (Dubinsky and Jokiel, 1994). Thereby, nutrients required for cellular growth are restricted in respect to the flux of carbon, leading to an excessive accumulation of photosynthetic products which cannot be used for growth, and are instead translocated to the host. It has been estimated that up to 95% of fixed carbon is translocated to the host where it is primarily utilised by the host to support respiration as well as mucus production (Muscatine, 1965; Falkowski et al., 1984; Crossland, 1987; Wild et al., 2004; Bachar et al., 2007; Tremblay et al., 2015). While being rich in energy, translocated photosynthates have been described as "junk food" due to being poor in nitrogen (Falkowski et al., 1984). The majority of the photosynthate released by the symbiont has been found to be in the form of glycerol (Muscatine, 1967). Other compounds that are translocated include sugars, amino acids, organic acids, lipids, and fatty acids (reviewed by: Yellowlees et al., 2008; Venn et al., 2008). Thus, organic nitrogen is translocated to the host in the form of amino acids. Indeed, several studies have reported the flux of nitrogen from the zooxanthellae to the host, thus calling into question whether translocated photosynthates can really be considered as junk food (Wang and Douglas, 1999; Tanaka et al., 2006; Pernice et al., 2012; Béraud et al., 2013; Kopp et al., 2013). However, a lot of uncertainty still remains over what major compounds are translocated and how these are allocated by the host, and little is known about minor translocated compounds.

One controversial topic in cnidarian-dinoflagellate metabolism is what controls the translocation of photosynthetic products. One proposition is that by prohibiting symbiont proliferation, surplus photosynthetic produce is generated which can be translocated to the host (Dubinsky and Berman-Frank, 2001). However, this could also result in carbon storage rather than release. One observation has been that isolated *Symbiodinium* incubated in homogenated host tissue release a substantially greater amount of photosynthate than *Symbiodinium* incubated in sea water (Trench, 1971; Muscatine et al., 1972; Grant et al., 2006; Biel et al., 2007). This lead to the proposition that a 'host release factor' (HRF) stimulates the release of photosynthates. The HRF is suggested to be protein based, due to

its heat-sensitivity (Sutton and Hoegh-Guldberg, 1990). Yet, it is likely species-specific and cannot be generalised. In *Pocillopora damicornis* it was proposed to consist of a suite of free amino acids since these stimulate photosynthate release as well as increasing the rate of photosynthesis (Gates et al., 1995). The non-protein amino acid taurine was found to trigger photosynthate release in zooxanthellae isolated form the anemone *Aiptasia pulchella* (Wang and Douglas, 1997). Experimental evidence suggests that HRF affects carbon metabolism of the algal symbiont by elevating glycerol biosynthesis, and at the same time, limiting triglyceride synthesis which would provide a storage compound for excess fixed carbon (Grant et al., 2006, 2013; Biel et al., 2007). Yet, still very little is known about the mechanism that controls the release of photosynthates in the coral-dinoflagellate symbiosis.

1.1.1.3. Regulation of the zooxanthellae population *in hospite*

Proliferation of the zooxanthellae population *in hospite* is subject to regulation in order to maintain a favourable ratio of host to symbiont cells which is a necessity for symbiosis stability. Thereby, synchronisation of host and algal growth ensures that the algal symbionts cannot overgrow the host. Control mechanisms of algal population growth can occur both pre- and post-mitotically.

Cell cycle progression is regulated by light-dark stimulation. Blue light alone has been found to stimulate entry into DNA synthesis stage of the cell cycle (S) while darkness is required for completion of cytokinesis (Wang et al., 2008). Consequently, a dial rhythmicity in cell cycle progression is often observed, with a peak in the mitotic rate (the proportion of the population undergoing division) observed at the end of the dark period (Fitt and Cook, 2001; Hoegh-Guldberg, 1994). Yet, mitotic rates of zooxanthellae *in hospite* are considerably lower than those measured for zooxanthellae in culture (Falkowski et al., 1984). Low division rates are reflected in the elongated growth stage of the cell cycle (G1) in the symbiotic state (Smith and Muscatine, 1999). These observations signify the implementation of control processes which limit cell cycle progression. The cell cycle itself is subject to tight regulation by checkpoints which responds to cellular and environmental cues, ensuring adequate resource availability required for completion of cell division. Nutrient limitation is therefore a key regulator of zooxanthellae population dynamics, uncoupling photosynthesis from cellular growth (Falkowski et al., 1993). Large increases in zooxanthellae population densities have been observed in response to

dissolved inorganic nitrogen enrichment (Muller-Parker et al., 1994b; Stambler et al., 1991; Marubini and Davies, 1996). Yet, host feeding rather than dissolved inorganic nutrient availability in anemones and hydroids has been found to support high mitotic rates (Cook et al., 1988; McAuley and Cook, 1994; Fitt and Cook, 2001; Smith and Muscatine, 1999). This is suggestive of symbiont proliferation being coupled to growth of the host tissue. Furthermore, algal growth rates during repopulation of an aposymbiotic anemone were observed to be similarly high as cultured zooxanthellae, followed by a decline in mitotic rates when a steady state density was reached (Berner et al., 1993). Similarly, an inverse relationship between zooxanthellae density and mitotic rate has been described in corals recovering from a bleaching event (Jones and Yellowlees, 1997). These studies indicate that zooxanthellae proliferation rates are limited by the habitable space available to populate, as well as resources since the competition for available nutrients will augment with rising density and increased self-shading will decrease light availability. Accordingly, pre-mitotic regulation of zooxanthellae population proliferation does not occur by active host control, but rather, by density dependent negative feedback. However, it has also been hypothesised that host release factors which stimulate the release of photosynthates could play a role in active control of cell cycle progression (Falkowski et al., 1993; Gates et al., 1995).

Post-mitotic control of zooxanthellae population densities occurs by the elimination of zooxanthellae from the host. This can involve either expulsion of the algal cells by exocytosis, or degradation of zooxanthellae within the endodermal host cells (Weis, 2008). A study by Baghdasarian and Muscatine identified a linear correlation between the rates of algal division and expulsion (Baghdasarian and Muscatine, 2000). Furthermore, cells undergoing division were found to be preferentially expelled. However, symbiont expulsion was not consistently found to be the driving mechanisms of zooxanthellae population control in all cnidarian species investigated. Evidence for digestion of zooxanthellae by the host has also been identified. This can occur either by autophagy (Downs et al., 2009) or by the fusion of lysosomes with symbiosomes (Chen et al., 2005). Rates of zooxanthellae degradation have also been measured to match rates of algal division (Titlyanov et al., 1996). Finally, zooxanthellae can also be lost from the symbiosis by means of programmed cell death, apoptosis or necrosis, processes which can be stimulated by biochemical or environmental stimuli (Weis, 2008). Thus, a set of mechanisms function in concert to ensure the maintenance of a stable symbiosis.

1.1.2. Nutrient acquisition and partition

In order to sustain growth, essential nutrients must be acquired from the environment. Of particular importance are nitrogen and phosphorus. Nitrogen is a constituent of proteins, nucleic acids, as well as of the reducing agent NADPH required for anabolic processes, and is thus a necessity for proper cell function and growth. Phosphorus is a constituent of DNA, RNA and phospholipids, and is required for the functioning of many enzymes and signalling pathways, as well as having a vital role in energy requiring biochemical pathways as a constituent of ATP and NADPH.

Due to the symbiosis with zooxanthellae, reef corals are capable of obtaining nutrients from multiple sources, both autotrophically and heterotrophically. This mixotrophic and opportunistic nature of corals allows them to thrive within the oligotrophic tropical waters often referred to as the blue desert. Yet, the relative importance of these different sources of nitrogen and phosphorus to the coral host and the algal symbiont remain controversial, an aspect with which this thesis is concerned. This thesis focuses on the roles of dissolved inorganic nutrients and heterotrophic feeding (Figure 2.2).

1.1.2.1. Dissolved inorganic nutrients

Nitrogen is acquired from the seawater, primarily as dissolved inorganic nitrogen (ammonium NH_4+, nitrate NO_3^-, and nitrite NO_2^-). The preferred form of nitrogen, due to its low energetic cost of absorption, is NH_4^+ which can be assimilated by both the coral host and the zooxanthellae (Grover et al., 2002). In both symbiotic partners, assimilated NH_4^+ is converted into glutamate, the end product of both the glutamine synthetase/glutamine 2-oxoglutarate amino transferase (GS/GOGAT) and the NADPH-glutamate dehydrogenase (GDH) pathways in *Symbiodinium*, and by the NADPH-GDH pathway in the host (Summons and Osmond, 1981; Roberts et al., 1999, 2001).

Pulse-chase experiments of corals exposed to seawater enriched with isotopically labelled NH_4^+ have shown that zooxanthellae, who incorporate a much larger proportion of NH_4^+ than the host within the first hour of exposure, represent the primary site of NH_4^+ assimilation within the holobiont (Grover et al., 2002; Pernice et al., 2012). Following the sudden incorporation of large amounts of nitrogen, zooxanthellae form temporary nitrogen stores in the form of uric acid crystals (Clode et al., 2009; Kopp et al., 2013). This likely occurs via the purine catabolism pathway since transcripts encoding the enzyme xanthine

dehydrogenase, which catalysed the conversion of xanthine to uric acid and subsequently to allontoin, were found to be present in *Symbiodinium spp.* (Kopp et al., 2013). Succeeding re-mobilisation of these nitrogen stores leads to translocation of nitrogenous compounds to the host where it is mostly incorporated into protein and mucous production (Kopp et al., 2013).

As opposed to the coral host, zooxanthellae are also capable of assimilating nitrate (NO_3^-) and nitrite (NO_2^-) since the required enzymes for its reduction to NH_4^+ are only found in the symbiotic algae (Yellowlees et al., 2008; Crossland and Barnes, 1977). Nitrate reductase (NR) reduces NO_3^- to NO_2^- in the cytoplasm, followed by its reduction to NH_4^+ which is catalysed by nitrite reductase (NiR) in the plastids. The uptake rates for both NH_4^+ and NO_3^- are concentration dependent, with increased uptake rates occurring with increasing availability (Muscatine and D'Elia, 1978; Grover et al., 2003). Rates of algal NO_3^- uptake are higher under low NH_4^+ concentration indicating that NH_4^+ is favoured as a nitrogen source (Crossland and Barnes, 1977). Despite the access to nitrate and nitrite being limited to the zooxanthellae, the nitrogen derived from this source also becomes incorporated into the host tissue fraction (Tanaka et al., 2006).

The assimilation and incorporation of phosphate by corals has been the subject of fewer investigations than that of nitrogen. Zooxanthellae are thought to generally be phosphate limited due to increased proliferation rates observed with elevated phosphate levels as well as the high activity of algal alkaline phosphatase (Jackson et al., 1989). Seawater phosphate enrichment results in enhanced NH_4^+ uptake (not the case for NO_3^-), implying a greater phosphate than nitrogen limitation (Godinot et al., 2011b). Corals can assimilate dissolved inorganic phosphorus (phosphate PO_4^{3-}). The disability of azooxanthellate corals to assimilate phosphate from the seawater, indicates that the zooxanthellae are responsible for its uptake (D'Elia and Webb, 1977). Furthermore, phosphate uptake increases in light. Due to the negative charge of phosphate, uptake must be mediated by active transport and carrier-mediated transport. The uptake of phosphate across host membranes is expected to occur via a sodium/phosphate symporter (Godinot et al., 2011b). Two acid phosphatases (phosphatases P-1 and P-2) have been isolated from zooxanthellae of *Acropora formosa* (Jackson et al., 1989). P-1 is suggested to mobilise the intracellular phosphate storage compound, polyphosphate. P-2 is proposed to function in the hydrolysis of phosphate esters, and could thereby provide a mechanism by which to translocate phosphate from the host cytoplasm into the symbiosime for active uptake by the symbiont. Following the

assimilation of phosphate little is known about the partition and allocation of phosphorus within the symbiosis.

1.1.2.2. Dissolved organic nutrients

Additional to dissolved inorganic forms, nitrogen can also be taken up from the surrounding sea water in dissolved organic forms. Important compounds of dissolved organic nitrogen include urea and dissolved free amino acids. The uptake of urea is both concentration and light dependent (Grover et al., 2006). The extent of incorporation of nitrogen derived from urea uptake was considerably higher in the host fraction than in the algae (Grover et al., 2006). Similarly, the uptake of dissolved free amino acids was also light-enhanced and the obtained nitrogen was primarily retained within the host tissue fraction (Grover et al., 2008; Al-Moghrabi et al., 1993).

A study by Grover and colleagues combined the uptake rates of both dissolved inorganic and organic nitrogen with the nitrogen requirements of tissue growth in *Stylophora pistillata* and estimated that these nutrient pools can satisfy the total daily nitrogen demand. Thereby, dissolved inorganic and organic nitrogen accounted for around 75% and 25% of the daily nitrogen requirements respectively, thus placing considerably value on the activity of zooxanthellae for the maintenance of the nutrient status of the coral holobiont.

1.1.2.3. Heterotrophic feeding

A further mechanism of carbon, nitrogen and phosphorus uptake in reef corals is heterotrophic feeding. Many coral species are capable of capturing particles with their tentacles by mucous adhesion or by firing of specialised stinging cells, the nematocysts, upon prey contact (Yonge, 1930). Thereby, corals can feed on a range of live and detrital particulate organic matter including zooplankton, phytoplankton, nano- and picoplankton, bacteria, and organic matter contained in sediments (reviewed by: Houlbrèque and Ferrier-Pagès, 2009). However, the relative importance of heterotrophy in respect to autotrophy remains controversial. It has been estimated that for the coral *Stylophora pistillata* heterotrophic feeding on zooplankton, nano- and picoplankton can supply approximately 3.2µg of nitrogen cm^{-2} day^{-1} (Houlbrèque and Ferrier-Pagès, 2009). Furthermore, some corals obtain up to 60% of their fixed carbon from heterotrophic feeding on zooplankton (Grottoli et al., 2006). It has been suggested that corals depend on heterotrophic nutrient

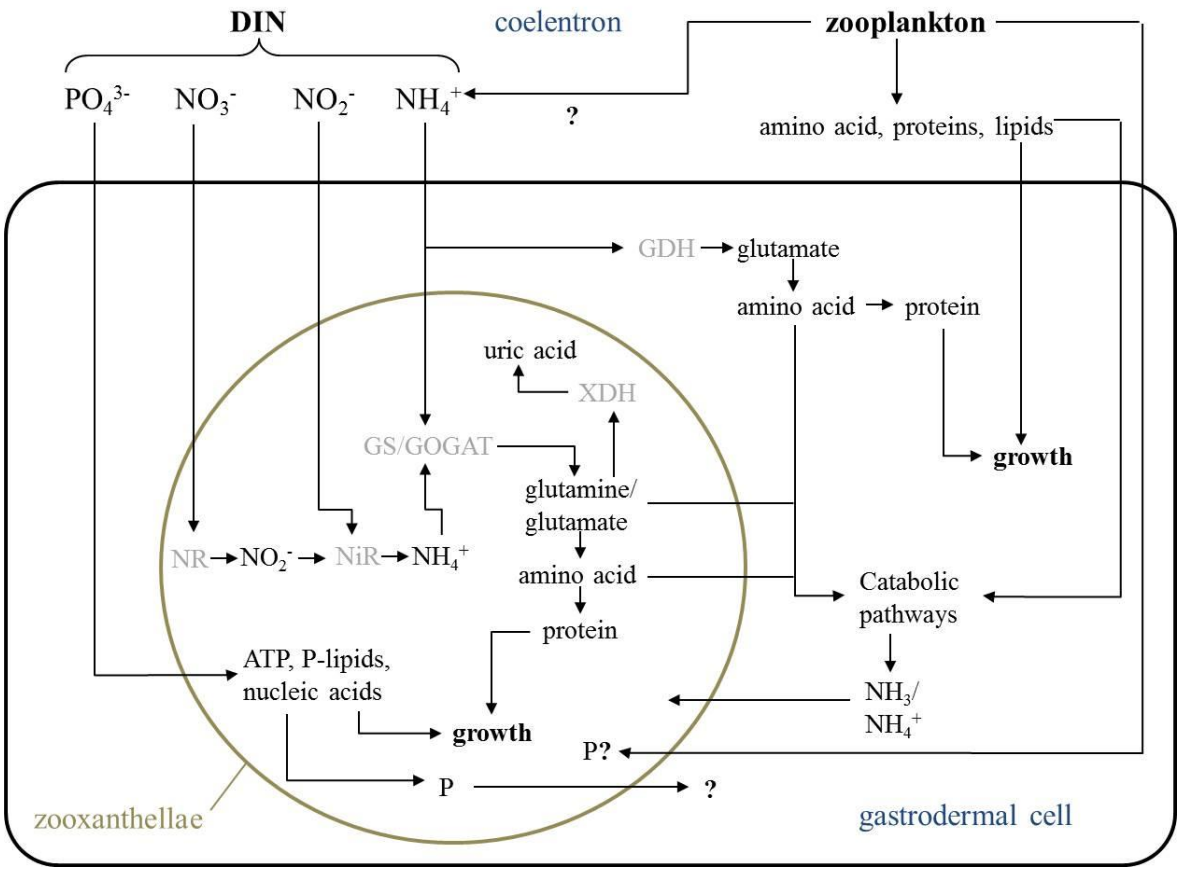

Figure 1.2| The assimilation of nitrogen and phosphorus by dissolved inorganic nutrient uptake and heterotrophic feeding. Diagram depicting the assimilation of dissolved inorganic nutrients (DIN) and particulate organic matter (zooplankton) by the coral holobiont. These are the two key nutrient sources investigated in this thesis. Ammonium (NH_4^+) can be assimilated by both the coral host and the symbiont, both of which possess enzymes required for its metabolism into glutamate which is used for protein biosynthesis (GS/GOGAT and GDH in zooxanthellae, GDH in the host). Only the zooxanthellae possess the enzymes required for reduction of nitrate (NO_3^- by NR) and nitrite (NO_2^- by NiR) into NH_4^+. Excess nitrogen can be stored in the form of uric acid within the zooxanthellae. Nitrogen-rich compounds are translocated from the zooxanthellae to the host Phosphate (PO_4^{3-}) is assimilated by the zooxanthellae. It is not known if phosphorus-rich compounds are translocated to the host. The host acquires nitrogen and phosphorus through heterotrophy. Digestion of zooplankton in the host coelenteron likely liberates NH_4^+ which can also be assimilated by the zooxanthellae. It is not known if heterotrophic phosphorus becomes available to the zooxanthellae. Catabolic processes of the host releases NH_4^+ as a metabolic waste product which is recycled by the zooxanthellae. DIN primarily support cellular growth of the zooxanthellae while heterotrophic nutrients sustain growth of the coral host. Enzymes are shown in grey. Adapted from Pernice et al. 2012

input to sustain their growth, whereas compounds derived through translocation from the zooxanthellae are only utilised to support respiration. Indeed, nitrogen and carbon acquired through heterotrophy are predominantly retained by the host tissue fraction, although both nutrients are also incorporated into the algal fraction (Piniak et al., 2003; Tremblay et al., 2015). Feeding has been shown to increase zooxanthellae density, rates of photosynthesis, rates of calcification, as well as protein and lipid content of both coral host and symbionts, thus leading to greater coral biomass (Houlbrèque et al., 2003, 2004; Tolosa et al., 2011; Cook et al., 1988). The allocation of heterotrophically acquired carbon has been shown to depend on the level of light irradiance, however finding on the specific effects of combined light irradiation have yielded contradictory results for the different species investigated (Treignier and Grover, 2008; Tremblay et al., 2014).

Importantly, heterotrophic feeding has largely been observed to be an opportunistic nutrient source, with rates of feeding and allocation of heterotrophically derived nutrients being dependent on the environmental situation (Anthony and Fabricius, 2000; Grottoli et al., 2006; Palardy et al., 2008). Thereby, heterotrophy is, for example, thought to play a larger role for corals living at greater depth due to the reduced supply of photosynthates at lower light irradiance (Palardy et al., 2008). Furthermore, not all coral species depend on heterotrophy to the same extent due to large differences in the capacity for predation (Grottoli et al., 2006; Ferrier-Pagès et al., 2010; Connolly et al., 2012). The significance of heterotrophic feeding in sustaining health of the coral holobiont is discussed below in relation to coral resilience to adverse environmental conditions.

1.1.2.4. Nitrogen fixation

Additional to the zooxanthellae, reef corals are associated with a variety of microbes. Nitrogen fixation by symbiotic diazotrophs, the conversion of dinitrogen (N_2) into ammonia, constitutes an additional source of nitrogen (Lesser et al., 2007; Rädecker et al., 2015). The highest rates of nitrogen fixation have been reported to occur in the early morning and evening (Lesser et al., 2007). Isotope analysis is indicative of the zooxanthellae benefitting primarily from this nitrogen source (Lesser et al., 2007). Nitrogen fixation is energetically costly, and likely only contributes a small proportion to the overall nitrogen uptake of the coral host and the zooxanthellae (Rädecker et al., 2015). Yet, the ubiquitous distribution and vertical transfer of diazotrophs is suggestive of a functional importance of nitrogen fixation to reef corals (Lema et al., 2012, 2014).

1.1.2.5. Nutrient recycling within the symbiosis

With the observation that corals in the aposymbiotic state (without zooxanthellae) have a greater rate of ammonia excretion than when in the symbiotic state, it was implied that the ammonia derived as a metabolic waste product from host catabolic processes is assimilated by the zooxanthellae (Muscatine and D'Elia, 1978; Rahav et al., 1989). In turn, organic nitrogen is translocated back to the host in the form of amino acids (Wang and Douglas, 1999). Thereby nitrogen is retained and recycled within the symbiosis. The cycling of nitrogen originating from nitrate assimilation by the zooxanthellae has been confirmed by a study employing ^{15}N isotope tracer (Tanaka et al., 2006). Accordingly, it is expected that, despite nutrients derived through the uptake of dissolved organic nutrients and heterotrophy being primarily incorporated into the host tissue fraction (Grover et al., 2006; Piniak et al., 2003), the resulting increase in host metabolic processes would result in a consequential increase in the supply of ammonium to the zooxanthellae. Heterotrophic nitrogen has been shown to be exchanged between the host and the zooxanthellae resulting in long term retention of the nutrient (Tremblay et al., 2015). In support of these observations, when studying the proteomes of anemones in symbiotic and aposymbiotic states, a ammonium transporter was found to only be expressed in the symbiotic state, indicating an increased need for nitrogen trafficking (Oakley et al., 2015). Additional to the interactions between the host animal and the zooxanthellae, associated nitrifying and denitrifying microbes also contribute to the internal cycling of nitrogen (Rädecker et al., 2015). Thus, additional to the high efficiency of nutrient uptake, the coral holobiont is adept at nutrient conservation. However, there is no evidence for the recycling of phosphorus within the symbiosis.

1.1.3. Coral bleaching – Functional breakdown of the symbiosis

1.1.3.1. Causes of bleaching

The effective maintenance of the coral-zooxanthellae symbiosis is highly sensitive to environmental stress caused by perturbations in temperature, irradiance, salinity, sedimentation, nutrient levels, and disease. The stress response results in the breakdown of the coral-zooxanthellae symbiosis leading to coral bleaching, the loss of symbiont pigmentation or expulsion of the zooxanthellae by the host (Hoegh-Guldberg, 1999). The term bleaching refers to the white appearance of the coral after loss of the brown

zooxanthellae since the white carbonate skeleton can be seen through the transparent coral tissue. Bleaching results in severe energy deficiency of the host and frequently leads to mortality. Corals can survive for short periods in a bleached state and may recover their symbionts if the environmental perturbation ceases. However, they suffer much reduced growth and calcification and may endure greater incidence of disease.

The most profound cause of coral bleaching is heat stress. There is a tight correlation between warmer-than-normal temperature and coral bleaching (Jokiel and Coles, 1990; Glynn, 1993; Hoegh-Guldberg, 1999; Lesser, 1997; Warner et al., 1999). Corals are believed to live close to their thermal limit during summer. Generally, bleaching occurs when the summer water temperature maxima is 1 to 2°C higher than normal for 3 to 4 weeks (Hoegh-Guldberg, 1999). However, there is no single threshold for bleaching for a single location or species, as seen by the often patchy occurrence of bleaching (Hughes 2003). Especially geographic variance of bleaching threshold within a species provides evidence for an on-going evolution of temperature tolerance (Hughes et al., 2003). Tolerance was found to be particularly high for species in the Arabian Gulf where temperatures can be up to 10°C higher than the maximal summer temperature in cooler regions (Hume et al., 2013). Furthermore, other factors often act synergistically with high temperature, lowering the threshold of temperature-induced bleaching (Wiedenmann et al., 2013). Particularly solar irradiation impairs the tolerance of corals to high temperature stress by damaging the photosynthetic machinery of the zooxanthellae (Brown, 1997).

Contemporary climate change caused by the increasing atmospheric concentrations of greenhouse gas is causing sea surface temperatures to rise at an unprecedented rate, causing significant ecological impacts (Walther et al., 2002). According to the intergovernmental panel on climate change (IPCC) mean global surface temperature has risen by 0.85°C between 1880 and 2012. Over the past century tropical oceans have increased in temperature by 1-2°C (Hoegh-Guldberg, 1999). Global warming of the ocean is predicted to continue throughout the 21st century, the extent to which the release of anthropogenic carbon into the atmosphere can be reduced. It has been estimated that the thermal tolerance of corals will need to increase by 0.2-1.0°C per decade in order to persist (Donner et al., 2005). Climate change mediated warming of the tropical oceans is accentuated by intermittent El Niño Southern Oscillation (ENSO) events which are believed to be increasing in intensity and frequency, causing coral bleaching at large geographical scales, termed mass bleaching. The most severe mass bleaching event was

recorded in 1997/98 as the consequence of an ENSO event. A subsequent mass bleaching event took place in 2010. A strong ENSO event initiated the latest global bleaching event which began in 2014 and is predicted to continue to spread during 2016 (National Oceanic and Atmospheric Administration). The bleaching and mortality of reef corals impedes their metabolic exchange with other organisms, thereby affecting essential biogeochemical processes and impacting the reef ecosystem (Wild et al., 2011). The magnitude of bleaching events is predicted to increase further in the next decades, presenting a severe threat to the survival of coral reefs.

1.1.3.2. Mechanisms of bleaching

The molecular pathways and cellular events that ultimately result in coral bleaching are still not fully understood. However, the underlying process that causes bleaching is the production of reactive oxygen species, leading to oxidative stress of the host, causing damage to membranes, proteins and DNA (Lesser, 2006; Weis, 2008). High temperature and combined irradiance stress can induce damage to the photosynthetic apparatus of zooxanthellae by causing photoinhibition of photosynthetic electron transport coincident with a continued high absorption of excitation energy (Smith et al., 2005). Particularly photosystem II (PSII) is believed to be a primary target of damage due to increased destabilisation of D1 protein which exceeds the rate of its repair (Warner et al., 1999). Further, it has been suggested that ribulose 1,5-bisphosphate carboxylase-oxygenase (Rubisco), the enzyme responsible for carbon fixation, becomes damaged by thermal stress, thereby decreasing the rate of consumption of ATP and NADPH, the products of photosynthetic electron transport (Jones et al., 1998). A further sight of primary damage is suggested to be the thylakoid membranes (Tchernov et al., 2004). Increased membrane fluidity in response to heat stress compromises membrane integrity which results in the destabilisation of the photosystems and in the uncoupling of photosynthetic electron transport from ATP synthesis (Tchernov et al., 2004). The consequence to damage of any of these targets is the build-up of electrons. If the flux of electrons overwhelms non-photochemical dissipation mechanisms which convert excitation energy into heat, the production of reactive oxygen species results through photochemical dissipation whereby the reduction of O_2 in the place of $NADP^+$ by the Mehler reaction takes place, forming superoxide (O_2^-), and in turn, hydrogen peroxide (H_2O_2) and hydroxyl radicals (•OH) which diffuse into the host tissue (Smith et al., 2005; Lesser, 2006). Both the zooxanthellae and the host possess antioxidant enzymes. However, if the production of reactive oxygen

species exceeds the antioxidant capacity, then a cascade of cellular damage occurs, leading to apoptosis and necrosis of host cells, ultimately leading to mortality (Downs et al., 2002; Weis, 2008; Tchernov et al., 2011). Thus, in order to limit oxidative damage, the elevated production of reactive oxygen species triggers the degradation of zooxanthellae within the host, exocytosis of zooxanthellae by the host or the shedding of host cells containing zooxanthellae (Weis, 2008).

1.1.4. The role of the nutrient environment in reef coral resilience

1.1.4.1. A changing nutrient environment

Corals are generally adapted to a nutrient-poor environment. Yet, their natural nutrient environment is increasingly becoming altered. Human population expansion is resulting in increased land clearing for urbanisation and logging, leading to increased industrial runoff, sedimentation, and sewage discharge along with reduced abundance of buffering environments such as mangroves. Furthermore, the rising pressure on food production is leading to increased agricultural expansion and fertiliser usage. Additionally, an increasing rate of major storms and rainfall is causing enhanced runoff of terrestrially sourced sediments, nutrients and pollutants. The net effect is increased nutrient loading of coastal waters, particularly effecting bays which experience less circulation and reefs in close proximity to river mouths (Szmant, 2002; Fabricius, 2005; Brodie et al., 2012; D'Angelo and Wiedenmann, 2014; Voss et al., 2013). This is often associated with increased turbidity which limits benthic irradiance (Fabricius, 2005). Furthermore, climate change is predicted to intensify coastal upwelling of nutrient rich waters (Bakun et al., 2015; Di Lorenzo, 2015). Consequential of the rapid turnover of dissolved inorganic nutrients by pelagic communities, nutrient enrichment is generally believed to constitute a local stressor to effected reef communities (Furnas et al., 2005). However, secondary effects of stimulated phytoplankton blooms are expected to disrupt the nutrient environment on a larger scale, both in space and time, by precipitating the limitation of key nutrients (D'Angelo and Wiedenmann, 2014). On the other hand, climate change is also causing increased stratification of the upper ocean, thereby reducing nutrient availability required for primary production (Chavez et al., 1999; Behrenfeld et al., 2006). Thus, corals are expected to face increased incidences of both nutrient enrichment and impoverishment. Particularly the effect of nutrient enrichment on reef corals has been subject of many

investigations (reviewed by: Fabricius, 2005; D'Angelo and Wiedenmann, 2014). However, the complexity of interacting affects mean that the response of a coral reef to nutrient enrichment is context dependent (D'Angelo and Wiedenmann, 2014; Riegl et al., 2015). Consequently, experimental findings have yielded contradictory results, leading to a degree of uncertainty on whether nutrient enrichment acts synergistically or antagonistically with increasing sea surface temperature to induce the demise of coral reefs.

1.1.4.2. Dissolved inorganic nutrient enrichment

1.1.4.2.1. Indirect effects on reef corals

Increased nutrient loading, particularly of nitrogen and phosphorus, can result in eutrophication which is detrimental to coral reefs (Szmant, 2002; Hughes et al., 2007). Phytoplankton blooms can deplete corals of essential resources by limiting light, oxygen, and key nutrients. Such increases in primary productivity have the potential of disrupting nutrient ratios, for example by increased nitrogen fixation of blooming *Trichodesmium spp*. (D'Angelo and Wiedenmann, 2014). Moreover, a shift in the benthic community from coral and crustose coralline algae cover to algal turf and fleshy macro algae can take place, leading to a loss of habitat complexity and the associated biodiversity (Lapointe, 1997; Szmant, 2002). This process is aggravated by the overfishing of key grazing species (Hughes, 1994; Mumby et al., 2006). A net increase in nutrient flux can be beneficial by increasing the productivity of a reef up until a threshold at which the daily primary production exceeds what can be consumed by the grazing community of the reef (Szmant, 2002). Consequently, coral reefs are also observed to flourish in the presence of relatively high dissolved inorganic nutrient concentrations (Stuhldreier et al., 2015). Yet, past this threshold, cover of macro algae will begin to increase and coral cover will decrease, resulting in reef degradation. Thereby, top-down and bottom-up factors interact to control the community structure of coral reefs (D'Angelo and Wiedenmann, 2014). Thus, high nutrient availability becomes a threat to coral reefs if this interaction is thrown out of balance through destructive anthropogenic activities. This interaction with top-down regulation makes it difficult to establish nutrient thresholds which elicit an eutrophication response. Globally, overfishing is considered to constitute a greater pressure to coral reef ecosystems than nutrient enrichment alone (Szmant, 2002). Elevated nutrient levels also increase the prevalence of corallivorous predators such as the crown of thorns starfish, large outbreaks of which have been detrimental to corals on the Great Barrier Reef (Brodie

et al., 2005). Furthermore, the abundance of bioeroders has also been documented to increase in response to nutrient enrichment, competing with corals for space and compromising the integrity of the reef (Fabricius et al., 2012). Nutrification has also been associated with increased incidence and severity of coral diseases which was related to coral mortality and a decreased bleaching threshold (Bruno et al., 2003; Vega Thurber et al., 2014).

1.1.4.2.2. Direct effects on reef corals

Experimental enrichment of dissolved inorganic nutrients has been observed to increase zooxanthellae densities and algal protein content (Dubinsky et al., 1990; Stambler et al., 1991; Muller-Parker et al., 1994b; Marubini and Davies, 1996). Additionally, increased cellular chlorophyll content and photosynthetic rates have been measured (Dubinsky et al., 1990; Muller-Parker et al., 1994b; Ferrier-Pagès et al., 2000). It is proposed that the elevated availability of dissolved inorganic nutrients and consequential expansion of the zooxanthellae population alters the metabolic interactions of the symbiosis by impairing the translocation of photosynthetic products to the host (Dubinsky and Jokiel, 1994). This has negative repercussions to the physiological performance of the coral holobiont, resulting in reduced rates of calcification, linear extension and reproductive success (Marubini and Davies, 1996). Reduced calcification has been observed to occur in regions affected by upwelling of nutrient rich waters, although it was unclear whether this was cause by nutrient enrichment or the reduction in sea surface temperature, or a combination of the two (Wellington and Glynn, 1983). Yet, these direct effects on the zooxanthellae and coral host have not consistently been observed, as some studies found that dissolved inorganic nutrient enrichment had either no, or inconsistent effects on zooxanthellae and host physiology (Ferrier-Pagès et al., 2001; Koop et al., 2001; Nordemar et al., 2003). Negative impacts of dissolved inorganic nutrient enrichment have predominantly been attributed to nitrogen enrichment (Muscatine et al., 1989b; Stambler et al., 1991). However the enrichment with phosphate alone has also been observed to decrease growth rates (Ferrier-Pagès et al., 2000). Thus, direct effects of dissolved inorganic nutrient enrichment have been subject to controversial findings (Fabricius, 2005), likely as a result of differences in chemical forms used, enrichment concentrations, exposure times, study species, and levels of light irradiance (Shantz and Burkepile, 2014). More robust studies are therefore required using long-term, controlled experimental conditions in order to

establish definitive effects of different dissolved inorganic nutrient concentrations to the functioning of the coral-zooxanthellae symbiosis.

A link between water quality and upper thermal bleaching threshold on the Great Barrier Reef was determined by means of using chlorophyll a concentration as a proxy for nutrient loading, showing that nutrient enrichment, which prevailed on inshore reefs due to terrestrial runoff, was associated with lower bleaching thresholds (Wooldridge, 2009). The significance of this impact was considered to be as much as 2.0-2.5°C (Wooldridge, 2009). This correlation between nutrient enrichment and increased bleaching sensitivity was also reported for reefs in southern Florida (Wagner et al., 2010). Several studies provide a mechanistic understanding of how nutrient enrichment increases the susceptibility of corals to bleaching. Firstly, an increased zooxanthellae density and cellular pigment content stimulated by heightened nutrient concentrations results in a darker colouration of the coral (Fabricius, 2005). Correspondingly, a gradient of coral communities has been documented on the Great Barrier Reef, with coastal corals being darker in colouration than offshore corals (Fabricius, 2006). Coral pigmentation has been shown to alter the thermal microenvironment of the coral (Fabricius, 2006). Thereby darker corals display higher surface temperatures due to increased thermal absorption which can exacerbate thermal stress, leading to decreased bleaching thresholds (Fabricius, 2006). Furthermore, a study by Cunning et al. conceptualised that corals with an increased ratio of zooxanthellae to host cells are more susceptible to bleaching due to a cumulatively higher production of reactive oxygen (Cunning and Baker, 2012). Thereby, the higher zooxanthellae densities harboured by corals exposed to nutrient enrichment would trigger a bleaching response at a lower level of stress compared to corals harbouring more favourable symbiont densities. A study by Wiedenmann et al. concluded that the negative impact of dissolved inorganic nutrient enrichment is derived from a resulting imbalance in the proportions of available nitrogen and phosphorus (Wiedenmann et al., 2013). Thereby, enrichment of nitrate alone induced phosphorus starvation of the proliferating zooxanthellae population. This was associated with a decreased irradiance- and thermally-induced bleaching threshold. It was proposed that homeostatic responses of the zooxanthellae aiming to recycle internal stores of phosphorus resulted in compromised integrity of the thylakoid membranes (Wiedenmann et al., 2013). The loss of thylakoid membrane integrity and resulting increase in the production of reactive oxygen species has previously been reported as a mechanism of bleaching initiation (Tchernov et al., 2004).

Thus, both by indirect and direct impacts, prevailing evidence links enrichment of dissolved inorganic nutrients with negative effects towards coral reef ecosystems and a decrease in reef coral resilience to interacting stressors (D'Angelo and Wiedenmann, 2014). An altered dissolved inorganic nutrient environment therefore threatens to exasperate the effects of climate change (Riegl et al., 2015), making water quality of major concern to the management of coral reefs (Brodie et al., 2010; Kroon et al., 2014; Aswani et al., 2015).

1.1.4.3. Heterotrophic compensation

Stressors such as increased temperature raise the metabolic cost that is required to maintain cellular homeostasis. At the same time, adverse environmental conditions can result in a diminished energy supply by autotrophy due to 1) decreased light availability such as occurs by high turbidity, 2) increased zooxanthellae photoinhibition, or 3) decreased zooxanthellae density caused by bleaching. Consequently, the host must resort to the use of energy reserves in the form of lipid, protein or carbohydrate stores in order to survive (Rodrigues and Grottoli, 2007). However, the trophic flexibility of corals allows for the increase in heterotrophic feeding rates and a shift in the use from autotrophic to heterotrophic carbon in order to satisfy daily energy requirements (Anthony and Fabricius, 2000; Grottoli et al., 2006; Palardy et al., 2008). Thereby, up to 100% of the daily metabolic energy demand can be met by means of feeding, when photosynthetically sourced carbon diminishes (Grottoli et al., 2006). Indeed, increased feeding rates have been observed to occur as soon as increased sea water temperatures are experienced (Ferrier-Pagès et al., 2010). Furthermore, significantly increased incorporation of heterotrophic carbon into coral biomass was recorded almost a year following a bleaching event in two reef coral species (Hughes and Grottoli, 2013). This either indicates that the recovery period is extremely long or that a change in trophic behaviour could be a mechanism of adaptation to provide greater resilience to future stress events. It has also been demonstrated that heterotrophic nutrient input limits photophysiological damage to zooxanthellae caused by thermal stress, thereby increasing bleaching resilience (Borell and Bischof, 2008; Hughes et al., 2010; Hoogenboom et al., 2012). However, heterotrophic plasticity is species-specific, leading to the proposition that corals which are effective at heterotrophic feeding have a competitive advantage over those with a greater dependency on autotrophy (Grottoli et al., 2006; Connolly et al., 2012; Anthony and Fabricius, 2000; Ferrier-Pagès et al., 2010).

Thus, high prey availability could mitigate the effects of climate change by increasing the chances of survival and recovery following a bleaching event. Nevertheless, this only holds true for some species, thus compromising diversity. Furthermore, this depends on a healthy zooplankton population which is often in low or patchy abundance. The climate change driven decrease in primary production is predicted to reduce zooplankton availability, particularly in the tropical oceans (Behrenfeld et al., 2006; Chust et al., 2014). On the other hand, nutrient pollution in coastal environments increases primary productivity, leading to heightened prey abundance (D'Angelo and Wiedenmann, 2014). However, this often coincides with increased turbidity and sedimentation which can offset the nutritional benefits brought about by increased prey abundance (Fabricius, 2005; Fabricius et al., 2013), as well as negative secondary effects to the functioning of the coral reef ecosystem (D'Angelo and Wiedenmann, 2014). Additionally, when in combination with imbalanced dissolved inorganic nutrient availability, an increased availability of particulate food has been shown to compromise coral resilience (Ezzat et al., 2015). It therefore remains controversial whether or not increased availability of particulate food is beneficial towards coral resilience.

1.1.5. The role of symbiont genotype in determining reef coral resilience

Even in the absence of interacting local stressors, coral-zooxanthellae associations must increase their thermal tolerance in order to survive future warming trajectories (Donner et al., 2005; Logan et al., 2014). A critical aspect required for projections of climate change impact to coral reef persistence is therefore the understanding of the capacity of reef corals to acclimate and adapt to future environmental perturbations. Despite acclimation efforts being apparent in corals (Gates and Edmunds, 1999), it is feared that the rate of ocean warming will outpace the natural scope for adaptation. Yet, it is argued that one mechanism by which corals can acclimate to higher temperatures more rapidly is by harbouring more thermally tolerant symbionts (Baker, 2001; Berkelmans and van Oppen, 2006; Jones et al., 2008).

The genus *Symbiodinium* has been classified into lineages, clades A-H, based on phylogenetics using the nuclear small and large subunit ribosomal DNA, of which clades A-D, F, and G are associated with scleractinian corals (LaJeunesse, 2001). According to analysis of the highly variable internal transcribed spacers (ITS1/2), each clade is

comprised of distinct types, thus resulting in a great diversity of *Symbiodinium*. Although most corals harbour one dominant *Symbiodinium* type, they can generally associate with multiple clades, with different types often present as background populations (Silverstein et al., 2012).

Symbiodinium types, both at cladal and subcladal level, differ in their sensitivity to thermal stress (Sampayo et al., 2008). Notably, clade D is considered to be a high temperature specialist, on account of the temperature at which photoinhibition occurred being comparatively higher in clade D compared to clade C (Rowan, 2004). Correspondingly, clade D symbionts confer a higher bleaching resistance to their coral host (Berkelmans and van Oppen, 2006). The *Symbiodinium* population within a host could change by two mechanisms. Firstly, by switching, in which symbionts are expelled and new symbionts are acquired from the environment. Or secondly, by shuffling, in which the relative dominance of different genotypes that are already harboured within the host are altered. Thereby, the dominance of a symbiont with high thermal resistance following recovery conveys greater bleaching resistance to future temperature perturbations (Silverstein et al., 2015). Thermal acclimation of *Acropora millepora* by means of community shuffling from a clade C to clade D dominated community resulted in a gain in heat tolerance in the range of 1-1.5°C (Berkelmans and van Oppen, 2006). However, the majority of corals are symbiont-specialists, harbouring only a single clade or even subclade, and are thus unlikely to associate with new symbiont types during thermal stress (Goulet, 2006). The ecological relevance of symbiont plasticity as a mechanism of coral acclimation to global climate change is therefore controversial.

Symbiodinium types also differ in the metabolic advantage which they provide to the host, meaning that changes to the symbiont community constitute a trade-off between temperature tolerance and physiological performance. Under steady-state conditions clade D is measured to have a lower photochemical efficiency (Cunning et al., 2015), and a decreased capacity for carbon and nitrate assimilation (Baker et al., 2013), resulting in reduced translocation of photosynthates, and impairment of host trophic plasticity, growth, and fecundity (Jones and Berkelmans, 2010, 2011; Leal et al., 2015). However, the inverse holds true when exposed to thermal stress during which the physiological performance of clade D symbionts is maintained while that thermally sensitive types decreases. Consequently, clade D is generally in low abundance, only dominating symbiont communities on reefs exposed to high temperatures or turbidity, and has been coined a

selfish opportunist (Stat and Gates, 2011). A recent study concluded that the transition to a clade D dominated community only takes place following severe bleaching in combination with a high recovery temperature (Cunning et al., 2015).

The mechanisms underlying the functional diversity of different *Symbiodinium* genotypes are poorly characterised. Differences in reactive oxygen production have been implicated to play a role in thermal sensitivity (Suggett et al., 2008). A further study has suggested that thylakoid membrane saturation may be involved in conveying differential thermal sensitivities (Tchernov et al., 2004). The involvement of the chloroplast membranes in the distinction of clade D *Symbiodinium* to other genotypes has been verified by transcriptional analysis (Ladner et al., 2012; Barshis et al., 2014). Membrane composition does indeed play an important role in thermal acclimation in higher plants (Welti et al., 2002; Chen et al., 2006). Yet, the polar lipid composition has never been investigated in coral-associated zooxanthellae.

1.1.6. Membrane remodeling as a mechanism of acclimation and adaptation to environmental stress in photosynthetic organisms

1.1.6.1. Relating lipid biochemistry to environmental perturbations

Polar lipids provide the matrix of cellular membranes by assembling into a lipid bilayer which forms biological barriers, forming the structure of the cell and allowing for compartmentalisation within cells which is necessary for the complex functions performed by cellular organelles. This is attributed to the amphipathic nature of polar lipids, having a hydrophobic tail and a hydrophilic head, connected via a glycerol backbone. The tail is constituted of two fatty acyl molecules at sn-1 and sn-2 positions of glycerol which differ in length of the hydrocarbon chain as well as in the degree of their unsaturation which is determined by the number of double bonds between adjacent carbon molecules. The head group at sn-3 denotes the lipid class, with phospholipids containing a phosphate group and glycolipids containing a sugar moiety. Key algal lipid classes are shown in Figure 2.3. The range of possible headgroup moieties combined with the spectrum of fatty acyls results in a tremendous complexity in polar lipid biochemistry.

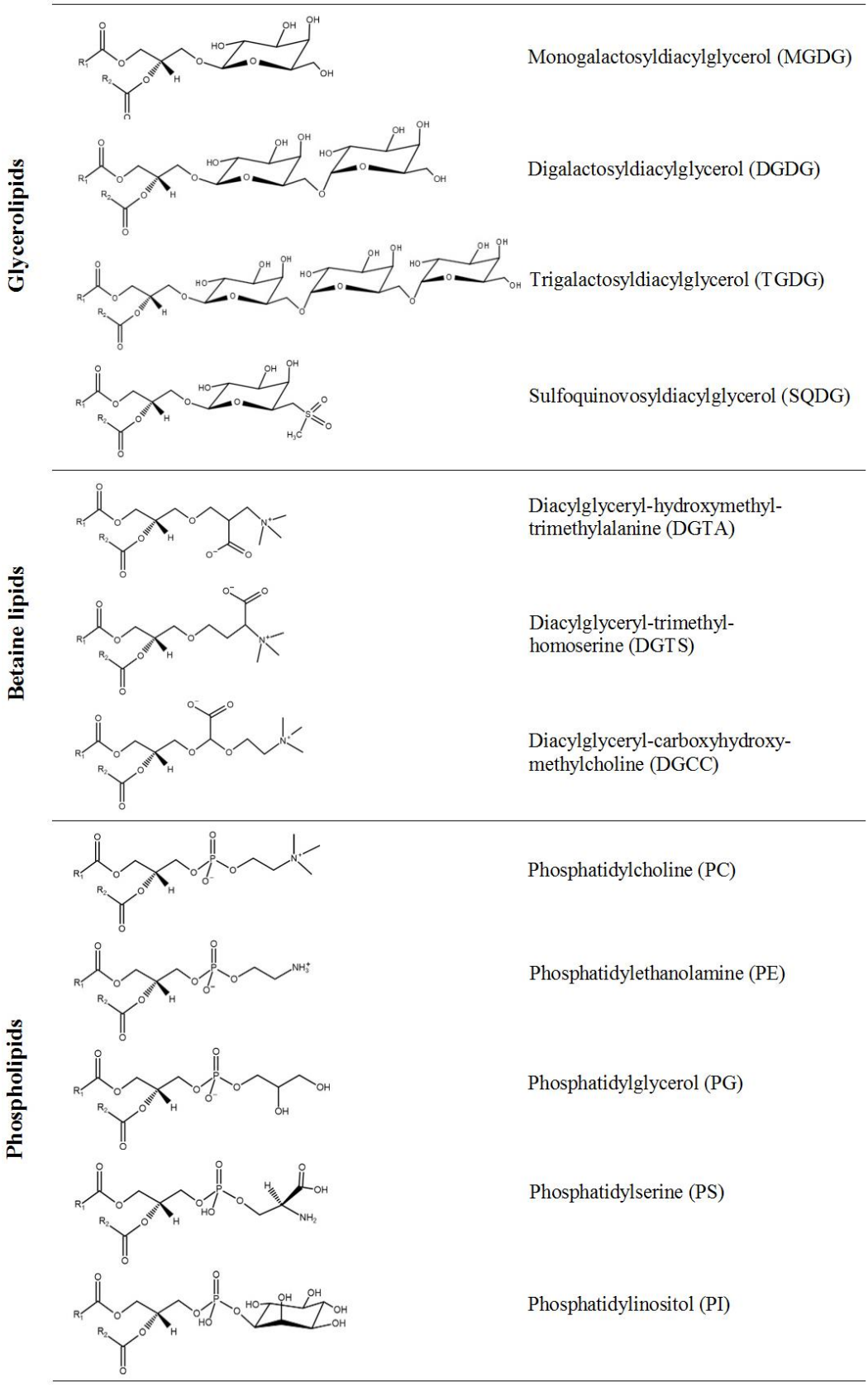

Figure 1.3| Key families of polar lipids prevalent photosynthetic organisms depicting chemical structures of head groups

The specific composition of lipid molecules affects the physiological properties of membranes, most notably, membrane fluidity. Membrane fluidity relates to its melting temperature, with a more fluid membrane having a lower melting temperature, and is regulated by the fatty acyl length and degree of unsaturation, the ratio of bilayer-stabilising to non-stabilising lipids, the size, hydrophobicity and charge of head groups, and the ratio of cholesterol and proteins to lipids. An increase in membrane fluidity affects membrane dynamics and integrity, resulting in increased membrane permeability and impairs the function of integral proteins such as ion channels, enzymes, and, most critically for photosynthetic organisms, the photosynthetic apparatus. Consequently, remodeling of chloroplast membranes is a fundamental process of photosynthetic organisms in response to a fluctuating environment such as changes in temperature (Welti et al., 2002; Zheng et al., 2011). Adaptations of the physical characteristics of membranes in response to sub-lethal temperature increases can lead to long term thermal acclimation, called acquired thermotolerance (Horváth et al., 1998; Chen et al., 2006; Saidi et al., 2011). However, plants and algae can also differ in their inherent ability to tolerate high temperature without pre-acclimation.

Additionally, cellular membranes have been shown to possess a great amount of flexibility in their composition, providing a buffering mechanism in response to nutrient stress. Under normal growth conditions of the higher plant *Arabidopsis thaliana*, it has been estimated that phospholipids hold one third of cellular organic phosphorus (Poirier et al., 1991). The homeostatic response to phosphorus starvation involves the remobilisation of this store in order to redirect this essential nutrient towards more vital cellular functions such as the production of ATP (Van Mooy et al., 2009; Frentzen, 2004). This is possible due to the substitution of phospholipids by non-phosphorus containing lipids with similar chemical properties. On the other hand, membrane lipid replacement is not a principal response to nitrogen limitation since polar lipids are not believed to constitute a considerable store of cellular nitrogen (Gaude et al., 2007). However, substantial changes to lipid metabolism constitutes the stress response to either phosphorus or nitrogen limitation, resulting in a significant accumulation of neutral lipids, independent of the limiting nutrient (Hu et al., 2008).

Thus, the polar lipid composition provides biomarkers signifying environmental stress responses and adaptation to specific environmental conditions. Lipid biomarkers that have been observed in response to a range of abiotic stressors are summarised in table 2.1.

Table 1.1| Characteristic changes to the membrane composition of photosynthetic organisms provide biomarkers indicative of responses to specific nutrient environments.

Lipid biomarker	Abiotic stress	Description	Organisms	Reference
↑ **SFA/PUFA**	High temperature	The degree of fatty acid unsaturation is decreased in response to high temperature. This has particularly been observed for DGDG in chloroplast membranes. The double bonds within unsaturated fatty acids are also a prime target of attack by reactive oxygen species, thus favouring a decrease in PUFAs	Cyanobacteria, *Arabidopsis thaliana*	(Wada et al., 1994; Falcone et al., 2004; Chen et al., 2006)
↑ **TAG**	High temperature	Decreases in lipid unsaturation are thought to occur largely via deacylation and de novo fatty acid synthesis, resulting in the translocation of PUFAs to TAGs, thus leading to TAG accumulation	*Arabidopsis thaliana*	(Higashi et al., 2015)
↓ **MGDG/DGDG**	High temperature	While DGDG is a bilayer forming lipids, MGDG forms non-bilayer structures (inverted hexagonal) when not in contact with proteins. The proportion of non-bilayer structures has been observed to increase in response to heat stress, resulting in a decrease in the MGDG/DGDG ratio in order to preserve thylakoid membrane integrity. Correspondingly, mutations resulting in impaired DGDG biosynthesis result in increased heat sensitivity.	*Arabidopsis thaliana*	(Chen et al., 2006)
↓ **PC/PE**	Freezing/ dehydration	PC is a bilayer forming lipid, but the smaller headgroup of PE results in the formation of hexagonal structures. The decrease in molar ratio of PC and PE during cold stress results in increased formation of non-bilayer structures which causes freezing damage. An increase in the PC/PE ratio is therefore associated with increased tolerance to cold in higher plants.	*Arabidopsis thaliana*	(Welti et al., 2002)

Lipid biomarker	Abiotic stress	Description	Organisms	Reference
↑ **TGDG**	Freezing/ high salinity	In order to prevent damage cause by cellular dehydration an increase in the biosynthesis of oligogalactolipids at the expense of MGDG has been observed, increasing the ratio of bilayer- to non-bilayer forming lipids within the outer chloroplast envelope membrane, thereby preventing membrane fusion which could occur due to organelle shrinkage.	*Arabidopsis thaliana*	(Moellering et al., 2010)
↑ **SQDG/PG**	Phosphorus starvation	Phospholipids comprise a considerable store of cellular P which is recycled during P starvation by the replacement of PG with SQDG within the thylakoid membranes which is possible due to the shared anionic nature of these lipids.	*Arabidopsis thaliana*	(Frentzen, 2004; Wiedenmann et al., 2013)
↑ **Betaine Lipids/PC**	Phosphorus starvation	The betaine lipids DGTA/S and DGCC can substitute of PC within extraplastidic membranes in response to P starvation.	Phytoplankton	(Van Mooy et al., 2009)
DGDG localisation	Phosphorus starvation	DGDG is only localised within chloroplast membranes under normal conditions but is trafficked to the plasma membrane during P starvation in order to substitute for PC.	*Arabidopsis thaliana*	(Härtel et al., 2000)
↑ **TAG**	Nitrogen and/or phosphorus limitation	Lipid metabolism commonly shifts from the production of polar lipids to that of neutral lipids due to reduced cell division (reduced need for membrane biosynthesis) and due to redirection of photosynthates from production of N- and P- rich molecules to that of hydrocarbons.	various microalgae	(Hu et al., 2008)

Studies of membrane remodelling have predominantly been conducted in the higher plant *Arabidopsis thaliana*, yet particularly the chloroplast membrane composition, composed of the galactolipids MGDG and DGDG as well as SQDG and PG as minor components, is highly conserved among photosynthetic organisms (Mizusawa and Wada, 2012), thus making these findings applicable to microalgae. Indeed, an increase in the SQDG/PG ratio in response to phosphate starvation, which was first observed in *A. thaliana*, has also been identified as a biomarker of phosphorus starvation in *Symbiodinium* hosted by reef corals (Wiedenmann et al., 2013). The full polar lipid biochemistry of *Symbiodinium* has not been elucidated, yet has great potential in furthering our understanding of acclimation and adaptation of the coral-zooxanthellae symbiosis.

1.1.6.2. Current knowledge of coral lipidomics – fatty acids

Due to the great complexity of lipid biochemistry, lipid analysis of corals and their symbionts has primarily focused on the analysis of fatty acids. Dominant fatty acid species that have been identified in *Symbiodinium* include 14:0, 16:0, 16:1, 18:0, 18:1, 18:3, 18:4, 18:5, 20:5 and 22:6 (Papina et al., 2003; Kneeland et al., 2013; Imbs et al., 2014; Chen et al., 2015). Particularly a high content of 22:6ω3 has been suggested to be a marker of dinoflagellates as it is rare in other microalgae (Zhukova and Aizdaicher, 1995). Additionally, 18:3, 18:4, 18:5, and 20:5 have been proposed as *Symbiodinium* fatty acid markers (Papina et al., 2003; Imbs et al., 2014; Chen et al., 2015). Yet, no clear trend in the fatty acid profile is apparent depending on symbiont type, host species, or whether they are in culture or *in hospite* (Imbs et al., 2014; Chen et al., 2015; Kneeland et al., 2013).

Zooxanthellae contain a higher relative PUFA content compared to their hosts (Papina et al., 2003). Unlike plants, animals cannot synthesize fatty acids with a double bond beyond the Δ9 position (due to lack of Δ9, Δ12, Δ15 desaturases), which are necessary for the production of ω3 and ω6 polyunsaturated fatty acids, and thus, must obtain these from photosynthetic organisms. The occurrences of ω3 fatty acid markers within the host fraction indicate that PUFAs are translocated from the symbionts to the host (Papina et al., 2003). Consequently, coral bleaching results in a significant decrease in PUFA content of the host tissue (Bachok et al., 2006). This is likely exacerbated by the proposed preferential usage of fatty acids for respiration during stress in order to maintain host metabolism (Tolosa et al., 2011). Bleached corals must instead rely on stored lipids or on the uptake of PUFAs through heterotrophic feeding on phytoplankton, the capacity of which is species

specific and often insufficient, thus highlighting the importance of fatty acid trafficking within the coral-algal symbiosis (Grottoli et al., 2006; Rodrigues et al., 2008).

The role played by the degree of fatty acid saturation in determining the thermal sensitivity of different Symbiodinium types has been investigated by several studies. The retention of thylakoid membrane integrity during exposure to high temperatures was observed in thermally resilient symbiont types, including clade D, while the same temperature treatment resulted in compromised stacking capacity of thylakoids in thermally sensitive types (Tchernov et al., 2004). This was associated with a significant increase in the relative abundance of 18:1 compared to 18:4 fatty acids, thus concluding that an increase in thylakoid membrane saturation regulates thermal sensitivity. However, two further studies found that thermal sensitivity of *Symbiodinium* type had no effect on the degree of fatty acid saturation of both unstressed and thermally-stressed samples (Díaz-Almeyda et al., 2010; Kneeland et al., 2013). Furthermore, the thermal threshold initiating a decrease in C18 PUFA content was found to be lower in clade C compared to clade D *Symbiodinium* (Kneeland et al., 2013). However, the lipid classes associated with fatty acids had not been identified. As suggested by Kneeland et al., the analysis of total fatty acid profiles cannot differentiate between fatty acids associated with polar lipids or storage lipids, thus making it relatively uninformative considering that in other photosynthetic organisms the decrease in chloroplast PUFA content in response to thermal stress has been found to occur by transfer of PUFA from galactolipids to TAGs, thus retaining the PUFAs within the cell (Légeret et al., 2015). The analysis of the polar lipid composition is therefore needed in order to provide greater insight into the lipid biochemistry underlying thermal tolerance in *Symbiodinium*. A greater understanding of the functional role of membrane composition in coral-associated zooxanthellae as well as the capacity of membrane remodeling in driving thermal acclimation and adaptation would aid in the projections of reef coral persistence during future global climate scenarios.

1.2. Knowledge gaps and aims of this thesis

Of critical concern to the persistence of the coral reef ecosystem is the understanding of how the nutrient environment impacts the stability of the coral-zooxanthellae symbiosis and its resilience to global climate change. Notably, terrestrial sources of nutrient pollution could largely be manageable (Kroon et al., 2014). It is therefore, fundamental to advance our awareness of how this non-climatic factor affects the symbiosis in order to implement science driven management strategies so as to promote coral reef resilience (Aswani et al., 2015). Yet, many aspects of coral nutrient biology are still elusive, making the management of the nutrient environment subject to continued debate. It remains largely unclear how the essential nutrients, nitrogen and phosphorus, are partitioned and allocated within the symbiosis, as well as what the principal source of these nutrients is to the coral host and to the algal symbiont. Particularly little is known about the uptake and distribution of phosphorus within the symbiosis. It has only recently been demonstrated that a particular threat of anthropogenic nutrient pollution is the disruption of the ratio of dissolved inorganic nitrogen and phosphorus (Wiedenmann et al., 2013). This necessitates a greater comprehension of how imbalanced dissolved inorganic nutrient availabilities impact the functioning of the coral-zooxanthellae symbiosis. The importance of nitrogen and phosphorus ratios in heterotrophic form has never been considered. Indeed, heterotrophy has largely only been recognised as a source of carbon. Furthermore, effective tools for the identification of nutrient stress in reef corals are required.

Increasing coral resilience through the management of the nutrient environment bides time in the race against climate change. Yet, global warming of sea surface temperatures is predicted to continue, the rate of which being dependent on the ability of the human population to rapidly reduce carbon emissions (IPCC 2013). Ultimately, reef building corals need to adapt in order to persist within future climate change scenarios (Logan et al., 2014). It is important to grasp what specific mechanisms promote a heightened tolerance to various environmental stress parameters in order to predict the capacity of reef corals to acclimate and adapt to a rapidly changing environment. The underlying mechanism of the differential inherent tolerance of diverse *Symbiodinium* types to higher temperatures is not understood. The polar lipid composition of zooxanthellae has never been characterised, yet could provide greater insight into fundamental mechanisms of thermal resistance and provide a tool with which to study the capacity of reef corals to acclimate and adapt to

increasing temperatures, as well as to recognise responses to other perturbations to the physicochemical environment.

This thesis sets out to explore both of these essential aspects of coral biology: responses of the symbiosis to the nutrient environment and the role of zooxanthellae membrane composition in inherent thermal tolerance. Firstly, this thesis aims to characterise phenotypes of the symbiosis in respect to different nutrient environments in order to establish cellular biomarkers which are representative of nutrient availability and signify nutrient stress, which could aid in the effective monitoring and management of coral reef ecosystems. In doing so, this thesis aims to investigate the relative importance of two major sources of nutrients to the functioning of the coral-zooxanthellae symbiosis: the assimilation of dissolved inorganic nutrients and heterotrophic feeding. Furthermore, this thesis aims to assess the importance of the ratio of nitrogen and phosphorus, both in dissolved inorganic and heterotrophic form, in respect to the steady-state functioning of the symbiosis as well as to the resilience to thermal stress. Secondly, this thesis aims to elucidate the underlying distinctions in the polar lipid biochemistry of two zooxanthellae genotypes in order to understand what adaptations of the symbiont may explain the heightened thermal tolerance of specific coral-zooxanthellae associations. Thereby, the aim is to characterise biochemical markers of a thermally resistant phenotype, with the potential of advancing the study and understanding of reef coral acclimatisation and adaptation to climate change.

Major research questions of this thesis are:

1. **Can heterotrophy compensate for the lack of dissolved inorganic nutrient availability?**

2. **Is a dissolved inorganic nutrient imbalance caused by the enrichment of either dissolved inorganic nitrogen or phosphate equally detrimental to the physiology of reef corals?**

3. **Can imbalanced growth of the zooxanthellae be induced by a disproportional intake of heterotrophic nitrogen and phosphorus?**

4. **Do inherent differences in the membrane composition of *Symbiodinium* types underpin their diverse thermal sensitivity?**

1.3. Approach and thesis outline

This thesis is divided into four results chapter which are written in the format of scientific publications, each with an introduction, methods, results, and discussion section. The first three chapters are concerned with the effects of the nutrient environment on the coral-zooxanthellae symbiosis, addressing the first three research questions in turn. The final results chapter aims to answer the fourth research question by investigating the polar lipid biochemistry of two *Symbiodinium* types with contrasting thermal sensitivities. Finally, a synthesis chapter provides broader interpretations and conclusions of the presented findings, and outlines future research trajectories.

All studies encompassing this thesis were conducted using reef coral specimens cultured in the experimental mesocosm facility of the University of Southampton. This allowed for controlled experimental conditions. Studies presented in this thesis stand apart from past investigations on the effects of the nutrient environment on reef corals by applying long-term experimental treatments. This enabled the establishment of adapted phenotypes as compared to the study of an immediate response to a change in the nutrient environment. The nutrient environment was manipulated by adjusting the dissolved inorganic nutrient concentrations within distinct aquaria systems as well as by subjecting specimens to different feeding regimes. Additionally, the light and temperature of separate tank units within a given system could be altered so as to subject the test specimens to stress conditions. Thus, the interacting effects of multiple factors could be examined. All studies on the effects of different nutrient conditions (chapters 2-4) used *Euphyllia paradivisa* harbouring clade C1 *Symbiodinium* as the model organism. The analysis of *Symbiodinium* polar lipid biochemistry (chapter 5) was conducted in collaboration with the Centre for Biomedical Research Mass Spectrometry Unit at Southampton General Hospital lead by Professor Tony Postle. The study organisms for this latter study were clade C and D *Symbiodinium* harboured by distinct genotypes of *Acropora valida* cultured under oligotrophic conditions. The key hypothesis and approach of each chapter are outlined below:

Chapter 2 Ultrastructural biomarkers in symbiotic algae reflect the availability of dissolved inorganic nutrients and particulate food to the reef coral holobiont

H_1 Heterotrophic feeding can compensate for long-term deprivation of dissolved inorganic nutrients in a reef coral.

This study assesses the relative importance of two nutrient sources to reef corals: dissolved inorganic nutrients and particulate food. Macroscopic and transmission electron microscope analysis are used to characterise the phenotypes of the coral-zooxanthellae association subjected to replete and limited dissolved inorganic nitrogen and phosphate availability in combination with the presence and absence of heterotrophic feeding. By the analysis of the zooxanthellae ultrastructure, cellular biomarkers representative of nutrient availability to zooxanthellae *in hospite* are identified which could aid in the monitoring of nutrient stress in reef corals. Additionally, the effects of the different nutrient environments on the dial cell cycle of zooxanthellae *in hospite* are characterised. Taken together, this study allows for the inference of the relative contribution of each nutrient source to the nutrient status of the coral host and the zooxanthellae.

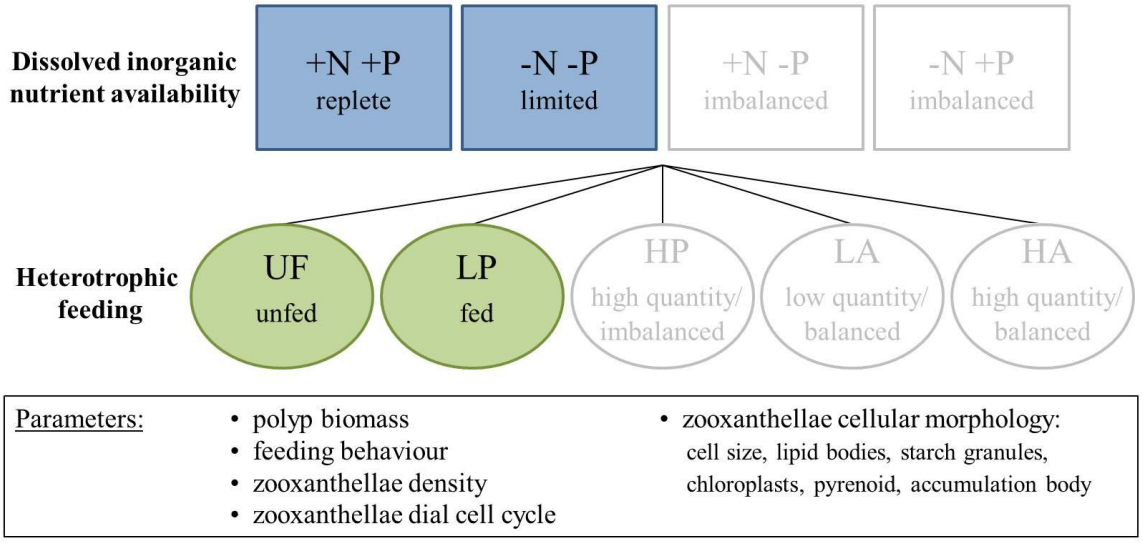

Figure 1.4| Experimental design for chapter 2. Two dissolved inorganic nutrient treatments are coupled to the presence of absence of heterotrophic nutrient input.

Chapter 3 The coral-zooxanthellae symbiosis is significantly more dependent on an external supply of phosphorus than nitrogen

H_2 The imbalanced nutrient environment resulting from the enrichment of dissolved inorganic nitrogen alone is more detrimental to the functioning of the coral-zooxanthellae than the imbalance resulting from the enrichment of phosphate alone.

This study investigates the relative importance of dissolved inorganic nitrogen and phosphate to the functioning of the coral-zooxanthellae symbiosis. Additional to the contrast of high and limited availability of both nitrate and phosphate studied in chapter 2, the phenotypes of the coral-zooxanthellae symbiosis subjected to imbalanced dissolved inorganic nutrient availabilities are characterised. The nutrient imbalance is caused either by the enrichment with nitrate alone, or by that of phosphate alone, thereby inducing the limitation of phosphorus or nitrogen respectively. By the same principle of chapter 2, the effects of these different nutrient environments are assessed by macroscopic analysis of coral polyps as well as by the study of the zooxanthellae density and ultrastructure by transmission electron microscopy. Cellular biomarkers representative of these two forms of nutrient imbalance are identified. This study implicates which form of nutrient imbalance is most detrimental to the health of reef corals.

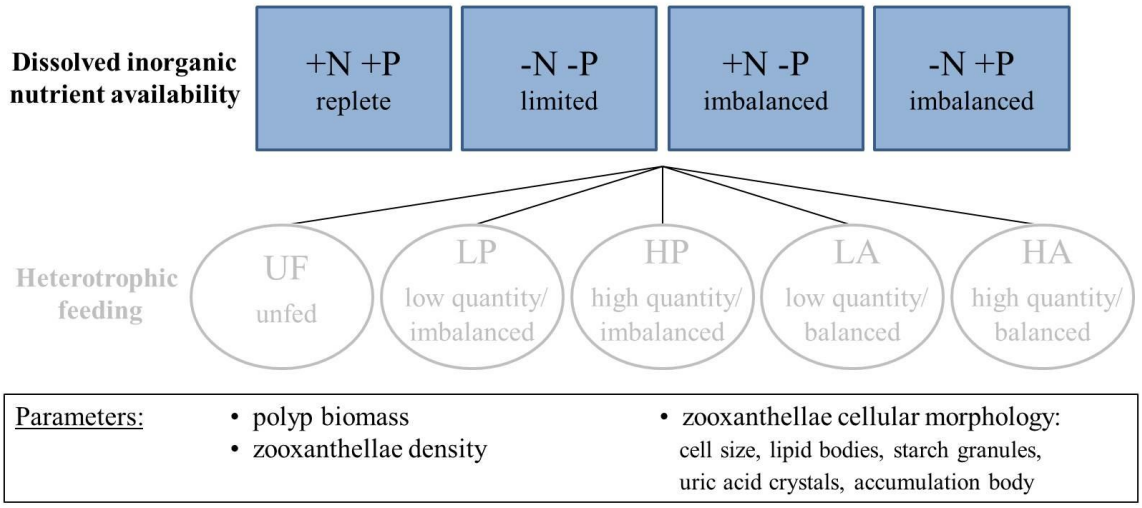

Figure 1.5| Experimental design for chapter 3. *Euphyllia paradivisa* polyps are subjected to four dissolved inorganic nutrient treatments. The repercussions of two types of nutrient imbalance are compared.

Chapter 4 Heterotrophic feeding is only beneficial towards coral stress resilience if nitrogen and phosphorus intake is balanced

H_3 Disproportional intake of heterotrophic nitrogen and phosphorus results in imbalanced growth of the zooxanthellae population, leading to impairment of heat stress tolerance.

This study assesses the importance of food quality, in terms of the balance of heterotrophic nitrogen and phosphorus intake, as well as food quantity on the nutritional benefit provided by particulate food intake. The interacting effects of balanced and imbalanced heterotrophic nutrient intake and different dissolved inorganic nutrient availabilities on the nutrient status of the coral-zooxanthellae symbiosis are studied. Additionally, this study investigates how the imbalanced intake of heterotrophic nutrients in combination with limited or imbalanced dissolved inorganic nutrient availability affect the thermal stress resilience of the coral host and the zooxanthellae.

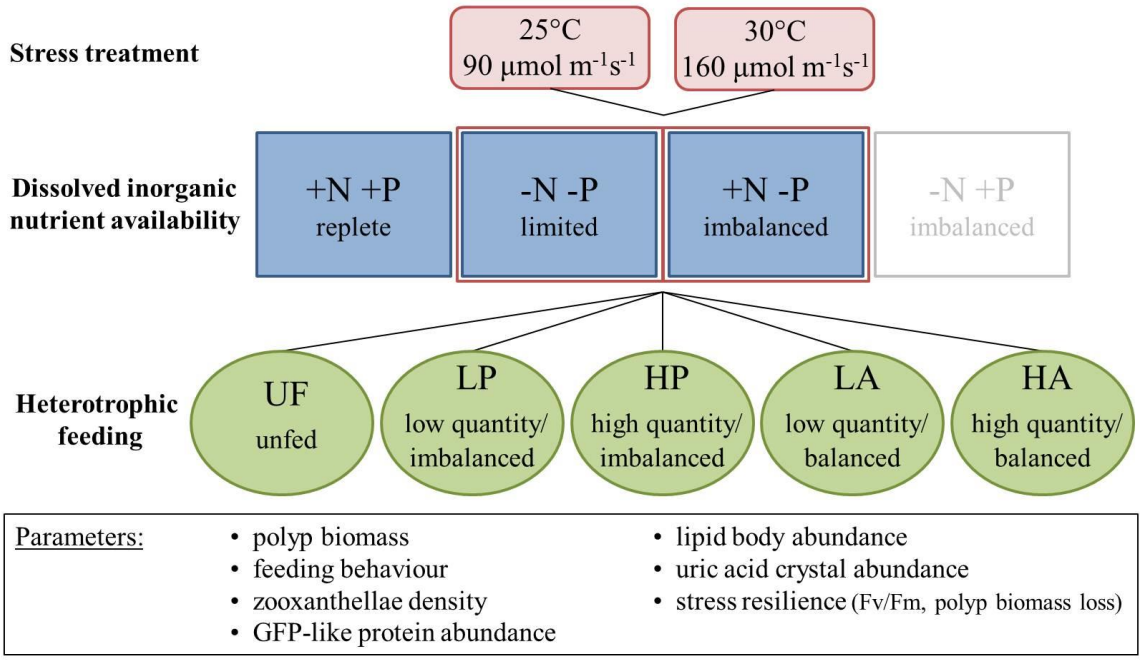

Figure 1.6| Experimental design for chapter 4. This chapter assesses the interacting effects of dissolved inorganic nutrient availability and heterotrophic feeding. Five feeding treatments are analysed, taking into account the value of food quality and quantity. The effects of the different feeding treatments in combination with limited and imbalanced dissolved inorganic nutrient availability on the thermal stress resilience of the coral host and the zooxanthellae are examined.

Chapter 5 Distinct lipid profiles of two clades of endosymbiotic algae isolated from the same coral host species give new insight into the basis of their divergent heat stress tolerance

H_4 The membrane composition of the thermally tolerant clade D *Symbiodinium* is distinct from that of the thermally sensitive clade C, and is principally attributed to differences in the composition of chloroplast membranes.

In this study the polar lipid biochemistry of clade C and D *Symbiodinium* subjected to the same environmental conditions is characterised using high performance liquid chromatography coupled to electrospray ionisation tandem mass spectrometry. Key differences in the membrane composition are identified and related to the varying thermal tolerance of these two clades.

Chapter 2: Ultrastructural biomarkers in symbiotic algae reflect the availability of dissolved inorganic nutrients and particulate food to the reef coral holobiont

Sabrina Rosset, Cecilia D'Angelo, Jörg Wiedenmann

[Published as: Rosset S, D'Angelo C, Wiedenmann J (2015) Ultrastructural biomarkers in symbiotic algae reflect the availability of dissolved inorganic nutrients and particulate food to the reef coral holobiont. Frontiers in Marine Science, 2:1-10. (Excluding dial cell cycle analysis)]

Author contributions:

Cecilia D'Angelo and Jörg Wiedenmann established and maintained the different nutrient environments and cultured *E. paradivisa* under the respective experimental treatments. All authors contributed to the experimental design. Sabrina Rosset conducted TEM analysis of all samples and analysed the zooxanthellae dial cell cycle. Cecilia D'Angelo provided measurements of polyp biomass parameters. All authors contributed to the writing of the manuscript.

2.1. Abstract

Reef building corals associated with symbiotic algae (zooxanthellae) can access environmental nutrients from different sources, most significantly via the uptake of dissolved inorganic nutrients by the algal symbiont and heterotrophic feeding of the coral host. Climate change is expected to alter the nutrient environment in coral reefs with the potential to benefit or disturb coral reef resilience. At present, the relative importance of

the two major nutrient sources is not well understood, making predictions of the responses of corals to changes in their nutrient environment difficult. Therefore, we have examined the long-term effects of the availability of different concentrations of dissolved inorganic nutrients and of nutrients in particulate organic form on the model coral *Euphyllia paradivisa*. Coral and algal biomass showed a significantly stronger increase in response to elevated levels of dissolved inorganic nutrients as compared to the supply with particulate food. Notable alterations to the dial pattern of zooxanthellae division rates are suggestive of considerable alterations to the metabolic interactions of the zooxanthellae and the coral host in response to dissolved inorganic nutrient deprivation. Also, changes in the zooxanthellae ultrastructure, determined by transmission electron microscopy (TEM), were mostly driven by the availability of dissolved inorganic nutrients under the present experimental conditions. The larger size of symbiont cells, their increased accumulation of lipid bodies, a higher number of starch granules and the fragmentation of their accumulation body could be established as reliable biomarkers of low availability of dissolved inorganic nutrients to the coral holobiont.

2.2 Introduction

Coral reefs provide important ecosystem services by supporting a vast biodiversity, coastal protection and food supply for millions of coastal inhabitants. They are of substantial economic value to fisheries and the recreation and tourism industries (Moberg and Folke, 1999). Corals reefs are threatened by global warming and a broad range of human impacts (Baker et al., 2008; van Hooidonk et al., 2013; D'Angelo and Wiedenmann, 2014). Their habitat-forming scleractinian species have a certain potential to adapt/acclimatise to elevated temperatures (Logan et al 2014) and regional coral populations can stand unusual levels of heat stress (Hume et al., 2013; Barshis et al., 2013). However, it is uncertain whether these temperature tolerant forms will extend their geographic range in the warming oceans since local adaptations can prevent their wider distribution (D'Angelo et al., 2015). Therefore, it is questionable whether coral reefs will deliver their ecosystem services in the future.

Shallow, warm water reefs are commonly found in oligotrophic waters where the nitrogen and phosphorus containing nutrients that are required to sustain cellular growth (Falkowski et al., 1984; Yellowlees et al., 2008) are scarce in both dissolved and particulate forms

(Dubinsky and Jokiel 1994; but see Szmant 2002). The success of reef-building corals in these environments can be attributed to their symbiotic association with unicellular algae of the genus *Symbiodinium* (zooxanthellae). This symbiosis enables the holobiont to access both nutrient pools, dissolved inorganic and organic nutrients (NH_4^+, NO_3^-, PO_4^{3-}, urea, free amino acids) which can be assimilated by the zooxanthellae (D'Elia and Webb, 1977; Grover et al., 2006, 2008), and organic nutrients in particulate form which can be accessed by the host via heterotrophic feeding on zooplankton, bacteria and suspended particulate matter (Yonge, 1930; Johannes et al., 1970; Bak et al., 1998; Anthony, 2000; Heidelberg et al., 2004; Yahel et al., 2005). Additionally, the zooxanthellae acquire ammonium derived from host catabolic pathways, thereby efficiently retaining and recycling nitrogen within the holobiont (Muscatine and D'Elia, 1978; Rahav et al., 1989; Wang and Douglas, 1998). In addition, bacterial nitrogen fixation could potentially represent an additional source of nitrogen for corals as reviewed by (Rädecker et al., 2015)..

The limited availability of nutrients is thought to restrict the growth of zooxanthellae *in hospite* (Muscatine et al., 1989b). While experimental evidence indicates that this limitation is mostly due to an insufficient supply with nitrogen (Fabricius, 2005; Wiedenmann et al., 2013; D'Angelo and Wiedenmann, 2014), a limited availability of phosphorus has also been suggested to constrain algal proliferation (Rands et al., 1993; Yellowlees et al., 2008). The nutrient-limited zooxanthellae in shallow water corals in oligotrophic environments experience an often sufficient exposure to photosynthetic active radiation (Dubinsky & Jokiel 1994). While CO_2 supply for the algal cells is not unlimited in these corals (Muscatine et al. 1989), it seems to be less limiting than the nutrient availability given that photosynthesis and carbon fixation are largely uncoupled from cellular growth as indicated by the transfer of substantial amounts of photosynthetically fixed carbon from the zooxanthellae to the host (Falkowski et al., 1993; Dubinsky and Jokiel, 1994). This carbon transfer can help the algae to maintain a favourable chemical balance (Falkowski et al., 1993; Dubinsky and Jokiel, 1994). The coral host benefits from the translocated photosynthates which support energy and mucus production (Muscatine, 1965; Falkowski et al., 1984; Crossland, 1987; Bachar et al., 2007).

The capacity of the symbiotic algae to assimilate dissolved inorganic nutrients renders them sensitive to changes in environmental nutrient levels (Muscatine et al. 1989) and these disturbances can directly increase the susceptibility of corals to bleaching, the often fatal breakdown of the symbiotic association (Wiedenmann et al., 2013; Cunning and

Baker, 2013; Vega Thurber et al., 2014). In particular, phosphate starvation of zooxanthellae which can result from imbalanced nitrate enrichment has been shown to reduce the threshold for heat and light stress-mediated bleaching (Wiedenmann et al., 2013). Dissolved inorganic nutrient deprivation resulting from competition with other organisms such as blooming phytoplankton was also suggested as a potential cause for increased susceptibility of corals to thermal bleaching (D'Angelo and Wiedenmann, 2014). In contrast, supplementation with inorganic nitrogen and particulate food has the potential to mitigate negative effects of heat stress on zooxanthellae photosynthesis (Béraud et al., 2013; Hoogenboom et al., 2012). The supply with nutrients from heterotrophic feeding of the host has also been shown to promote coral recovery after episodes of bleaching (Grottoli et al., 2006).

Global change-driven modifications of the nutrient environment is likely to affect coral reefs due to A) the increased nutrient enrichment of coastal waters and associated negative effects due to human population growth and the intensified use of coastal areas (D'Angelo and Wiedenmann, 2014) and B) the nutrient impoverishment of oceanic waters due to stronger stratification of the water column promoted by warming surface waters (Behrenfeld et al., 2006). The latter conditions prevailed during the 1997/98 coral die-off at Galapagos when the El Niño Southern Oscillation (ENSO)-mediated reduction of major upwelling resulted in nutrient deficiency (Chavez et al., 1999) and an associated drop in surface water temperatures (Riegl et al., 2015). Such reduction in productivity can also result in a decrease of zooplankton biomass (Roemmich and McGowan, 1995; Chust et al., 2014), further depriving corals from vital nutrients by impairing heterotrophic feeding. Therefore, future changes in nutrient fluxes in coral reefs in oceanic environments may act in combination with increased heat stress levels (Logan et al., 2014) to accelerate reef decline. In contrast, the higher food availability in coastal waters that may result from the expected nutrient-fueled increase in primary production could result in a trophic shift to predominantly heterotrophic coral communities (Anthony and Fabricius, 2000) and possibly mitigate some of the direct negative effects of nutrient enrichment on coral physiology (D'Angelo and Wiedenmann, 2014). However, it is yet unclear whether the potentially beneficial (Grottoli et al., 2006) or adverse (Fabricius et al., 2013) effects of greater food abundance on reef coral will dominate in the future. In particular, the interactive effects of host feeding in combination with high or low availability of dissolved inorganic nutrients on the physiology of the coral holobiont are not well understood.

Many previous studies focused either on the effects of enrichment with dissolved inorganic nutrients without controlling feeding (Stambler et al., 1991; Marubini and Davies, 1996; Ferrier-Pagès et al., 2000), or analysed the effects of feeding without comparative investigation of dissolved inorganic nutrient enrichment (Muller-Parker et al., 1996; Houlbrèque et al., 2004; Hoogenboom et al., 2010; Tolosa et al., 2011; Tremblay et al., 2014). Studies that did consider both nutrient sources, subjected corals to short-term treatments ranging from 2 to 4 weeks (Muscatine et al. 1989; Dubinsky et al. 1990; Smith & Muscatine 1999; Titlyanov et al. 2000). Since some physiological responses of corals to changes in environmental conditions such as the photoacclimation of the host can take up to 6 weeks to reach a fully acclimated state (Gittins et al., 2015), long-term experiments are required to define endpoints in the acclimation process. Biomarkers of such acclimation responses hold high potential to serve as indicators of changes in nutrient environments in coral reef waters which are otherwise difficult to detect due to rapid uptake and turnover of dissolved inorganic nutrients by pelagic communities (Furnas et al., 2005).

We have therefore assessed the combined effects of the availability of dissolved inorganic nutrients and particulate food on the performance of the coral holobiont. Long-term experiments were conducted in which the corals together with their symbionts were exposed to different nutrient environments for >1.5 years. We used transmission electron microscopy (TEM) to examine the ultrastructure of the algal symbionts and to establish biomarkers reflecting the nutrient environment. The results of our study provide novel insights into the complex nutrient physiology of the coral-*Symbiodinium* association.

2.3. Methods

2.3.1. Experimental design

E. paradivisa is widely distributed in the central Indopacific, American Samoa and the Red Sea. It is characterised by large polyps and long tentacles which enable the coral to take up comparably large food items. The tentacles can be easily removed and yield high quality zooxanthellae preparations due to the lack of contamination by skeletal remains. Hence, *E. paradivisa* represents an excellent model species to study the effects of heterotrophic feeding. The corals were cultured in the experimental mesocosm of the Coral Reef Laboratory at the National Oceanography Centre Southampton (D'Angelo and

Wiedenmann, 2012). The experimental units were maintained at high nutrient (HN) (NO_2^- /NO_3^- ~6.5µM/phosphate ~0.3µM) or low nutrient (LN) (NO_2^-/NO_3^- ~0.7µM/phosphate ~0.006µM) conditions, correspondingly producing a nutrient replete and a nutrient limited environment (D'Angelo and Wiedenmann, 2012, Wiedenmann et al., 2013). High nutrient levels were maintained by continuous low level dosing of sodium nitrate and disodium hydrogen phosphate solutions. Low nutrient levels were maintained through the addition of Rowaphos phosphate removal matrix (Rowa) as well as daily low level dosing of ethanol. NH_4^+ and NO_2^- concentrations were negligible or low, respectively, in comparison to NO_3^-. Therefore, values of total dissolved nitrogen represent mostly NO_3^- (Wiedenmann et al., 2013). Polyps of selected replicate colonies from both nutrient conditions were individually fed three times per week with defined portions of prawn muscle tissue (one portion = ~2.15mg dry weight, ~4.83cal). Fed and unfed colonies were cultured side by side within the respective experimental tanks to ensure that they experienced identical conditions apart from the deviating feeding regime. The services of a commercial provider (Eurofins) were used to determine the nutrient content of the food. A single portion offered to a polyp per feeding event contained ~170µg N and ~6.9µg P. The amount of particulate food used in the experiments falls in the order of magnitude discussed to be available to corals in the natural environment (Johannes et al., 1970; Heidelberg et al., 2004; Yahel et al., 2005). To test satiation threshold of the corals exposed to different nutrient environments, feeding was increased to five times per week. Food intake was measured as the percentage of polyps that ingested the offered portions. Food that was not taken up by the polyps within 30 min was removed from the tank and recorded. Corals were cultured at a constant temperature of 25°C and a photonflux of ~150µmol m^{-2} s^{-1} with a 10/14 hour light/dark cycle. Four experimental treatments were established: HN/unfed; HN/fed; LN/unfed; and LN/fed. Polyps were cultured under these conditions for over 1.5 years prior to sampling.

2.3.2. Determining of the symbiont phylotype

Tentacles of *E. paradivisia* were harvested, sonicated for 15 minutes in deionised water (MilliQ, Millipore) water and homogenised using a micropestle. Zooxanthellae were separated from tissue homogenate by five consecutive centrifugation (2500 g) and wash steps with sterile-filtered seawater. Genomic DNA was extracted and the *Symbiodinium spp*. ribosomal DNA section, covering partial 18S, full ITS1, 5.8S, and ITS2, and partial 28S regions, was amplified by a PCR (Hume et al. 2013). The PCR product was cloned

using StrataClone PCR cloning kit (Aligent Technologies). Plasmid DNA was purified using a QIAprep Spin miniprep kit (Qiagen). Sequencing was performed by Macrogen. S*ymbiodinium spp.* subclade C1 was identified by comparing the ITS2 region (220bp) with reference sequences by BLAST searches (www.ncbi.nlm.nih.gov/ blast).

2.3.3. Polyp wet weight and protein content

Five polyps were collected from colonies exposed to each of the experimental conditions. The polyp was cut off at the border between live tissue and exposed skeleton using a hacksaw. Polyps were allowed to drip-off for 2 min on absorbent tissue. Their weight was then determined and the individual polyps were transferred in 50 ml Falcon tubes with 10 ml MilliQ water. The polyps were homogenated using a pestle and vigorous shaking. The homogenate was adjusted to 20 ml with MilliQ water. The samples were subsequently centrifuged for ten minutes at 2500g, the supernatant was transferred to a clean tube and the volume of homogenate was determined. Aliquots (2 ml) were removed and centrifuged at 20000g. The supernatant was used to measure host protein content using the BCA protein assay following the protocols from the manufacturers (Pierce-Thermo Scientific, USA). The protein content of the individual polyps was calculated by multiplying the protein concentration of the subsamples with the total recovered volume of tissue homogenate.

2.3.4. Dial patterns of zooxanthellae mitotic rate

Tentacles from selected groups of colonies were sampled and pooled every hour within a 24-hour period for each nutrient treatment. To achieve replication, sampling was conducted for three 24-hour periods, with one day being omitted from sampling in between consecutive sampling days. Polyps were fed at ~12:00 on days prior to the start of a sampling period (16:00). However, they were not fed during the course of the 24-hour sampling period. Tentacles were stored at -20°C immediately after sampling. Tentacle samples were homogenised and the zooxanthellae were extracted and washed as mentioned above. Zooxanthellae samples were fixed in seawater with 5% formaldehyde at 4°C overnight. Subsequently, the zooxanthellae were bleached of their pigments by the slow addition of methanol:acetic acid (3:1) while mixing to give a 7:3 solution of methanol/acetic acid : sterile filtered sea water and stored overnight at -20°C. Samples were washed in sea water and stained by incubation with 2µg/ml DAPI (4′,6-Diamidino-2-phenylindole dihydro-chloride, Sigma-Aldrich) for 15 minutes in the dark. DAPI is a cell

permeable fluorescent probe which binds to the minor groove of DNA. Samples were washed once to remove excess DAPI. Finally, 3µl of stained cell suspension was placed on a microscope slide. 250 cells were counted at x1000 magnification using oil immersion (Immersol, Zeiss) on a fluorescence microscope with excitation and emission filters suitable for the visualisation of DAPI. The proportion of cells undergoing karyokinesis (Figure 3.1b: division of the nucleus) and cytokinesis (Figure 3.1c: division of the cytoplasm) were recorded. A mean division rate of a given time point which was above the total mean of the division rate (midpoint between maximum and minimum percentage recorded) was considered as a significant increase in mitotic activity and thus, as a peak in the division rate within the dial cycle. The mean total mitotic rate of one dial cycle was assessed by integration of the area under the curve.

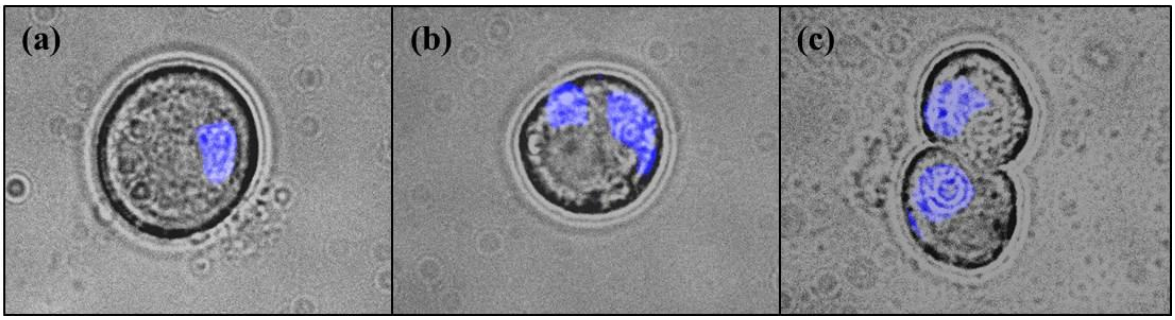

Figure 2.1| Stages of mitosis in zooxanthellae. DAPI-stained zooxanthellae were imaged using a fluorescence microscope. Images taken with light and with fluorescence filters were overlaid to depict the nucleus/nuclei within the cell. **(a)** A cell with a single nucleus. **(b)** A cell that has undergone karyokinesis. **(c)** Cells are undergoing cytokinesis.

2.3.5. Transmission electron microscopy

2.3.5.1. Sample preparation

The polyps of *E. paradivisia* showed a tendency to contract towards the end of the dark period and expanded again at the beginning of the light period. Since a full expansion of the polyps facilitates the harvest of samples with comparable size, tentacles were collected within the first hour of the light period. Per experimental condition, three tentacles were sampled, each of them being removed from a different colony. Tentacles were chosen which were well exposed to light and located around the centre of the polyp. Samples were fixed for 1h in 3% glutaraldehyde, 4% formaldehyde, and 14% sucrose in 0.1M PIPES buffer at pH 7.2. The central section of the fixed tentacles was cut out with a razor blade

and used for downstream analyses. Post fixation of specimens was performed with 1% osmium tetroxide followed by staining with 2% uranyl acetate, dehydration with a graded ethanol series, and embedding in Spurr's resin. Blocks were sectioned using an ultra microtome and the samples were mounted on 200Cu grids. For each tentacle, 3-5 thin sections (<100nm thick) were obtained, each from a different region of the tentacle specimen so as to avoid imaging the same algal cell twice. Grids were stained with lead citrate for 5 minutes. Further sections (~500nm) were prepared for light microscopy analyses.

2.3.5.2. Electron micrograph acquisition

Imaging was performed on a Hitatchi H7000 transmission electron microscope. A minimum of 30 zooxanthellae cell sections were imaged, using three or more cut sections per tentacle. The 3-4 cells with the largest visible diameter were selected for imaging per grid square to ensure that the imaged cell cross-section was as close as possible to the centre of the cell. A total of 100 micrographs of individual zooxanthellae (x6000 magnification) were analysed for each condition. Additionally, 9 micrographs per condition were taken at x1000 magnification.

2.3.5.3. Micrograph analysis

Each imaged cell was analysed using Fiji (Schindelin et al., 2012) to determine the area of the cell section and the area occupied by chloroplasts, lipid bodies, pyrenoid starch sheath, pyrenoid core, and the accumulation body. Additionally, the number of starch granules per cell as well as the number of breaks within each accumulation body was counted. The area occupied by lipid bodies was expressed as percentage of the total cell section area. The pyrenoid and the accumulation body were not visible in each micrograph, especially in LN samples due to the larger cell size. The number of analysed structure is indicated in the legend to Figure 3. The size of the pyrenoid starch sheath was only considered when the pyrenoid stalk was visible to reduce bias caused by the position of the section through the pyrenoid. Chloroplasts were analysed in 20 randomly chosen micrographs per treatment.

Zooxanthellae density was estimated by point counting in quadrants of known size, using micrographs at x1000 magnification as well as semi-thin sections viewed with a light microscope.

2.3.6. Statistical analysis

Data was tested for normality using the Shapiro-Wilk test and for equal variance using Levene's test. Data that was not normally distributed was log transformed prior to further testing. For the statistical analysis of zooxanthellae cell size, chloroplasts, pyrenoid starch sheath, pyrenoid core, lipid bodies, and accumulation body size, results from all micrographs were pooled as one population (Table A1.1). Thus, replication was achieved by the analysis of individual algal cells obtained from tentacles of different colonies and from within different regions of each tentacle, subject to comparable sampling schemes. For the analysis of the number of starch granules per algal cell and the number of breaks per accumulation body, means were taken from each of the three processed tentacles per treatment (Table A1.2). Statistically significant effects induced by the differences in the nutrient environment were determined by a two-way analysis of variance (ANOVA) with the two factors being: dissolved inorganic nutrient availability and heterotrophic feeding (Table A1.3). This was followed by a Tukey's Test for pairwise comparison (Table A1.4). For data that did not meet the assumptions required for a 2-way-ANOVA after transformation, the non-parametric Scheirer-Ray-Hare test was applied. $P < 0.05$ was considered to be significant in all instances.

2.4. Results

2.4.1. Effects of nutrient availability on the coral biomass

Exposure to experimental treatments was conducted for >1.5 years, ensuring that our results reflect the fully acclimated state of the coral-zooxanthellae symbiosis. Polyps of *Euphyllia paradivisa* corals hosting *Symbiodinium* Clade C1 kept at high levels of dissolved inorganic nutrients (HN) were visibly larger than those kept at low levels of dissolved inorganic nutrients (LN) (Figure 3.2). Heterotrophic feeding did not modify the appearance of corals in the HN treatment. At LN levels, however, feeding resulted in increased polyp biomass and protein content per polyp as compared to unfed specimens (Figure 3.3a).

Corals from the HN conditions were visibly darker as compared to the LN treatment (Figure 3.2) due to significantly higher zooxanthellae densities (Figure 3.3b). In contrast,

heterotrophic feeding had no significant effect on zooxanthellae density, independent from the availability of dissolved inorganic nutrients in the water.

Notably, while corals from the HN and LN treatments were offered the same amount of particulate food, the food uptake varied among the two conditions. Under LN availability, 100% of the polyps ingested the portion food offered to them whereas on average ~30-40% of the polyps of HN corals rejected the food (Figure 3.3c).

2.4.3. Effects of nutrient availability on the mitotic index of zooxanthellae

Both feeding and dissolved inorganic nutrient availability affected the dial cell cycle of the zooxanthellae. When considering cells undergoing either karyokinesis or cytokinesis in determining the total mitotic rate, a significant peak in the zooxanthellae division rate was observed just before the start of the light period (Figure 3.4a). This peak occurred irrespective of the nutrient environment, yet the highest division rate at this time point was measured for HN/fed samples. Additionally, LN/fed samples were measured to have a significant peak in division rate 9:00, 12:00, and most significantly, again at 17:00-18:00. LN/unfed samples were also observed to have a second peak in division rate 19:00. Yet, when integrating the area under the curve for one dial cycle, the total mitotic rate was relatively consistent, only being slightly higher in LN/fed samples (Figure A1.2).

It was expected that the proportion of cells undergoing cytokinesis could be overestimated as a result of cells sticking together, thus leading to an error in measure of the total proportion of cells undergoing division. Consequently, the results of cells undergoing karyokinesis only were also shown which represent a more reliable measure of the effects of the different nutrient environments on the dial cell cycle (Figure 3.4b). HN/fed samples were still only observed to have one significant peak in division rate, at the end of the dark period. Yet, the major peak for LN/fed samples appears to be shifted to 11:00. Unfed samples, irrespective of dissolved inorganic nutrient availability, displayed a peak in division both at 7:00 and 11:00. Furthermore, LN samples had a peak in division at 17:00-18:00. LN/unfed samples had an additional peak at 2:00, giving four major peaks in division during the dial cycle.

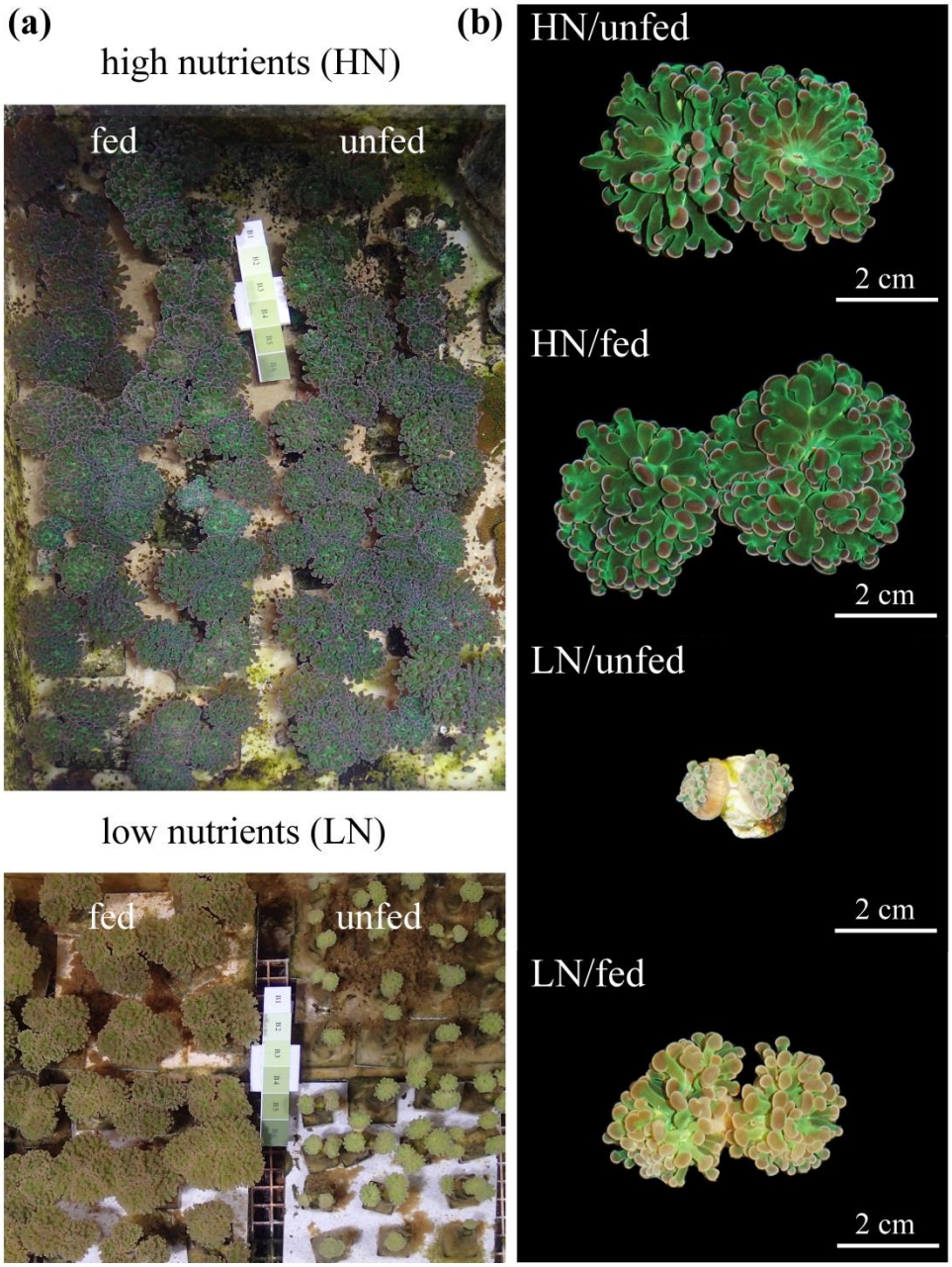

Figure 2.2| Effects of the dissolved inorganic nutrient availability and heterotrophic feeding on *E. paradivisa* polyp biomass. (a) Photographs of corals cultured under high or low availability of dissolved inorganic and particulate organic nutrients. **(b)** Close ups of individual polyps.

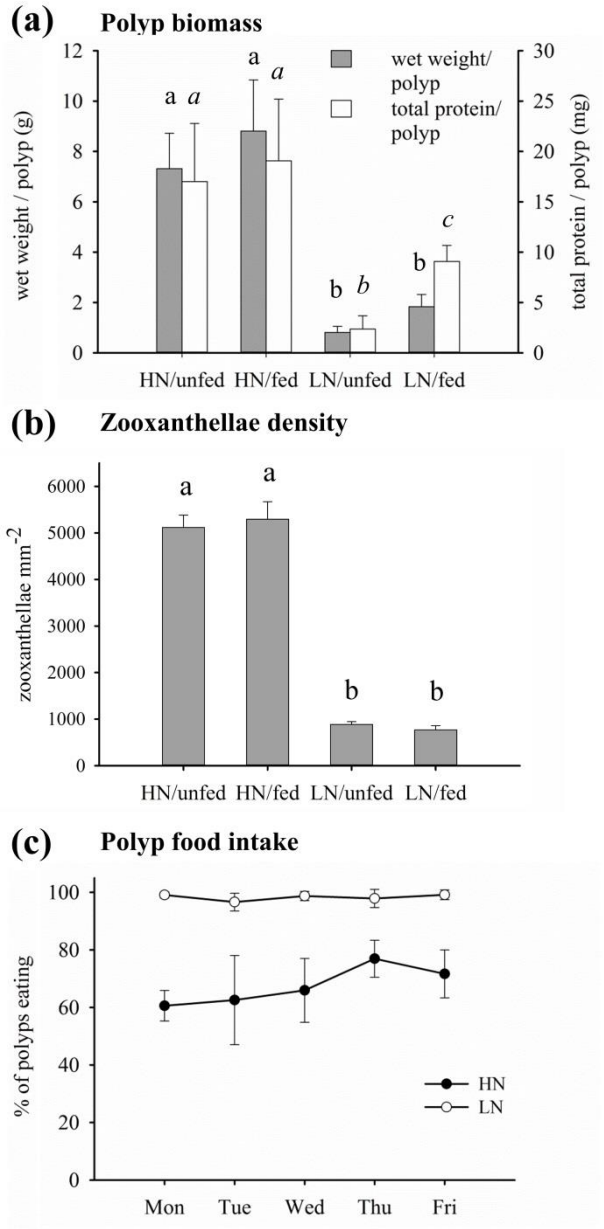

Figure 2.3| Effects of the dissolved inorganic nutrient availability and heterotrophic feeding on zooxanthellae density, and feeding behaviour. **(a)** Wet weight and total protein content of whole polyps (HN/unfed n = 5, HN/fed n = 4, LN/unfed n = 4, LN/fed n = 5). **(b)** Zooxanthellae cell density per mm^2 of ~250nm thick tentacle sections (n = 4). **(c)** Daily food intake of polyps measured as per cent of polyps feeding (n = 4). Data are presented as mean and standard deviation. Different letters indicate statistically significant differences among treatments.

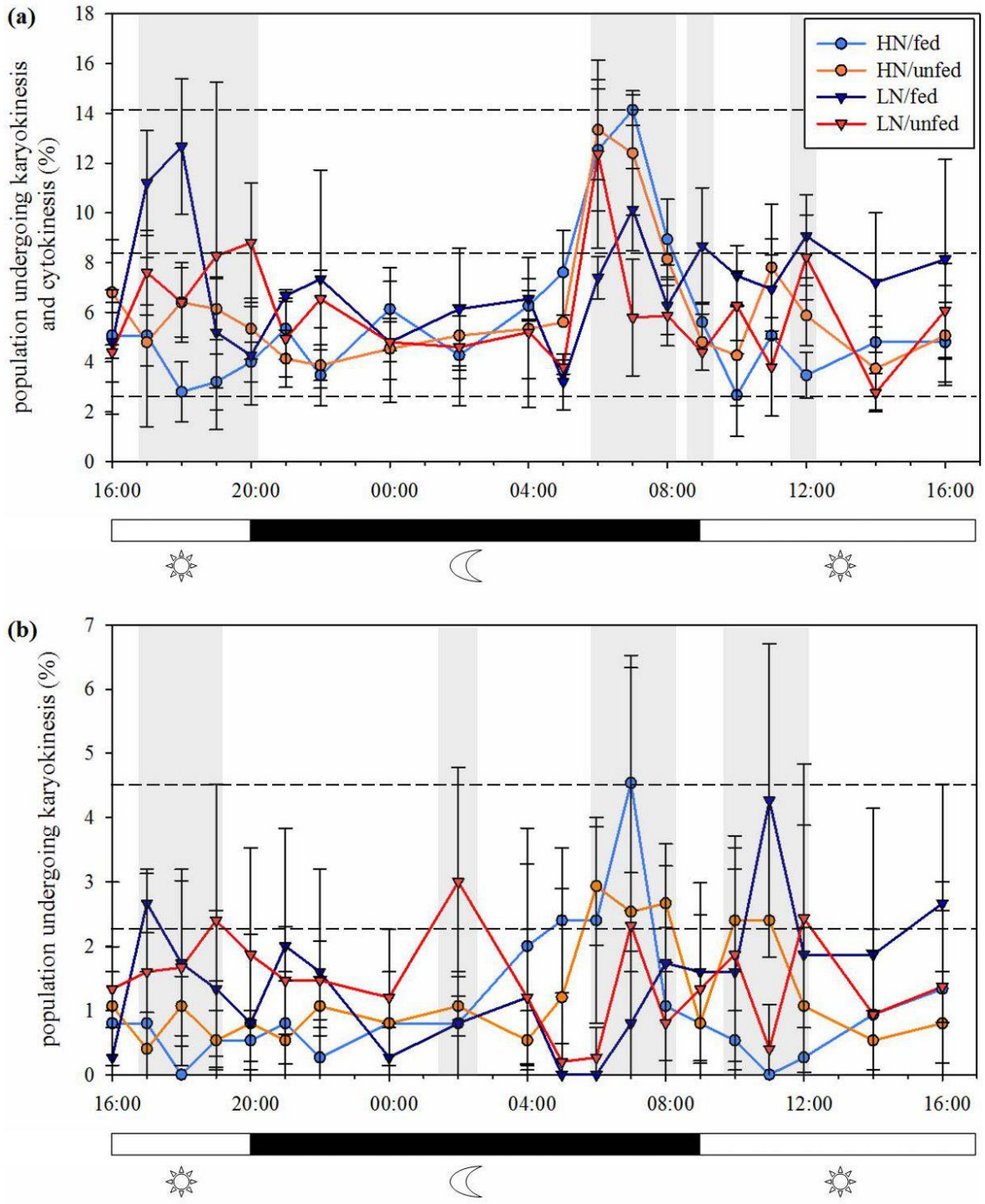

Figure 2.4| Effects of the nutrient environment on the dial pattern of zooxanthellae mitotic index. (a) Percentage of zooxanthellae population undergoing either karyokinesis or cytokinesis. **(b)** Percentage of zooxanthellae population undergoing karyokinesis only. Time points at which the division rate of zooxanthellae of any nutrient treatment reached above 50% of the measured range are marked by grey bars. HN/fed (pale blue), HN/unfed (orange), LN/fed (dark blue), LN/unfed (red).

2.4.2. Effects of nutrient availability on the ultrastructure of zooxanthellae

The zooxanthellae ultrastructure was analysed using TEM (Figures 3.5 & 3.6). Compared to zooxanthellae from HN corals, the size of algal cells was significantly larger in the LN treatment, with feeding resulting in a further increase under this condition (Figure 3.5 & 3.6a). Neither the availability of dissolved inorganic nutrients nor host feeding affected the abundance of chloroplasts within the zooxanthellae or the extension of the starch sheath surrounding the pyrenoid (Figures 3.6b-c and A1.1). The pyrenoid core, in contrast, was significantly larger in algal cells of the LN/fed treatment as compared to the other treatments (Figure 3.6d).

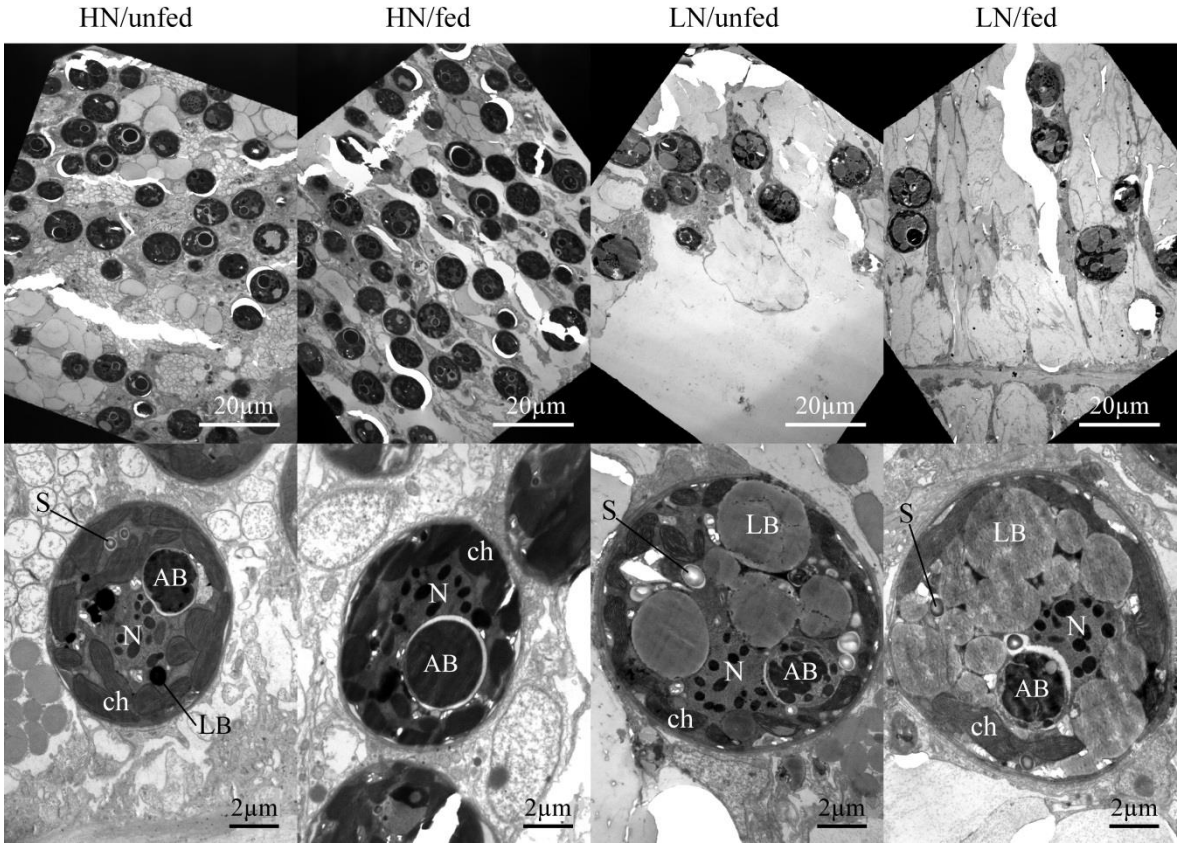

Figure 2.5| Effects of the dissolved inorganic nutrient concentration and heterotrophic feeding on zooxanthellae population density and ultrastructure *in hospite*. Representative micrographs of tentacle sections showing the zooxanthellae population within the host endoderm (magnification x1000, top panels) and zooxanthellae cell sections representing the mean ultrastructure resulting from each nutrient treatment (magnification x6000, lower panels). AB: accumulation body, ch: chloroplast, LB: lipid body, N: nucleus with condensed chromosomes, P: pyrenoid, S: starch granule.

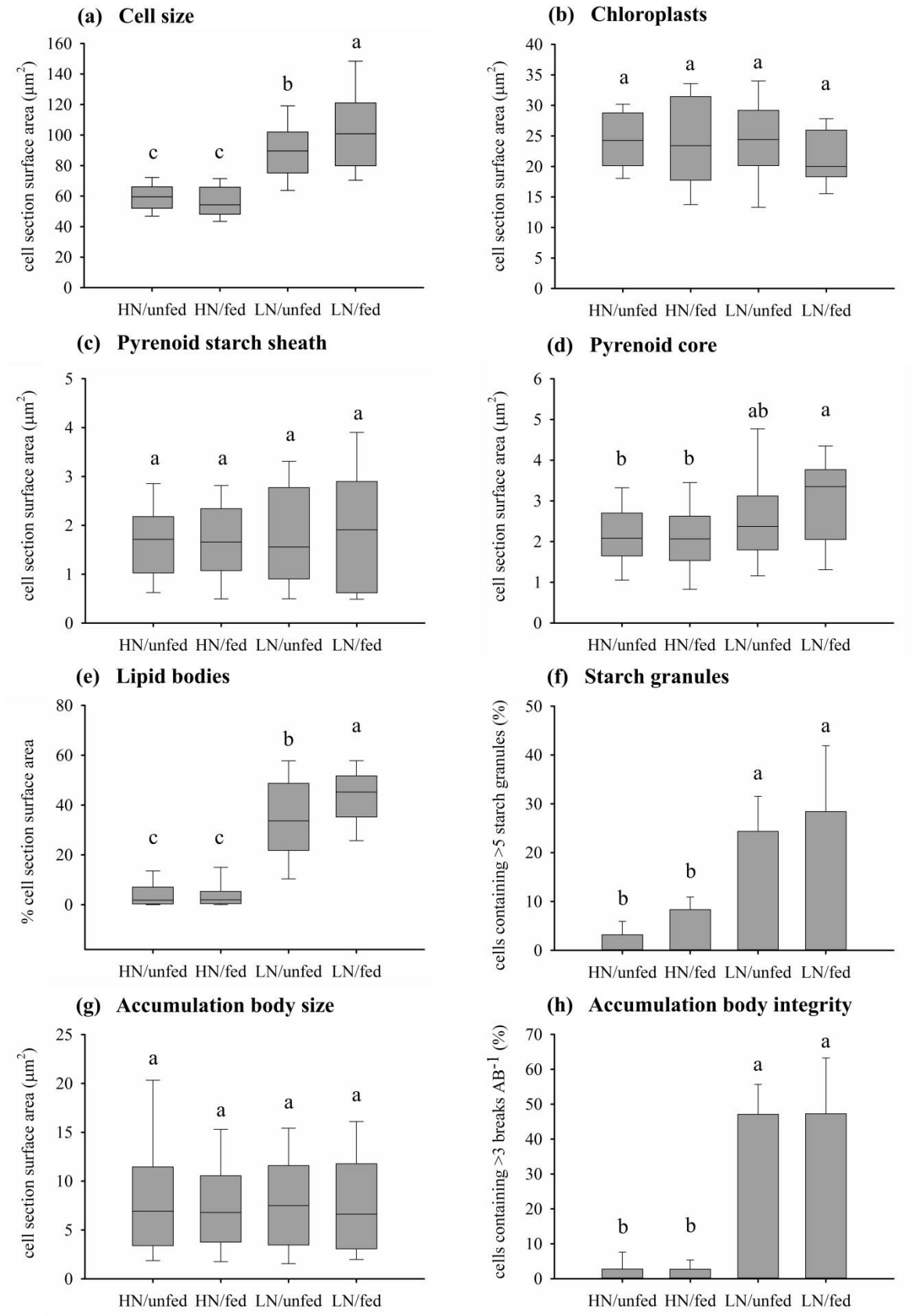

Figure 2.6| Effects of the dissolved inorganic nutrient concentration and heterotrophic feeding on zooxanthellae. **(a)** Cell size measured as zooxanthellae section surface area (µm^2) (n =

100). **(b)** Chloroplast abundance measured as section surface area (μm^2) (n = 20). **(c)** Accumulation of starch around the pyrenoid measured as section surface area (μm^2) (HN/unfed n = 38, HN/fed n = 32, LN/unfed n = 22, LN/fed n = 18). **(d)** Size of pyrenoid core measured as cell section surface area (μm^2) (n = same as (C). **(e)** Accumulation of lipid bodies measured as per cent of cell section surface area (n = 100). **(f)** Abundance of starch granules represented as per cent of cells containing greater than one starch granule (n = 3). **(g)** Size of accumulation body measured as section surface area (μm^2) (HN/unfed n = 75, HN/fed n = 81, LN/unfed n = 39, LN/fed n = 46). **(h)** Accumulation body integrity measured as the per cent of accumulation bodies containing greater than one break (n = 3). Box plots: the vertical line within each box represents the median. The box extends from the first to the third quartile and whiskers extend to the smallest and largest non-outliers. Outliers are not shown. Bar charts represent mean and SD. Statistically significant differences of pairwise comparison (Tukey's post hoc) are indicated by the use of different letters.

Lipid body accumulation increased significantly in zooxanthellae kept under LN conditions and was further enhanced when the LN corals were fed (Figures 3.6e & A1.1). Also, starch granules were more abundant in zooxanthellae from LN corals compared to HN samples (Figure 3.6f). A statistically insignificant increase in starch granule accumulation was detected in response to host feeding irrespective of availability of dissolved inorganic nutrients.

The size of the accumulation body did not respond to the difference in nutrient availability (Figure 3.6g) but it showed a striking fragmentation in a significantly higher amount to algal cells from LN corals (Figures 3.6h & A1.1). This fragmentation response was unaffected by the feeding regime of the corals.

2.5. Discussion

We have conducted the first long-term study of the combined effects of different dissolved inorganic nutrient concentrations and particulate food availability on the reef coral holobiont in order to establish biomarkers of the respective conditions.

2.5.1. Effects of nutrient availability on the coral biomass

We found that polyp biomass and the protein content per polyp were higher in HN corals compared to corals exposed to low dissolved inorganic nutrient levels (Figures 3.2 and

3.3a). Zooxanthellae densities were also increased by the HN treatment but they were not affected by heterotrophic feeding (Figure 3.3b). This access to nutrients in the particulate form only increased the polyp protein content under LN conditions and to a much lesser extent as the supply to HN levels. Hence, our results indicate that the availability of high amounts of dissolved inorganic nutrients, accessible to the coral holobiont mostly via the symbionts (D'Elia and Webb, 1977; Crossland and Barnes, 1977; Yellowlees et al., 2008; Godinot et al., 2009), provide substantial benefits to the coral host. This is further supported by the reduced food ingestion rates of HN polyps (Figure 3.3c), since lower prey capture rates can indicate satiety of corals (Ferrier-Pagès et al., 2003).

Our results suggest that nitrogen and phosphorus acquired through dissolved inorganic nutrient assimilation become available to the coral host in significant amounts and are used to promote growth. Clearly, under the present experimental conditions, the supply of dissolved inorganic nutrients appears to be more important for the gain of biomass of the coral holobiont than the supply with particulate food, suggesting a substantial translocation of nitrogen-containing compounds from the symbiont to the host (Wang and Douglas, 1999; Tanaka et al., 2006; Pernice et al., 2012; Béraud et al., 2013; Kopp et al., 2013). However, it remains uncertain how the dissolved inorganic nutrients were partitioned and allocated within the HN-exposed holobiont. A transfer to the host might occur by means of (A) translocation of nitrogen- and phosphorus-rich molecules to the host (Pernice et al., 2012), or (B) digestion of the zooxanthellae (Titlyanov et al., 2006).

Considering the response of the zooxanthellae density to nutrient availability, similar observations have been reported for *Stylophora pistillata*, in which daily host feeding with *Artemia salina* nauplii in natural, oligotrophic sea water resulted in a smaller increase in zooxanthellae densities compared to dissolved inorganic enrichment ($20\mu M\ NH_4^+ + 2\mu M\ PO_4^{3-}$) (Muscatine et al., 1989b; Dubinsky et al., 1990).

2.5.2. Effects of nutrient availability on the dial cycle of zooxanthellae cell division

We observed that both dissolved inorganic nutrient and particulate food availability influenced the mitotic index (proportion of population undergoing cell division) of zooxanthellae during the dial cycle. Cellular division rates are known to be significantly reduced as a result of the symbiotic state, most likely due to a restriction in nutrient access imposed by the host in order to maintain a favourable ratio of algal to host cells (Smith and Muscatine, 1999). Typically, a dial rhythmicity in cell division is observed with one peak

in the mitotic index occurring at the end of the dark period, with a maximum of approximately 8-15% of the population undergoing cytokinesis at this time (Fitt and Cook, 2001; Wang et al., 2008; Cook et al., 1988).

In agreement with past observations, a peak in the mitotic index was observed to occur at the end of the dark period in all samples (Figure 3.4). For HN/fed samples this was the only peak in the division rate during the dial cycle. Yet, particularly the absence of dissolved inorganic nutrients resulted in multiple peaks in zooxanthellae division rate. Notably, the total mitotic index measured over the course of one dial cycle was relatively consistent, only being higher in LN/fed samples (Figure A1.2). This indicates that the proportion of the population undergoing division is relatively steady despite large differences in population density, thus displaying a constant turnover rate of the zooxanthellae population *in hospite*. Contrary to these observations, past studies have observed the mitotic index to decrease in response to nutrient deprivation, and zooxanthellae division to be particularly dependent on heterotrophic nutrient input in model sea anemones (Cook et al., 1988; Fitt and Cook, 2001; Smith and Muscatine, 1999; Hoegh-Guldberg, 1994). In the current study, heterotrophic nutrients only stimulated an increase in total division rate when combined with diminished dissolved inorganic nutrient availability. The disparity to past observations is likely the result of differences in nutrient exposure time since the current study analysed a steady-state of the symbiosis rather than the response to an immediate change in nutrient availability, thus highlighting the value of long-term experiments.

The rhythmicity of zooxanthellae division was more notably affected by dissolved inorganic nutrient limitation than by the absence of heterotrophic feeding. It is hypothesised that, within the LN treatment, peaks in zooxanthellae division rate were generated by spikes in nutrient availability within the symbiosis. Thus, particulate food input resulted in a significant peak in cell division approximately 5-6 hours following prey ingestion, suggesting that nutrient release following digestion could induce a progression of the cell cycle into mitosis in a proportion of the algal population. However no response to heterotrophic nutrient input was observed when feeding was coupled to high dissolved inorganic nutrient availability. Finally it is suggested that the host may assimilate the zooxanthellae directly as a mechanism of obtaining nitrogen and phosphorus during nutrient limited conditions (Titlyanov et al., 2006), consequently resulting in rhythmical releases of ammonia following catabolism of the symbionts by the host, thus leading to

multiple peaks in algal division rates as a result of the LN/unfed condition. Further investigation is required to confirm if such proposed fluxes of nutrients occur within the symbiosis. Yet, it is apparent that a diminished supply of dissolved inorganic nutrients greatly changes the dynamics of the zooxanthellae population *in hospite* and ultimately, the functioning of the symbiosis.

2.5.2. Effects of nutrient availability on the ultrastructure of zooxanthellae

Our TEM analysis of the zooxanthellae ultrastructure revealed that symbionts from LN corals were characterised by increased cell sizes and large accumulations of energy storage bodies (lipid bodies and starch granules) (Figures 3.5 and 3.6a,e,f). Comparable changes in cellular characteristics were described for free-living microalgae (Hu et al. 2008 and references therein; Msanne et al. 2012) and zooxanthellae under nutrient limitation (Hoegh-Guldberg, 1996; Muller-Parker et al., 1996; Weng et al., 2014). Specifically, increased cell volumes have been observed for nitrogen-deprived zooxanthellae in culture (Jiang et al., 2014) and in the free-living dinoflagellate *Heterocapsa sp.* (Latasa and Berdalet, 1994). The increase in cell size under nutrient limitation may be associated with a longer growth phases, thus leading to a slower progression through the cell cycle (Vaulot et al., 1987; Smith and Muscatine, 1999).

The accumulation of neutral lipids and starch granules in zooxanthellae from LN corals is also in line with previous observations (Berner and Izhaki, 1994; Hoegh-Guldberg, 1996; Muller-Parker et al., 1996). Such an increase in carbon-rich storage products could result from the uncoupling of carbon fixation from cellular growth (i.e. high photosynthetic production) in combination with a reduced energy demand of the nutrient limited cells (Hu et al., 2008; Vítová et al., 2015).

The accumulation body, a cellular compartment thought to accumulate cellular waste products (Taylor, 1968) showed a characteristically fragmented appearance in a significantly increased amount of zooxanthellae from LN corals as compared to those from HN exposure, which qualifies as a novel indicator of nutrient limitation in zooxanthellae (Figures 235 and 3.6h).

None of the ultrastructural changes indicative for zooxanthellae from LN corals (increases in cell size, in numbers/extent of lipid and starch bodies, and in the frequency of accumulation body fragmentation) were reduced by heterotrophic feeding, hence nutrients

acquired through feeding were not sufficient at alleviating the nutrient stress imposed by the LN treatment. On the contrary, there was a slight trend for these markers to be further increased in zooxanthellae from fed LN corals, suggesting that feeding may even aggravate the algal nutrient limitation under the present experimental conditions, an observation that calls for further study.

The amount of food offered to the corals was within the range discussed to be available to corals in various reef settings (Johannes et al., 1970; Heidelberg et al., 2004; Yahel et al., 2005). However, the 100% uptake rate of LN corals suggests that they were not fed to satiation (Figure 3.3c). Therefore, more pronounced responses might result from an increased food supply even if such high prey availability appears unrealistic under natural conditions. On the other hand, the nutritious value of the offered food might have been inadequate, an aspect that should be analysed in depth by future studies on heterotrophic feeding.

While corals show some plasticity in acquiring nutrients from different sources (Anthony & Fabricius, 2000; Borell & Bischof, 2008; Connolly et al., 2012; Ferrier-Pagès et al., 2010; Grottoli et al., 2006), our results assign a crucial importance to the uptake of dissolved inorganic nutrients for the performance of both the host and zooxanthellae. This strong dependence can help to explain positive effects of dissolved inorganic nutrient availability on corals (Bongiorni et al., 2003) as well as negative responses to nutrient starvation as observed under skewed N:P ratios (Wiedenmann et al., 2013; D'Angelo and Wiedenmann, 2014).

The findings of our study indicate that despite their symbiotic life style, zooxanthellae show responses to nutrient limitation in the water column comparable to free-living algae (Hu et al., 2008; Msanne et al., 2012). Thereby, our results highlight the limited capacity of the coral host to fully isolate the symbionts from the influence of the chemistry of the surrounding seawater.

The analysis of the ultrastructural biomarkers confirmed our observations at the macroscopic level that the corals were more affected by the supply of dissolved inorganic nutrients than by the uptake of particulate food. This supports the notion that the nutrient status of the symbionts *in hospite* is strongly dependent on the uptake of dissolved inorganic nutrients (Dubinsky and Jokiel, 1994)

These conclusions, however, cannot be taken as support for the assumption that (anthropogenic) nutrient enrichment will generally benefit coral reefs (D'Angelo and Wiedenmann, 2014) but call for further analyses of the effects that the global/climate change-mediated alteration of the nutrient environment will have on coral reefs (D'Angelo and Wiedenmann, 2014; Riegl et al., 2015). Due to the fast uptake and turnover of dissolved inorganic nutrients coral reef waters, it is difficult to establish the prevailing nutrient conditions for reef monitoring purposes solely by analysing the water chemistry (Furnas et al., 2005) in addition, high-content biomarkers are required to inform coral reef management about disturbances of the natural nutrient environment (Wiedenmann & D'Angelo 2014). The novel biomarkers indicative of the nutrient status of zooxanthellae established in the present study have a high potential for environmental monitoring applications since they enable to discriminate responses to different nutrient sources at the cellular and subcellular level and reflect the nutrient exposure history.

Chapter 3: The coral-zooxanthellae symbiosis is significantly more dependent on an external supply of phosphorus than nitrogen

Sabrina Rosset, Adam J. Reed, Cecilia D'Angelo, Jörg Wiedenmann

Author contribution:

Cecilia D'Angelo and Jörg Wiedenmann established the +N+P, -N-P and +N-P nutrient systems and cultured *E. paradivisa* under these respective nutrient conditions. Adam Reed established the -N+P nutrient system. All authors contributed to the experimental design. Sabrina Rosset conducted the TEM analysis of all samples. All authors contributed towards the interpretation of the results. Sabrina Rosset wrote the chapter. Cecilia D'Angelo provided comments on the chapter.

3.1. Abstract

Increasing enrichment of coastal waters with dissolved inorganic nutrients occurs as a result of a range of anthropogenic activities and constitutes a significant local pressure to coral reefs. Notably, this can disrupt nitrogen to phosphorus ratios favourable to reef ecosystems, thereby precipitating deprivation of the limiting nutrient. The repercussions of a nutrient imbalance to reef corals remains poorly understood. Long term cultivation of *Euphyllia paradivisa* harbouring clade C1 *Symbiodinium* in the presence of replete (+N+P), limiting (-N-P), or imbalanced (+N-P, -N+P) availability of nitrate and phosphate ensured the development of phenotypes representative of the respective nutrient environments. Effects on zooxanthellae morphology were analysed by transmission electron microscopy. Deprivation of phosphorus alone resulted in a similar response to the limitation of both nitrogen and phosphorus: severe reduction of coral and algal biomass as well as a mean zooxanthellae cellular morphology marked by large cell size and storage

body accumulation. However, limitation of only nitrogen did not compromise polyp biomass or algal population size, likely due to the capacity of recycling nitrogen within the coral holobiont. This demonstrates a greater dependence of zooxanthellate corals towards the supply of phosphorus over nitrogen. Yet, energy storage body accumulation was significantly increased due to phosphate enrichment signifying nutrient stress. Taken together, morphological biomarkers were able to discriminate between different forms of nutrient stress, providing a promising tool for the management of nutrient pollution.

3.2. Introduction

Coral reefs are globally threatened by climate change and a range of anthropogenic pressures which often act synergistically, leading to increasing incidences of coral disease and bleaching events (Goreau and Hayes, 1994; Sheppard, 2003; Hoegh-Guldberg et al., 2007; Hughes et al., 2007; Baker et al., 2008; van Hooidonk et al., 2013; D'Angelo and Wiedenmann, 2014; Logan et al., 2014). Ascending rates of coral reef degradation endanger the associated valuable ecosystem services (Moberg and Folke, 1999). It is increasingly clear that the nutrient environment plays a large role in determining coral reef resilience (Szmant, 2002; Fabricius, 2005; D'Angelo and Wiedenmann, 2014). Anthropogenic nutrification of coastal waters poses a significant local stressor contributing to coral reef decline, thus requiring the implementation of efficient management strategies (Brodie et al., 2010; Kroon et al., 2014; Aswani et al., 2015). However, the repercussions of different nutrient environments to the functioning of the coral-zooxanthellae symbiosis are still not fully elucidated.

Reef corals often thrive in oligotrophic environments, in which essential nutrients required for growth are very limited. An important source of nutrients to reef corals is the assimilation of dissolved inorganic nutrients (NH_4^+, NO_3^-, PO_4^{3-}) from the water column (Muscatine and D'Elia, 1978). While the coral host is capable of ammonium uptake (Grover et al., 2002; Pernice et al., 2012), the assimilation of nitrate and phosphate is attributed to endosymbiotic algae called zooxanthellae (D'Elia and Webb, 1977; Crossland and Barnes, 1977; Grover et al., 2003; Godinot et al., 2009; Pernice et al., 2012). Additionally, the zooxanthellae recycle ammonium excreted as a metabolic waste product by the host, thereby efficiently retaining nitrogen within the holobiont (Muscatine and

D'Elia, 1978; Rahav et al., 1989; Wang and Douglas, 1998). However, internal recycling of phosphorus has not been reported.

The sensitivity of zooxanthellae proliferation *in hospite* in response to increased availability of dissolved inorganic nitrogen, lead to the proposition that the symbionts generally experience nutrient limitation *in hospite* (Muscatine et al., 1989a). This nutrient limitation underpins the functioning of the symbiosis as it results in a chemical imbalance of nitrogen and phosphorus relative to carbon, thereby decoupling photosynthetic carbon fixation from cellular growth (Dubinsky and Jokiel, 1994). This results in the translocation of a large proportion of photosynthates to the coral host where it fuels respiration and mucous production (Muscatine, 1965; Falkowski et al., 1984; Crossland, 1987; Bachar et al., 2007).

Anthropogenic nutrient loading of oceans, especially of coastal waters, caused by atmospheric deposition through the combustion of fossil fuels, use of agricultural fertilizers, erosion, and riverine and sewage discharge, is continuously rising (Fabricius, 2005; Brodie et al., 2012; D'Angelo and Wiedenmann, 2014). Nutrification can have profound indirect effects on coral reefs, detrimental to ecosystem structure and function, including: 1) increased phytoplankton blooms and phase-shifts to macro-algae which outcompete corals for light, oxygen and nutrients (Szmant, 2002; D'Angelo and Wiedenmann, 2014), 2) outbreaks of predators such as crown-of-thorns starfish (Brodie et al., 2005), and 3) increased incidence of coral disease (Vega Thurber et al., 2014). Furthermore, nutrient pollution affects coral physiology directly. Enrichment of dissolved inorganic nutrients is proposed to alleviate zooxanthellae nutrient limitation, thereby promoting cellular growth and proliferation which has negative repercussions on photosynthate translocation to the host, consequently leading to decreases in coral growth, calcification and reproductive rates (Stambler et al., 1991; Marubini and Davies, 1996; Ferrier-Pagès et al., 2000). On the other hand, ample dissolved inorganic nutrient availability has been shown to be fundamental to the nutritional status of both the coral host and the zooxanthellae (chapter 3, Rosset et al., 2015). Direct physiological effects are dependent on the type of nutrient, nutrient concentrations, study species, and the environmental context, resulting in conflicting perceptions (Shantz and Burkepile, 2014; Gil, 2013). Nutrient enrichment has also been shown to act synergistically with high temperature and irradiance stress, thereby increasing the susceptibility of corals to coral

bleaching which is often fatal (Nordemar et al., 2003; Wooldridge, 2009; Wagner et al., 2010; Cunning and Baker, 2013; Fabricius et al., 2013; Wiedenmann et al., 2013).

The ratio at which dissolved inorganic nitrogen to phosphorus occurs within the ocean can be seen as a tipping point between nitrogen or phosphorus limitation of marine photosynthesis along with assimilated carbon. On coral reefs this ratio is found to be in an approximate range of 4.3:1 (Crossland et al., 1984), 6.4:1 (Furnas et al., 1995), to 7.2:1 (Smith et al., 1981), which is lower than the cellular composition of phytoplankton (16:1 (Redfield, 1958)), implying that coral reefs are generally more nitrogen limited. Different sources of nutrient pollution vary in the types and concentrations of nitrogen and phosphorus that are released, with the potential of disrupting the nitrogen to phosphorus ratio favourable to coral reef waters (Conley et al., 2009; Voss et al., 2013). Disproportionally high nitrate availability has previously been shown to result in phosphorus limitation of proliferating algal symbionts and was related to a decreased coral bleaching threshold (Wiedenmann et al., 2013). Although geographical differences are apparent, anthropogenic emission of nitrogen is generally not paralleled by that of phosphorus, fluxes of which are less perturbed by human activity (Peñuelas et al., 2013). One example for the occurrence of a nutrient imbalance is Discovery Bay in Jamaica, where enrichment with groundwater borne nitrate has been measured to result in a dissolved inorganic nitrogen to phosphorus ratio of 72:1 (Lapointe, 1997). Similarly, a reef at Guarajuba beach in Brazil was subjected to nutrification by contaminated groundwater which resulted from a high rate of coastal urbanisation, leading to a dissolved inorganic nitrogen to phosphorus ratio of ~47:1 (Costa et al., 2000). Both reefs endured consequential eutrophication.

In order to support science driven management of nutrient pollution, it is critical to gain a greater understanding of the repercussions of an imbalanced nutrient environment to the functioning of the coral-algal symbiosis. Previous studies on the direct effects of dissolved inorganic nutrient availability on reef corals generally do not consider disruptions in nitrogen to phosphorus ratios induced by enrichment treatments (Fabricius, 2005). Furthermore, short treatment exposure times often do not allow for the development of nutrient limitation resulting from an imbalanced nutrient environment. In the present study *Euphyllia paradivisa* harbouring C1 *Symbiodinium* (Rosset et al. 2015) was cultured with different availabilities of dissolved inorganic nutrients for over 6 months, ensuring the development of representative phenotypes in response to replete and limiting availability

of both nitrogen and phosphorous, as well as to an imbalanced nutrient environment (enrichment of either nitrate or phosphate only). Transmission electron microscopy (TEM) was used to study changes in zooxanthellae morphology, thereby identifying cellular biomarkers of nutrient stress which could provide valuable tools for reef monitoring purposes.

3.3. Methods

3.3.1. Coral culture

Within an experimental mesocosm (D'Angelo and Wiedenmann, 2012) four distinct nutrient conditions were established in individual tank units by manipulation of dissolved inorganic nitrogen and phosphate concentrations: 1) nutrient replete (+N+P: N = 10.97µM, P = 1.81µM, N:P = 6.1 : 1), 2) nutrient limited (-N-P: N = 0.16µM, P = 0.32µM, N:P = 0.5 : 1), 3) nutrient imbalance by nitrate enrichment (+N-P: N = 64.52µM, P = 0.53µM, N:P = 121.3 : 1), and 4) nutrient imbalance by phosphate enrichment (-N+P: N = 0.06 µM, P = 3.57 µM, N:P = 1 : 59.5). High levels of dissolved inorganic nitrogen and phosphate were maintained by continuous low level dosing of sodium nitrate and/or disodium hydrogen phosphate solutions respectively. Daily low level dosing of ethanol suppressed dissolved inorganic nitrogen concentrations. Low phosphate levels were maintained through the addition of Rowaphos phosphate removal matrix (Rowa). Because levels of ammonia (NH_4^+) were found to be insignificant in comparison to nitrate (NO_3^-) and nitrite (NO_2^-), dissolved inorganic nitrogen in the mesocosm was considered to be represented by nitrate and nitrite only (Wiedenmann et al., 2013). The N:P ratios given must be considered as an approximation due to large fluctuations of this value when measuring extremely low nutrient concentrations. Nevertheless, the +N+P treatment represents an N:P ratio which is in the range commonly measured on coral reefs (Szmant, 2002). In the -N-P treatment both dissolved inorganic nitrogen and phosphate availability is very limited, making the ratio less significant. Within the remaining two treatments, +N-P and -N+P, the N:P ratio is imbalanced, precipitating conditions of either phosphorus or nitrogen limitation respectively as a result of an enrichment with either nitrate or phosphate. The phosphorus limitation of zooxanthellae *in hospite* resulting from a disproportionally high concentration of dissolved inorganic nitrogen relative to phosphate has previously been

established (Wiedenmann et al., 2013). Colonies of *Euphyllia paradivisa* (D'Angelo and Wiedenmann, 2012) were cultured in each nutrient treatment at a constant temperature of 25°C and a photonflux of ~150 µmol m^{-2} s^{-1} with a 10/14 hour light/dark cycle. The corals were cultured within the +N+P, -N-P, and the +N-P treatments for >1.5 years. Colonies were moved from the -N-P system into the -N+P system 6 months prior to sampling. Corals cultured within the +N-P treatment were maintained at lower light intensity (~30 µmol m^{-2} s^{-1}) due to mortality following very long exposure to this nutrient availability at higher light irradiation. +N-P samples were exposed to ~150 µmol m^{-2} s^{-1} for 3 months prior to sampling.

3.3.2. Polyp size

Polyp size was determined by measuring the mean length of polyp tissue cover down the side of the skeleton for each individual polyp using callipers.

3.3.3. Transmission electron microscopy

3.3.3.1. Sample preparation and imaging

For each experimental treatment, three tentacles of *E. paradivisa* were sampled, each taken from a distinct colony at the beginning of the light period when the polyps were well expanded. Sampled tentacles were located towards the centre of each polyp to ensure that they were well exposed to light. Specimens were fixed and imaged as described in chapter 3. Briefly, tentacles were fixed (3% glutaraldehyde, 4% formaldehyde, 0.1 M PIPES buffer containing 14% sucrose at pH 7.2) and then cut to obtain only the central section of each tentacle, post-fixed using 1% osmium tetroxide, stained with 2% uranyl acetate and dehydrated with a graded ethanol series before being embedded in Spurr's resin. Semi-thin tentacle sections (~250 nm) were cut and stained with a solution of 1% toluidine blue and 1% borax for light microscope observations. For each specimen 3-5 thin sections (<100 nm thick) were obtained that were > 20µm apart from each other, so as to eliminate the chance of imaging the same algal cell twice. Thus, for each experimental treatment a minimum of nine sections were obtained, originating from three tentacles. Sections were stained with lead citrate and imaged on a Hitatchi H7000 transmission electron microscope. For each grid square (Cu200), only the 3-4 largest zooxanthellae were imaged in order to maximise the chance that the imaged cell section was as close as possible to the central diameter of the cell, thereby reducing bias on cell size. For each tentacle, a minimum of 30

zooxanthellae cells were imaged, using 3 or more cut sections. A total of 100 micrographs of individual zooxanthellae (x6000 magnification) were acquired for each treatment.

3.3.3.2. Micrograph analysis

All micrographs were analysed using Fiji (Schindelin et al., 2012). Cell size of individual zooxanthellae was measured as the cell section surface area. Furthermore, the sectional area of lipid bodies, starch granules and uric acid crystals was determined within each cell, and presented as a percentage of the cell section surface area. Lipid body accumulation was additionally assessed through a biochemical assay using the lipophilic dye Nile Red (method A2.1). Accumulation body integrity was measured by the degree of its fragmentation by counting the number of breaks within the periphery of each body. The accumulation body was not always visible within the analysed zooxanthellae sections; especially in nutrient limited samples, either due to the enlarged cell size reducing the chance of the accumulation body being visible at the chosen section through the cell, or due to the absence of an accumulation body in a proportion of zooxanthellae exposed to this treatment (+N+P n = 81, -N-P n = 39, +N-P n = 87, -N+P n = 84). Zooxanthellae density was estimated by measuring the size of the endoderm and counting the contained zooxanthellae, using semi-thin sections viewed on a light microscope at x40 magnification.

3.3.4. Statistical analysis

For the results on zooxanthellae morphological parameters, statistical replication was achieved by the analysis of 100 distinct algal cells, originating from three tentacles and from different areas within each tentacle (n = 100) (Table A2.1). For zooxanthellae density a mean value was obtained for each processed tentacle (n = 3) (Table A2.2). Data was tested for normality using the Shapiro-Wilk test and log transformed if found to be non-normally distributed. Statistically significant effects resulting from the difference in dissolved inorganic nutrient availability were determined by one-way analysis of variance (ANOVA) (Table A2.3), followed by Tukey's post hoc test for pairwise comparison (Table A2.4). Certain parameters were not normally distributed even after transformation, and significant differences within these parameters were therefore determined by the non-parametric Kruskal-Wallis one way ANOVA on ranks. $P < 0.05$ was considered to be significant in all instances.

3.4. Results

In comparison to polyps cultured under nutrient replete (+N+P) conditions, polyp size was greatly reduced as a result of the nutrient limited (-N-P) and the high nitrate imbalanced (+N-P) nutrient treatments (Figures 4.1 and 4.2a). Among these conditions, the polyp size was lower in the -N-P treatment as compared to the +N-P treatment (Figures 4.1 & 4.2a). However, nutrient imbalance induced by phosphate enrichment (-N+P) resulted in an increase in the length of skeletal tissue cover compared to +N+P specimens. Although, visually the polyps cultivated within the +N+P treatment appeared to be fatter and more expanded compared to those exposed to the -N+P treatment (Figure 4.1).

The -N-P as well as the +N-P nutrient conditions resulted in the coral host harbouring greatly reduced zooxanthellae population densities compared to +N+P samples (Figures 4.1 and 4.2b). This was reflected in the difference in polyp colour, with +N+P polyps being visibly darker than polyps cultured within the -N-P and +N-P treatments (Figure 4.1). However, the zooxanthellae density of specimens within the -N+P treatment was comparable to that of the +N+P treatment, despite the diminished supply of dissolved inorganic nitrogen.

Compared to zooxanthellae harboured by polyps within the +N+P treatment, the zooxanthellae cell size was significantly larger within corals of the +N-P treatment (Figure 4.3a). Reduced availability of both nitrate and phosphate in the -N-P treatment resulted in even larger zooxanthellae cell size. On the other hand, cell size was not affected by the -N+P treatment, remaining equivalent to that of +N+P samples.

Both the accumulation of lipid bodies and starch granules were significantly higher in zooxanthellae experiencing nutrient imbalanced conditions as compared to samples exposed to the +N+P treatment (Figures 4.1 and 4.3b-c). Although there was a higher accumulation of these energy storage bodies in the absence of both nitrate and phosphate, as opposed to lack of phosphate alone, these differences were not statistically significant. Lipid body abundance was equivalent within both imbalanced treatments. Yet, the accumulation of starch granules was most considerable in response to nitrogen limitation alone, leading to a substantially greater abundance in the -N+P, as compared to the -N-P and +N-P treatments. As a control for the method of transmission electron micrograph

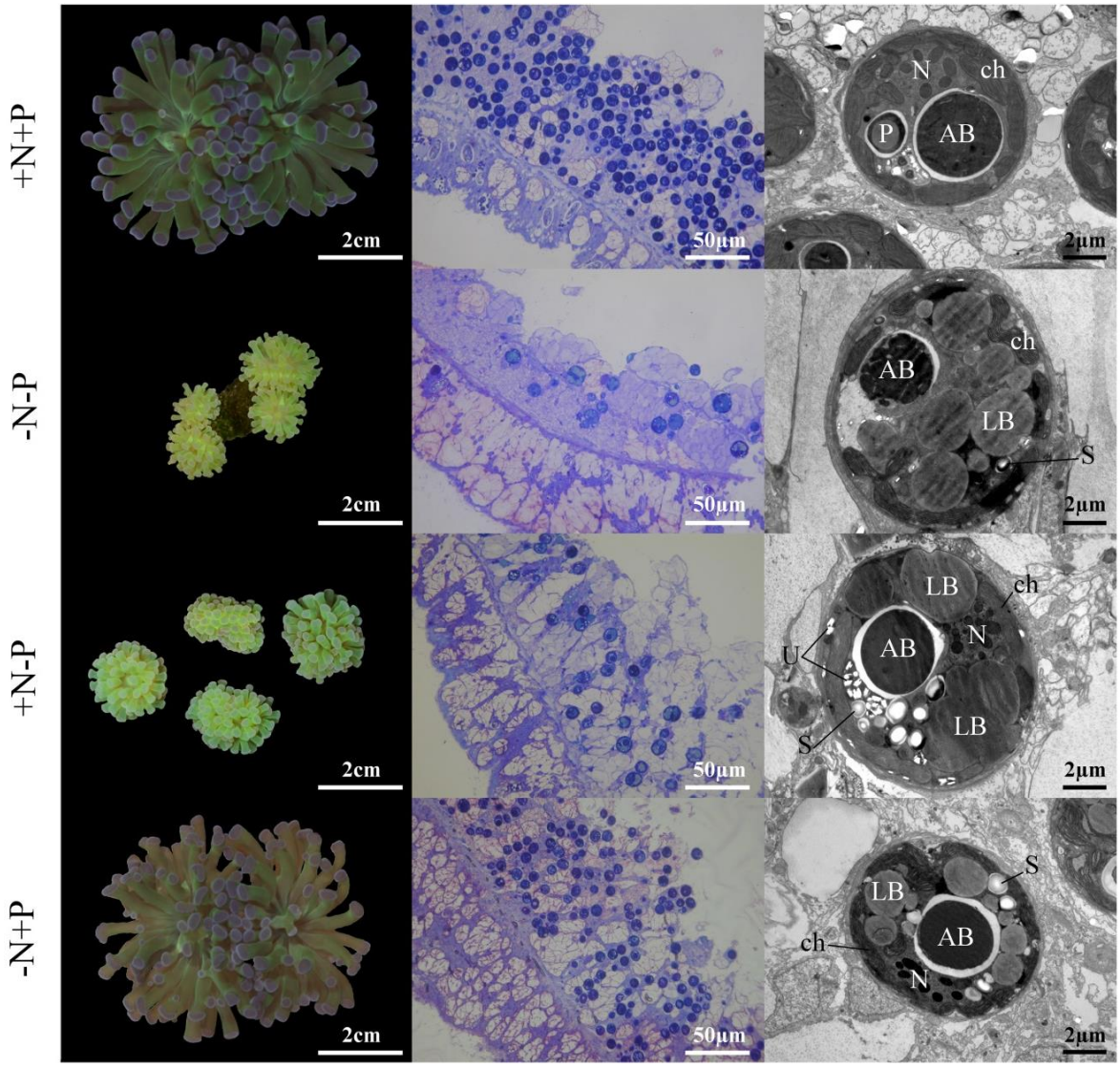

Figure 3.1| Effects of dissolved inorganic nutrient availability on polyp size, zooxanthellae density and mean cellular ultrastructure. Right panels show the polyp macrostructures. Middle panels show the zooxanthellae density contained within the endoderm (x400 magnification). Left panels show micrographs representing the mean ultrastructures of zooxanthellae (x6000 magnification). AB: accumulation body, ch: chloroplast, LB: lipid body, N: nucleus with condensed chromosomes, P: pyrenoid, S: starch granule, U: uric acid crystals.

analysis, neutral lipid accumulation was also determined by a biochemical assay, employing the lipophilic dye Nile Red (method A2.1). The differences in lipid body accumulation in response to varying dissolved inorganic nutrient availability determined by TEM and by Nile Red corresponded extremely well (Figure A2.1a). Furthermore, neutral lipid abundance as determined by Nile Red did not fluctuate significantly depending on sampling time within the dial cycle (Figure A2.1b).

The accumulation of uric acid crystals was substantially higher in response to the +N-P treatment as opposed to the other nutrient environments (Figure 4.3d). On the other hand, fragmentation of the accumulation body, was significantly increased in zooxanthellae of the -N-P treatment, while zooxanthellae harboured by corals experiencing high nutrient availability, balanced (+N+P) or imbalanced (+N-P, -N+P), were found to have intact accumulation bodies (Figure 4.3e).

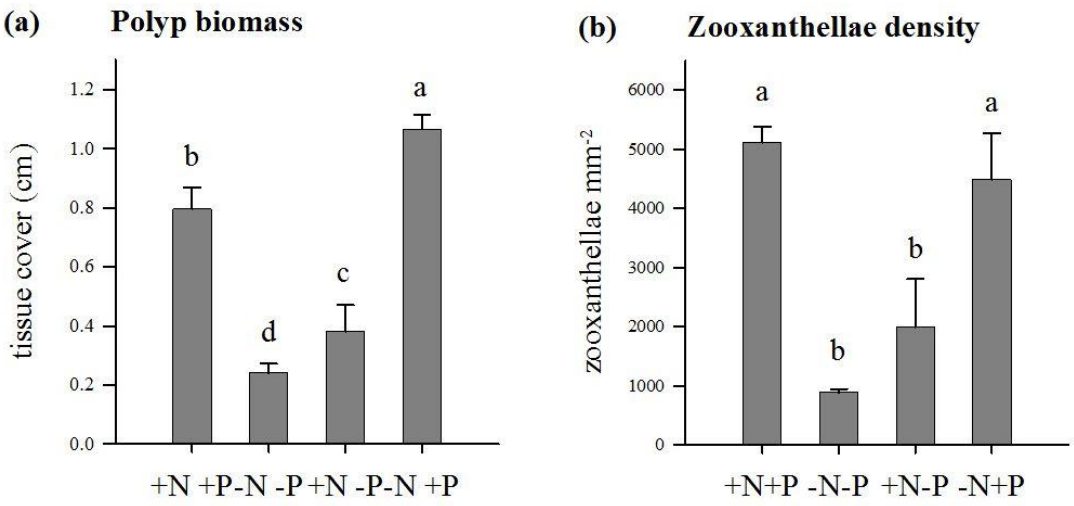

Figure 3.2| Effects of dissolved inorganic nutrient availability on polyp biomass and zooxanthellae density. (a) Polyps size given as the length of skeletal tissue cover (cm). **(b)** Zooxanthellae density. Values are given as mean ± S.D. Statistically significant differences are indicated by the use of different letters.

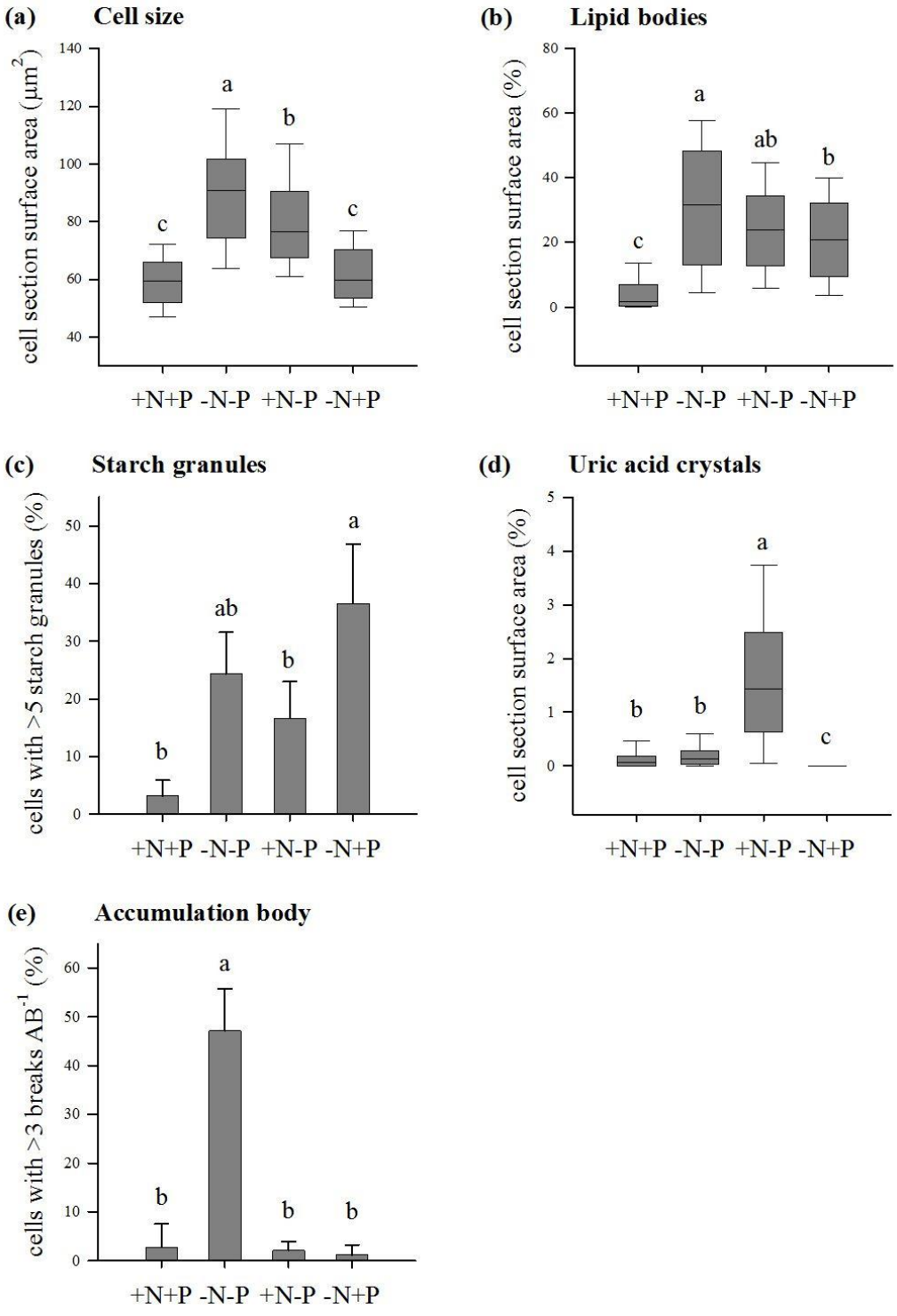

Figure 3.3| Effects of dissolved inorganic nutrient availability on the zooxanthellae ultrastructure. (a) Cell size measured as cell section surface area (μm^2). **(b)** Lipid body accumulation measured as the percentage of the cell section surface area. **(c)** Starch granule abundance measured as the percentage of cells containing >5 granules. **(d)** Uric acid crystal accumulation measured as the percentage of the cell section surface area. **(e)** Accumulation body integrity measured as the percentage of cells >3 breaks within the periphery of the accumulation body. Statistically significant differences are indicated by the use of different letters.

3.5. Discussion

In order to gain further insight into the response of the coral-zooxanthellae symbiosis to an imbalanced nutrient environment, the reef coral *Euphyllia paradivisa* harbouring clade C1 *Symbiodinium*, was exposed to either replete (+N+P) or limited (-N-P) dissolved inorganic nutrient concentrations, or to an imbalanced nutrient environment (+N-P, -N+P). Long term cultivation ensured the development of definitive phenotypes representative of the respective nutrient availability.

3.5.1. Effects on polyp size and on the zooxanthellae population *in hospite*

The deficiency of either both nitrate and phosphate (-N-P), or of phosphate alone (+N-P), was found to have a profound effect on the size of *E. paradivisa* polyps, with polyps cultured in the nutrient replete treatment (+N+P) being significantly larger in comparison (Figures 4.1 and 4.2a). Correspondingly, zooxanthellae population density *in hospite* was also greatly reduced in the -N-P and +N-P treatments as compared to the +N+P treatment (Figures 4.1 and 4.2b). Yet, limitation of nitrate alone (-N+P) did not reduce polyps size or zooxanthellae density, these parameters being comparable to corals within the +N+P treatment. Hence, these findings suggest that a sufficient supply of dissolved inorganic nutrients is necessary for the maintenance of a large polyp biomass and high zooxanthellae density, and that these are most significantly limited by the supply of phosphate as opposed to nitrate.

Nitrate and phosphate are assimilated from the water column by the zooxanthellae and cannot be accessed by the coral host directly (D'Elia and Webb, 1977; Crossland and Barnes, 1977; Yellowlees et al., 2008; Godinot et al., 2009). Therefore, in order for the large size of polyps within the +N+P treatment to be sustained over such a long time period, these nutrients are expected to be partitioned within the holobiont, either by incorporation into translocated photosynthates (Wang and Douglas, 1999; Tanaka et al., 2006; Pernice et al., 2012; Béraud et al., 2013; Kopp et al., 2013) or by digestion of the zooxanthellae (Titlyanov et al., 2006; Downs et al., 2009). Hence, as a result of a diminished supply of dissolved inorganic nutrients, particularly phosphate, either the nutritional quality of the zooxanthellae themselves or of the photosynthates which they translocate to the host is insufficient to sustain an increase in host biomass.

The zooxanthellae population density *in hospite* is not solely dependent on the favourability of abiotic factors, but is also subject to host control. The host places an upper threshold on the zooxanthellae standing stock to ensure the maintenance of a favourable host to algal cell ratio in which the symbionts do not overgrow the host tissue, thus making symbiont density subject to space constraint (Jones and Yellowlees, 1997). It is expected that the zooxanthellae population size harboured by polyps within the +N+P treatment represents the maximal steady-state density which can be accommodated, while a decrease in population size results as a consequence of diminished nutrient supply within the remaining treatments. Accordingly, the inverse correlation between zooxanthellae density and cell size which was observed implies that nutrient deprivation affected the rate of algal cellular growth and division, details of which still require further investigation.

It is proposed that insufficient translocation of nitrogen- and phosphorus-rich molecules to the host, due to diminished availability of the respective nutrients, leads to the assimilation of zooxanthellae as a nutrient source directly in order to satisfy the energy demand of the host. Thereby, the zooxanthellae population size *in hospite* is affected by the rate of algal degradation by the host, as has previously been suggested (Titlyanov et al., 1996). Yet, the limitation of nitrogen alone resulted in an insignificant restriction of symbiont population size, suggesting a low rate of algal degradation by the host and thus, an adequate supply of nutrient-rich photosynthates being translocated to the host despite diminished availability of nitrate in the water.

The coral-algal symbiosis is known to be highly efficient at recycling stores of nitrogen, with waste nitrogen from host catabolic processes becoming available to the symbionts once more (Muscatine and D'Elia, 1978; Rahav et al., 1989; Wang and Douglas, 1998). However, the current findings suggest that the same does not hold true for phosphorus, implying that phosphorus is instead accumulated by the host, likely as a means of skeletogenesis (Godinot et al., 2011a). Consequently, zooxanthellate corals are markedly more vulnerable to phosphorus limitation than to the deprivation of nitrogen. A greater dependency on phosphorus rather than nitrogen supply has previously been reported in *Stylophora pistillata* (Godinot et al., 2011b). The fixation of dinitrogen by coral associated diazotrophs (reviewed in Rädecker et al., 2015) may further contribute to the greater reliance on the continuous uptake of phosphorus over nitrogen.

3.5.2. Storage body accumulation is indicative of nutrient stress

Besides being observed to have a greatly enlarged mean cell size, zooxanthellae morphology resulting from the -N-P treatment was characterised by a large accumulation of energy storage bodies (lipid bodies and starch granules) (Figures 4.1 and 4.3a-c). These features have been reported to be biomarkers of the nutrient limited phenotype (chapter 3, Rosset et al., 2015) and have formerly been observed in nutrient limited zooxanthellae (Berner and Izhaki, 1994; Hoegh-Guldberg, 1996; Muller-Parker et al., 1996; Weng et al., 2014) as well as in free living microalgae (Hu et al., 2008; Li et al., 2008; Wang et al., 2009). This increase in hydrocarbon storage is likely a repercussion of photosynthetic carbon fixation decoupling from cellular growth, leading to a decrease in the biosynthesis of nitrogen- and phosphorus-rich molecules (Msanne et al., 2012).

The morphology of zooxanthellae harboured by corals within the +N-P and -N+P nutrient systems were similarly marked by a significant increase in the accumulation of both lipid bodies and starch granules, the latter being most considerable as a result of the -N+P treatment. Thus, biomarkers of low nutrient stress were apparent as a result of nutrient imbalance. These results, therefore, demonstrate clearly that, despite being exposed to either nitrogen or phosphorus enriched conditions, the zooxanthellae are experiencing nutrient deprivation as a consequence of imbalanced nutrient ratios. Significantly, these findings demonstrate that despite there being little observable limitation to growth of the coral or its symbionts as a result of nitrogen limitation alone, morphological analysis indicates that the cellular metabolism of the zooxanthellae is severely impacted by the experienced nutrient limitation, thus making the overall health of the holobiont deceiving when observing the macrostructure alone.

3.5.3. Morphological biomarkers discriminate between the nutrient environments

The cellular morphology of zooxanthellae experiencing an imbalanced nutrient environment as a result phosphorus limitation alone was highly marked by a significant accumulation of uric acid crystals (Figures 4.1 and 4.3d). Uric acid deposits have previously been shown to accumulate temporarily in zooxanthellae after a pulse of nitrogen enrichment (Kopp et al., 2013). It has been hypothesized that uric acid crystals form a transitory storage of assimilated nitrogen which is later remobilised to sustain the nitrogen requirements of both the host and the symbionts (Clode et al., 2009; Kopp et al., 2013). Thus, as a consequence of luxury uptake, the disproportionately high concentration of

nitrogen relative to phosphorus experienced by corals cultured in the +N-P treatment leads to the storage of excess nitrogen in the form of uric acid within the zooxanthellae. Storage of nitrogen within zooxanthellae and associated high cellular N:P ratio has previously been observed in response to ammonium enrichment, (8 weeks 20µM NH_4^+ as compared to >1µM NH_4^+, 0.1 µM PO_4^{-3}) (Muller-Parker et al., 1994a). On the contrary, nutrient imbalance resulting in nitrogen limitation resulted in algal cells lacking such nitrogen stores completely.

On the other hand, the loss of accumulation body integrity was characteristic only of zooxanthellae experiencing limitation of both nitrate and phosphate (Figures 4.1 and 4.3e). Such a fragmented appearance of this cellular body, which is believed to function as a deposit of cellular waste products (Taylor, 1968), was thus only apparent in samples of the -N-P treatment and represents a marker of severe nutrient deprivation.

Taken together, the analysis of the zooxanthellae ultrastructure allows for the discrimination of the nutrient environment experienced by the coral holobiont. This understanding is of interest for environmental monitoring of coral reefs, especially since fast uptake of dissolved inorganic nutrients by benthic communities often makes it difficult to discern what nutrient concentrations a coral reef is being exposed to (Furnas et al., 2005; Rosset et al., 2015).

3.5.4. Implications for the management of coastal nutrient pollution

This study highlights the great sensitivity of zooxanthellate corals to dissolved inorganic nutrient availability and demonstrates the immense importance of a balanced supply of nitrogen and phosphorus. Particularly nitrogen pollution greatly compromises the physiology of reef corals (Shantz and Burkepile, 2014). Consequential nutrient imbalance has been shown to result in a decreased bleaching threshold (Wiedenmann et al., 2013). Despite the greater dependence on phosphorus availability and the lack of apparent negative effects of phosphate enrichment to coral macrostructure, resulting nutrient imbalance nevertheless lead to nutrient stress of the zooxanthellae, the implications of which remain to be fully elucidated. An abnormally high concentration of phosphorus is therefore not advocated as being beneficial to reef ecosystems. Phosphate enrichment has in fact been observed to result in increased coral skeleton porosity, compromising skeletal integrity (Dunn et al., 2012). It is therefore imperative to manage anthropogenic nutrient pollution of coastal environments in order to maintain nitrogen to phosphorus ratios that

are favourable to reef ecosystems (Furnas et al., 1995; Szmant, 2002), thereby sustaining balanced cellular growth of corals and promoting resilience towards interacting stressors. The monitoring of zooxanthellae cellular ultrastructure in combination with coral macrostructure could aid in the identification and discrimination of nutrient stress experienced within coral reefs.

Chapter 4: Heterotrophic feeding is only beneficial towards coral stress resilience if nitrogen and phosphorus intake is balanced

Sabrina Rosset, Adam J Reed, Luke Morris, Cecilia D'Angelo, Jörg Wiedenmann

Author contribution:

Sabrina Rosset and Luke Morris maintained the experimental feeding treatments. Adam Reed monitored and maintained the dissolved inorganic nutrient concentrations within the different experimental systems. Sabrina Rosset, Adam Reed, Cecilia D'Angelo and Jörg Wiedenmann contributed to the experimental design. Luke Morris produced the data for zooxanthellae density, lipid body accumulation and GFP-like protein abundance as part of his MSc research project which was designed and supervised by Sabrina Rosset. Adam Reed helped with the set-up of the stress treatments and monitored the progression of the stress treatment photographically. Sabrina Rosset produced all other data and wrote this chapter. Cecilia D'Angelo provided comments.

4.1. Abstract

Reef coral species that are competent at heterotrophic feeding have been proposed to have a competitive advantage in light of climate change due to the increased stress resilience provided by heterotrophy through enhanced energy provision to the host and by mitigation of photoinhibition in the zooxanthellae. In dissolved inorganic form, the ratio of nitrogen and phosphorus is crucial to the steady-state functioning and to the thermal resilience of the coral-zooxanthellae symbiosis. The value of heterotrophic phosphorus and the importance of food quality in terms of the nitrogen and phosphorus ratio have never been investigated. This study assesses the interacting effects of nitrogen and phosphorus in dissolved inorganic and in heterotrophic form to the steady-state physiology and to the stress resilience of the coral host and the zooxanthellae. Polyps of *Euphyllia paradivisa*,

subjected to different dissolved inorganic nutrient environments, were fed with two types of food, balanced or nitrogen-enriched, both at natural and maximal food quantities. Dissolved inorganic nitrogen and phosphate availability was shown to be more critical to the physiology of the coral holobiont compared to heterotrophic feeding. Food quality had significant effects on coral physiology and stress resilience. Enriched intake of heterotrophic nitrogen resulted in imbalanced growth of the zooxanthellae. Consequently, heterotrophic feeding was only beneficial towards the stress resilience of the zooxanthellae if heterotrophic nitrogen and phosphorus intake was balanced. This indicates that heterotrophy is valuable as a source of phosphorus to the coral host as well as to the zooxanthellae and demonstrates that the nutritional quality of prey items is critical when considering the beneficial effects of heterotrophic feeding. This raises the concern of heterotrophy being damaging to reef coral health and resilience if the food quality is compromised through anthropogenic pollution.

4.2. Introduction

Reef corals are well adapted to the oligotrophic environment they live in through their mixotrophic nature, obtaining carbon, nitrogen and phosphorus through autotrophy by means of their endosymbiotic algae which fix carbon photosynthetically and assimilate dissolved inorganic nutrients from the water column (Muscatine and Porter, 1977; Muscatine, 1990), as well as through heterotrophy by predation on zooplankton, bacteria and particulate organic matter (Yonge, 1930; Johannes et al., 1970; Bak et al., 1998; Anthony, 2000; Heidelberg et al., 2004; Yahel et al., 2005). The nutrient environment plays a critical role in determining the capacity of reef corals to tolerate environmental stress such as increased sea surface temperatures (Szmant, 2002; Fabricius, 2005; D'Angelo and Wiedenmann, 2014). Yet, an increase in nutrient availability has the potential of being either favourable or detrimental towards coral resilience, making the management of nutrient pollution and the prediction of the repercussions of climate change driven fluctuations to the nutrient environment highly complex. Anthropogenic dissolved inorganic nutrient enrichment can generate adverse indirect effects to reef corals by inducing eutrophication and increased outbreaks of predators and disease (Szmant, 2002; Brodie et al., 2005; Vega Thurber et al., 2014), and compromise coral physiology directly by disrupting natural nutrient ratios (Wiedenmann et al., 2013). On the other hand,

increased prey abundance is thought to enhance the capacity of corals to tolerate stress (Grottoli et al., 2006; Borell and Bischof, 2008). However, the interacting effects of varying availabilities of nitrogen and phosphorus in dissolved inorganic or heterotrophic forms to the functioning of the coral-algal symbiosis under steady-state and adverse conditions remain poorly understood.

The comprehension of how nitrogen and phosphorus derived from different sources affect the functioning of the symbiosis requires an understanding of how these nutrients are partitioned and allocated within the symbiosis. Piniak et al. found that 10-20% of assimilated ^{15}N following prey ingestion was found in zooxanthellae, however, the rapid appearance of which indicating either uptake of rapidly catabolised nitrogen or assimilation of digested material directly from the coelenteron, rather than translocation of nitrogenous compounds from the host (Piniak et al., 2003). Similarly, another study reported that, while a higher incorporation rate of heterotrophic nitrogen was measured in the host fraction than in the zooxanthellae, nitrogen nevertheless became rapidly available to the zooxanthellae following predation (Tremblay et al., 2015). Yet, it remains unknown whether heterotrophically acquired phosphorus becomes available to the zooxanthellae.

Photosynthates that are translocated from the zooxanthellae to the host had previously been considered as 'junk food' that only consisted of hydrocarbons which were used by the host to sustain respiration and mucus production (Falkowski et al., 1984). Accordingly, it has been suggested that heterotrophic nutrient input is required to support coral growth (Houlbrèque et al., 2003; Hoogenboom et al., 2010). Yet, it is apparent that nitrogen-rich compounds are also translocated to the host (Wang and Douglas, 1999; Tanaka et al., 2006; Pernice et al., 2012a; Béraud et al., 2013; Kopp et al., 2013). Indeed, in the absence of heterotrophic nutrient input, dissolved inorganic nutrients in forms that can only be assimilated by the zooxanthellae can sustain a healthy physiology and growth of the coral holobiont, indicating that these nutrients are more equally partitioned among the zooxanthellae and the host (chapter 3: Rosset et al., 2015). However, it is unclear if this occurs through the active translocation of the assimilated nutrients to the host, or if the host obtains these nutrients largely through the digestion of the proliferating zooxanthellae (Titlyanov et al., 2006). Nevertheless, the same nutritional benefit was not observed when the only nutrient input was heterotrophy, thus making nutrient acquisition in dissolved inorganic form more critical to the health of reef corals (Rosset et al., 2015). Yet, the role played by the nutritional quality of prey items was questioned.

Many studies have reported vast beneficial effects of heterotrophic feeding towards the health and physiology of reef corals, as well as their symbionts. Feeding has been shown to increase host biomass (Houlbrèque et al., 2003; Hoogenboom et al., 2010; Treignier and Grover, 2008; Tremblay et al., 2014), calcification, (Houlbrèque et al., 2003; Hoogenboom et al., 2010; Treignier and Grover, 2008; Tremblay et al., 2014), and protein and lipid concentrations (Houlbrèque et al., 2003; Connolly et al., 2012; Rodrigues and Grottoli, 2007; Treignier and Grover, 2008). Reported effects of feeding on zooxanthellae include increases in density (Titlyanov et al., 2000), mitotic index (Cook et al., 1988; McAuley and Cook, 1994; Fitt and Cook, 2001), chlorophyll content and photosynthetic rate (Houlbrèque et al., 2003; Borell and Bischof, 2008), as well as decreased starch and lipid content (Muller-Parker et al., 1996). Furthermore, heterotrophy has been observed to increase thermal and irradiance induced stress tolerance of the coral holobiont by mitigating photoinhibition of PSII (Borell and Bischof, 2008), as well as providing more energy needed to alleviate the induced metabolic stress and support recovery (Grottoli et al., 2006; Rodrigues and Grottoli, 2007; Ferrier-Pagès et al., 2010).

The uptake of nutrients by heterotrophic feeding is subject to a great degree of plasticity as corals can shift from being primarily autotrophic to being primarily heterotrophic. Thus, an increase in heterotrophic feeding rate as well as in the per cent contribution of heterotrophically acquired carbon to host respiration has been measured in response to diminished photosynthetically sourced carbon, such as occurs due to increasing depth (Palardy et al., 2008), increased shading (Anthony and Fabricius, 2000), decreased light irradiance (Hoogenboom et al., 2010), loss of zooxanthellae through bleaching, or increased zooxanthellae photoinhibition (Grottoli et al., 2006). However, heterotrophic plasticity is not only situation-, but also species-specific (Grottoli et al., 2006; Borell and Bischof, 2008; Connolly et al., 2012; Anthony and Fabricius, 2000; Ferrier-Pagès et al., 2010). These findings lead to the proposition that corals with the capacity of increasing the rate of heterotrophic feeding are more resilient to environmental stress due to the ability of supporting their energy demand solely by heterotrophic nutrient uptake (Grottoli et al., 2006; Hughes and Grottoli, 2013). Conflicting with this notion, a shift to a predominantly heterotrophic community has been observed to be detrimental to coral stress tolerance due to the associated increase in turbidity (Fabricius et al., 2013). Furthermore, heterotrophy has been observed to be deleterious when in combination with imbalanced dissolved inorganic nutrient availability (Ezzat et al., 2015).

Various studies have demonstrated the importance of heterotrophy as a source of carbon and nitrogen to the coral holobiont. However, no previous study has considered the value of heterotrophic phosphorus intake to the functioning of the coral-algal symbiosis. In dissolved inorganic form, the ratio of nitrogen to phosphorus is crucial for balanced growth of the coral (chapter 4). Particularly a disproportionally high intake of dissolved inorganic nitrogen is detrimental to coral physiology (chapter 4) and results in a decreased stress tolerance (Wiedenmann et al., 2013). In the current study it was hypothesised that, analogous to the consequences of dissolved inorganic nitrogen enrichment, a comparatively high intake of heterotrophic nitrogen compared to phosphorus can precipitate nutrient stress in zooxanthellae by causing imbalanced growth, thus questioning the generalisation that heterotrophy is beneficial towards coral stress resilience. The aims of this study were to determine how the balance of heterotrophic nitrogen and phosphorus intake affects the nutritional benefits achieved through heterotrophic feeding towards the physiology and stress resilience of the coral host and the zooxanthellae, and to assess how this interacts with varying availabilities of dissolved inorganic nitrogen and phosphate.

4.3. Methods

4.3.1. Coral culture: dissolved inorganic nutrient and feeding treatments

Colonies of *Euphyllia paradivisa* harbouring clade C1 *Symbiodinium* were cultured within the experimental mesocosm at the University of Southampton (D'Angelo and Wiedenmann, 2012; Rosset et al., 2015). Colonies were distributed among three separate systems which were maintained at different concentrations of dissolved inorganic nutrients: (1) nutrient replete system, having high concentrations of nitrate and phosphate (+N+P: N = 10.97µM, P = 1.81µM, N:P= 6.1 : 1)), (2) nutrient limited system, having very low concentrations of nitrate and phosphate (-N-P: N = 0.16µM, P = 0.32µM, N:P= 0.5 : 1), and (3) nutrient imbalanced system, having a high concentration of nitrate but a low concentration of phosphate (+N-P: N = 64.52µM, P = 0.53µM, N:P= 121.3 : 1). Corals were maintained at these nutrient conditions for >2 years. All three systems were maintained at 25°C. Corals within the +N+P and -N-P systems were exposed to a light irradiation of 90µmol m^{-2} s^{-1}. Corals cultured within the +N-P system were exposed to a light irradiation of 30µmol m^{-2} s^{-1} due to mortality when exposed to higher irradiation for a

long time period, but were moved to the higher light environment 4 weeks prior to sampling.

Within each nutrient system, polyps were exposed to five feeding treatments, using two types of foods at two quantities: (1) high level of prawn (HP), (2) low level of prawn (LP), (3) high level of Artemia (HA), (4) low level of Artemia (LA), and (5) unfed (UF). The prawn used was frozen muscle tissue and the Artemia was frozen adult *Artemia salina*. The two types of food were analysed for total nitrogen and phosphorus content using a commercial food testing company (Eurofins food testing UK ltd). The prawn tissue contained a significantly higher total nitrogen content compared to the Artemia. However, the total phosphorus content was not significantly different. As a result, the prawn had a higher N:P ratio than the Artemia, thus providing a food source which is imbalanced (Figure 5.1e).

The large polyp size of *E. paradivisa* allowed for targeted feeding and monitoring of food intake. If the prey item was not ingested after 20-30 minutes, food items were removed. Polyps were fed five days per week for ten weeks and subsequently fed seven days per week for two weeks prior to sampling. Polyps that were fed at a high level were fed twice daily with large portions (~8 hour interval between feeding times), and polyps that were fed at a low level were fed once daily with small portions. The mean dry weight of large and small food portions was ~7.3mg and ~2.1mg respectively. Total daily intake of nitrogen and phosphorus by heterotrophic feeding was calculated by combining portion weight, known nitrogen and phosphorus content, and the mean percentage of daily polyp food ingestion (mean taken over five weeks of feeding) within each feeding regime. The low level of feeding was considered as being representative of realistic food abundance (Johannes et al., 1970; Houlbrèque and Ferrier-Pagès, 2009). However, feeding polyps with large portions twice per day was representative of unrealistic prey availability and served to establish a phenotype demonstrative of the maximum effects brought about by intake of the particular food. The satiety of polyps undergoing the high feeding regimes was demonstrated by the reduced rate of food ingestion, which was especially apparent when fed for the second time during the day.

As a control study to demonstrate that the difference in food quality between the Artemia and prawn is not attributed to the content of polyunsaturated fatty acids (PUFA), polyps within the -N-P system that had been unfed for over one year were subjected to four

feeding treatments: Artemia, prawn, prawn enriched with PUFA, unfed. Five colonies with a sum total of nine polyps were maintained within each feeding treatment for 16 weeks. Polyps were fed once per day, five days per week. The enrichment with PUFA was achieved by blotting prawn portions dry and soaking these within a commercial cod liver oil rich in 20:5 and 22:6 fatty acids. The length of polyp skeletal tissue cover was monitored and photographs and Fv/Fm measurements were taken at the start and at the end of the treatment (Figure A3.3).

4.3.2. Uric acid crystal accumulation measured by transmission electron microscopy

The accumulation of uric acid crystals was previously established as a biomarker of a nutrient imbalance resulting from disproportionally high nitrogen availability (Chapter 4). In order to determine if heterotrophic feeding on an imbalanced food source (prawn) induces phosphorus limitation in zooxanthellae, uric acid crystal abundance was analysed by transmission electron microscopy in samples within the -N-P system exposed to the HP, HA and UF treatments, and compared to the result previously obtained from samples exposed to imbalanced dissolved inorganic nutrients (+N-P/UF). Tentacles from three polyps on distinct colonies were sampled at 2pm (five hours after feeding). Tentacles were only sampled from polyps that ingested the food received that morning. Tentacles were fixed, sectioned and imaged as described in chapters 3 and 4. Cell section and uric acid crystal surface areas were measured using Fiji (Schindelin et al., 2012).Uric acid crystal abundance was calculated as the percentage of the cell section surface area (n = 100).

4.3.3. Analysis of zooxanthellae density

Tentacles were sampled from four distinct colonies from each experimental treatment, thus providing four replicates per treatment. Tentacles were homogenised by sonication within a waterbath for 10 minutes, followed by vigorous disruption using a micro pestle. Following centrifugation of the homogenate at 2500xg for 2 minutes, 100µl of the supernatant was removed and the total host protein concentration was measured using the Pierce BCA assay kit according to the manufacturer's instructions. Zooxanthellae were purified by repeated washing and centrifugation with filtered sterile seawater and counted using a haemocytometer. Zooxanthellae density was determined by normalising algal cell number to host protein concentration.

4.3.4. Analysis of GFP-like protein concentration

The supernatant obtained following tentacle homogenisation was used to determine GFP-like protein concentration by measuring fluorescence intensity using a fluorescence spectrophotometer (Varian Cary Eclipse) using an excitation wavelength of 475nm and an emission wavelength of 504nm. The fluorescence intensity was normalised to total protein content.

4.3.5. Analysis of zooxanthellae neutral lipid content

Lipid body accumulation has been established as a biomarker of nutrient limitation in zooxanthellae (Chapters 3 and 4). Neutral lipid content was measured using the fluorescent dye Nile Red (9-diethylamino-5-benzo[α]phenoxazinone) which emits a yellow/orange fluorescent signal in the presence of neutral lipids (Greenspan et al., 1985). Nile Red (Sigma-Aldrich Ltd.) was dissolved in dimethyl sulfoxide (DMSO) as a 1mg ml^{-1} stock solution. Purified zooxanthellae were standardised to $7x10^5$ cells ml^{-1} by dilution in sterile seawater. Cells were stained in 2μg ml^{-1} Nile Red with 5% DMSO (Kou et al., 2013). Samples were shaken for 40 seconds, incubated in the dark at room temperature for 5 minutes, and measured in a 96-well plate using a fluorescence spectrophotometer (Varian Cary Eclipse) with an excitation wavelength of 528nm. Emission spectra were obtained in the range of 550-750 nm with 576 nm being recorded as the Nile Red fluorescence emission corresponding to neutral lipids. The relative fluorescence intensity (RFI) was obtained by subtraction of the fluorescence intensity of the auto-fluorescence of unstained zooxanthellae and of Nile Red in seawater, from that of the stained zooxanthellae.

4.3.6. Measure of polyp biomass

As a measure of polyp size, the length of the tissue covering the outside of the skeleton was measured using callipers.

4.3.7. Stress treatment exposure and monitoring

Colonies cultured within the -N-P and the +N-P systems were exposed to a stress treatment of increased light irradiance and temperature. This was conducted within the same systems as control colonies were maintained in, but in separate tank units within each system. Within the -N-P system five colonies of each feeding treatment, each holding three polyps, were relocated to the stress treatment tank. Colonies were spaced out within the tank to

form five groups, with each including one colony from each feeding treatment, thereby limiting effects of any microenvironments within the tank. Within the +N-P system five individual polyps of each feeding treatment were placed within the stress treatment tank and allowed to acclimate to the increased light irradiation (90µmol m^{-2} s^{-1}) for two weeks. Subsequently the light intensity was increased from 90 to 160µmol m^{-2} s^{-1} with one day at 120 and one day at 150µmol m^{-2} s^{-1} in between. The temperature was raised from 25 to 26°C and these conditions (160/26) were maintained for eight days. This was followed by a further increase in temperature by one degrees C per day until a final temperature of 30°C was reached. Polyps were fed daily throughout the stress treatment.

The effects of the stress treatment exposure were monitored by the daily measurement of the maximum quantum yield of PSII (Fv/Fm) using pulse amplitude modulated fluorometry (Diving PAM - Heinz Walz GmbH). Two readings were taken from each polyp within the -N-P treatment, with each colony counting as one replicate (n = 5) for the determination of mean ± S.D. of Fv/Fm. Within the +N-P treatment each individual polyp was considered as one replicate (n = 5) and was measured three-four times. Additionally, every three days, the polyp tissue cover was measured using callipers and the polyps were photographed for the determination of changes in polyp expansion. The percentage of polyps ingesting received food items was monitored. The feeding behaviour of control polyps within the -N-P system was also monitored. Due to the scarcity of polyps remaining in the +N-P control tank unit (three polyps per feeding treatment), the feeding behaviour of the polyps in this system which were exposed to the stress treatment was also compared to that of the controls from the -N-P system.

4.3.8. Statistical analysis

The significant difference in total nitrogen and phosphorus content between the prawn and Artemia was determined by a t-test (Table A3.3). Significant effects of the different nutrient environments on food ingestion rates, zooxanthellae density, GFP-like protein fluorescence intensity, zooxanthellae lipid body abundance and steady-state polyp tissue cover were determined by two-way analysis of variance (ANOVA) with the two factors being dissolved inorganic nutrient availability and feeding treatment (Tables A3.1, 3.7). This was followed by Tukey's test for multiple pairwise comparisons (Tables A3.2, 3.8-11). Data that was not normally distributed was log transformed prior to analysis. Significant differences in uric acid crystal abundance were determined by a one-way

ANOVA followed by Tukey's test (Tables A3.5, 3.6). Significant effects of dissolved inorganic nutrient availability and feeding treatments on stress resilience was assessed by linear regression analysis of Fv/Fm and tissue cover decline. The slope for Fv/Fm decline was determined for each replicate, using data obtained as of the onset of maximum temperature stress (T15) up until measurements could no longer be taken for -N-P/UF samples (T38). Due to non-normal distribution, significant effects on the rate of Fv/Fm decline was determined by non-parametric Scheirer-Ray-Hare test using all slope values (Table A3.12). Linear regression for the decline in skeletal tissue cover was performed, assessing the percentage decline in tissue length, taking the length at the first day of 30°C exposure as the 100% value for each polyp (Figure A3.2). The obtained values for the slopes of the regression lines were used for a two-way ANOVA and Tukey's post hoc test in order to determine significant effects of the feeding treatments and dissolved inorganic nutrient availability on the rate of decline in tissue cover caused by stress treatment exposure (A3.13, 3.14). A three parameter sigmoid curve was fit to data of food ingestion during stress exposure and the inflection point of each curve was taken as a measure of the effects of food quality and quantity on changes in feeding behaviour. $P < 0.05$ was considered as significant in all instances.

4.4. Results

4.4.1. Food quality and feeding behaviour

The quality of two types of foods used for heterotrophic feeding of *E. paradivisa* polyps was tested by comparison of the total nitrogen and phosphorus content. The molar ratio of nitrogen to phosphorus was found to be twice as high in the prawn as compared to the Artemia due to significantly higher total nitrogen content in the prawn (Figure 5.1e). However, the total phosphorus content was not significantly different. Therefore, food type had a significant effect on the total intake of nitrogen by heterotrophic feeding (Figure 5.1f). This difference is expected to be attributed to the nature of the tissue, with prawn constituting only of muscle tissue whereas the Artemia consists of whole animals. Thus, the prawn represents a relatively imbalanced food source. It remains possible that other differences in nutritional quality of the two foods contribute to the different effects exhibited towards the coral holobiont. Only, the possible role of polyunsaturated fatty acid concentration was evaluated by enriching the prawn with PUFAs. This enrichment had no significant effect on polyp biomass, colouration or Fv/Fm (Figure A3.2).

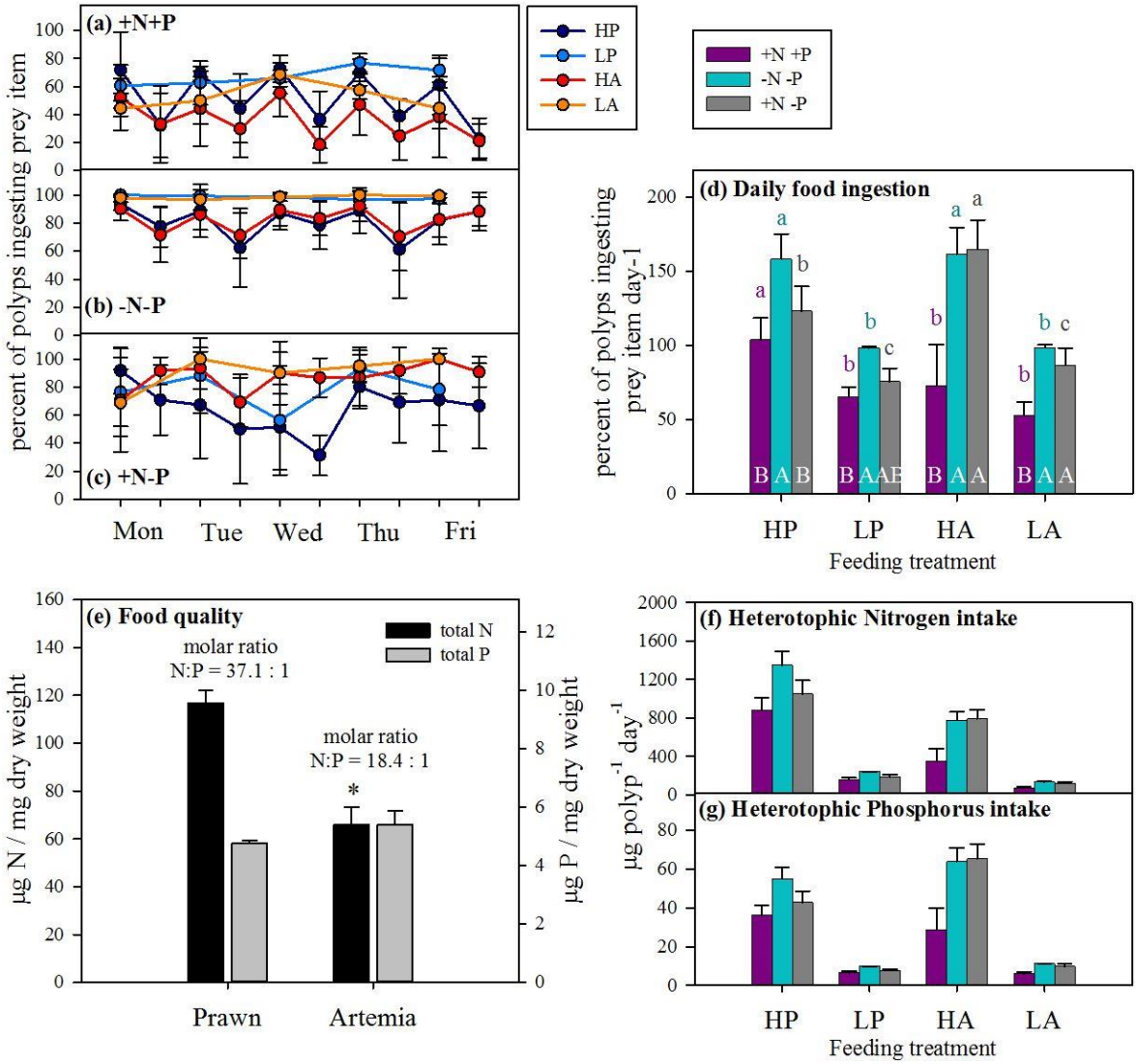

Figure 4.1|Feeding behaviour, food quality and total heterotrophic nitrogen and phosphorus intake. Mean daily feeding behaviour over five weeks of feeding for **(a)** +N+P system polyps, **(b)** -N-P system polyps, and **(c)** +N-P system polyps. High level of prawn (HP – dark blue) and high level of Artemia (HA - red) were fed twice per day with large portions. Low level prawn (LP – pale blue) and low level Artemia (LA - orange) were fed once per day with small portions. **(d)** Daily total mean percentage of polyps ingesting food items. **(e)** Total nitrogen (N - black) and phosphorus (P - grey) content of prawn muscle tissue and adult *Artemia salina* were measured and the molar ratio of nitrogen to phosphorus was determined for each food type. Asterisk indicates a significant difference between the two types of food. **(f)** Total intake of nitrogen by heterotrophic feeding (portion size x N content x percentage food ingestion). **(g)** Total intake of phosphorus by heterotrophic feeding (portion size x P content x percentage food ingestion). All data is given as mean and S.D. Statistically significant differences for **(d)** are shown by the use of different letters: lower case letters indicate significant effects of feeding within each nutrient treatment; upper case

letters indicate significant effects of the nutrient environment within each feeding treatment. $P < 0.05$ is considered significant in all instances.

Dissolved inorganic nutrient availability as well as food quality effected polyp feeding behaviour (Figure 5.1a-d). Polyps within the +N+P system were observed to have a significantly lower percentage of daily food ingestion compared to polyps experiencing limitation of dissolved inorganic nutrients, indicating satiety as a result of the high concentrations of nitrate and phosphate in the water (Figure 5.1a-d). Polyps within the -N-P system receiving prawn displayed a higher feeding rate than polyps within the +N-P system on the same food type (Figure 5.1d). However, the feeding rate on Artemia was equally high within the -N-P and +N-P systems. Polyps receiving only small food items once per day had a prey ingestion rate of close to 100%, whereas those exposed to a high level of feeding had a much lower rate of prey ingestion, especially when fed for the second time in the day (Figure 5.1a-c), thus demonstrating satiety as a result of the high feeding level and verifying that the resulting phenotypes were representative of a maximum rate of heterotrophy.

4.4.2. Biomarkers of coral and zooxanthellae nutrient stress

Uric acid crystal accumulation is a biomarker of nutrient imbalance resulting from a disproportionally high availability of nitrogen compared to phosphorus (chapter 4). The HP feeding treatment in combination with limited dissolved inorganic nutrient availability (-N-P) resulted in a very high accumulation of uric acid crystals, comparable to that observed within samples exposed to an imbalanced ratio of dissolved inorganic nutrients (+N-P/UF) (Figure 5.2). On the other hand, the HA feeding treatment as well as the absence of feeding within the -N-P system resulted in a very low occurrence of uric acid crystals.

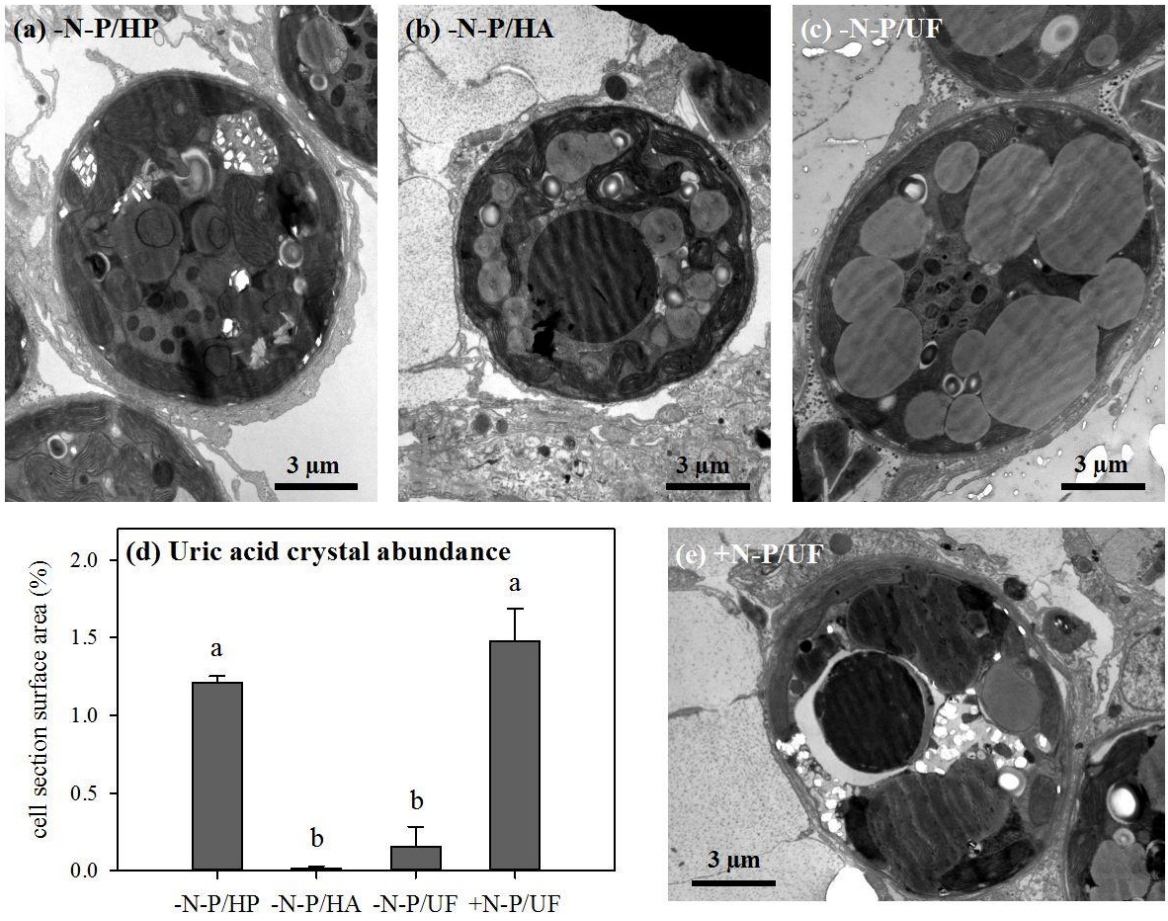

Figure 4.2| Uric acid crystal accumulation is a biomarker of a nutrient imbalance resulting from nitrogen enrichment. Micrographs of zooxanthellae at x6000 magnification show the mean cellular ultrastructure resulting from three feeding treatments within the nutrient limited system (-N-P) as well as that resulting from the high nitrate imbalanced system in the absence of feeding (+N-P): **(a)** high level of prawn (HP/-N-P), **(b)** high level of Artemia (HA/-N-P), **(c)** unfed (UF/-N-P). **(d)** mean and S.D. of cellular uric acid crystal abundance. **(e)** unfed (UF/+N-P). The use of different letters indicates significant differences, with $P < 0.05$ considered significant. (d) Micrograph of uric acid crystals within a vacuole, imaged within an algal cell exposed to the -N-P/HP treatment.

Zooxanthellae density was greatly decreased as a result of diminished availability of phosphate within the -N-P and +N-P systems (Figure 5.3a). Heterotrophic feeding had no effects on zooxanthellae density irrespective of food quality or quantity when combined with high concentrations of nitrate and phosphate. However, within the -N-P and +N-P systems feeding had significant effects on algal density which was highest as a result of the HA feeding treatment in the former and as a result of the LA feeding treatment in the latter.

Zooxanthellae density was lowest in unfed polyps in the -N-P system and was observed to increase as a result of the LP feeding treatment and to increase further as a result of HP or LA feeding regimes. However, feeding on prawn had no significant effect on density within the +N-P system. Interestingly, with the exception of unfed samples which displayed relatively high GFP-like protein fluorescence intensity, a significant positive correlation between zooxanthellae density and GFP-like protein fluorescence was demonstrated for all other conditions, thus making fluorescence a potentially useful biomarker for determination of the nutrient status of this species (Figures 5.3c, A3.1).

Neutral lipid accumulation by zooxanthellae was very low as a result of high dissolved inorganic nutrient availability and was not affected by heterotrophic feeding within this system (Figure 5.3b). Neutral lipid abundance was significantly higher as a result of diminished dissolved inorganic nutrient concentrations. Only the HA feeding treatment resulted in differences in neutral lipid abundance which were statistically insignificant among the three nutrient systems. Thus, the HA feeding treatment limited neutral lipid accumulation within the -N-P and +N-P treatments while the lack of feeding resulted in the highest accumulation of neutral lipids.

The length of skeletal tissue cover was measured as a parameter for polyp size (Figure 5.3d). The lack of phosphate availability resulted in a significant decrease in tissue cover length. All feeding treatments resulted in a slight increase in tissue cover when in combination with the +N+P treatment. Much larger feeding effects were apparent within the -N-P and +N-P treatments. HA resulted in the highest tissue cover within the -N-P treatment, followed by HP, these being higher than corresponding samples from the +N+P treatment. LA resulted in a tissue cover similar to HP, while LP resulted in a lesser tissue cover. Within the +N-P system both HA and LA resulted in a large increase in tissue cover. Yet feeding with prawn did not significantly increase the tissue cover as compared to unfed samples.

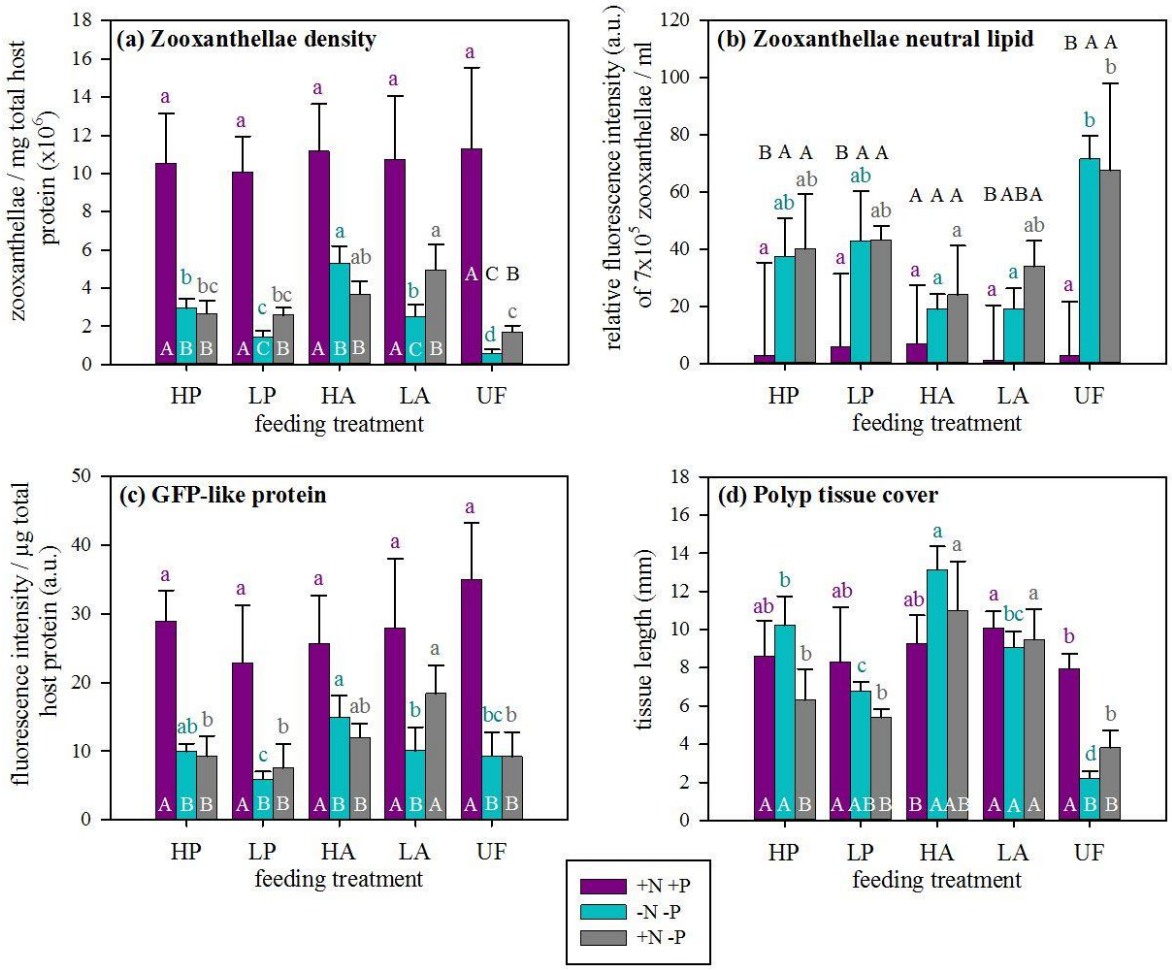

Figure 4.3| Biomarkers for the analysis of coral and zooxanthellae nutrient status. **(a)** Zooxanthellae population density normalised to host protein content. **(b)** Neutral lipid accumulation in zooxanthellae measured as the relative fluorescence intensity of Nile red at a concentration of $7x10^5$ cells ml^{-1}. **(c)** GFP-like protein concentration measured as fluorescence intensity normalised to host protein content. **(d)** Length of polyp skeletal tissue cover as a measure of polyp biomass. All measurements were conducted for polyps exposed to five feeding treatments within three distinct dissolved inorganic nutrient environments: high feeding level with prawn (HP), low feeding level with prawn (LP), high feeding level with Artemia (HA), low feeding level with Artemia (LA), unfed (UF), replete (+N+P, magenta), limited (-N-P, blue), and imbalanced (+N-P, grey) dissolved inorganic nutrient availability. All data is given as mean and S.D. Statistically significant differences are shown by the use of different letters: lower case letters indicate significant effects of feeding within each nutrient treatment; upper case letters indicate significant effects of the nutrient environment within each feeding treatment. $P < 0.05$ is considered significant in all instances.

4.4.3. Impact of the nutrient environment on coral and zooxanthellae stress resilience

Photosystem II efficiency measured as Fv/Fm was used as an indication of zooxanthellae health during exposure to a combined light irradiance and temperature stress treatment. Concomitantly, polyps were documented photographically and the length of their skeletal tissue cover as well as their feeding behaviour was measured in order to infer the effect of the stress treatment to the coral host.

Prior to onset of the stress treatment, Fv/Fm of UF samples within the -N-P system was significantly lower compared to all fed samples, however no differences were measured among the fed samples. Yet, food quality had a significant effect on zooxanthellae stress resilience. As the stress treatment progressed, values measured for prawn fed samples became similar to those measured for UF samples (Figure 5.4a). The rate of decline in Fv/Fm following exposure to 30°C was similar for HP, LP and UF samples, while that of HA and LA samples was lower (Figure 5.6a). Fv/Fm of HP samples dropped below what is considered as a healthy value (0.5) after nine days of exposure to 30°C. Yet, Fv/Fm of HA samples only dropped below a mean reading of 0.5 after 18 days at 30°C. A similar pattern was observed within the +N-P system, however the rate of Fv/Fm decrease was slower compared to that observed within the -N-P system, with the mean reading for HP and HA samples dropping below 0.5 following 14 and 24 days of exposure to 30°C respectively.

The different feeding treatments produced the same effects on the rate of decline in polyp skeletal tissue cover as was observed for the rate of Fv/Fm decline. Thus, within the -N-P treatment, the rate of decline was observed to be slightly faster for HP, LP and UF samples than for HA and LA samples (Figure 5.6b). Yet, these differences were not statistically significant. Within the +N-P treatment, the tissue receded fastest as a result of the HP feeding treatment, and slowest in response to the LA feeding treatment (Figure 5.6b). Yet, it must be noted that the start point for tissue cover decline varied hugely as a result of the different feeding treatments (Figure 5.5). Contrary to what was observed for the rate of Fv/Fm decline, the rate of skeletal tissue cover decline was more rapid as a result of imbalanced dissolved inorganic nutrient availability.

Food ingestion declined gradually as a result of stress treatment exposure, with no polyps ingesting offered food items anymore at the end of the treatment (Figure 5.8). The rate of decline in food ingestion, measured by the inflection point of the fit sigmoid curves, was affected by the feeding regime and dissolved inorganic nutrient availability. The HP feeding regime declined fastest, while the LA feeding regime could be maintained for the longest upon exposure to the stress treatment. The ingestion of prawn, both with a high and low level of feeding, declined in polyps within the -N-P system prior to those within the +N-P system, yet dissolved inorganic nutrient availability had no effect on the rate of decline in the ingestion of Artemia.

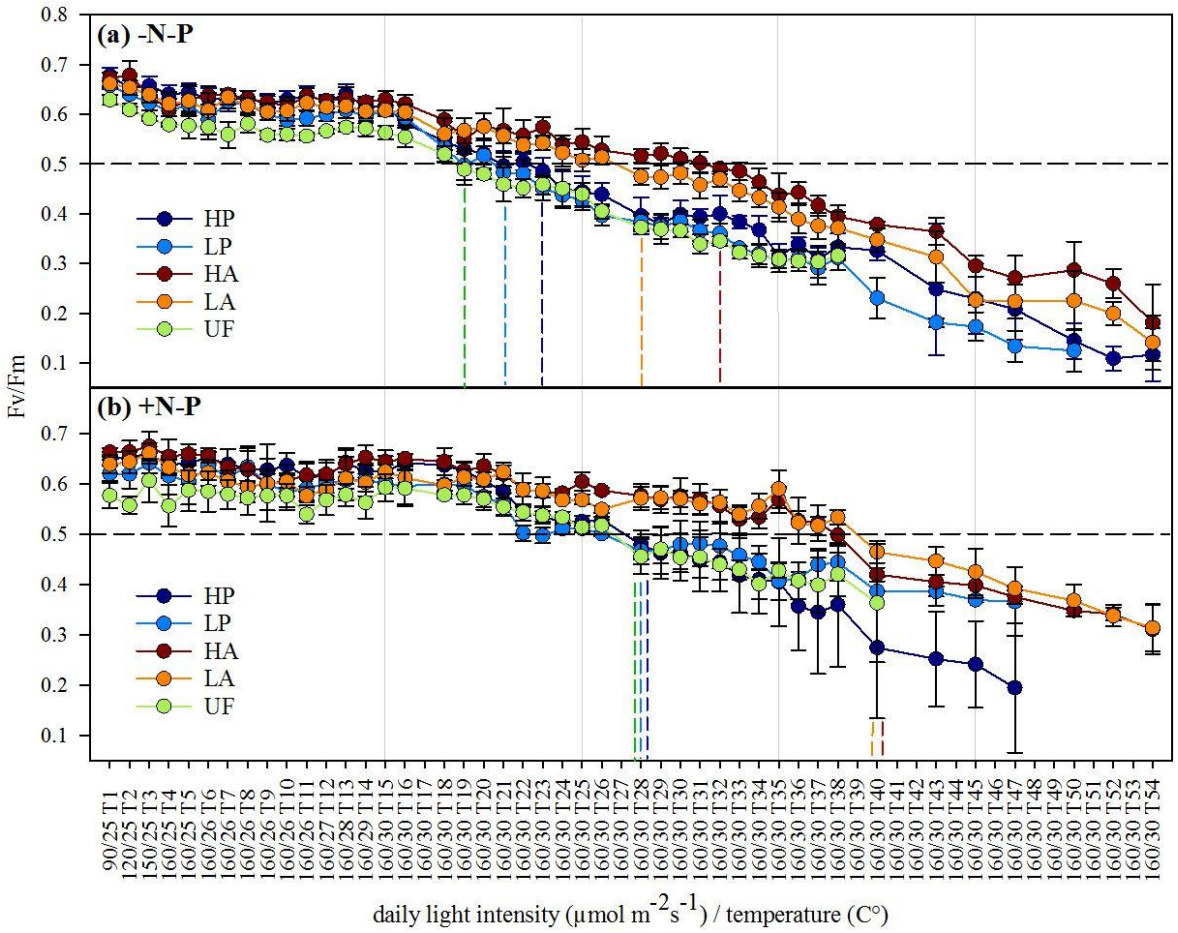

Figure 4.4| Daily Fv/Fm measurement during the course of the stress treatment. **(a)** Nutrient limited treatment (-N-P), **(b)** nutrient imbalanced treatment (+N-P). Data are given as mean ± S.D. Data points stop once the signal became too low for accurate measurement or became subject to interference by algal overgrowth. Vertical dashed lines mark the days at which values dropped below a healthy value of 0.5 for each treatment. High level of prawn (HP, dark blue), low level of prawn (LP, pale blue), high level of Artemia (HA, red), low level of Artemia (LA, orange), unfed (UF, green).

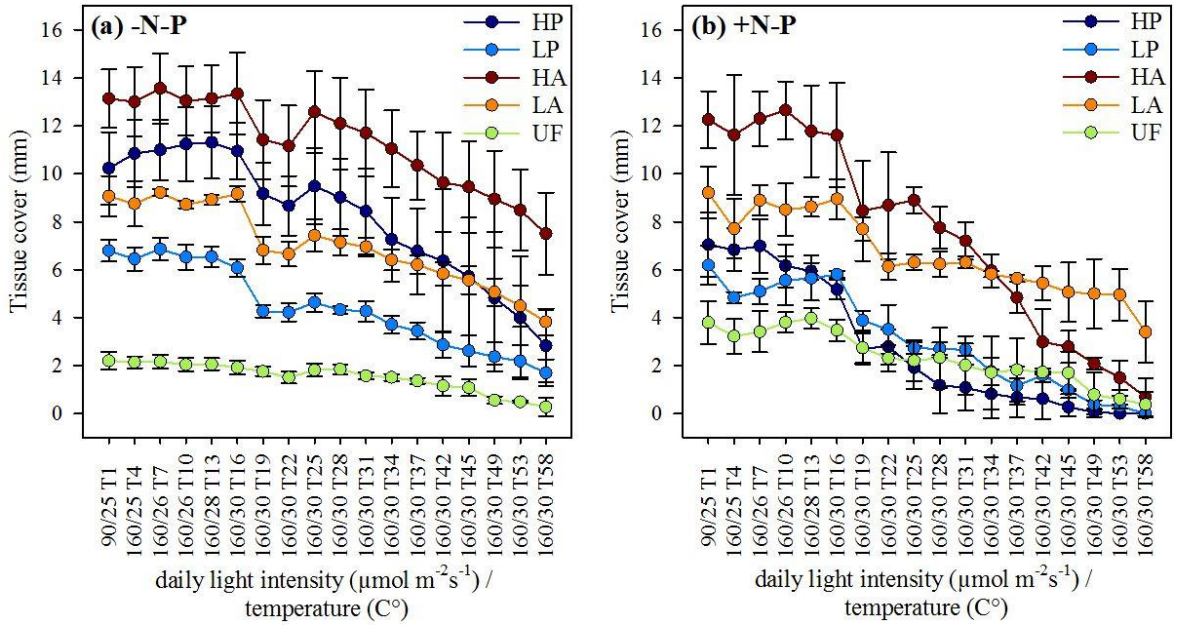

Figure 4.5| Measurement of polyp skeletal tissue cover during the course of the stress treatment. **(a)** Nutrient limited treatment, **(b)** nutrient imbalanced treatment. Data are given as mean ± S.D.

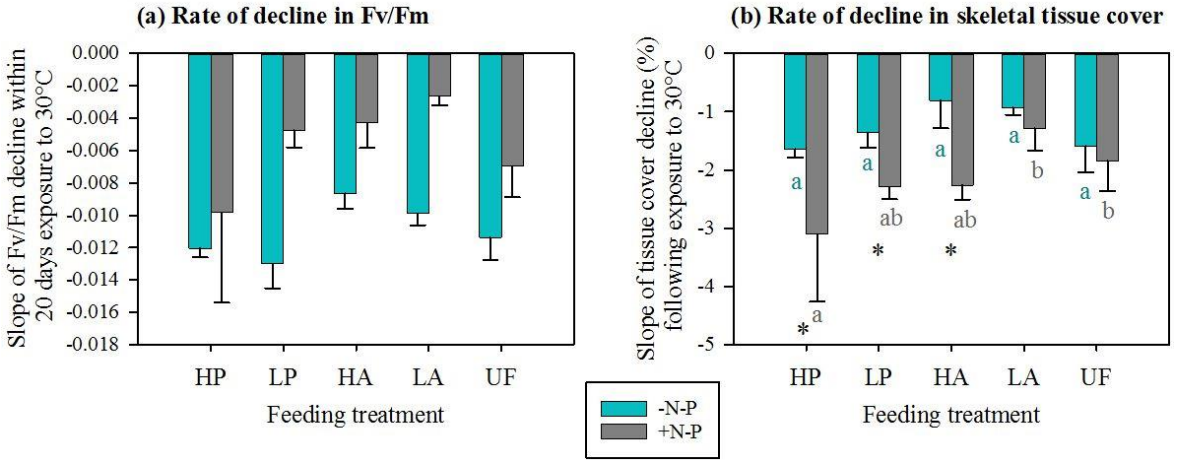

Figure 4.6| Rates of decline in zooxanthellae and coral host health following stress exposure. Mean and S.D. of the slopes of linear regression in **(a)** Fv/Fm and **(b)** polyp skeletal tissue cover. For (a) significant effects of feeding and dissolved inorganic nutrient availability was examined by non-parametric analysis due to non-normal distribution, therefore no pairwise comparison could be conducted. For (b) Significant effect of the feeding treatments within each nutrient system is indicated by the use of different letters. Significant effects of dissolved inorganic nutrient availability within each feeding regime are indicated by the use of an asterisk.

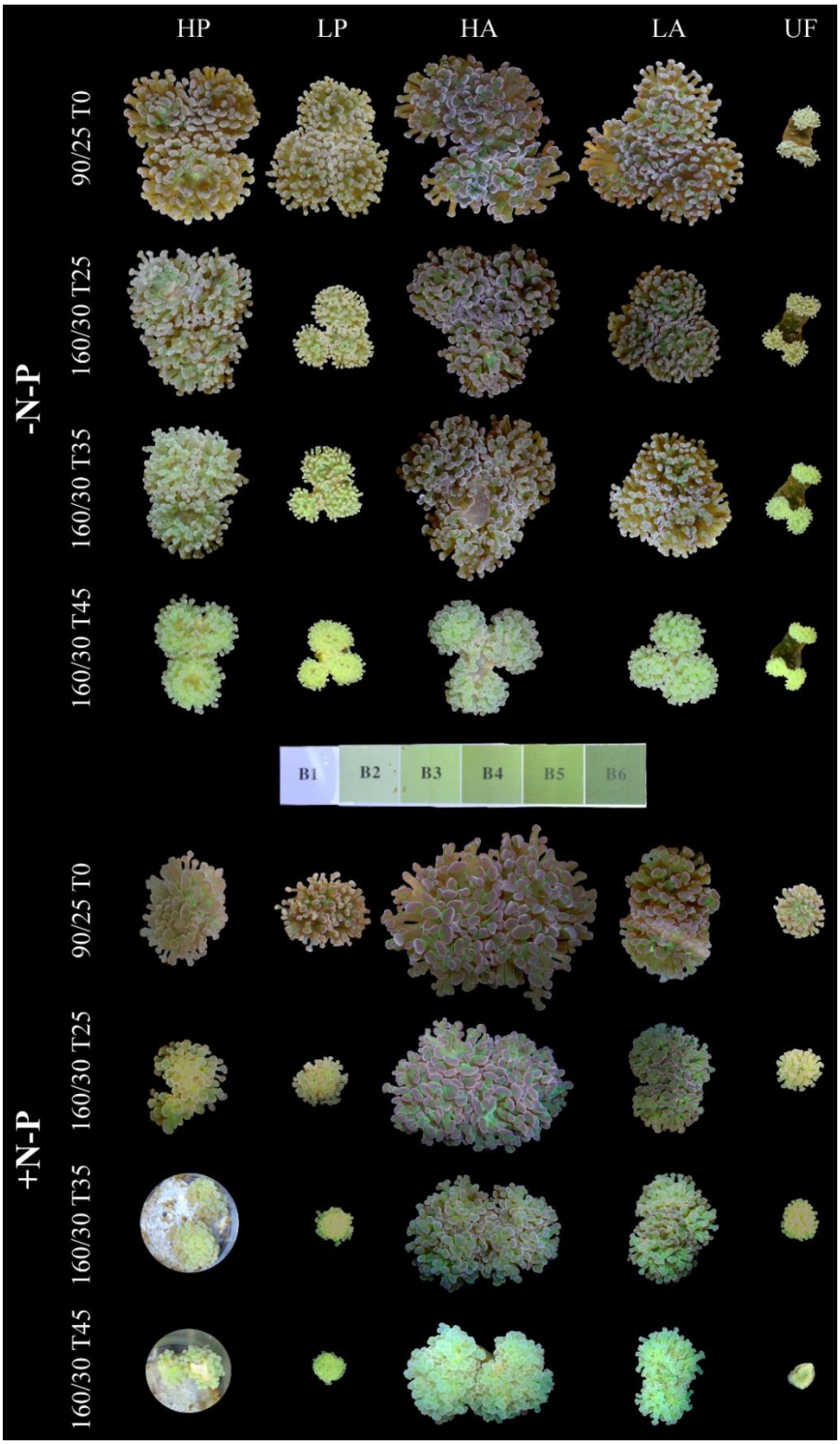

Figure 4.7| Progression of polyp deterioration during the course of the stress treatment within the -N-P and +N-P systems. Four time points are shown for each treatment. All -N-P colonies constitute three polyps, +N-P colonies range from three to one single polyp. +N-P/HP polyps detached from the skeleton. High level of prawn (HP), low level of prawn (LP), high level of Artemia (HA), low level of Artemia (LA), unfed (UF).

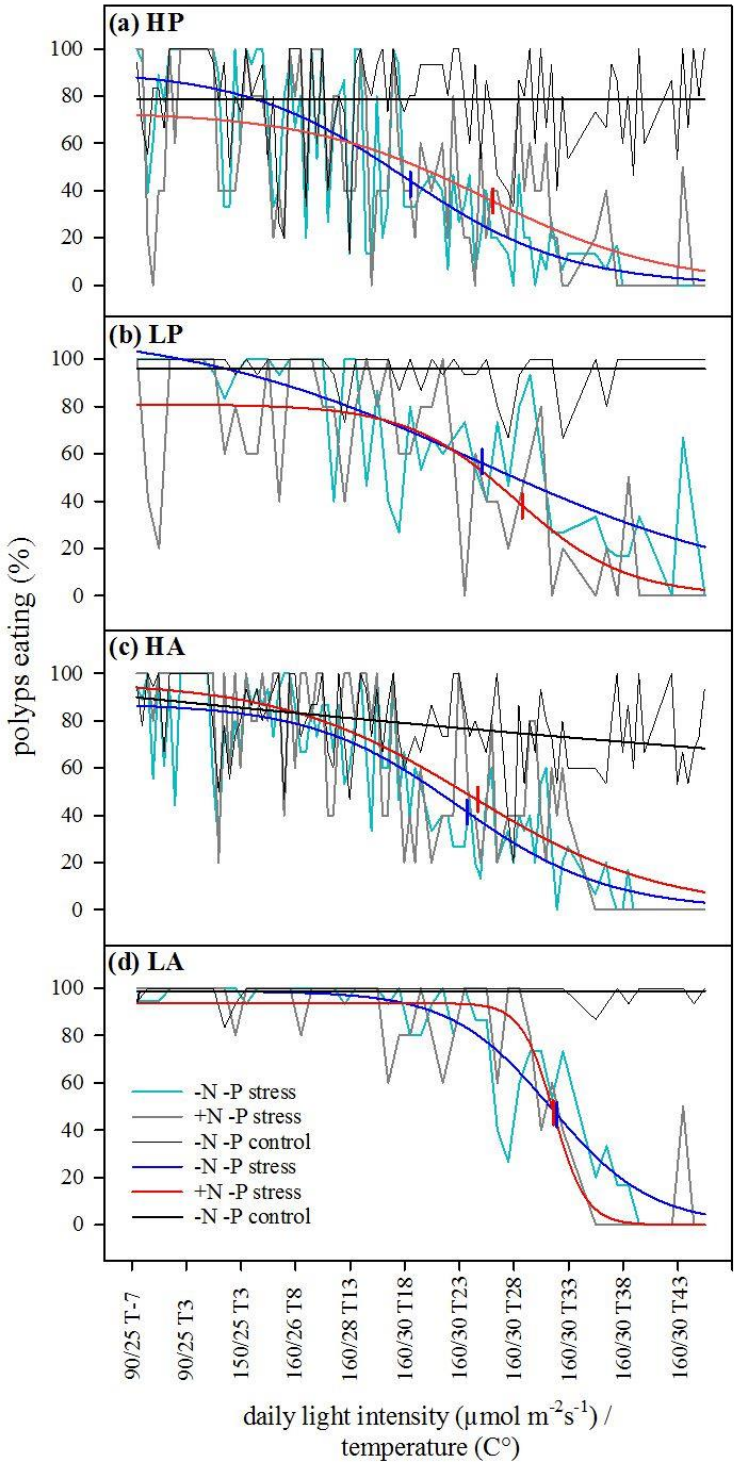

Figure 4.8| Polyp feeding behaviour during the course of the stress treatment. The percentage of polyps taking in offered prey items was measured. **(a)** High level prawn (HP) fed twice daily, **(b)** low level prawn (LP) fed once daily, **(c)** high level Artemia (HA) fed twice daily, **(d)** low level Artemia (LA) fed once daily. Three parameter sigmoidal curves were fit to the data for better visualisation of the decline in food ingestion rate. The inflection points are marked on the curves.

4.5. Discussion

In this study the interacting effects of two principal sources of nitrogen and phosphorus to reef corals, the uptake of dissolved inorganic nutrients and heterotrophic feeding, were evaluated in order to determine which source is the dominant driver of the nutrient status of the coral host and its endosymbiotic algae. A balanced ratio of dissolved inorganic nitrogen to phosphate availability has previously been shown to be critical for coral health and stress tolerance (Wiedenmann et al. 2013; Chapter 4). Here, we examined how a disproportionally high intake of nitrogen relative to phosphorus through heterotrophic feeding affects coral and algal physiology and stress resilience, providing the first study of food quality when considering the beneficial effects of heterotrophy to reef corals.

4.5.1. Imbalanced growth caused by heterotrophic feeding

Uric acid crystals constitute a cellular storage of excess nitrogen (Kopp et al., 2013), a large accumulation of which signifying an imbalance in the uptake of nitrogen relative to phosphorus (Chapter 4). A high level of uric acid crystal abundance was previously observed as a result of dissolved inorganic nitrogen enrichment (Chapter 4). The ratio of nitrogen to phosphorus was considerably higher in the prawn compared to the Artemia, resulting in a higher uptake of heterotrophic nitrogen as a result of feeding on this food source (Figure 5.1e,f). Consequently, a high level of uric acid crystal accumulation was observed in zooxanthellae harboured by prawn fed polyps within the -N-P system, comparable to that observed in samples experiencing an imbalanced dissolved inorganic nutrient environment (Figure 5.2). On the other hand, a balanced intake of heterotrophic nitrogen and phosphorus by feeding on Artemia resulted in a very small abundance of uric acid crystals. These findings demonstrate that imbalanced growth is not only caused by enrichment of dissolved inorganic nitrogen (Wiedenmann et al. 2013; Chapter 3), but also by heterotrophic feeding on nitrogen enriched prey, implying that heterotrophy by the coral host can precipitate nutrient stress (phosphorus limitation) in zooxanthellae.

4.5.2. The interacting effects of heterotrophy and dissolved inorganic nutrient uptake on the nutrient status of a reef coral

In agreement with what was previously observed in *E. paradivisa* (chapter 3), dissolved inorganic nutrient availability had a significant effect on polyp feeding behaviour (Figure 5.1a-d). The decreased rate of prey ingestion when exposed to replete dissolved inorganic

nutrient availability (+N+P) signifies that the nutrient requirements of the coral host are largely satisfied by means of dissolved inorganic nutrient assimilation by the zooxanthellae. Interestingly, a significant degree of heterotrophic plasticity was also observed in response to food quality. Polyps exposed to imbalanced dissolved inorganic nutrient concentrations ingested the nutrient balanced food (Artemia) at the same rate as polyps cultured in the nutrient limited environment, but displayed a comparably lower uptake of the nitrogen enriched food (prawn) (Figure 5.1a-d). This signifies that a greater degree of satiety is reached due to the high uptake of heterotrophic nitrogen when in combination with high dissolved inorganic nitrogen availability. These findings are conflicting with observations in other species in which increased dissolved inorganic nutrient availability resulted in heightened prey ingestion rates which was hypothesised to relate to the high energy demand of the prey ingestion and digestion process (Leal et al., 2015; Ezzat et al., 2015).

In the presence of a high concentration of dissolved inorganic nutrients, heterotrophic feeding largely had no effects on the physiology of the coral host or the zooxanthellae (Figure 5.3). On the other hand, when deprived of dissolved inorganic nutrients, heterotrophy resulted in a partial recovery of the experienced nutrient stress, apparent by increased zooxanthellae density, increased polyp size, and decreased algal neutral lipid accumulation. Nevertheless, despite simulating greatly exaggerated prey abundance, heterotrophy could not compensate for insufficient dissolved inorganic nutrient availability. Yet, this finding applies predominantly to the nutrient status of the zooxanthellae and not to that of the host. Indeed, polyp size was larger when a high level of feeding was combined with diminished dissolved inorganic nutrient supply than when combined with high dissolved inorganic nutrient concentrations, either as a consequence of the lower zooxanthellae density or due to higher prey ingestion rate. On the other hand, zooxanthellae density was very low even when subjected to a high level of heterotrophic nitrogen and phosphorus. These observations indicate that nutrients acquired through heterotrophy are not equally partitioned between the coral host and the zooxanthellae which is in agreement to what has previously been reported (Piniak et al., 2003). Thus, heterotrophy is observed to primarily provide benefit to the physiology of the coral host while, on the contrary, assimilated dissolved inorganic nutrients appear to be partitioned more equally within the coral holobiont. Nevertheless, the increased zooxanthellae density and diminished neutral lipid accumulation in samples receiving the -N-P/HA treatment

compared to the -N-P/HP treatment indicates that both heterotrophic nitrogen and phosphorus become available to the zooxanthellae.

Food quality had a significant effect on the benefits provided by heterotrophy. Particularly when in the presence of an imbalanced dissolved inorganic nutrient environment, the ingestion of prey that was balanced in terms of nitrogen and phosphorus content resulted in a considerably higher increase in zooxanthellae density and polyp size (Figure 5.3), despite the difference in food quality being driven by an increase in nitrogen content rather than by a decrease in phosphorus content (Figure 5.1e). Moreover, polyp size was considerably larger as a result of the LA feeding treatment as compared to the HP feeding treatment within the +N-P system, thus placing a greater value on food quality over quantity, and highlighting the importance of nutrient balance to coral health.

4.5.3. The effects of heterotrophic nitrogen and phosphorus uptake on coral stress resilience

The ratio of heterotrophic nitrogen and phosphorus intake had a considerable effect on coral stress resilience. Phosphate deprivation precipitated by dissolved inorganic nitrogen enrichment has previously been observed to increase thermal sensitivity of reef corals (Wiedenmann et al., 2013). Concurrent with this study, imbalanced nutrient intake by the ingestion of nitrogen enriched prey also decreased coral stress tolerance relative to corals receiving a balanced input of heterotrophic nutrients. Zooxanthellae stress resilience, measured by the rate of decline in photosynthetic efficiency of PSII (Fv/Fm), was not enhanced in samples feeding on prawn relative to unfed samples, irrespective of food quantity (Figures 5.4, 5.6a). Moreover, even a low feeding rate on Artemia resulted in a significant increase in zooxanthellae stress resilience relative to prawn-fed or unfed samples. In a study by Borell & Bischof a high photosynthetic efficiency of PSII was maintained in zooxanthellae harboured by fed corals exposed to heat stress, while a significant decline in Fv/Fm was measured in unfed corals (Borell and Bischof, 2008). The current findings are in agreement with this observation, implicating that heterotrophic feeding can significantly increase the stress tolerance of zooxanthellae by limiting chronic photoinhibition, however only if the intake of heterotrophic nitrogen and phosphorus is balanced.

Correspondingly, the stress resilience of the coral host, measured by the rate at which the skeletal tissue cover receded with exposure to 30°C, was also only increased in response to

a balanced intake of heterotrophic nitrogen and phosphorus. Thus, when in combination with limited dissolved inorganic nutrient availability, polyp biomass was lost at a faster rate in response to the prawn-fed or unfed treatment compared to the Artemia-fed samples, though this difference was not significant (Figure 5.6b). Furthermore, within the +N-P treatment, the biomass of polyps exposed to the HP feeding treatment declined at an even faster rate than unfed samples. Additionally, for both food types, a low level of feeding was observed to be more beneficial to coral stress tolerance when in combination with imbalanced dissolved inorganic nutrient availability. Yet, the effects of the different feeding treatments to the rate of decline in polyp biomass was much less notable than the effects observed for the decline in Fv/Fm, indicating that the ratio of heterotrophic nitrogen and phosphorus intake is more critical for the stress response of the zooxanthellae than for that of the coral host (Figure 5.6). However, the starting point for polyp biomass was significantly increased as a result of heterotrophy, meaning that it would take longer for all biomass to be lost during stress exposure (Figures 5.5 and 5.7). Thus, contrary to what was observed for the zooxanthellae, heterotrophy did not considerably limit the effects of heat stress to the coral host, but supplied it with more energy reserves in the form of biomass, thus providing a greater chance of survival and recovery as a result of feeding. This is in agreement with past observations (Grottoli et al., 2006; Connolly et al., 2012). Yet, the extent of this benefit provided by heterotrophy was strongly dependent on the balance of heterotrophic nitrogen and phosphorus intake.

The stress treatment resulted in a gradual decline in the food ingestion rate in all feeding treatments (Figure 5.8). The feeding rate on prawn declined faster than that on Artemia, and polyps receiving large portions reduced their ingestion rates earlier than those receiving small portions. The latter observation likely relates to the greater physical effort needed to ingest a prey item of larger size. The former observation does indicate that a balanced intake of heterotrophic nutrients provided the polyps with more energy needed to maintain feeding efforts. Interestingly, the ingestion rate of prawn declined slower in the +N-P system compared to the -N-P system, despite polyps within the imbalanced nutrient system having a comparatively lower initial feeding rate on the prawn. On the other hand, dissolved inorganic nutrient availability had no effect on the decline in feeding rate on Artemia. Several studies have observed feeding rates to increase in response to temperature stress in certain species (Ferrier-Pagès et al., 2010). This was not observed in the current

study, possibly because feeding rates were already increased in order to compensate for diminished dissolved inorganic nutrient availability.

A high availability of nitrate in the +N-P system increased the stress resilience of zooxanthellae relative to those experiencing deprivation of both nitrate and phosphate, with the rate of decline in Fv/Fm being slower within the +N-P system (Figures 5.4 and 5.6a). Yet, the decline in health of the coral host, measured by the rate of reduction of skeletal tissue cover, was more severe as a result of imbalanced dissolved inorganic nutrient availability (Figure 5.5 and 5.6b). Interestingly, the mechanism of polyp biomass decline was different in the two nutrient systems. Within the -N-P system the skeletal tissue cover receded steadily up to the edge of the corallite skeleton and then continued to recede along the inside edge of the skeleton until either no tissue biomass remained or the persisting polyp was overgrown by bacterial films. Contrary, within the +N-P system, skeletal tissue cover receded rapidly until the edge of the skeleton followed by complete detachment of the polyp from the skeleton. This process occurred particularly rapidly in response to the HP treatment (Figure 5.5). The inconsistency of this process among the two nutrient environments speaks against this being a general escape strategy of *E. paradivisa*. Rather, it is proposed that phosphorus deprivation resulting from the nutrient imbalance hinders the connection between the calicoblastic epithelium and the skeleton, likely due to impairment of calcification as a result of imbalanced nutrient availability. Enrichment of nitrate alone has previously been observed to decrease the calcification rate and, moreover, was found to be particularly deleterious when in combination with heterotrophic feeding (*Artemia salina*) (Ezzat et al., 2015).

4.5.4. Implications for coral reefs

This study demonstrated that heterotrophy provides considerable benefit, particularly to the coral host, yet that a balanced and plentiful supply of dissolved inorganic nutrients is more critical for the sustenance of the coral holobiont physiology. Thus, even highly exaggerated prey abundance cannot compensate for dissolved inorganic nutrient deprivation in *E. paradivisa*. Importantly, heterotrophy only increased coral stress resilience when the intake of heterotrophic nitrogen and phosphorus was balanced. This highlights the value of heterotrophy as a source of phosphorus to the symbiosis. Particularly in coastal environments, which are highly susceptible towards nutrient pollution through various anthropogenic activities, the ratio of dissolved inorganic nitrogen and phosphate can

become imbalanced (Peñuelas et al., 2013). If nitrogen enrichment is passed down the food chain, increasing the N:P stoichiometry of zooplankton, this has the potential of aggravating the resulting phosphorus limitation of the zooxanthellae in species that have a high capacity for predation. Thus, the benefit of heterotrophic feeding towards the stress resilience of reef coral species that rely heavily on predation (Grottoli et al., 2006) may be lost or even become deleterious if the food source becomes nutritionally imbalanced. The negative repercussions of a nutrient enrichment often do not persist a great distance from the source of the pollution due to the fast uptake and turnover of the nutrients by pelagic communities (Furnas et al., 2005). Yet, the finding that imbalanced growth can be caused by heterotrophy raises the possibility of a coastal nutrient imbalance precipitating phosphorus limitation of corals located on more distant reefs as a result of the dispersal of a phytoplankton bloom and the thereon feeding zooplankton away from the source of the imbalance. However, the ecological relevance of this concept remains to be investigated. Yet, it is apparent that the nutritional quality of prey items is critical when considering the benefit of heterotrophic feeding towards the physiology and stress resilience of reef corals. It is therefore vital to manage disruptions to natural nitrogen and phosphorus ratios in coastal environments in order to support a high resilience of coral reefs to climate change driven increases in sea surface temperatures.

Chapter 5: Distinct lipid profiles of two clades of endosymbiotic algae isolated from the same coral host species give new insight into the basis of their divergent heat stress tolerance

Sabrina Rosset[1], Cecilia D'Angelo[1], Grielof Koster[2], Joost Brandsma[2], Alan Hunt[2], Anthony Postle[2], Jörg Wiedenmann[1]

1. *Coral Reef Laboratory, University of Southampton, Waterfront Campus, SO14 3ZH Southampton, UK*
2. *Faculty of Medicine, University of Southampton, Southampton General Hospital, SO16 6YD Southampton, UK*

Author contribution:

Cecilia D'Angelo and Jörg Wiedenmann designed the study and cultured the coral specimens used. Cecilia D'Angelo and Sabrina Rosset optimised the method for lipid analysis. Sabrina Rosset prepared the samples and collected and analysed all data. Grielof Koster, Joost Brandsma, Alan Hunt and Anthony Postle provided assistance with method development and data interpretation. Sabrina Rosset wrote the chapter. Cecilia D'Angelo provided comments.

5.1. Abstract

The polar lipid biochemistry of two clades of *Symbiodinium* (C and D) harboured by reef corals were analysed, providing the first detailed description of the *Symbiodinium* lipidome. The identification of inherent differences in membrane composition is a promising target for the understanding of the underlying basis of the differing thermal sensitivity in these endosymbiotic algae. Different genotypes of the reef coral *Acropora*

valida harbouring either clade C or D *Symbiodinium* were cultured under controlled laboratory conditions, providing a model for a host- and environment-independent comparison of these clades. Twelve classes of polar lipids were analysed by electrospray ionisation tandem mass spectrometry (ESI-MS/MS). The lipid biochemistry was shown to be distinct in the two clades, particularly apparent by differences in the degree of DGDG and SQDG saturation, as well as large differences in the abundance of MGDG, TGDG, DGCC, PC, and PG. PC was shown to be present in both diacyl and mono-alkyl forms, the ratio of which was also clade dependent. The observed increase in chloroplast membrane saturation and decrease in the MGDG:DGDG ratio of clade D samples likely relates to the heightened thermal resistance of this clade. Yet, the most significant differences in the lipid biochemistry were associated with extraplastidic membranes, providing compelling evidence for true metabolic and physiological differences among *Symbiodinium* clades.

5.2. Introduction

The symbiosis of reef-building corals with dinoflagellates of the genus *Symbiodinium*, allows corals to thrive in an often highly oligotrophic environment due to the algae's capacity of assimilating dissolved inorganic nutrients and to the translocation of a considerable proportion of photosynthates to the coral host (Muscatine and Porter, 1977; Falkowski et al., 1984; D'Elia and Webb, 1977). Yet, increasing sea surface temperatures precipitated by climate change is placing immense pressure on reef corals globally, threating the valuable ecological and economic services provided by coral reefs (Hughes et al., 2003; Baker et al., 2008; Wild et al., 2011; Logan et al., 2014). Heat stress can result in coral bleaching which is the loss of the algal symbionts and/or their pigments from the coral host and often leads to mortality due to resultant energy deficiency of the coral (Brown, 1997). The exact mechanisms triggering coral bleaching are not fully understood, yet likely involve the loss of thylakoid membrane stability, resulting in impairment of photosystem function and ultimately, in the increased production of reactive oxygen species which cause cellular damage of the host animal (Warner et al., 1999; Lesser, 1997; Tchernov et al., 2004). Yet, corals can associate with genetically distinct *Symbiodinium* types which vary in their thermal sensitivity, thereby influencing the capability of its coral host to withstand heat stress (Rowan, 2004). Particularly clade D has been famed for its high thermal tolerance (Berkelmans and van Oppen, 2006; Jones et al., 2008). However, physiological and biochemical differences that characterise *Symbiodinium* types and

underpin their varied ecological roles remain very poorly understood. Grasping what traits distinguish thermally tolerant from thermally sensitive *Symbiodinium* types is critical in order to study and predict the capacity of reef corals to acclimate and adapt to future climate change scenarios.

Remodeling of cellular membranes by photosynthetic organisms is a fundamental homeostatic response to various abiotic stressors and a principal method of adaptation to different environments (Welti et al., 2007; Zheng et al., 2011). Key to this process is the adaptation of membrane fluidity which entails changes to fatty acid chain length and degree of unsaturation, the ratio of bilayer stabilising and non-stabilising lipids, the size, hydrophobicity and charge of polar lipid headgroups, and the ratio of cholesterol and proteins to polar lipids (Sato et al., 1996; Hartmann, 1998; Lee, 2004; Mizusawa et al., 2009). Heat stress induces an increase in membrane fluidity which impacts membrane dynamics and integrity, giving rise to increased membrane permeability and impairment of the function of integral proteins such as ion channels, enzymes, and, most critically for photosynthetic organisms, the photosynthetic apparatus (Horváth et al., 2012; Wada et al., 1994). Correspondingly, particularly adaptation of the chloroplast lipid composition has been well studies in plants and algae exposed to temperature stress (Moellering and Benning, 2011). The lipid composition of thylakoid membranes is highly conserved (Mizusawa and Wada, 2012), being composed predominantly of the neutral galactolipids MGDG and DGDG, as well as the anionic lipids SQDG and PG which are minor components. In response to heat stress the ratio in which MGDG and DGDG occur has been observed to decrease (Chen et al., 2006; Légeret et al., 2015). This is explained by the fact that DGDG is a bilayer forming lipid while MGDG forms non-bilayer structures (inverted hexagonal) when not in contact with proteins (Simidjiev et al., 2000). The proportion of non-bilayer structures increases with heat stress, thus compromising membrane integrity (Chen et al., 2006). Consequently, a decrease in the ratio of MGDG to DGDG functions to retain thylakoid membrane integrity (Chen et al., 2006). Additionally, an increase in the degree of DGDG saturation is a prevalent response to high temperature stress (Chen et al., 2006). The identification of inherent differences in chloroplast lipid composition is therefore a principal hypothesis for the understanding of varying heat stress tolerance of *Symbiodinium* types.

Previous studies on the lipids of *Symbiodinium* associated with reef corals have only focused on the fatty acid composition and predominantly analysed *Symbiodinium* in

culture. A high abundance of the polyunsaturated fatty acids (PUFAs) 18:3, 18:4, 18:5, 20:5 and 22:6 have been proposed to be *Symbiodinium* fatty acid markers (Papina et al., 2003; Imbs et al., 2014; Chen et al., 2015). An inherent increase in thylakoid membrane saturation has previously been suggested to underlie *Symbiodinium* thermal tolerance due to an observed decrease in the degree of C18 fatty acid unsaturation along with the maintenance of thylakoid membrane integrity during exposure to high temperature stress in types with high thermal tolerance (Tchernov et al., 2004). However, two further studies found that thermal sensitivity had no effect on the degree of fatty acid unsaturation of both unstressed and thermally-stressed *Symbiodinium* (Díaz-Almeyda et al., 2010; Kneeland et al., 2013). Importantly, the analysis of total fatty acid profiles cannot differentiate between fatty acids associated with polar lipids or storage lipids, thus making it relatively uninformative considering that in other photosynthetic organisms the decrease in chloroplast PUFA content in response to thermal stress has been found to occur by transfer of PUFA from galactolipids to triacylglycerols (TAGs), thus retaining the PUFAs within the cell (Légeret et al., 2015; Hemme et al., 2014). While the degree of fatty acid unsaturation may indeed play a role in thermal stress tolerance of the coral-algal symbiosis, the analysis of associated lipid classes is needed in order to obtain a true picture of the importance of algal membrane composition to the resilience of reef corals.

Elucidating the *Symbiodinium* lipidome would provide great insight into biochemical differences between clades and further our understanding of the adaptability of the coral-algal symbiosis to a changing environment. This study aimed to identify key inherent differences in the membrane composition of two *Symbiodinium* clades harboured by reef corals and known for possessing different thermal sensitivities. Thereby, we provide the first detailed analysis of *Symbiodinium* polar lipid composition *in hospite*, as analysed by electrospray ionisation tandem mass spectrometry (ESI-MS/MS). The cultivation of distinct genotypes of *Acropora valida* harbouring either clade D or clade C *Symbiodinium*, under controlled laboratory conditions, provided an excellent model for a host- and environment-independent analysis of the *Symbiodinium* lipidome. The lipid biochemistry of these two clades was shown to be distinct, providing extensive evidence of true metabolic and biochemical differences among *Symbiodinium* clades, and giving insight into the underlying biochemical basis of thermal tolerance in this organism.

5.3. Methods

5.3.1. Coral culture and sample preparation

Colonies of three distinct genotypes of *Acropora valida* were cultured within a single tank unit of the experimental mesocosm at the University of Southampton (D'Angelo and Wiedenmann, 2012). Corals were cultured at a constant temperature of 25°C and light intensity of 150µmol s^{-1} m^{-2} with a 12/12 hour light/dark cycle. Measurable nutrients in the water were representative of oligotrophic conditions (NO_3^- ~0.65µM, PO_4^{3-} ~0.21µM).

Symbiodinium spp. were sampled from three separate fragments of each of the three *A. valida* genotypes, giving three replicates per genotype. The algal cells were extracted by spraying coral fragments with sterile seawater using an airbrush and purified by repeated steps of centrifugation (2500 x g) and washing of the pellet in sterile seawater. Due to the extraction of algal cells from host tissue, the possibility of the samples not being completely free of host material must be considered. Furthermore, it is not clear whether the symbiosome membrane complex, including the host-derived outer symbiosome membrane, which surrounds the algal cells in the symbiotic state is retained within the purified symbiont preparations (Wakefield et al., 2000). However all samples and replicates were processed in the same way, thus making preparations consistent. Algal cells obtained in each extract were counted using a haemocytometer and mean cell size was measured by microscopic analysis to ensure that there was no significant difference in cell size.

5.3.2. *Symbiodinium* spp. phylotyping

Genomic DNA was extracted and the ribosomal DNA section including the ITS2 and surrounding regions were amplified by PCR using specific primers (Hume et al., 2013). The PCR product was cloned using StrataClone PCR cloning kit (Aligent Technologies) and plasmid DNA was purified using a QIAprep Spin miniprep kit (Qiagen). Sequencing was performed by Macrogen. *Symbiodinium* type was identified by comparison of sequences of the ITS2 region (220bp) with reference sequences by performing BLAST searches (www.ncbi.nlm.nih.gov/ blast). Two host genotypes (one brown and one purple colour morph) were identified as harbouring clade C of the same type (C3k: eg. GenBank: GU111904.1). The third genotype (purple colour morph) was identified as harbouring clade D (D1a: eg. GenBank: JN558080.1). Hereafter, samples of clade C *Symbiodinium*

isolated from the brown *A. valida* colour morph are referred to as CA, and clade C isolated from the purple host colour morph are referred to as CB.

5.3.3. Lipid extraction

Symbiodinium cell pellets were standardized to contain an equal cell number ($2x10^6$) before extracting total lipids by modified Bligh and Dyer method (Bligh and Dyer, 1959). Accordingly, cell pellets were re-suspended in 800µl Hank's balanced salt solution (HBSS) followed by the sequential addition of 1ml dichloromethane, 2ml methanol, 1ml dichloromethane and 1ml of demineralised water with vigorous mixing after the addition of each solvent. Samples were centrifuged for 10 minutes (40'000 g) to achieve phase separation. The lower organic phase was transferred into a glass vial, dried under a stream of nitrogen gas at 37°C, and stored at -20°C.

5.3.4. Lipid analysis

5.3.4.1. Chromatography conditions

Dried lipid extracts were dissolved in 100% methanol and delivered onto a diol column (PrincetonSPHERE 100 DIOL 100Å 5µ, 150 x 2.1mm) using an Agilent 1100 LC system with an autosampler (Agilent Technologies). The diol column was maintained at a constant temperature of 22°C. Chromatographic separation of lipids was achieved by using a gradient of 100% solvent A to 48% solvent A over 20 minutes, followed by an increase to 28.5% solvent A in 5 minutes. The final solvent ratio was maintained for 10 minutes. Solvent flow was 0.4ml/minute. Solvents constituted of (by volume): solvent A = 800:200:0.9:0.36 *n*-hexane:isopropanol:formic acid:25% aqueous ammonium hydroxide; solvent B = 900:100:0.9:0.36 isopropanol:water:formic acid:25% aqueous ammonium hydroxide, as in (Popendorf et al., 2013). The result of lipid class separation by means of this method is shown in Figure A4.1.

5.3.4.2. Mass spectrometry conditions

Analysis of the lipids was performed using a triple quadrupole tandem mass spectrometer with electrospray ionisation interface (ESI-MS/MS) (Xevo, Waters, UK) (Han and Gross, 2005). Instrument parameters were set as follows: the source temperature was 150°C, desolvation temperature was 200°C, 3.22kV to electrospray capillary, 50V cone energy, and the collision gas used was N_2. The lipid classes Monogalactosyldiacylglycerol

(MGDG), Digalactosyldiacylglycerol (DGDG), Trigalactosyldiacylglycerol (TGDG), Sulfoquinovosyldiacylglycerol (SQDG), Diacylglyceryl hydroxymethyl trimethyl-b-alanine (DGTA), Diacylglyceryl trimethyl homoserine (DGTS), Diacylglyceryl carboxyhydroxymethylcholine (DGCC), Phosphatidylcholine (PC), Phosphatidylethanolamine (PE), Phosphatidylglycerol (PG), Phosphatidylserine (PS), and Phosphatidylinositol (PI) were identified by the use of precursor or neutral loss scans specific to diagnostic head group fragments of each lipid class (Table 6.1). Each scan of a particular lipid class produced a total ion current chromatogram representative of all lipid species within the given class. The total abundance of a given lipid class was determined by integration of the respective chromatogram peak area (Table A4.1). The relative abundance of individual lipid species within each class was determined by integration of the spectral peak areas and determination of the percent contribution of each peak area to the total (Tables A4.2-4.17). For this means, a threshold of 2% was set, with peak areas above this threshold considered as significant components of a respective lipid class. All chromatograms and mass spectra were processed using Masslynx software (Waters, UK). For each chromatogram and mass spectra, background noise was subtracted and the data was smoothed prior to analysis. Processed mean spectra for each analysed lipid class are presented in appendix 4.

Table 5.1: Mass spectrometry conditions for the analysis of twelve classes of polar lipids by ESI-MS/MS

Lipid group	Lipid class	Molecular ion	Scan type	Precursor or neutral loss mass	Ionisation energy	Collision energy (V)
Glycolipids	MGDG	$[M+NH_4]^+$	Neutral loss	179	ES+	22
	DGDG	$[M+NH_4]^+$	Neutral loss	341	ES+	24
	MGDG/ DGDG	$[M+NH_4]^+$	Precursor	243	ES+	58
	TGDG	$[M+NH_4]^+$	Neutral loss	503	ES+	28
	SQDG	$[M+NH_4]^+$	Neutral loss	261	ES+	24
Betaine lipids	DGCC	$[M+H]^+$	Precursor	104	ES+	40
	DGTS/A	$[M+H]^+$	Precursor	236	ES+	32
Phospholipids	PC	$[M+H]^+$	Precursor	184	ES+	32
	PE	$[M+H]^+$	Neutral loss	141	ES+	28
	PG	$[M+NH_4]^+$	Neutral loss	189	ES+	18
	PS	$[M+H]^+$	Neutral loss	185	ES+	22
	PI	$[M+NH_4]^+$	Neutral loss	241	ES-	41

5.3.4.3. Lipid quantification

Lipid classes were quantified by the indirect method employing lipid standards (Avanti polar lipid). Thereby, the abundance of each lipid class was extrapolated from a standard curve of chromatogram peak areas determined at different concentrations of each lipid standard. This served as a control, verifying that lipids were measured within a linear range of their concentration. PS and PI were not quantified. Furthermore, no lipid standards were commercially available for DGCC or TGDG. For the latter lipid classes, different concentrations of a *Symbiodinium* sample were measured in order to confirm the linear response of signal intensity to lipid concentration.

The *Symbiodinium* galactolipids, MGDG and DGDG, were not compatible with corresponding commercial standards. This was noted due to the significantly higher signal intensity of *Symbiodinium* MGDG and DGDG compared to MGDG and DGDG standards when using NL179 and NL341 scans as compared to using the alternative scans, NL197 and NL359, which resulted in the inverse observation. These two sets of neutral loss scans differ in the retention of a water molecule by the head group fragment. It is proposed that *Symbiodinium* MGDG and DGDG are chemically distinct from the plant galactolipid standards. The possibility of them being ether lipids was ruled out by the analysis of the ultimate masses of key species by Fourier-transform MS. While certainly being glycolipids, it is proposed that they possess a different sugar moiety than galactose. Further analysis of *Symbiodinium* glycolipids is required in order to establish the exact chemical configurations of these lipid classes. In order to quantify MGDG and DGDG the precursor scan 243 ES+ was employed which produced equal signal intensity for sample and standard lipids. Samples and standards were re-suspended and combined using the solvent dichloromethane:methanol:50mM sodium acetate in water, 300:665:35 (Welti et al., 2003). This solution was loaded by direct infusion with 5µl/min flow rate. A collision energy of 58V was used which produced equal signal intensity for MGDG and DGDG spectra. Thereby galactolipid standards were used as internal standards, allowing for direct comparison within the obtained mass spectra. For the purpose of the comparison of MGDG and DGDG abundance among the analysed *Symbiodinium* clades, both results obtained from NL179/341 and P241 scans were considered.

5.3.5. Statistical analysis of data

The data are expressed as mean ± standard deviation (n = 3). Significant differences in lipid class abundance as well as in lipid class composition between the three samples were determined by one way analysis of variance (ANOVA) followed by Tukey's test for pairwise comparison (Sigmaplot). Differences were considered to be significant with $P < 0.05$.

Colonies of the same colour morph harbouring either clade C (CB) or D were used as direct comparison of cladal differences in lipidome composition. The remaining genotype harbouring clade C (CA) was used as a control to determine that differences identified were indeed clade dependent.

5.4. Results

5.4.1. Glycolipids

Clade D was measured to have a lower abundance of MGDG (Figure 6.1a). Yet, the relative abundance of lipid species comprising MGDG was the same for both clades (Figure 6.1b). Furthermore, no difference in the abundance of DGDG was recorded (Figure 6.1c). Both MGDG and DGDG mainly constituted of 38:9 and 38:10 in both clades. However, the composition of DGDG species differed between the two clades. Clade D contained a higher relative abundance of 36:8, 36:9 and 38:9, while clade C contained a higher relative abundance of 36:6, 38:10 and 42:11 (Figure 6.1d).

Both clades were also found to contain TGDG, this lipid class being significantly more abundant in clade C compared to clade D (~3-fold higher) (Figure 6.1e). TGDG was mostly comprised of 30:0, 32:0, 38:9 and 38:10, however, the relative abundance of TGDG lipid species differed between the two clades with clade C containing a significantly higher relative abundance of 30:0, 32:0, 34:1, and 36:0, and clade D containing a greater relative abundance of 34:4, 34:5, 36:8, 36:9, and 38:9 (Figure 6.1f).

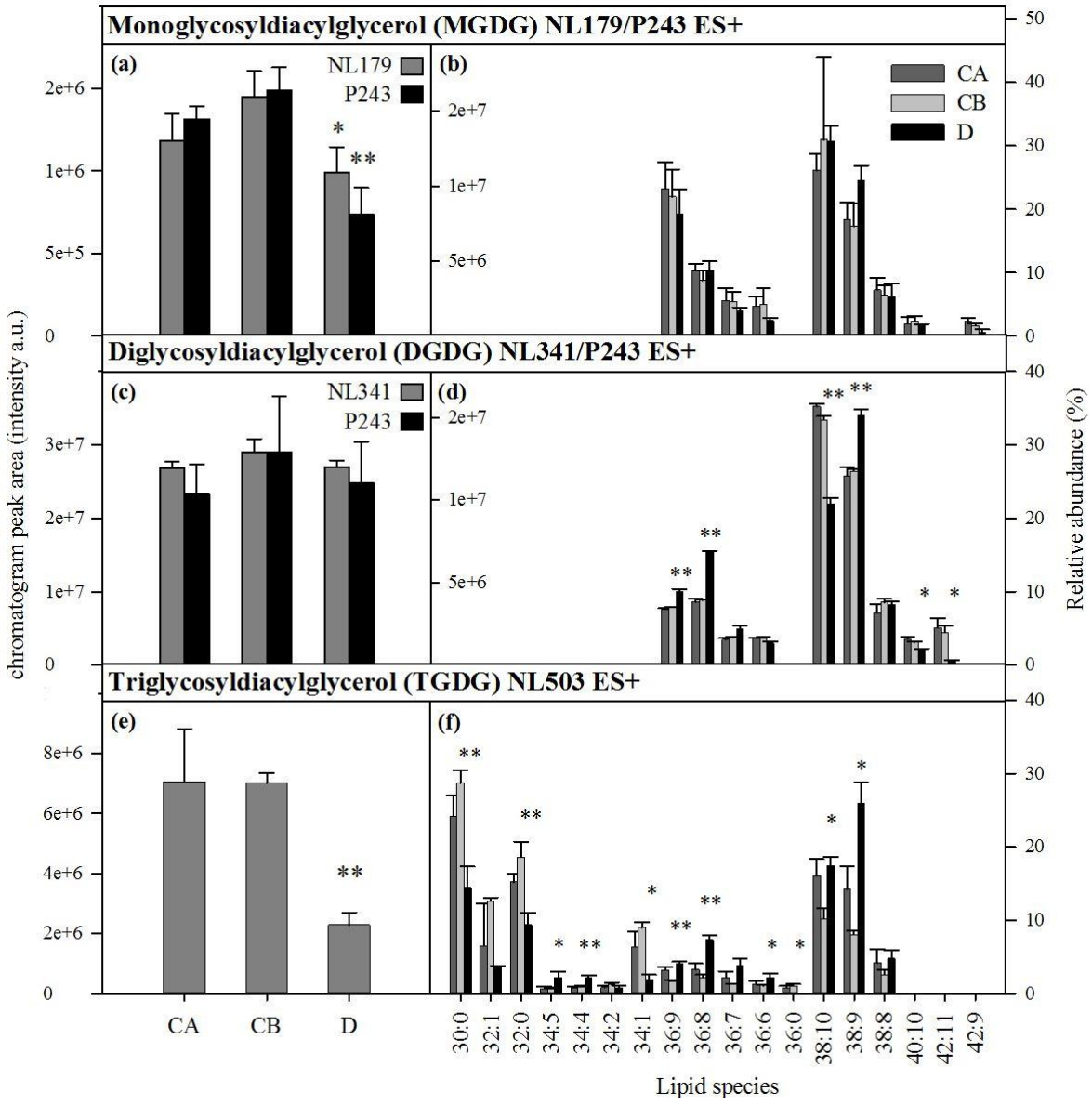

Figure 5.1| Glycolipid abundance and composition. Total lipid class abundance measured as signal intensity of integrated chromatogram peak area for **(a)** MGDG, **(c)** DGDG and **(e)** TGDG. Total abundance of MGDG and DGDG were determined both by neutral loss (grey) and by precursor scans (black). Relative composition of lipid species measured as the percent contribution to total lipid class for **(b)** MGDG, **(d)** DGDG and **(f)** TGDG. The colour legend depicted in graph (b) also applies to (d) and (f): CA (dark grey), CB (pale grey), and D (black). CA = *Symbiodinium* clade C isolated from brown *A. valida* colour morph, CB = *Symbiodinium* clade C isolated from purple *A. valida* colour morph, D = *Symbiodinium* clade C isolated from purple *A. valida* colour morph. Significant differences between samples CB and D are indicated by the use of asterisk. * = $p<0.05$, ** = $p<0.001$.

No significant difference in the concentration of SQDG was apparent between the two clades (Figure 6.2a). Yet, the composition of SQDG species was clade-specific, with clade C containing a higher relative abundance of 30:1 but a lower relative abundance of 32:0 compared to clade D (Figure 6.2b).

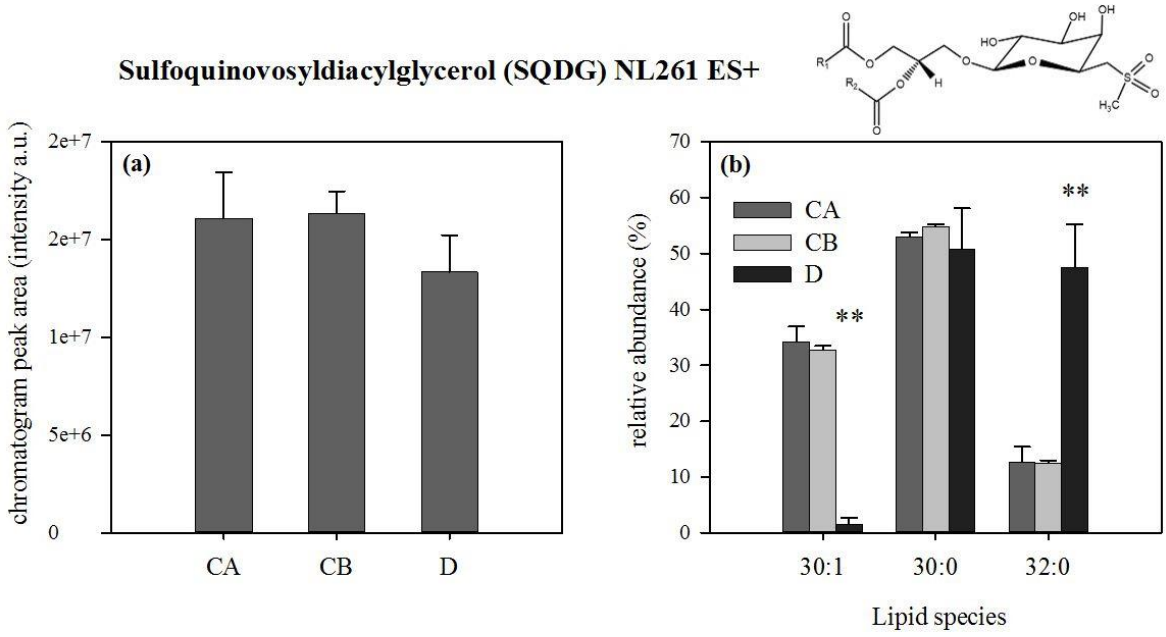

Figure 5.2| SQDG abundance and composition. (a) SQDG signal intensity measured by integration of chromatogram peak area. **(b)** Relative composition of SQDG lipid species measured as percentage contribution of total: CA (dark grey), CB (pale grey), and D (black). CA = *Symbiodinium* clade C isolated from brown *A. valida* colour morph, CB = *Symbiodinium* clade C isolated from purple *A. valida* colour morph, D = *Symbiodinium* clade C isolated from purple *A. valida* colour morph. Significant differences between samples CB and D are indicated by the use of asterisk. * = $p<0.05$, ** = $p<0.001$.

5.4.2. Betaine lipids

The *Symbiodinium* lipidome was found to have a very high abundance of the betaine lipid DGCC. The other known betaine lipids DGTA and DGTS were not detected. A very large difference in the abundance of DGCC was observed between clade C and D (Figure 6.3a). Clade C lipidomes were compromised of ~4.8-fold higher DGCC content compared to clade D. The relative abundance of DGCC species was also considerably different between the two clades (Figure 6.3c). Clade C DGCC was comprised predominantly by 38:6 and also contained high amounts of 36:5 and 38:5. Clade D DGCC was comprised largely of

44:12 and 42:11. However, clade D was measured to contain a higher abundance of lyso-DGCC (~2.6-fold higher). Clade D contained mostly 22:6 and also relatively high amounts of 20:5 and 18:0. Clade C lyso-DGCC species were comprised largely of 16:0 with 22:6, 20:5 and 18:0 also being relatively abundant (Figure 6.3b).

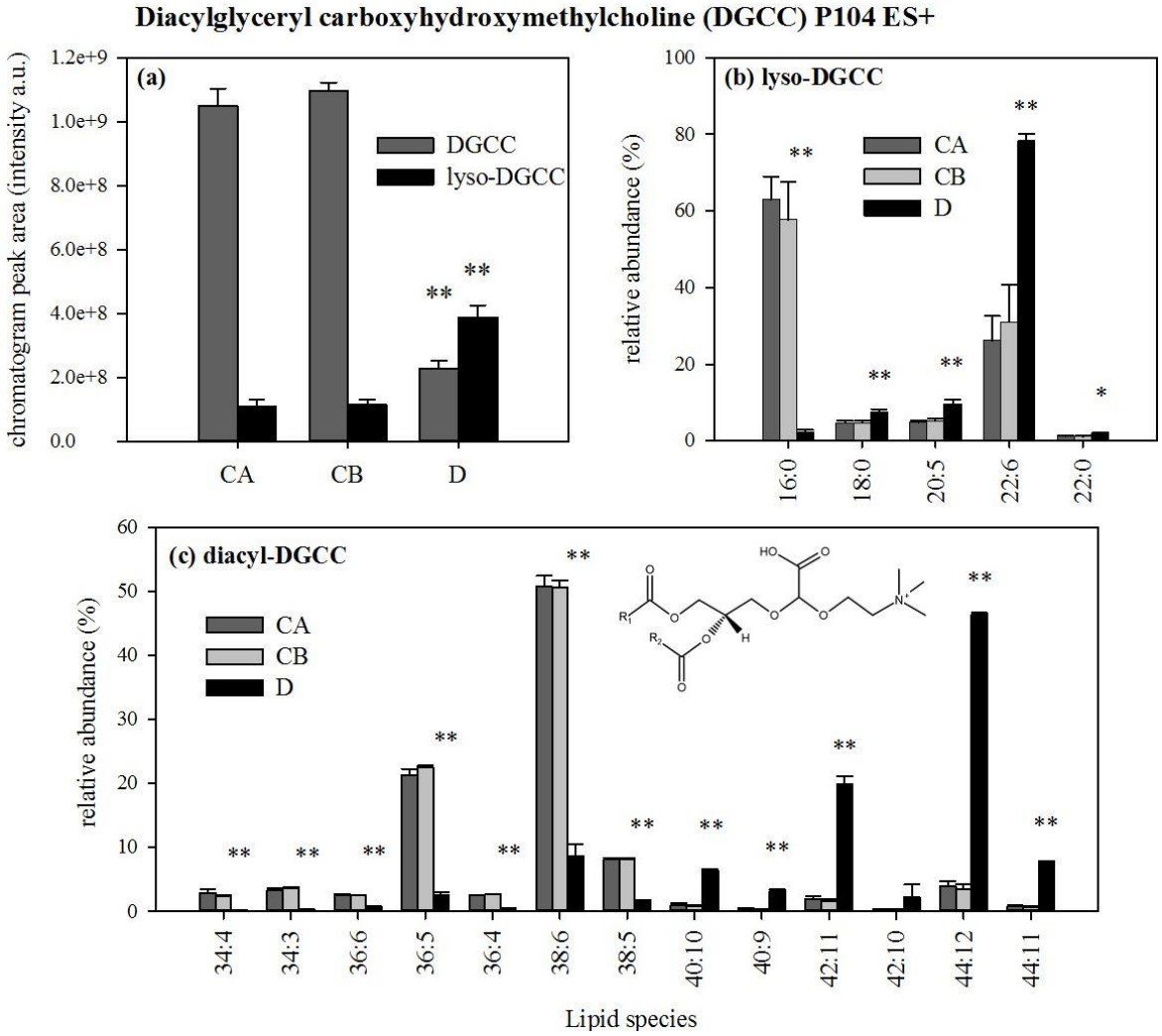

Figure 5.3| DGCC abundance and composition. (a) Total lipid class abundance measured as signal intensity of integrated chromatogram peak area for DGCC (grey) and lyso-DGCC (black). Relative composition of lipid species measured as percent contribution to total lipid class for **(b)** lyso-DGCC and **(c)** diacyl-DGCC. The same colour legend applies to (b) and (c): CA (dark grey), CB (pale grey), and D (black). CA = *Symbiodinium* clade C isolated from brown *A. valida* colour morph, CB = *Symbiodinium* clade C isolated from purple *A. valida* colour morph, D = *Symbiodinium* clade C isolated from purple *A. valida* colour morph. Significant differences between samples CB and D are indicated by the use of asterisk. * = $p<0.05$, ** = $p<0.001$.

5.4.3. Phospholipids

Clade D *Symbiodinium* contained a significantly larger amount of PC compared to clade C (~1.7-fold increase) (Figure 6.4a). In both clades PC was found to be present as diacyl and as mono-alkyl forms. This was inferred due to the different retention times of PC species,

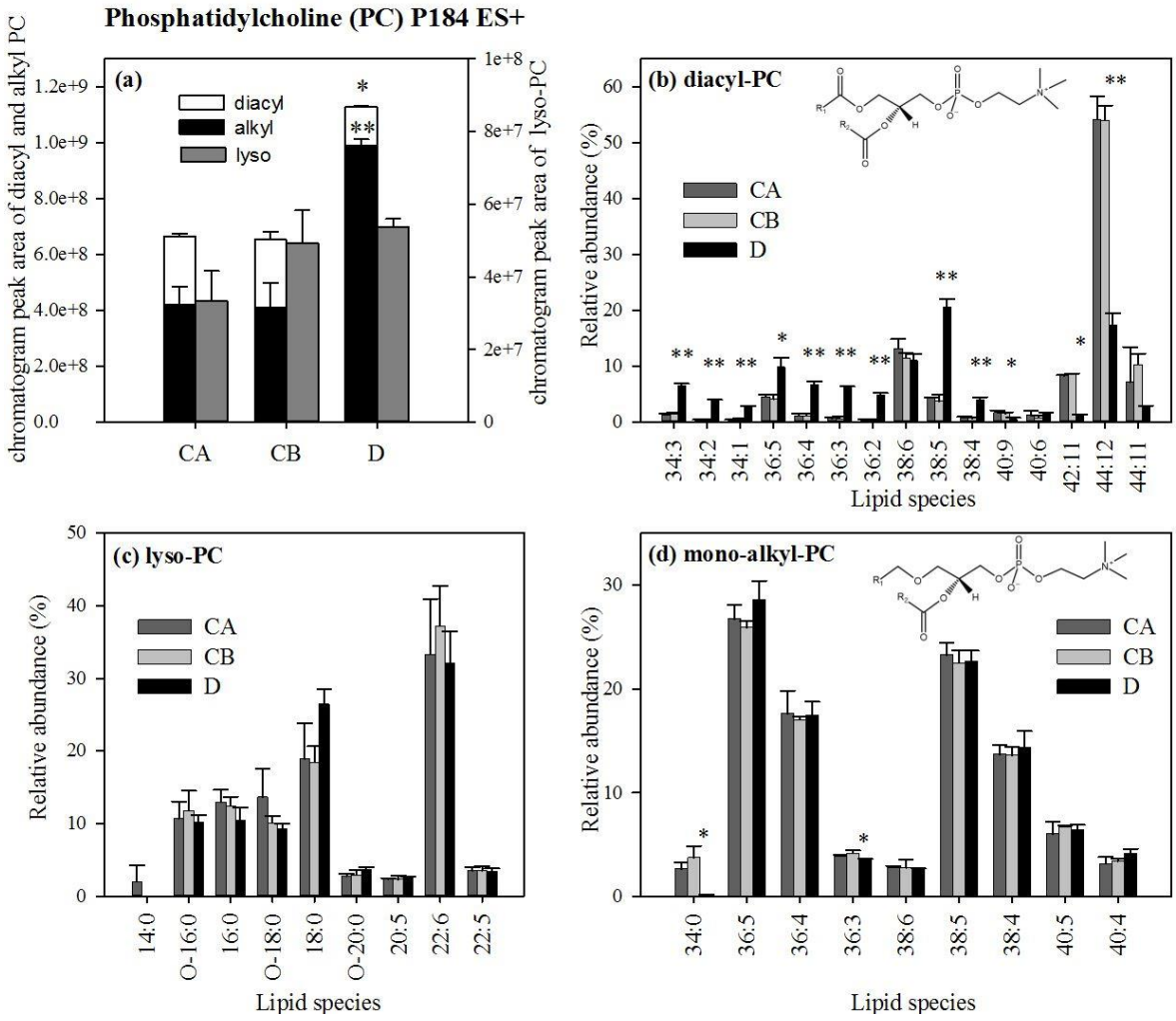

Figure 5.4| PC abundance and composition. (a) Total lipid class abundance measured as signal intensity of integrated chromatogram peak area for diacyl- (white), lyso- (dark grey) and mono-alkyl-PC (black). Relative composition of lipid species measured as percent contribution to total lipid class for **(b)** diacyl-PC, **(c)** lyso-PC and **(d)** mono-alkyl-PC. The prefix O- indicates that the lyso species contains an alkyl ether rather than an acyl chain. The same colour legend applies to (b), (c) and (d): CA (dark grey), CB (pale grey), and D (black). CA = *Symbiodinium* clade C isolated from brown *A. valida* colour morph, CB = *Symbiodinium* clade C isolated from purple *A. valida* colour morph, D = *Symbiodinium* clade C isolated from purple *A. valida* colour morph. Significant differences between samples CB and D are indicated by the use of asterisk. * = $p<0.05$, ** = $p<0.001$.

with mono-alkyl species eluting in a peak prior to the diacyl species (Figure A4.10a). Of these, mono-alkyl species were the dominant form of PC. While clade D had a higher abundance of both diacyl and mono-alkyl PCs, particularly mono-alkyl forms of PC were significantly higher within clade D (~2.4-fold higher). There is thus a difference in the ratio of diacyl to mono-alkyl forms apparent between the clades (diacyl : alkyl D = 1 : 7.2; C = 1 : 1.7). Yet, there was no significant difference in the relative composition of mono-alkyl PC species between the clades (Figure 6.4d). Mono-alkyl PCs largely constituted of 36:4, 36:5 38:4, 38:5 and 40:4, 40:5. However, differences in the relative abundance of diacyl PC lipid species were apparent, with clade D having an increased abundance of species expected to be composed of shorter and more saturated fatty acids (34:1, 34:2, 34:3, 36:2, 36:3, 36:4, 38:5) while clade C contained a very high abundance of the longer and more unsaturated fatty acid-containing 44:12 (likely 22:6/22:6), as well as higher relative abundance of 42:11 (likely 22:6/20:5) and 44:11 (likely 22:6/22:5) (Figure 6.4c). No significant difference in the abundance or in the species composition of lyso-PC was measured between the clades (Figure 6.4b). Abundant lyso-PC species identified included alkyl 16:0 and 18:0 and acyl 16:0, 18:0 and 22:6.

The NL141 scan corresponding to the loss of the PE headgroup fragment resulted in two peaks (Figure A4.11a). The first peak was identified as PE. This lipid class was observed to be significantly more abundant in clade C samples (Figure 6.5a). The second chromatogram peak represents ceramide PE (Cer-PE), the abundance of which was much higher than PE and did not differ significantly among the analysed samples (Figure 6.5c). The relative abundance of PE and Cer-PE species was the same in both clades (Figure 6.5b,d). The PE and Cer-PE lipid species could not be determined due to the possibility of these being diacyl, mono-alkyl, or mono-alkenyl species.

The abundance of PG was significantly lower (~4.6-fold) in clade D compared to clade C (Figure 6.5e). The composition of PG species was also very different between the two clades (Figure 6.5f). PG was dominated by 36:4, 36:9 and 36:10 in clade C while clade D PG composition was comprised predominantly of the more saturated from, 36:3, while also containing a higher relative abundance of 40:7.

PS abundance was higher in clade D compared to clade C, yet spectra obtained were not very consistent between replicate colonies, making this difference statistically insignificant (Figure 6.6a). PS was largely composed of 40:4 in both clades (Figure 6.6b).

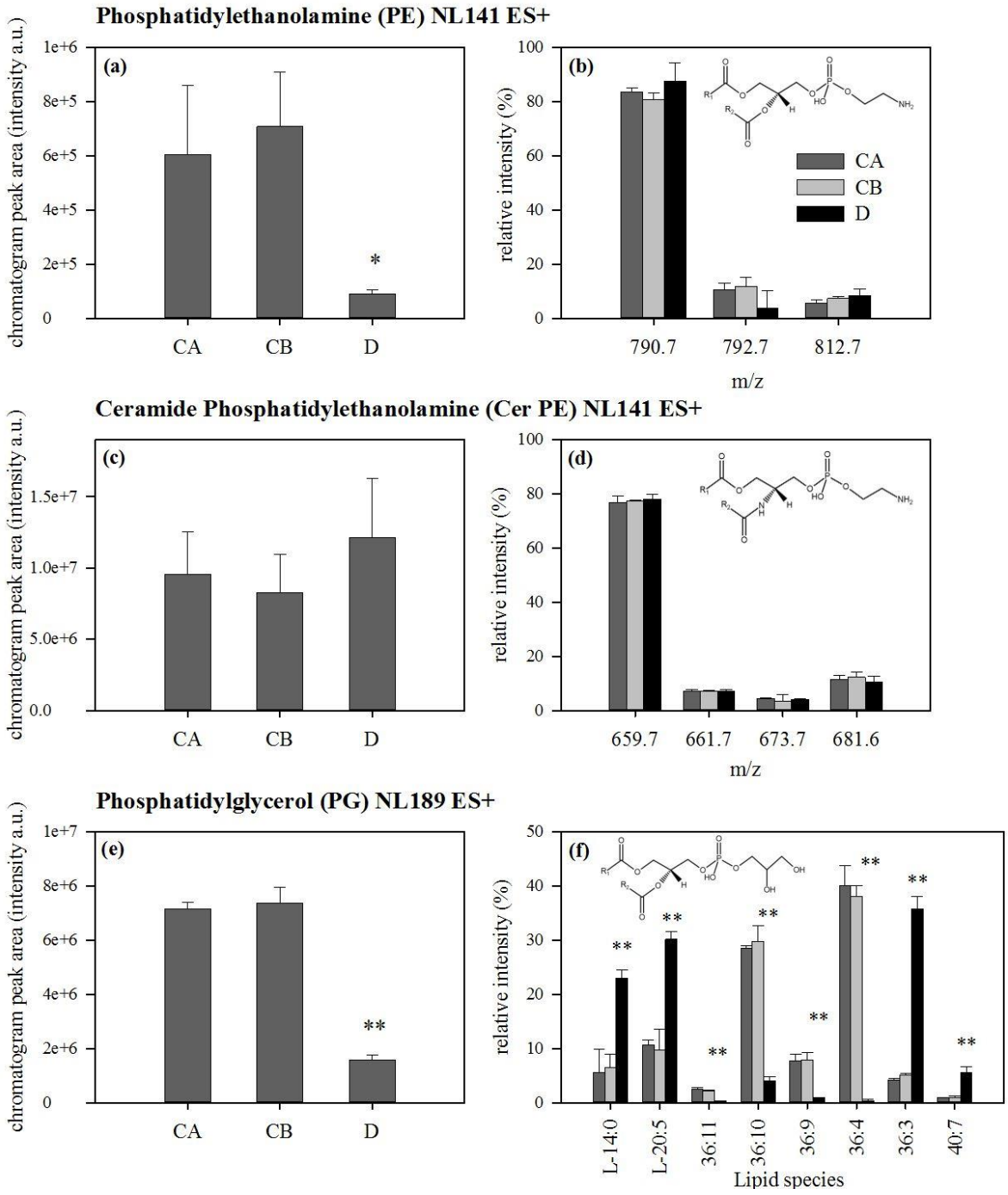

Figure 5.5| PE, Cer-PE, and PG abundance and composition. Total lipid class abundance measured as signal intensity of integrated chromatogram peak area for **(a)** PE, **(c)** Cer-PE and **(e)** PG. Relative composition of lipid species measured as percent contribution to total lipid class for **(b)** PE, **(d)** Cer-PE and **(f)** PG. The same colour legend applies to (b), (d) and (f): CA (dark grey), CB (pale grey), and D (black). CA = *Symbiodinium* clade C isolated from brown *A. valida* colour morph, CB = *Symbiodinium* clade C isolated from purple *A. valida* colour morph, D = *Symbiodinium* clade C isolated from purple *A. valida* colour morph. Significant differences between samples CB and D are indicated by the use of asterisk. * = $p<0.05$, ** = $p<0.001$.

PI was also detected and constituted predominantly of 32:1 (Figure 6.6b). Similarly to PS, clade D was observed to contain a slightly higher abundance of PI compared to clade C, however, due to inconsistency in the total abundance measured between replicates, this difference was not considered to be significant (Figure 6.6c).

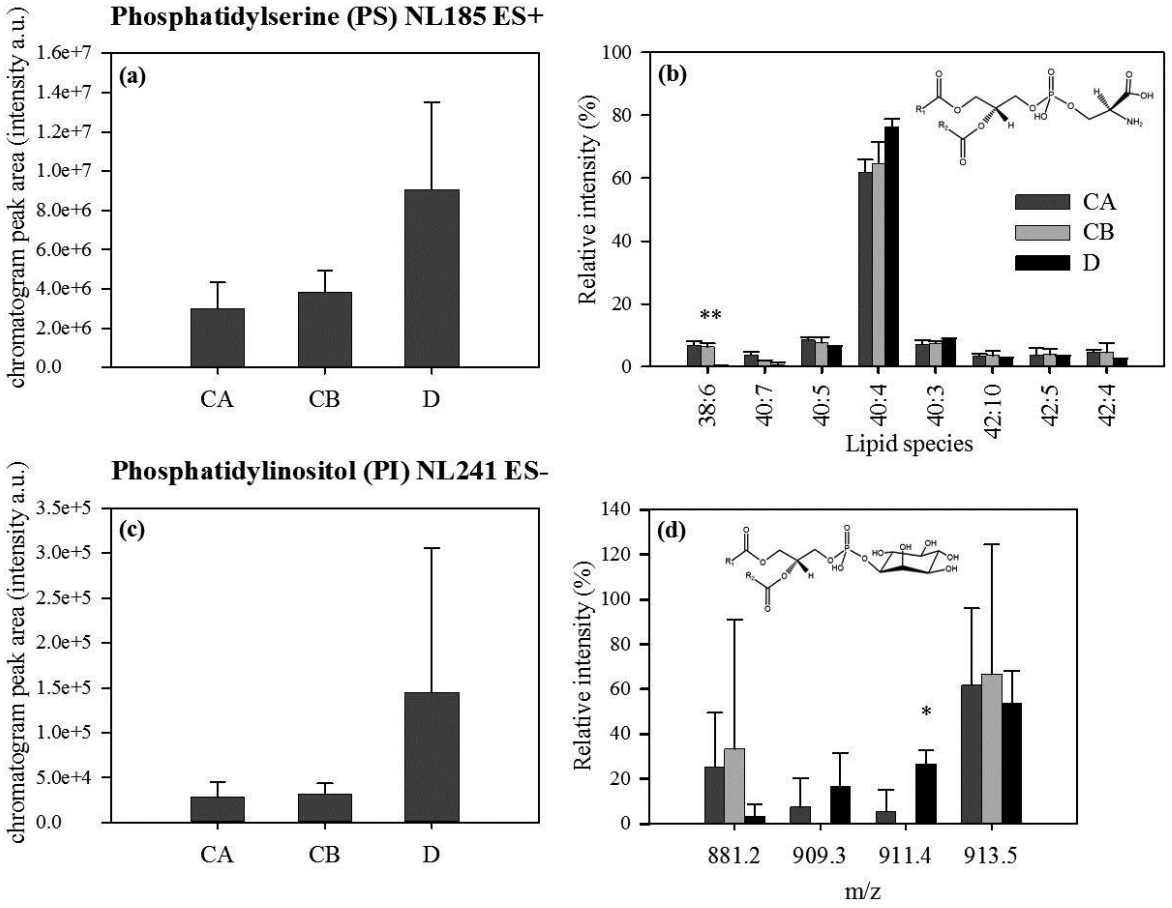

Figure 5.6| PS and PI abundance and composition. Total lipid class abundance measured as signal intensity of integrated chromatogram peak area for **(a)** PS and **(c)** PI. Relative composition of lipid species measured as percent contribution to total lipid class for **(b)** PS and **(d)** PI. The same colour legend applies to (b) and (d): CA (dark grey), CB (pale grey), and D (black). CA = *Symbiodinium* clade C isolated from brown *A. valida* colour morph, CB = *Symbiodinium* clade C isolated from purple *A. valida* colour morph, D = *Symbiodinium* clade C isolated from purple *A. valida* colour morph. Significant differences between samples CB and D are indicated by the use of asterisk. * = $p<0.05$, ** = $p<0.001$.

5.4.4. Unknown lipids

Clade D contained a significantly increased abundance of an unknown lipid which was identified by a diagnostic fragmentation mass of 241 in positive ionisation mode (Figure A4.2). Dominant peaks included m/z 948.4, 950.2, and 976.1. Daughter scans of these were inconclusive, yet it is possible that these are TAGs. Neutral lipids were not analysed in this study and differences in their abundance remain to be investigated.

A dominant peak observed in clade C spectra was m/z 910.6. This peak was observed when using both P184 and P104 scans. Spectra of clade D samples contained a much lower abundance of this peak (Figure A4.2).

Additional differences in the spectra of total lipid extracts in positive ionisation mode were apparent between the two analysed clades, yet these specific spectral peaks could not be related to any known lipid class. Many lipids that constitute the *Symbiodinium* lipidome are therefore still unknown.

5.5. Discussion

The lipid biochemistry of *Symbiodinium* clades C and D, freshly isolated from the reef coral *A. valida*, was analysed by ESI-MS/MS, providing the first extensive description of *Symbiodinium* polar lipid composition. Despite being exposed to the same environmental conditions, the lipid biochemistry was shown to be distinct in these two clades which are known to have different thermal sensitivities, providing new insight into the basis of inherent stress tolerance in these endosymbiotic algae.

5.5.1. Chloroplast membrane composition

Both *Symbiodinium* clades analysed in this study were found to contain predominantly 38:9 and 38:10 species of MGDG and DGDG (Figure 6.1b,d) which likely correspond to 20:5/18:4 and 20:5/18:5 respectively, placing the analysed *Symbiodinium* clades within the C20/C18 cluster of peridinin-containing dinoflagellates (Gray et al., 2009b). In a study on the glycolipid profile of cultured *Symbiodinium microadriaticum* isolated from jellyfish, an increase in glycolipid saturation of the *sn*-2 fatty acid was observed in response to high temperature exposure, apparent by a decrease in the relative abundance of 18:4/18:5 and an

increase in that of 18:4/18:4 in both MGDG and DGDG (Leblond et al., 2015). Here, clade D was shown to contain a lower relative abundance of DGDG 38:10 and a higher relative abundance of DGDG 38:9 as compared to clade C, thus displaying an inherent increase in the ratio of 18:4- to 18:5- containing DGDG species (Figure 6.1d). Yet, the relative composition of MGDG was equal within the two clades (Figure 6.1b). This demonstrates that the photosynthetic membranes of clade D are more saturated compared to clade C. The resulting increase in membrane melting temperature may therefore be associated with the higher thermal tolerance characteristic of this clade.

The total MGDG abundance of clade D samples was observed to be decreased compared to that of clade C, yet the total abundance of DGDG did not differ (Figure 6.1a, c). Consequently, the ratio of MGDG:DGDG is decreased in clade D compared to clade C (Figure A4.3a). The ratio of these lipids critically regulates the fluidity of the thylakoid membranes. Thereby, a decrease in the MGDG:DGDG ratio has proven to be an important acclimation response to temperature stress in higher plants and algae (Chen et al., 2006; Légeret et al., 2015). Furthermore, the maintenance of a decreased MGDG:DGDG ratio following heat stress has been demonstrated to be an adaptive mechanism of acquired thermotolerance in *Arabidopsis thaliana* (Chen et al., 2006). In response to heat stress *Arabidopsis thaliana* decreased the MGDG:DGDG ratio by increasing the total abundance of DGDG, whereas the same response was related to a decrease in the total abundance of MGDG in the microalgae *Chlamydomonas reinhardtii*. Since it cannot be excluded that DGDG is also localised in extraplastidic membranes (Härtel et al., 2000), the interpretation of the MGDG:DGDG ratio must be taken with caution. However, it is possible that an inherent decrease in the MGDG:DGDG ratio of thylakoid membranes in clade D *Symbiodinium* contributed to its characteristic heat resistance. Yet, further investigation will be required to confirm this.

The oligogalactolipid TGDG was also identified as a component of the *Symbiodinium* lipidome, the total abundance of which being significantly higher in clade C compared to clade D (Figure 6.1e). The species 38:9 and 38:10 are abundant which is concurrent with TGDG being produced by galactolipid:galactolipid galactosyltransferase (GGGT) using MGDG and DGDG as substrates (Figure 6.1f) (Moellering and Benning, 2011). However, the short chain, saturated species 30:0, 32:0 and 32:1 had the greatest relative abundance. In a *Arabidopsis thaliana* mutant deficient in DGDG synthase function (*dgd1*), a large increase in DGDG rich in 16:0 within extraplastidic membranes was observed in response

to phosphorus starvation, suggesting that DGDG can be synthesized by a different pathway in order to substitute for PC (Härtel et al., 2000). It is therefore possible that TGDG is synthesized by two distinct pathways and could be partially localised in non-photosynthetic membranes. It has been proposed that the prevalence of TGDG in cold water adapted dinoflagellates suggests a role related to membrane fluidity as a result of the large headgroup decreasing membrane packing capacity (Gray et al., 2009a). Moreover, an accumulation of DGDG and TGDG at the expense of MGDG abundance functions to stabilise chloroplast membranes during freeze-induced dehydration in *A. thaliana* (Moellering et al., 2010). It is therefore conceivable that TGDG plays a role in the control of salinity associated cellular dehydration. Additionally, TGDG is suggested to play a role in ER to plastid lipid trafficking (Xu et al., 2003). While the functional role played by TGDG remains inconclusive, the significant difference observed in its abundance signifies a divergent glycolipid metabolism and is certainly expected to affect the physical properties of the chloroplast membranes.

The remaining lipid components of the photosynthetic membranes are PG and SQDG. Adaptation of the ratio at which these lipids occur within the plastidial membranes plays a role in the response to phosphate starvation, with SQDG being able to substitute for PG to some extent due to their shared anionic nature, thereby liberating an internal store of phosphorus (Wiedenmann et al., 2013). The total abundance of SQDG did not differ between the two clades (Figure 6.2a). However, the clade D lipidome contained a significantly greater relative abundance of 32:0 and a lower relative abundance of 30:1 as compared to clade C, thus making SQDG more saturated in clade D which could further contribute towards an increased integrity of thylakoid membranes at higher temperatures (Figure 6.2b).

PG was significantly more abundant in clade C compared to clade D (Figure 6.5e). Yet, it is unclear if this results in a greater PG:SQDG ratio within the thylakoid membranes of clade C or whether this reflects a greater abundance of PG in extraplastidial membranes. Furthermore, the relative composition of PG species was distinct in the two clades, with clade C containing considerably higher relative amounts of 36:10, 36:9 and 36:4, but a lower abundance of 36:3 and 40:7 (Figure 6.5f).

5.5.2. Differences in betaine lipid abundance and its ratio to PC

The betaine lipid DGCC was identified as a major component of the *Symbiodinium* lipidome. However, other known betaine lipids, DGTA and DGTS, were not detected. A very large difference in the quantity of DGCC was measured between clade C and clade D samples, with clade C containing a considerably higher abundance (Figure 6.3a). Furthermore, the relative composition of DGCC lipid species was distinct (Figure 6.3b).

Betaine lipids are non-phosphorus containing polar lipids whose molecular geometry and charge distribution greatly resemble that of PC (Dembitsky, 1996). Indeed, a negative correlation between the abundance of betaine lipids and PC has been observed in marine algae (Kato et al., 1996). Phospholipids constitute a considerable pool of cellular phosphorus (Martin et al., 2011). Consequently, a key homeostatic response to phosphorus starvation is the substitution of phospholipids for non-phosphorus containing lipids such as the substitution of PG for SQDG previously observed in coral-associated *Symbiodinium* (Wiedenmann et al., 2013). Equivalently, phytoplankton also substitute PC for DGCC under phosphate limited conditions (Van Mooy et al., 2009). Correspondingly, clade D did contain a significantly greater abundance of PC as compared to clade C (Figure 6.4a) which would agree with an inverse relationship in DGCC and PC abundance (Kato et al., 1996). Concurrently, the profiles of DGCC and diacyl-PC lipid species composition are also inversely related, noticeable for example for 42:11 and 44:12 which are expected to consist of the prominent *Symbiodinium* fatty acids 22:6/20:5 and 22:6/22:6 respectively (Papina et al., 2003; Imbs et al., 2014; Chen et al., 2015). However, this significant difference in the PC:DGCC ratio occurred despite exposure to the same nutrient environment. It is possible that this reflects a difference in the capacity of nutrient assimilation (Baker et al., 2013). Yet, clade C contained a significantly greater abundance of PG as compared to clade D, thus making other lipid markers of phosphorus-limitation inconsistent (Figure 6.2a and 6.5e).

Interestingly, clade D contained a significantly higher abundance of lyso-DGCC compared to clade C (Figure 6.3a). Lyso lipids possess only one fatty acyl moiety and are predominantly minor membrane components known to play a role as signalling molecules (Ryu, 2004). The abundance of lyso phospholipids has previously been observed to increase in response to freezing induced stress in higher plants (Welti et al., 2002). On the

other hand, lyso-DGTS abundance has been observed to increase in *C. reinhardtii* in response to heat stress (Légeret et al., 2015).

Due to the lack of understanding of DGCC biosynthesis pathway and function, the effect of a changing DGCC abundance on *Symbiodinium* physiology remains speculative. However, it is proposed that DGCC biosynthesis is likely subject to regulation other than phosphorus availability. Importantly, these results demonstrate that the lipid biochemistry of the two clades investigated is considerably different and that this goes beyond differences in the composition of photosynthetic membranes.

5.5.3. The significance of ether lipids

The *Symbiodinium* lipidome was characterised by the occurrence of ether lipids which differ from diacyl lipids in the acyl chain at the sn-1 position being linked to the glycerol backbone by an alkyl (plasmenyl) or alkenyl (plasmalogen) ether bond as opposed to an ester bond. This was particularly noted for PC, evidenced by the difference in retention time of mono-alkyl and diacyl species. The higher abundance of PC in clade D lipid extracts was particularly driven by the greater abundance of mono-alkyl PCs, thus producing an increased alkyl:diacyl PC ratio in this clade. PE and Cer-PE species were likely also ether-bonded. PC and PE are the most common lipid classes associated with ether lipids and the occurrence of ether linked PCs and PEs was previously reported in the anemone *Aiptasia pallida* in which PC species were identified as alkyl, while PE species were identified as alkenyl forms (Garrett et al., 2013). The functional significance of a high proportion of ether phospholipids is unclear. Ether lipids are known to alter membrane dynamics by closer membrane packing which reduces membrane fluidity and also promotes the formation of non-bilayer structures at lower temperatures than corresponding diacyl species (Lohner et al. 1984), thereby affecting membrane permeability and facilitating membrane fusion, the latter being important for vesicular fusion such as is needed for exocytosis.

5.5.4. Conclusions

Due to the lack of understanding of the functional roles of DGCC, TGDG and ether lipids, the biochemical and physiological implications of these vast differences in *Symbiodinium* lipid biochemistry remain speculative. Nevertheless, this study provides evidence that *Symbiodinium* clades are distinct in their biochemistry, metabolism and resultant

physiology which underpins their varying capacities to withstand environmental stressors such as increasing sea surface temperatures. More work is needed to fully grasp how the *Symbiodinium* membrane composition impacts the resilience of reef corals. Elucidating the mechanisms of lipid remodeling in clade C and D *Symbiodinium* during exposure to different environmental conditions is expected to provide further insight into the roles of major lipid classes in these algae. The sensitivity of membranes to the physicochemical environment means that the characterisation of the polar lipid composition of *Symbiodinium* provides a valuable tool with which to identify and comprehend stress responses of reef corals. Thereby, lipidomics holds great potential for furthering our understanding of the functioning of different coral-*Symbiodinium* associations, and the capacity reef corals to acclimate and adapt to a changing environment. This understanding is critical in order to predict future trajectories of coral reef ecosystems in response to climate change and to advance our management efforts to sustain coral reef resilience.

Chapter 6: Conclusions and outlook

6.1. Key findings and significance

6.1.1. Insight into the metabolic interactions of the coral-zooxanthellae symbiosis

The foundation of the coral-zooxanthellae symbiosis is the efficient assimilation and retention of nutrients within the symbiosis. This renders reef corals highly sensitive to perturbations to the nutrient environment which can occur in the form of both extremes of nutrient impoverishment and enrichment (D'Angelo and Wiedenmann, 2014). Particularly nutrient enrichment is considered a significant threat to coral reefs due to evidence supporting a positive correlation of elevated nutrient availability and bleaching susceptibility, as well as the threat of eutrophication which can result in community shifts and ecosystem degradation (Szmant, 2002). Additionally, nutrient enrichment is often related to pollution from a range of anthropogenic sources, thereby making it a local stressor which could be managed in order to mitigate the effects of climate change (Brodie et al., 2012). However the effectiveness of management strategies is dependent on scientific knowledge of what nutrient environment supports the greatest resilience of a specific reef ecosystem as well as the technology to assess and monitor the nutrient environment experienced by reef corals. However, the repercussions of different nutrient environments to the functioning of the coral-zooxanthellae symbiosis are still not fully understood.

The investigations of this thesis concerned with the effects of nutrient availability to the functioning of the *Euphyllia paradivisa – Symbiodinium* C1 association contributed significantly to our understanding of the nutrient biology of the coral-zooxanthellae symbiosis by giving new insight into the partition and cycling of nitrogen and phosphorus within the symbiosis. Many previous studies had investigated the effects of the nutrient environment to the functioning of the symbiosis, however findings were often contradictory (Fabricius, 2005; Shantz and Burkepile, 2014). The studies presented in this thesis stood apart from past investigations by conducting very long-term experimental treatments of at least six months of treatment exposure. Particularly, the development of a nutrient limited phenotype took a long time to manifest itself due to the apparent long memory of nutritional history in *Euphyllia paradivisa*. The establishment of long-term treatments was enabled by the use of the experimental mesocosm system established at the

University of Southampton (D'Angelo and Wiedenmann, 2012). This yielded true phenotypes of the symbiosis representative of different nutrient environments, as opposed to studying the immediate response to a change in nutrient availability.

Key to this investigation was teasing apart the effects of the essential nutrients, nitrogen and phosphorus, as well as of the two principal sources of these nutrients to reef corals: the assimilation of dissolved inorganic nutrients by the zooxanthellae and the uptake of particulate organic nutrients through heterotrophic feeding by the host. The relative value of nitrogen and phosphorus to the functioning of the symbiosis was assessed by means of exposure to imbalanced ratios of nitrate and phosphate as well as to the disproportionally high intake of heterotrophic nitrogen relative to heterotrophic phosphorus.

The prevailing consensus from many studies has been that dissolved inorganic nutrients, particularly dissolved inorganic nitrogen, lead to increased proliferation of the zooxanthellae and that nutrients translocated from the zooxanthellae to the host are used for energy provision through immediate catabolic processes, whereas heterotrophic nutrients are invested into growth of the coral host. Some studies concluded that dissolved inorganic nutrient enrichment decreased growth and calcification of the host due to proliferation of the zooxanthellae and resultant decreased translocation of photosynthates (Stambler et al., 1991; Marubini and Davies, 1996; Ferrier-Pagès et al., 2000). Yet, the results of this thesis demonstrate that dissolved inorganic nutrients alone sustain a healthy physiology and growth of the coral holobiont. This non-conformity is possibly explained by the difference in studying the immediate response of nutrient enrichment which would be related to a change in zooxanthellae density, versus the acclimatised, steady-state symbiosis at which the high density is already established. Results presented in this thesis are in support of several studies indicating the translocation of nitrogen-rich compounds to the host (Tanaka et al., 2006; Kopp et al., 2013). However, it is also inferred that the zooxanthellae provide the host with phosphorus following phosphate assimilation. This implies that dissolved inorganic nutrients are partitioned equally between the host and the zooxanthellae and are allocated towards growth of the host. However, the mechanism of this partition remains uncertain as it could occur via active translocation of nitrogen- and phosphorus-rich compounds to the host or by the degradation of zooxanthellae by the host (Titlyanov et al., 2006). Thus, according to the observations of this thesis, a high availability of dissolved inorganic nutrients is beneficial to the physiology of reef corals. This statement must be taken with caution. Indeed, under steady-state conditions within a

healthy unperturbed reef, corals can flourish in the presence of high concentrations of dissolved inorganic nutrients (D'Angelo and Wiedenmann, 2014; Stuhldreier et al., 2015). Yet, this places the corals as well as the reef ecosystem in closer proximity to a tipping point towards degradation if the steady-state conditions are disrupted. Some evidence suggests that even when nutrients are balanced, the high zooxanthellae densities and pigment content could make corals more susceptible to thermal and irradiance stress (Fabricius, 2006; Cunning and Baker, 2013). Indeed, *E. paradivisa* within the high nutrient treatment (+N+P) were not subjected to a stress treatment. Cunning and Baker hypothesised that a high zooxanthellae density represents a higher total abundance of 'reactive oxygen producing units', thus leading to greater cellular damage to the host at a given stress level. According to this proposition, it is possible that feeding on high quality food in combination with limited dissolved inorganic nutrient availability (Artemia/-N-P), which yields a large polyp size but considerably lower zooxanthellae density, constitutes a phenotype that is more resilient to thermal stress compared to corals exposed to the same food availability but in combination with high dissolved inorganic nutrients (Artemia/+N+P) which leads to a very high zooxanthellae density. Furthermore, in the presence of high dissolved inorganic nutrient concentrations the reef is highly dependent on top-down control to maintain a community structure dominated by coral cover (Hughes et al., 2007). This makes reefs highly susceptible to ecosystem degradation induced by overfishing. Nevertheless, it is argued that ample dissolved inorganic nutrient availability is critical for reef corals. The depletion of nutrients caused by increased stratification of the water column (Behrenfeld et al., 2006) therefore poses a significant threat to reef corals.

Consequently, heterotrophy had negligible effects on the symbiosis when in combination with high dissolved inorganic nutrient availability (Table 6.1). Furthermore, heterotrophic nutrient intake in combination with very limited dissolved inorganic nutrient availability could only achieve a similar phenotype, marked by large polyp size and high zooxanthellae density, if the intake of heterotrophic nutrients was considerably exaggerated relative to realistic natural prey abundance. The functioning and health of the coral-zooxanthellae symbiosis is therefore considerably more dependent on the supply of dissolved inorganic nutrient than to heterotrophic feeding. Although findings presented in this thesis cannot be generalised to all coral-zooxanthellae associations due to considerable species specificities (Ferrier-Pagès et al., 2010), it is believed that *Euphyllia paradivisa* is representative of coral species that are highly adept at predation. The extent to which heterotrophy can

Table 6.1| Summary of the interacting effects of balanced (HA: Artemia, high quantity) and imbalanced (HP: prawn, high quantity) heterotrophic nitrogen and phosphorus intake with varying dissolved inorganic nutrient availability. Differences are relative to the unfed condition within each of the three dissolved inorganic nutrient environments. Bold arrows indicate a large effect.

Dissolved inorganic nutrients	**+N+P**		**-N-P**		**+N-P**	
Heterotrophic feeding	**HP** imbalanced	**HA** balanced	**HP** imbalanced	**HA** balanced	**HP** imbalanced	**HA** balanced
Polyp size	=	=	↑	**↑**	=	↑
Food intake	low	low	high	high	low	high
Zooxanthellae density	=	=	↑	**↑**	=	↑
Lipid body content	=	=	↓	**↓**	↓	**↓**
Uric acid crystal content	n.a.	n.a.	**↑**	↓	n.a.	n.a.
Host stress resilience	n.a.	n.a.	=	↑	↓	=
Zooxanthellae stress resilience	n.a.	n.a.	=	↑	↓	↑

compensate for the loss of zooxanthellae nutrient assimilation during, and in the recovery of, a bleaching event, (Grottoli et al., 2006; Hughes and Grottoli, 2013) is therefore called into question. Nevertheless, heterotrophy did support a large increase in polyp biomass in the absence of dissolved inorganic nutrients. Also, despite the partition of heterotrophic nutrients being favoured towards the host fraction, both heterotrophic nitrogen and phosphorus became available to the zooxanthellae. This nutrient input increased the stress resilience of the zooxanthellae by maintaining photosynthetic efficiency during thermal stress, which is in agreement with past studies (Borell and Bischof, 2008). However, this benefit was only conferred if the nutritional intake by heterotrophy was balanced in terms of nitrogen and phosphorus content (Table 6.1), thus placing a high importance on the nutritional quality of prey items when considering the beneficial effects of heterotrophic feeding. On one side, this illustrates the value of heterotrophy as a source of phosphorus to the coral holobiont, whereas previous studies had only referred to heterotrophy as a source of carbon and nitrogen to the coral host. Yet, it also suggests that heterotrophy has the potential of being damaging to the zooxanthellae if the quality of prey items is compromised, thereby impacting the resilience of the coral holobiont. The finding that

heterotrophy itself can induce a nutrient imbalance of the zooxanthellae helps to explain why one study observed feeding to resulted in a decreased stress resilience of corals already exposed to imbalanced dissolved inorganic nutrient conditions (Ezzat et al., 2015). It is therefore important to consider how nutrient pollution is affecting the composition of particulate organic matter.

One major concern of anthropogenic nutrient pollution is the risk of disrupting natural ratios of dissolved inorganic nitrogen and phosphate that are favourable to reef environments (Wiedenmann et al., 2013; Peñuelas et al., 2013). This ratio is largely found to be below that of the Redfield ratio (16:1 - (Redfield, 1958)) (Szmant, 2002), indicating a tendency towards nitrogen limitation of primary production. The investigation of this thesis found that a nutrient imbalance inducing the limitation of phosphorus was considerably more detrimental to the functioning of the symbiosis than that inducing the limitation of nitrogen (Table 6.2). This demonstrated a greater dependency of the symbiosis to a continuous supply of phosphorus as compared to nitrogen. It was concluded that the efficiency at which nitrogen is recycled within the symbiosis renders the holobiont less dependent on the continuous external supply of nitrogen. This is based on the excretion of nitrogen being coupled to the metabolism of the host. Additionally, the association with nitrogen fixing microbes could contribute to the higher dependence on phosphorus (Rädecker et al., 2015). On the other hand, it is concluded that phosphorus is not cycled between the host and the symbiont, or at least not to the same extent, implying that phosphorus is instead largely incorporated into the host fraction by skeletogenesis (Dunn et al., 2012), or is lost from the symbiosis by being secreted in mucous (Wild et al., 2005). Nevertheless, phosphate enrichment alone did generate nutrient stress of the zooxanthellae through nitrogen limitation, the repercussions of which in terms of thermal stress resilience require further investigation. Thus, a greater emphasis is placed on the negative repercussions of nitrogen pollution. A primary driver of anthropogenic nitrogen loading is the runoff of agricultural fertilizers which could be limited by more efficient fertilizer usage (Fowler et al., 2013). But critically, it cannot be concluded that phosphorus pollution is not destructive. Phosphate enrichment has been associated with negative effects on skeletal integrity of corals (Dunn et al., 2012) and can stimulate phase shifts in community structure (Littler et al., 2010). Rather, it is essential to consider the nutrient environment in terms of the nutrient ratios when assessing nutrient stress of a reef ecosystem and in implementing management strategies. Furthermore, it has recently been theorised that

Table 6.2| Summary of key effects of different dissolved inorganic nutrient availabilities (nitrate and phosphate) on the coral-zooxanthellae symbiosis

		Nutrient condition			
		+N+P	**-N-P**	**+N-P**	**-N+P**
	Zooxanthellae nutrient status	nutrient replete growth	N/P co-limitation	P-starved	N-limited
	Zooxanthellae density	normal	low	low	normal
	Polyp size	normal	small	small	normal
Zooxanthellae ultrastructural biomarkers	**Cell size**	small	increased	increased	small
	Lipid body content	low	increased	increased	increased
	Starch granule content	low	increased	increased	increased
	Uric acid crystal content	low	low	increased	absent
	Accumulation body fragmentation	low	increased	low	low

targeted overfishing of large individuals and predatory fish can increase the N:P ratio of nutrient supply by fish communities (Allgeier et al., 2014). The additional pressure of overfishing could therefore exacerbate the repercussions of nutrient enrichment, not only at the level of community structure, but also by direct effects to coral physiology. Moreover, the finding that cellular imbalance of the zooxanthellae can also be triggered through heterotrophic feeding raises the possibility of a local disruption to natural nutrient ratios through point source pollution being passed on to higher trophic levels which could aggravate the nutrient imbalance of zooxanthellae harboured by corals with high feeding rates. Furthermore, this could result in a wider dispersal of the negative secondary effects of nutrient pollution. However, the ecological validity of this prospect remains to be assessed.

This thesis exemplified the tremendous plasticity of the coral-zooxanthellae symbiosis in terms of the nutrient environment, as well as the efficiency with which nutrients are recycled within the symbiosis. It is suggested that the dynamics of the symbiosis change in response to nutrient limitation by shifting towards increased dependency on the

assimilation of the zooxanthellae directly by the host when the translocation of nitrogen- and phosphorus-rich compounds to the host diminishes. It is inferred from the analysis of zooxanthellae densities and of the dial mitotic rates of zooxanthellae, that a given supply of dissolved inorganic nutrients supports a given standing-stock population density *in hospite*. A relatively constant proportion of population turnover during one dial cycle, therefore maintains these given densities. Dial cycles of zooxanthellae division and degradation have previously been reported to control the zooxanthellae population *in hospite* (Titlyanov et al., 2006). Under nutrient replete conditions, stimulation of zooxanthellae division is driven solely by the light-dark cycle, the initiation of mitosis therefore being subject to the cellular metabolism of the zooxanthellae alone (Wang et al., 2008). But, when severely deprived of an external supply of dissolved inorganic nutrients, peaks in algal division rates are suggested to be stimulated by internal fluxes of nutrients. These fluxes brought about by the cycling of nutrients between the host and algal fractions are therefore also proposed to be subject to dial rhythmicity. This highlights the sensitivity of the zooxanthellae to nutrient availability and provides a new perspective to the metabolic interaction of the coral host and its algal symbionts. Thereby the coral can survive even with very little external input of nutrients by essentially 'farming' its algal symbionts. However, the validity of this theory must be assessed by continued investigation.

6.1.2. The role of zooxanthellae lipid biochemistry in thermal tolerance of reef corals

According to predicted climate change trajectories coral-zooxanthellae associations need to dramatically increase their tolerance to continually rising sea surface temperatures in order to persist (Donner et al., 2005). Additionally, predicted increased incidence and severity of ENSO events will lead to frequent punctuated heat stress episodes, calling for a tremendous capacity of reef corals to tolerate and acclimatise to fluctuating perturbations of the physicochemical environment. Ultimately, corals and their algal symbionts must adapt through genetic modification in order to become more suited to warmer oceans (Logan et al., 2014). It is therefore of considerable interest to identify what coral and zooxanthellae associations are most resilient to climate change and what adaptations distinguish this heightened resilience. Several studies have demonstrated the potential for acclimation in reef corals (Bellantuono et al., 2012; Bay and Palumbi, 2015). Yet, we are only beginning to understand what cellular and molecular mechanisms contribute towards

acclimation and adaptation of the reef coral holobiont to climate change and it is feared that the rate of ocean warming will overwhelm the capacity of corals to adapt, leading to the prediction of a considerable loss to coral biodiversity within future oceans. The ultimate resilience to heat stress is determined by the specific coral and zooxanthellae combination. *Symbiodinium* is genetically diverse and significant differences in thermal sensitivity among clades and subclades have been recognised (Rowan, 2004), leading to the speculation that corals could acclimate more rapidly to climate change by switching their symbiont communities to harbour more thermally resistant algal symbionts (Berkelmans and van Oppen, 2006; Jones et al., 2008). Yet, the underlying mechanisms of enhanced thermal resistance of *Symbiodinium* are very poorly understood.

This thesis provides a considerable contribution towards our knowledge of underpinning molecular differences between thermally sensitive and resilient *Symbiodinium* clades and advances our understanding of the ability of reef corals to adapt to global climate change. A key finding of this investigation was that altered membrane composition constitutes an adaptation of the genus *Symbiodinium* to provide a beneficial resistance to heat stress. Previous studies had provided some evidence for the involvement of chloroplast membrane composition in determining thermal sensitivity of zooxanthellae (Tchernov et al., 2004; Ladner et al., 2012; Barshis et al., 2014), specifically implying that the degree of thylakoid membrane saturation played a significant role in increasing the thermal bleaching threshold (Tchernov et al., 2004). However, this had been disputed (Díaz-Almeyda et al., 2010; Kneeland et al., 2013). The investigation of this thesis provides the first characterisation of *Symbiodinium* polar lipid composition, and supports the involvement of chloroplast membrane composition in conveying heightened thermal tolerance. The thermally resistant clade D lipidome not only displayed increased saturation of key lipid species of the chloroplast membranes (DGDG and SQDG), but also a decrease in the ratio of MGDG:DGDG (Table 6.3). Both the lowered MGDG:DGDG ratio as well as heightened saturation of DGDG have been associated with acclimation and adaptation to heat stress in higher plants (Chen et al., 2006). These modifications relate to increased integrity of the photosynthetic membranes and stability of the photosynthetic apparatus at elevated temperatures (Chen et al., 2006). Thus, the adaptation of glycolipid metabolism of zooxanthellae has been established as a mechanism of enhanced thermotolerance in reef corals.

Table 6.3| Summary of the identified differences in polar lipid composition that distinguish a thermally tolerant *Symbiodinium* membrane phenotype (clade D) from a thermally sensitive membrane phenotype (clade C). Bold arrows signify a large difference.

		clade D thermally tolerant phenotype	
Lipid group	Lipid class	total class abundance	degree of saturation
Glycolipids	**MGDG**	↓	=
	DGDG	=	↑
	TGDG	↓	↑
	SQDG	=	↓
Betaine lipids	**DGCC**	↓	↓
	lyso-DGCC	↑	↓
Phospholipids	**diacyl-PC**	↑	↑
	mono-alkyl-PC	↑	=
	lyso-PC	=	=
	PE	=	=
	Cer PE	=	=
	PG	↓	↓
	PS	↑	=
	PI	↑	=

The finding that the chloroplast membrane composition was significantly different between clade D and C samples at ambient temperatures demonstrates that the difference in thermal resistance is explained by inherent distinctions in membrane composition as opposed to differential capacity for acclimation during heat stress exposure. This is in support of a transcriptional analysis of clade D and C *Symbiodinium* which identified significant differences in steady-state profiles, such as in the expression of heat shock proteins (Barshis et al., 2014). Therefore, an energetically costly heat shock response is likely initiated at a higher temperature in clade D compared to clade C due to perturbations of membrane fluidity taking place at higher temperatures. This could explain why the physiological performance of clade D symbionts is unaffected at higher temperatures while

that of more sensitive types decreased in response to heat stress (Baker et al., 2013). Similarly, thermally resilient coral species were reported to display considerable frontloading of thermal tolerance genes including heat shock proteins and antioxidant enzymes, and therefore displayed a reduced response to heat stress compared to more sensitive species which significantly up-regulated such genes during heat stress exposure (Barshis et al., 2013). The specific membrane composition of clade D symbionts therefore supports a greater degree of plasticity with respect to the physical environment compared to less thermally tolerant clades.

Most noteworthy to the comparison of lipid biochemistry of thermally sensitive and tolerant *Symbiodinium* clades, was the finding that the most compelling differences in membrane composition were identified in extraplastidic membranes (Table 6.3). Specifically, significant differences in the ratios of the betaine lipid DGCC and the phospholipid PC, as well as of diacyl and mono-alkyl PC species were apparent. A large difference in the total abundance of lyso-DGCC was also observed. The precise implications of these observations are not known due to a lack of understanding of the functional roles played by these lipids. It is therefore not known if these differences are involved in tolerance to temperature stress. Yet, it is inferred that the two clades analysed differ substantially in their lipid metabolism and nutrient allocation which could be a repercussion of different capacities for nutrient assimilation (Baker et al., 2013). DGCC and PC are expected to largely comprise the plasma membrane which forms the boundary of the cell. Due to the extraction of symbionts from host tissue, it is not clear if the analysed algal lipid extracts include lipids derived from the symbiosome membrane complex, or even from the host-derived outer symbiosime membrane, which constitutes the greatest limitation of this study. These membranes are critically involved in the exchange of metabolites, photosynthates, and signalling molecules between the host and the symbiont. It is possible that large differences in the composition of these membranes could affect the interaction between the host and the symbiont, thereby making the symbiosis fundamentally different among specific coral-zooxanthellae associations. The general conclusion inferred from this investigation is that genetically distinct clades and subclades of *Symbiodinium* may be physiologically more distinct than is currently known.

6.1.3. Cellular and biochemical biomarkers indicative of the status of reef corals

Nutrient pollution poses a major threat to coral reefs, yet it is a stressor that is manageable. Effective management requires the identification of perturbations in water quality and the association of a given cause of changes in water quality to the effect it is having on coral reefs. Yet, due to the rapid turnover of nutrients within the surface oceans it is difficult to perceive what nutrient environment prevails by direct measurement of the water chemistry (Furnas et al., 2005). Through the examination of phenotypes resulting from different nutrient environments, this thesis contributes novel tools for the assessment of nutrient stress in reef corals in the form of cellular biomarkers. Thereby, the analysis of zooxanthellae density along with cell size, storage body accumulation (lipid bodies, starch granules, uric acid crystals), and accumulation body integrity can give insight into the nutrient status of the coral. Under controlled laboratory conditions the analysis of these cellular biomarkers could discriminate between nutrient stress induced by the limitation of nitrogen (high density, small cell size, high accumulation of lipid bodies and very high content of starch granules), the limitation of phosphorus (low density, large cell size, high accumulation of lipid bodies, starch granules and uric acid crystals), or the limitation of both essential nutrients (low density, large cell size, high accumulation of lipid bodies and starch granules, fragmentation of accumulation body). This can be of particular value since the analysis of the coral macrostructure alone could be misleading, as exemplified by nutrient stress induced by the enrichment of phosphate alone.

Particularly the accumulation of neutral lipid in the form of cellular lipid bodies has been well studied in microalgae since it is of high value to the biofuel industry (Hu et al., 2008). While it is best documented as a response to nutrient limitation, lipid body accumulation is also stimulated by other stress parameters such as temperature, salinity, irradiance and pH (Hu et al., 2008). Lipid body accumulation should therefore be treated as a biomarker of general stress and should be considered along with other indicators and physicochemical measurements. Moreover, neutral lipid and starch are major products of photosynthesis and the accumulation of these storage bodies does take place under non-stressful conditions. Their abundance will therefore also relate directly to light availability. These biomarkers are therefore subject to natural variability which is a significant limitation. Reference thresholds in the accumulation of these compounds must therefore be established. It would also be important to consider sampling time since a previous study did describe a dial rhythmicity in lipid body abundance, with the accumulation increasing during the course of

the day, peaking at sunset, and returning to basal levels at night (Chen et al., 2011). Accordingly, it would be most informative to measure basal storage body accumulation at sunrise. However, major differences caused by sampling time were not identified in the current analysis. It may prove to be of value to consider the ratio of neutral lipid and starch, since the dominance of either starch or lipid production can be dependent on the environmental stimulus (Vítová et al., 2015). Indeed, it appeared that in zooxanthellae, nitrogen limitation favoured a lower ratio of neutral lipid to starch relative to the energy storage body production during phosphorus limitation. Additionally, it could be complementary to measure lipid body abundance within the host fraction. One study had previously observed that the translocation of lipid bodies to the host is decreased during temperature driven bleaching (Luo et al., 2009). On the other hand, nutrient limitation is expected to increase the translocation of neutral lipid to the host, thus leading to an increase in host lipid body abundance.

A further biomarker of nutrient availability which was identified but not discussed in detail is the abundance of GFP-like protein in *E. paradivisa*. A significant positive correlation was measured between zooxanthellae density and GFP-like protein concentration in response to changes in nutrient availability. GFP-like protein fluorescence has been shown to increase with increasing light irradiance, implying a photoprotective function of host fluorescence (Salih et al., 2000). Particularly blue light induces the upregulation of GFP-like proteins at the transcriptional level (D'Angelo et al., 2008). The accumulation of GFP-like protein in growth zones is hypothesised to facilitate the colonisation of this region by zooxanthellae through enhanced photoprotection (Wiedenmann et al., 2013). The positive correlation between GFP-like protein concentration and zooxanthellae density, at a constant light level, observed in this thesis is not in agreement with these findings since light availability within the tissue is expected to increase with a decreasing symbiont density due to reduced self-shading. The functional significance of this finding is therefore not clear. It is speculated that GFP-like protein could have a role in host-induced regulation of zooxanthellae proliferation since it absorbs blue light which is needed for stimulation of algal cell cycle progression. Nevertheless, host fluorescence could provide a useful non-invasive marker of zooxanthellae density in this coral species. However, the effects of interacting factors would need to be tested in order to determine what specificity to nutrient availability this marker has.

The most fundamental contribution provided by this study is the characterisation itself, of the polar lipidome of *Symbiodinium in hospite*. This had never been done before and involved considerable effort in method optimisation and in the classification of identified spectra. Cellular membranes are extremely sensitive to the physicochemical environment and have previously been described as primary sensors of environmental perturbations (Los et al., 2013; Horváth et al., 2012). Additionally, membranes in photosynthetic organisms display a considerable degree of plasticity depending on the availability of cellular phosphorus (Van Mooy et al., 2009; Wiedenmann et al., 2013). Consequently, an array of lipid biomarkers (summarised in table 2.1) can be used to infer acclimation to environmental stress parameters in photosynthetic organisms. A comprehensive understanding of membrane remodeling in coral-associated zooxanthellae would allow for the study of membrane characteristics of zooxanthellae *in situ* in order to identify and distinguish between environmental stress parameters and pinpoint populations which display greater traits of resilience. Such analysis could advance our management efforts by identifying local stressors which could be mitigated and aid in the establishment of refuges which hold greater promise of adapting to climate change. These biochemical markers could therefore not only serve to identify nutrient stress, but also be indicative of thermal acclimation and resilience. Thus, in the 'omics' era in which genomics, transcriptomics and proteomics are valued as specific tools for the identification of cause-and-effect relationships between an environmental stress factor and the response of an organism, this thesis advocates the contribution of lipidomics to provide key information for the effective management of coral reefs.

The combination of cellular and biochemical markers could provide higher specificity in the identification of nutrient stress relative to stress induced by other abiotic factors. Nutrient availability is commonly determined by proxy such as by the measurement of chlorophyll *a* as an indicator of phytoplankton biomass (Wooldridge, 2009) or by the measurement of nutrient content in the tissue of macroalgae (Mellors et al., 2005; Lapointe et al., 2010). However, the ecological relevance of these measurements to the health of reef corals is only inferred. The use of cellular and biochemical biomarkers would be complementary to the measurement of nutrient availability by proxies since it assesses the stress experienced by the coral directly, rather than the cause which may or may not result in stress depending on the context of the environment. Additionally, a bioindicator system has been proposed that uses physiological, population, and community parameters as

indicators of water quality (Cooper et al., 2009; Fabricius et al., 2012). Physiological markers include colony pigmentation and tissue thickness and surface rugosity of massive *Porites*. These markers are indicative of zooxanthellae density and coral growth (Cooper et al., 2009). A particularly useful biomarker of nitrogen pollution is the ratio of nitrogen isotopes (^{15}N:$^{14}N = \delta^{15}N$) within the coral skeleton, since this provides information on the anthropogenic source of nitrogen enrichment (Heaton, 1986; Risk et al., 2001). Effective biomarkers of nutrient availability at the level of population and community include the abundance of bioeroders, level of coral recruitment, taxonomic richness of hardcoral, octocoral and macroalgae, and the maximum depth of coral reef development (Cooper et al., 2009). These markers vary in response time, from short- to very long-term. The monitoring of nutrient stress by means of cellular and biochemical biomarkers of the zooxanthellae assesses a relatively rapid response to water quality and is therefore relevant for acute, non-lethal disturbance. These markers can therefore constitute an early warning system to changes in environmental conditions and can detect low levels of stress. These are highly desirable factors. Yet, a significant limitation of these biomarkers is that they are invasive, requiring a high level of sampling and replication in order to identify ecological effects. Furthermore, they are laborious and require specialised equipment and technical expertise which make their application unpractical for routine monitoring purposes. More work is therefore required to optimise the efficiency of these biomarkers and to test their validity and applicability *in situ*.

6.2. Future direction

While considerable insight into the metabolic interactions of the coral-zooxanthellae symbiosis has been gained, more evidence is required to support certain inferences made in this thesis. Of particular interest is advancing our understanding of phosphorus metabolism within the symbiosis, since the importance of this nutrient for the functioning of the symbiosis was emphasised by this thesis. Many studies have focused on carbon and nitrogen as essential nutrients of the coral-zooxanthellae symbiosis, yet comparatively little is known about the allocation of phosphorus. It would be valuable to study the partition of this nutrient between the host and the algal fraction in order to validate our assumption that phosphorus is largely not recycled within the symbiosis. Potentially, this could be achieved by the use of phosphorus radioisotopes. Alternatively, inductively coupled plasma mass

spectrometry (ICP-MS) should be sensitive enough to enable the measurement of phosphorus within different fractions of a reef coral. Coral fragments which had been exposed to long-term nutrient limited conditions could thereby be exposed to a spike of phosphate enrichment or heterotrophic phosphorus intake. The incorporation of phosphorus into host and algal fractions could subsequently be measured in a time series following exposure.

The effects of nutrient availability on the dial cell cycle dynamics of zooxanthellae requires further investigation. It is unclear how the turnover of a constant proportion of the symbiont population is regulated. It is possible that the host does have considerable active control over algal cell cycle progression. Algal division rates must be assessed alongside rates of degradation and expulsion in order to obtain a more complete picture of the symbiont population turnover under different nutrient conditions. A higher rate of algal degradation within corals exposed to nitrogen enrichment compared to specimens exposed to phosphorus enrichment would support the hypothesis that the steady-state stability of the symbiosis is largely driven by the translocation of phosphorus to the host. If the algal cells are regularly digested as a means of nutrient acquisition by the host, this must involve a signalling cascade that makes a proportion of algal cells susceptible to the host's immune response, leading to autophagy of the symbiosome contents. It is unknown if and how algal degradation in response to nutrient deprivation differs from the bleaching response in terms of signalling pathways. These processes remain largely uncharacterised. Additionally, the hypothesis that internal nutrient fluctuations derived from the cycling of nutrients between the host and the algal fraction stimulates bursts of zooxanthellae division, and that the resulting cycles of symbiont division and degradation can sustain the host under extremely oligotrophic conditions need to be further assessed.

Food quality was shown to be critical in determining the effects of heterotrophy on the coral-zooxanthellae symbiosis. In this thesis the ratio of nitrogen and phosphorus within prey items was considered. However, other nutritional qualities of food items must also be analysed. As a control study, it was shown that the level of polyunsaturated fatty acids within the food items had no impact on the macrostructure of the coral polyps. However, it is not known if this factor affects the stress resilience of the coral holobiont. Furthermore, other nutrients such as iron may also have played a role in the differences observed between prawn and *Artemia* fed polyps. The ecological significance of food quality should be examined by studying the effects of point source nutrient pollution on the community

composition and cellular stoichiometry of prey items. In terms of the deleterious effects of nutrient imbalance, it is expected that luxury uptake of dissolved inorganic nutrients by phytoplankton results in imbalanced cellular growth, as has been observed for the zooxanthellae. However, of greater relevance to reef corals, is the impact that this has on zooplankton communities on which they predominantly feed (Houlbrèque and Ferrier-Pagès, 2009). Additional to nutrients, toxins such as heavy metals could accumulate within prey items and cause deleterious effects to thereon feeding corals. Thus, the effects of anthropogenic pollution on heterotrophic feeding by reef corals needs to be further investigated in order to clarify in what environments that heterotrophy could be considered deleterious towards reef corals.

The cellular biomarkers proposed for the identification and management of nutrient stress in reef ecosystems need to be validated by *in situ* studies. It is likely that interacting effects may complicate the use of these markers. It is not known how these markers for nutrient stress would differ among diverse *Symbiodinium* types. A greater understanding of sources of variability is needed. Additionally, it would be useful to establish more efficient methods for the analysis of the described cellular parameters due to laborious work involved in the analysis by TEM. Thus, neutral lipid accumulation can be easily measured by spectrofluorometric assay. Similarly, the measurement of cellular uric acid accumulation was tested by the indirect uricase method which measured hydrogen peroxide as the end product of a reaction using the fluorescent probe Amplex red (Zhao et al., 2008). However this was unsuccessful due to extensive interference with the measurement of hydrogen peroxide. Thus, more work is required to establish the most efficient protocols.

It must be acknowledged that a considerable limitation to all of the studies on the effects of the nutrient environment to the functioning of the coral-zooxanthellae symbiosis presented in this thesis is the use of only one coral host and *Symbiodinium* species: *Euphyllia paradivisa* harbouring *Symbiodinium* clade C1. Moreover, only a single genotype of *E. paradivisa* was available. Thus, these studies were not conducted with true replication. It is recognised that both different coral species and *Symbiodinium* genotypes possess considerable differences in their nutrient biology (Ferrier-Pagès et al., 2010; Baker et al., 2013). Nevertheless, experimental work is often limited to a model organism. It is believed that *E. paradivisa* harbouring clade C1 *Symbiodinium* is an adequate representative of scleractinian corals. This is justified by the wide distribution of *E. paradivisa* within the

indo-pacific and the Red sea, and the common association of corals with clade C1 *Symbiodinium*. Importantly, the morphology of *E. paradivisa* makes this species highly adept at predation which is critical as a model for the effects of heterotrophy. However, the depth distribution of *E. paradivisa* is around 5-20 metres, making this species adapted to a low light environment. Future work must verify key findings of this thesis in other reef organisms and critically assess species specificities. An important progression will be to conduct similar studies with coral species adapted to a high light environment, such as a species of the Acroporidea family. Finally, studies must be conducted *in situ* on whole reef communities. This development is essential for the realisation of advancements in coral reef management strategies.

In order to further our understanding of the role of zooxanthellae lipid biochemistry to stress resilience in reef corals, functional roles of key lipid classes must be elucidated. DGCC was identified as the most abundant lipid of the clade C lipidome, yet the biosynthesis and regulatory pathways of this lipid remain unknown. Likewise, the significance of ether lipids and TGDG are poorly understood. Furthermore, the identity of some observed lipids remains unknown. Future work should establish 'membrane phenotypes' of specific *Symbiodinium* types *in hospite* by subjecting corals to different environmental conditions in controlled laboratory treatments. Analysis of membrane remodeling in response to different abiotic factors will allow one to infer biological function of key lipid classes. Analysis of the cellular localisation of lipid classes would further advance our understanding of lipid function. Specifically, DGDG could be localised both in plastidic and extraplastidic membranes depending on the environmental condition (Härtel et al., 2000). It is also proposed that TGDG could be localised in both membrane compartments and may even be synthesised by different pathways. Cellular localisation of lipid classes could be achieved by subcellular fractionation using differential centrifugation, or by immunolocalisation using antibodies specific to lipid headgroups. Furthering our understanding of membrane remodeling in zooxanthellae is not only relevant to reef corals, but also to other marine algae facing a changing environment.

Future analysis of membrane composition in corals could also advance our understanding of the functioning of the coral-zooxanthellae symbiosis. The comparison of the membrane composition of *Symbiodinium in hospite* and in culture subjected to the same nutrient availability could provide some further insight into the role of nutrient restriction by the

host in controlling symbiont proliferation and provide further insight into what constitutes the symbiotic state. Furthermore, characterisation of the host-derived outer symbiosome membrane as well as the symbiont-derived symbiosome membrane complex following exposure to different stress parameters could give further comprehension of inter-partner signalling and of the bleaching response. Both of these proposed investigations are technically complex due to the difficulties in *Symbiodinium* culture as well as in the isolation of specific membrane compartments, yet continuing progress may enable such investigations.

The most critical question to address in future research on *Symbiodinium* lipidomics is if and how membrane remodeling will continue to allow reef corals to acclimate and adapt to future climate change scenarios. This thesis demonstrated that membrane composition is diverse among different *Symbiodinium* clades and that the specific characteristics of the clade D lipidome likely contribute towards its heightened thermal resilience. Yet, due to host specificities (Goulet, 2006) and to the considerable metabolic trade-offs related to the association with clade D symbionts (Baker et al., 2013), a shift in global symbiont communities to a greater dominance of clade D symbionts as a mechanism of climate change mitigation remains under debate. Moreover, the potential for acclimation by means of membrane remodeling in other *Symbiodinium* types must be assessed. Indeed, certain clade C types are identified as being prevalent within very warm and highly fluctuating environments (Hume et al., 2015; Schoepf et al., 2015). The comparison of the lipid biochemistry of such thermally resilient clade C types to the identified lipidome of clade D *Symbiodinium* (under similar conditions) would provide an evaluation of whether specific polar lipid biomarkers are ubiquitously associated with high thermal tolerance of *Symbiodinium*. Additionally, the analysis of changes in polar lipid composition of the thermally sensitive clade C *Symbiodinium* characterised in this thesis, in response to sublethal temperature stress as well as following a significant recovery period would demonstrate what potential for acclimatisation this clade has in terms of modulating its lipid metabolism and whether heat stress exposure conveys acquired thermotolerance. Yet, a recent study found that a history of thermal stress had no effect on the bleaching susceptibility of a coral harbouring thermally sensitive clade C during consecutive heat stress exposure, which speaks against a capacity of rapid thermotolerance acquisition through acclimation (Silverstein et al., 2015). The vast differences in lipid biochemistry described between clade C and D *Symbiodinium* are the result of long-term evolutionary

divergence. Due to fast generation times and large population sizes, it is possible that evolutionary adaptation of microalgae such as *Symbiodinium* can occur in response to the pace of climate change (Irwin et al., 2015). However, the evolutionary capacity of reef corals to adapt to climate change predictions remains speculative. With the knowledge provided by the investigation of this thesis of what constitutes a thermally tolerant membrane phenotype, membrane remodeling provides a tool with which to investigate the scope of different coral-zooxanthellae associations to acclimate and adapt to warmer oceans. Recently, the controversial debate has been raised on whether assisted evolution of reef corals is necessary for the mitigation of global coral reef loss (van Oppen et al., 2015). If such intervention does become a realistic solution, then specific characteristics of *Symbiodinium* membrane composition are proposed to be an important consideration for the selection of high resilience.

Considerable scientific and social challenges must be overcome in order to preserve coral reefs and the valuable ecosystem services which they provide (Aswani et al., 2015). This thesis presents some advancement towards our understanding of how non-climatic factors affect reef corals and of the potential mechanisms by which corals might adapt to warming oceans. It is hoped that this insight can aid in the progress of critically needed conservation efforts.

Appendices

A1: Appendix for chapter 2

Table A1.1| Median, first quartile (25%) and third quartile (75%) of measured zooxanthellae cellular parameters

		HN/unfed	HN/fed	LN/unfed	LN/fed
Cell size (µm^2)	Median	59.44	54.32	89.65	100.83
	25%	51.99	48.10	75.164	79.9
	75%	66.02	65.84	101.99	121.10
Chloroplasts (µm^2)	Median	24.26	23.42	24.42	20.02
	25%	20.11	17.73	20.15	18.31
	75%	28.77	31.46	29.20	25.95
Lipid bodies (%)	Median	1.78	1.93	33.65	45.21
	25%	0.30	0.44	21.80	35.22
	75%	7.05	5.33	48.73	51.74
Pyrenoid starch sheath (µm^2)	Median	1.72	1.66	1.56	1.91
	25%	1.03	1.08	0.90	0.62
	75%	2.18	2.34	2.77	2.90
Pyrenoid starch core (µm^2)	Median	2.08	2.07	2.37	3.35
	25%	1.65	1.54	1.80	2.05
	75%	2.70	2.63	3.12	3.77
Accumulation body (µm^2)	Median	6.92	6.80	7.50	6.62
	25%	3.40	3.76	3.47	3.08
	75%	11.46	10.56	11.60	11.79

Table A1.2| Mean and SD of measured polyp parameters.

	HN/unfed	HN/fed	LN/unfed	LN/fed
Wet weight (g polyp^{-1})	7.32 ± 1.40	8.81 ± 2.03	0.81 ± 0.24	1.83 ± 0.49
Total protein (mg polyp^{-1})	17.01 ± 5.78	19.07 ± 6.12	2.37 ± 1.31	9.07 ± 1.59
Polyps feeding (% day^{-1})	-	67.54 ± 10.83	-	98.30 ± 2.25
Zooxanthellae density (cells mm^{-2})	5117.6 ± 266.7	5293.5 ± 378.6	887.1 ± 58.3	769.6 ± 90.8
Starch granules (% of cells containing >5)	3.18 ± 2.75	8.34 ± 2.58	24.35 ± 7.19	28.42 ± 13.47
AB integrity (% of AB containing >3 break)	2.78 ± 4.81	2.73 ± 2.64	47.12 ± 8.55	47.26 ± 15.98

Table A1.3| Results of the two-way ANOVA with the two factors: dissolved inorganic nutrient availability and heterotrophic feeding. Asterisk indicates use of the non-parametric Scheirer-Ray-Hare test.

Factor	df	*F* value	*p* value
Polyp weight			
DIN	1	132.587	**<0.001**
Heterotrophy	1	4.599	0.05
DIN x heterotrophy	1	0.163	0.692
Total	17		
Total protein			
DIN	1	36.126	**<0.001**
Heterotrophy	1	4.57	0.051
DIN x heterotrophy	1	1.281	0.277
Total	17		
Density			
DIN	1	379.548	**<0.001**
Heterotrophy	1	0.023	0.883
DIN x heterotrophy	1	0.381	0.554
Total	11		
Dial mitotic rate (K+C)			
DIN	1	12.213	**0.008**
Heterotrophy	1	4.481	0.067
DIN x heterotrophy	1	10.822	**0.011**
Total	11		
Dial mitotic rate (K)			
DIN	1	0.919	0.366
Heterotrophy	1	0.0616	0.810
DIN x heterotrophy	1	0.103	0.756
Total	11		
Cell size			
DIN	1	502.457	**<0.001**
Heterotrophy	1	2.480	0.116
DIN x heterotrophy	1	15.096	**<0.001**
Total	399		
Chloroplasts			
DIN	1	0.642	0.426
Heterotrophy	1	0.753	0.388
DIN x heterotrophy	1	0.774	0.382
Total	79		
Lipid bodies			
DIN	1	1084.119	**<0.001**
Heterotrophy	1	10.155	**0.002**
DIN x heterotrophy	1	8.153	**0.005**
Total	399		

Starch granules			
DIN	1	20.636	**0.002**
Heterotrophy	1	1.033	0.339
DIN x heterotrophy	1	0.014	0.908
Total	11		
Pyrenoid starch			
DIN	1	0.148	0.701
Heterotrophy	1	0.147	0.702
DIN x heterotrophy	1	0.384	0.537
Total	108		
Pyrenoid core			
DIN	1	11.618	**<0.001**
Heterotrophy	1	0.640	0.425
DIN x heterotrophy	1	1.354	0.247
Total	108		
Accumulation body size*			
DIN	1	0.015	0.903
Heterotrophy	1	0.268	0.605
DIN x heterotrophy	1	0.001	0.970
Total	240		
Accumulation body integrity			
DIN	1	121.945	**<0.001**
Heterotrophy	1	0.883	0.375
DIN x heterotrophy	1	2.831	0.131
Total	11		

Table A1.4| Results of Tukey's post hoc test of pairwise comparison for all measured parameters. No post hoc examination could be conducted following the use of non-parametric analysis

		DIN within unfed	DIN within fed	Feeding within HN	Feeding within LN
Wet weight (g polyp^{-1})	Diff of means	6.508	6.981	1.492	1.019
	q	11.111	11.918	2.548	1.741
	P	**<0.001**	**<0.001**	0.093	0.239
Total protein (mg polyp^{-1})	Diff of means	14.644	10.003	2.063	6.704
	q	7.142	4.879	1.006	3.270
	P	**<0.001**	**0.004**	0.489	**0.037**
Zooxanthellae density (cells mm^{-2})	Diff of means	213.169	227.126	8.693	5.265
	q	13.339	14.213	0.544	0.329
	P	**<0.001**	**<0.001**	0.601	0.750
Integrated mitotic rate (K+C)	Diff of means	1.188	39.333	6.800	31.345
	q	0.145	4.797	0.829	3.823
	P	0.888	**0.001**	0.431	**0.005**
Integrated mitotic rate (K)	Diff of means				
	q	n.a.	n.a.	n.a.	n.a.
	P				
Cell size (µm^2)	Diff of means	0.180	0.256	0.0225	0.0532
	q	18.530	26.301	2.311	5.460
	P	**<0.001**	**<0.001**	0.102	**<0.001**
Chloroplasts (µm^2)	Diff of means	0.113	2.424	0.0170	2.521
	q	0.0786	1.681	0.0118	1.748
	P	0.956	0.238	0.993	0.220
Lipid bodies (%)	Diff of means	4.079	4.854	0.0449	0.82
	q	30.071	35.781	0.331	6.042
	P	**<0.001**	**<0.001**	0.815	**<0.001**
Starch granules (% of cells with >5)	Diff of means	21.170	20.084	5.159	4.072
	q	4.662	4.423	1.136	0.897
	P	**0.011**	**0.014**	0.445	0.544
Pyrenoid starch sheath (µm^2)	Diff of means	0.0182	0.0779	0.0183	0.0778
	q	0.247	0.958	0.275	0.892
	P	0.862	0.500	0.846	0.530
Pyrenoid core (µm^2)	Diff of means	0.431	0.879	0.0699	0.377
	q	2.367	4.358	0.424	1.745
	P	0.097	**0.003**	0.765	0.220
Accumulation body size (µm^2)	Diff of means				
	q	n.a.	n.a.	n.a.	n.a.
	P				
Accumulation body integrity (% of AB with >3 break)	Diff of means	60.929	44.816	3.558	12.555
	q	12.726	9.360	0.743	2.622
	P	**<0.001**	**<0.001**	0.614	0.101

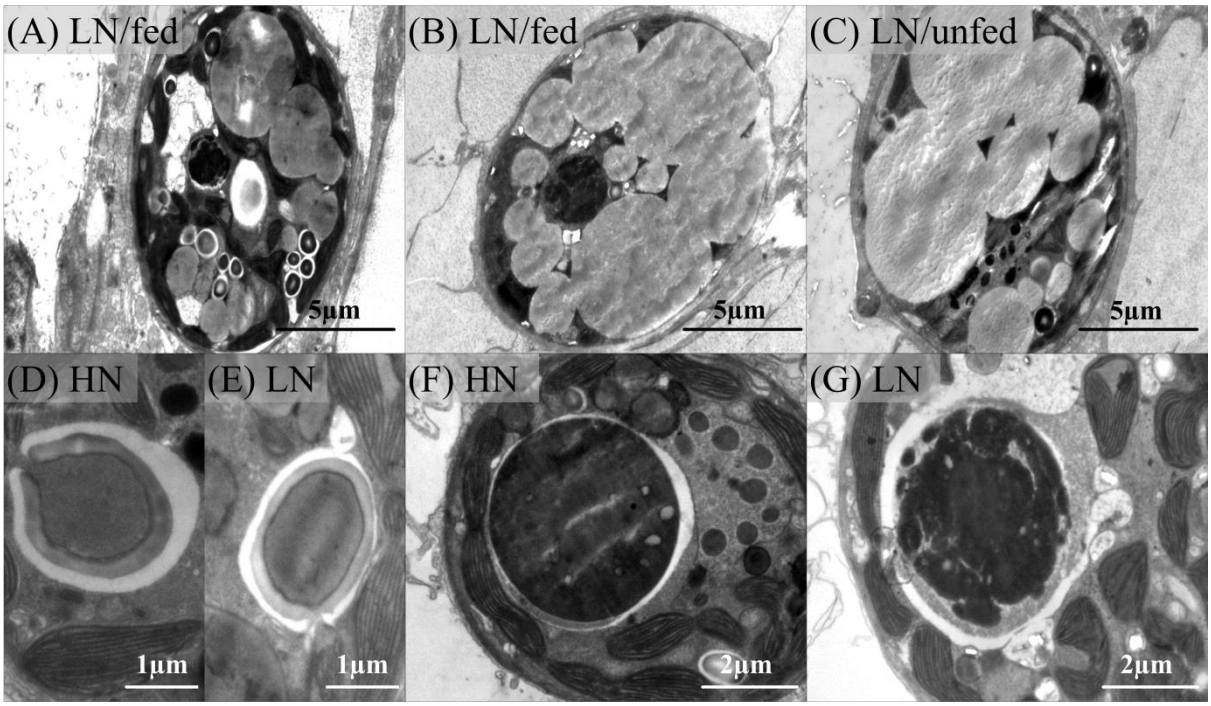

Figure A1.1| A) zooxanthellae of the LN/fed treatment containing a high number of starch granules. B) zooxanthellae of the LN/fed treatment containing a very large amount of lipid bodies. C) zooxanthellae of the LN/unfed treatment containing a very large amount of lipid bodies. D) pyrenoid in a zooxanthellae of the HN treatment. E) pyrenoid in a zooxanthellae of the LN treatment. F) accumulation body in a zooxanthellae of the HN treatment. G) accumulation body in a zooxanthellae of the LN treatment.

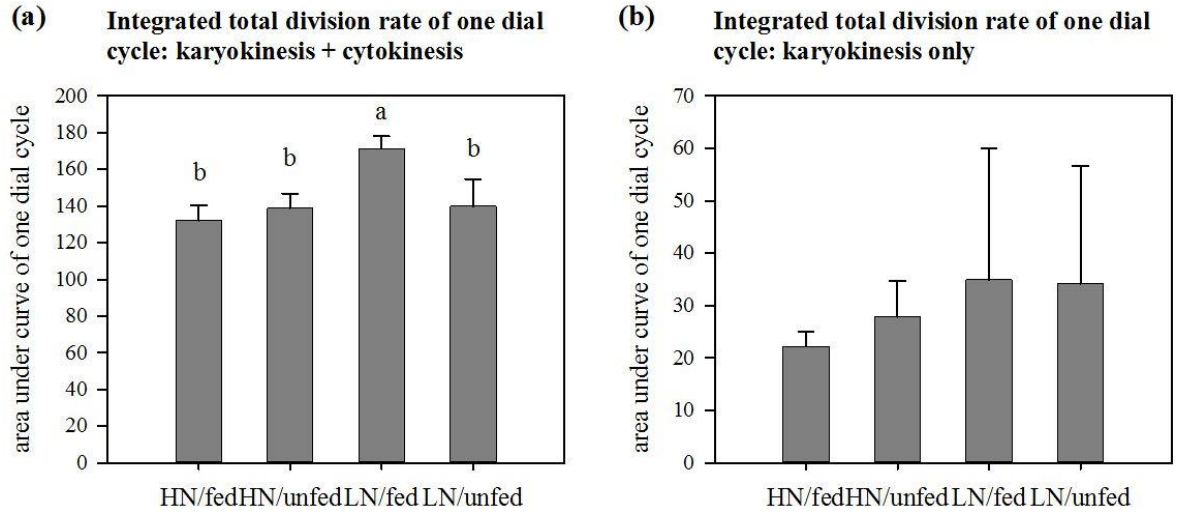

Figure A1.2| Integrated areas of zooxanthellae mitotic rate over one dial cycle. (a) Total of karyokinesis and cytokinesis. (b) Karyokinesis only. Mean ± S.D.

A2: Appendix for chapter 3

Table A2.1| Median, first quartile (25%) and third quartile (75%) of measured zooxanthellae morphological parameters (n = 100)

		+N +P	-N -P	+N -P	-N +P
Cell size (µm^2)	Median	59.44	90.72	76.61	59.60
	25%	51.99	74.15	67.42	53.57
	75%	66.02	101.67	90.51	70.23
Starch granules (%)	Median	0.58	1.49	1.53	2.78
	25%	0.00	0.69	0.48	1.73
	75%	1.50	2.69	3.52	4.05
Lipid bodies (%)	Median	1.78	31.62	23.92	20.79
	25%	0.30	12.98	12.66	9.45
	75%	7.05	48.34	34.40	32.14
Uric acid crystals (%)	Median	0.065	0.137	1.439	0.00
	25%	0.000	0.031	0.629	0.00
	75%	0.184	0.290	2.480	0.00
Accumulation body integrity (no. periphery breaks)	Median	0.00	3.00	0.00	0.00
	25%	0.00	2.00	0.00	0.00
	75%	0.00	5.00	1.00	0.00

Table A2.2| Mean and standard deviation of measured parameters (n = 10 for polyp volume, n = 3 for remaining parameters)

	+N +P	-N -P	+N -P	-N +P
Polyp biomass (cm)	0.795 ± 0.074	0.241 ± 0.031	0.381 ± 0.090	1.066 ± 0.048
Zooxanthellae density (cells mm^{-2})	5117.6 ± 266.7	887.1 ± 58.3	1987.9 ± 818.2	4489.0 ± 776.4

Table A2.3| Results of one-way ANOVA. Use of asterisk indicates use of non-parametric Kruskal-wallis one-way ANOVA on ranks.

	df	**F**	**P**
Polyp biomass (cm)	24	224.199	<0.001
Zooxanthellae density (cells mm^{-2})	11	36.032	<0.001
Cell size (μm^2)	399	92.080	<0.001
Starch granules (%)*	n.a.	n.a.	<0.001
Lipid body content (%)*	n.a.	n.a.	<0.001
Uric acid crystals (%)*	n.a.	n.a.	<0.001
AB integrity (no. periphery breaks)*	n.a.	n.a.	<0.001

Table A2.4| Results of Tukey's post hoc test of pairwise comparison for all measured parameters. Use of asterisk indicates performance of Tukey's test following non-parametric one-way ANOVA on ranks.

		+N+P vs -N-P	**+N+P vs +N-P**	**+N+P vs -N+P**	**-N-P vs +N-P**	**-N-P vs -N+P**	**+N-P vs -N+P**
Polyp volume (ml $polyp^{-1}$)	Diff of means	0.242	0.147	0.0664	0.0949	0.175	0.0804
	q	20.000	8.260	4.298	5.539	11.921	4.092
	P	**<0.001**	**<0.001**	**0.023**	**0.002**	**<0.001**	**0.033**
Zooxanthellae density (cells mm^{-2})	Diff of means	42.304	31.297	6.286	11.007	36.018	25.011
	q	12.628	9.342	1.876	3.286	10.751	7.466
	P	**<0.001**	**<0.001**	0.573	0.172	**<0.001**	**0.003**
Cell size (μm^2)	Diff of means	0.178	0.129	0.0224	0.0493	0.156	0.106
	q	20.097	14.531	2.532	5.567	17.565	11.999
	P	**<0.001**	**<0.001**	0.278	**<0.001**	**<0.001**	**<0.001**
Starch granules (%)*	Diff of ranks	8154.0	8911.5	15332.5	757.5	7178.5	6421.0
	q	7.053	7.708	13.262	0.655	6.209	5.554
	P<0.05	**Yes**	**Yes**	**Yes**	No	**Yes**	**Yes**
Lipid bodies (%)*	Diff of ranks	18762.0	15889.0	13857.0	2873.0	4905.0	2032.0
	q	6.228	13.743	11.986	2.485	4.243	1.758
	P<0.05	**Yes**	**Yes**	**Yes**	No	**Yes**	No
Uric acid crystals (%)*	Diff of ranks	3261.0	13833.0	10682.0	10572.0	13943.0	24515.0
	q	2.821	11.965	9.239	9.144	12.060	21.204
	P<0.05	No	**Yes**	**Yes**	**Yes**	**Yes**	**Yes**
Accumulation body integrity (no. periphery breaks)*	Diff of means	112.553	18.739	3.085	93.814	115.637	21.823
	q	6.863	1.442	0.235	5.785	7.092	1.695
	P	Yes	No	No	Yes	Yes	No

Method A2.1: Nile Red fluorescent dye

The fluorescent dye Nile Red emits a yellow/orange fluorescent signal in the presence of neutral lipids (Greenspan et al., 1985). This property was used to measure differences in zooxanthellae neutral lipid content depending on the experimental treatment, thus providing a method with which to verify the results of zooxanthellae lipid body content, as determined by TEM. Nile Red (Sigma-Aldrich Ltd.) was dissolved in DMSO as a 1 mg ml^{-1} stock solution. Tentacles of *E. paradivisia* were harvested at the start of the light period and zooxanthellae were isolated as described above. Zooxanthellae were counted using a haemocytometer and cell concentrations for all samples were standardised to $7x10^5$ cells ml^{-1} by dilution in sterile seawater. Cells were stained in 2 μg ml^{-1} Nile Red with 5% DMSO (Kou et al., 2013). Samples were shaken for 40 seconds, incubated at room temperature for 5 minutes, and measured in a 96-well plate using a Varian Cary Eclipse fluorescence spectrophotometer with an excitation wavelength of 528nm. Emission spectra were obtained in the range of 550-750 nm with 576 nm being recorded as the Nile Red fluorescence emission corresponding to neutral lipids. Relative fluorescence intensity (RFI) was obtained by subtraction of the fluorescence intensity of the zooxanthellae autofluorescence and of Nile Red in seawater, from that of the stained zooxanthellae. Results of RFI were normalised to cell size as determined by TEM, thereby making the results representative of neutral lipid content per cell volume which is directly comparable to the results of lipid body accumulation determined by TEM.

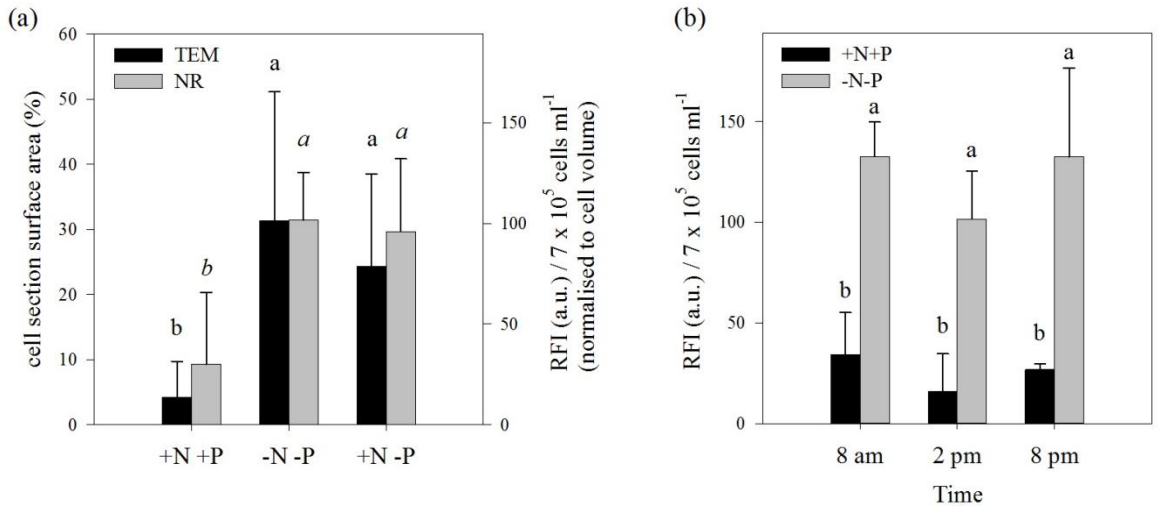

Figure A2.1| (a) zooxanthellae neutral lipid content measured by transmission electron microscopy (TEM) analysis and by relative fluorescence intensity of Nile Red (NR). (b) Fluctuation in lipid body accumulation within nutrient replete (+N+P) and nutrient limited (-N-P) samples measured at three time points in the dial cycle as, measured by the relative fluorescence intensity of Nile Red

Table A2.5| Results of one-way ANOVA. Use of asterisk indicates use of non-parametric Kruskal-wallis one-way ANOVA on ranks.

	df	**F**	**P**
Lipid body (TEM)*	n.a.	n.a.	<0.001
Lipid body (Nile Red)	11	8.666	0.008

Table A2.6| Results of Tukey's post hoc test of pairwise comparison. Use of asterisk indicates performance of Tukey's test following non-parametric one-way ANOVA on ranks.

		+N+P vs -N-P	**+N+P vs +N-P**	**-N-P vs +N-P**
Lipid body (TEM)	Diff of ranks	13377	11365.5	2011.5
	q	15.421	13.102	2.319
	P<0.05	**Yes**	**Yes**	No
Lipid body (Nile Red)	Diff of means	59.422	46.772	12.649
	q	5.588	4.399	1.190
	P	**0.009**	**0.031**	0.688

Table A2.7| Results of the two-way ANOVA for determination of significance in the difference of lipid body abundance over time measured by Nile Red relative fluorescence intensity. The two parameters are dissolved inorganic nutrient availability and time

	df	F	P
Nutrients	1	92.752	<0.001
Time	2	3.293	0.056
Nutrients* time	2	0.622	0.546
Total	27		

A3: Appendix for chapter 4

Table A3.1| Results of two-way ANOVA on the effects of dissolved inorganic nutrient availability (DIN) and food type on feeding behaviour, measured as the mean daily percentage of polyps ingesting food items (mean taken over five weeks)

Parameter	Factor	df	F	P
Rate of food ingestion	DIN	2	65.657	**<0.001**
	Food type	3	55.845	**<0.001**
	DIN x food type	6	8.075	**<0.001**
	Total	57		

Table A3.2| Tukey's test for multiple pairwise comparisons on the effects of dissolved inorganic nutrient availability and food type on feeding behaviour, measured as the mean daily percentage of polyps ingesting food items (mean taken over five weeks)

Comparison		**Feeding within +N+P**	**Feeding within -N-P**	**Feeding within +N-P**
HP vs. LA	Diff of means	50.974	59.726	36.584
	q	6.604	8.935	5.473
	P	**<0.001**	**<0.001**	**0.002**
HP vs. LP	Diff of means	38.471	59.844	47.433
	q	5.755	8.952	7.096
	P	**0.001**	**<0.001**	**<0.001**
HP vs. HA	Diff of means	31.078	3.174	41.511
	q	4.649	0.475	6.210
	P	**0.010**	0.987	**<0.001**
HA vs. LA	Diff of means	19.876	62.900	78.095
	q	2.578	9.410	11.683
	P	0.276	**<0.001**	**<0.001**
HA vs. LP	Diff of means	7.393	63.018	88.944
	q	1.106	9.427	13.306
	P	0.862	**<0.001**	**<0.001**
LP vs. LA	Diff of means	12.503	0.118	10.849
	q	1.620	0.0176	1.623
	P	0.664	1.000	0.662

Comparison		**DIN within HP**	**DIN within LP**	**DIN within HA**	**DIN within LA**
+N+P vs. -N-P	Diff of means	54.321	32.948	88.572	45.568
	q	8.126	4.929	13.250	5.904
	P	**<0.001**	**0.003**	**<0.001**	**<0.001**
+N+P vs. +N-P	Diff of means	19.317	10.355	91.905	33.707
	q	2.890	1.549	13.749	4.367
	P	0.113	0.522	**<0.001**	**0.009**
-N-P vs. +N-P	Diff of means	35.004	22.593	3.333	11.862
	q	5.236	3.380	0.499	1.774
	P	**0.002**	0.054	0.934	0.428

Table A3.3| Results of two-tailed t-test to determine significant difference in the total content of nitrogen and phosphorus within two food types

	df	t	P
Total N	4	9.456	**<0.001**
Total P	4	-2.399	0.074

Table A3.4| Significant effects of feeding treatment and dissolved inorganic nutrient availability (DIN) on the total intake of nitrogen and phosphorus by heterotrophic feeding determined non-parametric Scheirer-Ray-Hare test.

Parameter	Factor	df	SS/MS_{total}	P
Total N intake	DIN	2	3.334	0.189
	Food type	3	50.920	**<0.001**
	DIN x food type	6	0.412	0.999
	Total	57		
Total P intake	DIN	2	9.631	**0.008**
	Food type	3	44.862	**<0.001**
	DIN x food type	6	1.940	0.925
	Total	57		

Table A3.5| Mean and standard deviation of uric acid crystal abundance in zooxanthellae in the –N-P treatment, measured as % cell section surface area by micrograph analyses.

	HP	**HA**	**UF**
Uric acid crystal abundance (%)	1.211 ± 0.819	0.0143 ± 0.0386	0.156 ± 0.317

Table A3.6| Statistical significance of the effect of different feeding treatments on the accumulation of uric acid crystals. Pairwise multiple comparisons (Tukey's test) following a Kruskal-Wallis one-way ANOVA on ranks.

Comparison	Diff of Ranks	q	P<0.05
HP vs. HA	9232.000	16.376	**Yes**
HP vs. UF	6683.000	11.855	**Yes**
HA vs. UF	2549.000	4.522	**Yes**

Table A3.7| Results of two-way ANOVA with the two factors being dissolved inorganic nutrient (DIN) availability and feeding treatment.

Parameter	Factor	df	F	P
Zooxanthellae density	DIN	2	301.485	**<0.001**
	Feeding	4	36.151	**<0.001**
	DIN x feeding	8	18.483	**<0.001**
	Total	79		
Zooxanthellae neutral lipid	DIN	2	25.322	**<0.001**
	Feeding	4	5.298	**0.001**
	DIN x feeding	8	1.626	0.144
	Total	59		
GFP-like protein	DIN	2	91.881	**<0.001**
	Feeding	4	8.513	**<0.001**
	DIN x feeding	8	3.407	**0.003**
	Total	79		
Polyp tissue cover	DIN	2	8.600	**<0.001**
	Feeding	4	47.448	**<0.001**
	DIN x feeding	8	11.903	**<0.001**
	Total	100		

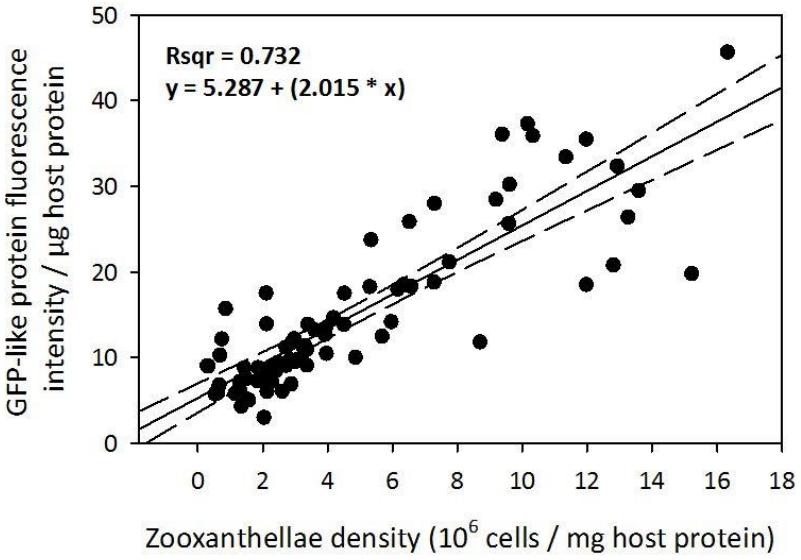

Figure A.3.1| Linear regression of GFP-like protein fluorescence intensity and zooxanthellae density showing a significant positive correlation. Regression line and 95% confidence intervals are shown. N = 80, F = 213.573, P = <0.001

Table A3.8| Results of Tukey's test for multiple pairwise comparisons following a two-way ANOVA on zooxanthellae density, with the two factors being dissolved inorganic nutrient availability (DIN) and feeding treatment.

Comparison		**Feeding within +N+P**	**Feeding within -N-P**	**Feeding within +N-P**
HA vs. LP	Diff of means	0.0407	0.561	0.152
	q	0.751	14.642	2.809
	P	0.984	**<0.001**	0.284
HA vs. HP	Diff of means	0.0276	0.254	0.145
	q	0.509	6.627	2.678
	P	0.996	**<0.001**	0.331
HA vs. LA	Diff of means	0.0225	0.330	0.121
	q	0.415	8.598	2.231
	P	0.998	**<0.001**	0.517
HA vs. UF	Diff of means	0.0113	0.978	0.336
	q	0.208	25.512	6.203
	P	1.000	**<0.001**	**<0.001**
UF vs. LP	Diff of means	0.0295	0.417	0.184
	q	0.543	10.870	3.393
	P	0.995	**<0.001**	0.129
UF vs. HP	Diff of means	0.0163	0.724	0.191
	q	0.301	18.885	3.525
	P	1.000	**<0.001**	0.105
UF vs. LA	Diff of means	0.0112	0.649	0.457
	q	0.207	16.914	8.433
	P	1.000	**<0.001**	**<0.001**
LA vs. LP	Diff of means	0.0182	0.232	0.273
	q	0.336	6.044	5.040
	P	0.999	**<0.001**	**0.006**
LA vs. HP	Diff of means	0.00508	0.0756	0.266
	q	0.0937	1.971	4.909
	P	1.000	0.634	**0.008**
HP vs. LP	Diff of means	0.0131	0.307	0.00714
	q	0.242	8.015	0.132
	P	1.000	**<0.001**	1.000

Comparison		**DIN within HP**	**DIN within LP**	**DIN within HA**	**DIN within LA**	**DIN within UF**
+N+P vs.	Diff of means	0.547	0.841	0.321	0.628	1.287
-N-P	q	11.649	17.913	6.825	13.366	27.416
	P	**<0.001**	**<0.001**	**<0.001**	**<0.001**	**<0.001**
+N+P vs.	Diff of means	0.595	0.589	0.478	0.334	0.803
+N-P	q	10.975	10.865	8.807	6.160	14.801
	P	**<0.001**	**<0.001**	**<0.001**	**<0.001**	**<0.001**
-N-P vs.	Diff of means	0.0481	0.252	0.157	0.294	0.485
+N-P	q	1.024	5.368	3.343	6.253	10.325
	P	0.750	**0.001**	0.054	**<0.001**	**<0.001**

Table A3.9| Results of Tukey's test for multiple pairwise comparisons following a two-way ANOVA on zooxanthellae lipid body accumulation, with the two factors being dissolved inorganic nutrient availability (DIN) and feeding treatment.

Comparison		**Feeding within +N+P**	**Feeding within -N-P**	**Feeding within +N-P**
HA vs. LP	Diff of means	1.031	23.923	19.133
	q	0.111	2.584	2.066
	P	1.000	0.371	0.593
HA vs. HP	Diff of means	4.222	18.533	16.041
	q	0.456	2.001	1.732
	P	0.998	0.621	0.737
HA vs. LA	Diff of means	5.763	0.112	9.909
	q	0.622	0.0121	1.070
	P	0.992	1.000	0.942
HA vs. UF	Diff of means	4.246	52.571	43.416
	q	0.459	5.677	4.689
	P	0.998	**0.002**	**0.015**
UF vs. LP	Diff of means	3.215	28.648	24.283
	q	0.347	3.094	2.622
	P	0.999	0.203	0.356
UF vs. HP	Diff of means	0.0239	34.039	27.376
	q	0.00258	3.676	2.956
	P	1.000	0.088	0.242
UF vs. LA	Diff of means	1.516	52.460	33.507
	q	0.164	5.665	3.618
	P	1.000	**0.002**	0.096
LA vs. LP	Diff of means	4.732	23.812	9.224
	q	0.511	2.571	0.996
	P	0.996	0.376	0.954
LA vs. HP	Diff of means	1.540	18.421	6.132
	q	0.166	1.989	0.662
	P	1.000	0.627	0.990
HP vs. LP	Diff of means	3.191	5.391	3.093
	q	0.345	0.582	0.334
	P	0.999	0.994	0.999

Comparison		**DIN within HP**	**DIN within LP**	**DIN within HA**	**DIN within LA**	**DIN within UF**
+N+P vs.	Diff of means	34.763	36.962	12.007	17.882	68.825
-N-P	q	3.754	3.992	1.297	1.931	7.432
	P	**0.029**	**0.019**	0.633	0.367	**<0.001**
+N+P vs.	Diff of means	37.323	37.225	17.060	32.732	64.723
+N-P	q	4.031	4.020	1.842	3.535	6.989
	P	**0.018**	**0.018**	0.401	**0.042**	**<0.001**
-N-P vs.	Diff of means	2.561	0.263	5.053	14.850	4.102
+N-P	q	0.277	0.0284	0.546	1.604	0.443
	P	0.979	1.000	0.921	0.499	0.948

Table A3.10| Results of Tukey's test for multiple pairwise comparisons following a two-way ANOVA on GFP-like protein fluorescence intensity, with the two factors being dissolved inorganic nutrient availability (DIN) and feeding treatment.

Comparison		**Feeding within +N+P**	**Feeding within -N-P**	**Feeding within +N-P**
HA vs. LP	Diff of means	0.0654	0.398	0.241
	q	1.027	8.844	3.784
	P	0.950	**<0.001**	0.069
HA vs. HP	Diff of means	0.0601	0.170	0.125
	q	0.944	3.764	1.958
	P	0.963	0.071	0.640
HA vs. LA	Diff of means	0.0278	0.182	0.183
	q	0.437	4.051	2.878
	P	0.998	**0.043**	0.261
HA vs. UF	Diff of means	0.138	0.221	0.132
	q	2.166	4.897	2.080
	P	0.546	**0.008**	0.585
UF vs. LP	Diff of means	0.203	0.178	0.109
	q	3.194	3.947	1.705
	P	0.172	0.052	0.748
UF vs. HP	Diff of means	0.0778	0.051	0.00771
	q	1.222	1.133	0.121
	P	0.909	0.929	1.000
UF vs. LA	Diff of means	0.110	0.0381	0.316
	q	1.730	0.846	4.958
	P	0.738	0.975	**0.007**
LA vs. LP	Diff of means	0.0932	0.216	0.424
	q	1.464	4.793	6.663
	P	0.838	**0.010**	**<0.001**
LA vs. HP	Diff of means	0.0323	0.0129	0.308
	q	0.508	0.287	4.837
	P	0.996	1.000	**0.009**
HP vs. LP	Diff of means	0.126	0.229	0.116
	q	1.972	5.080	1.826
	P	0.634	**0.006**	0.698

Comparison		**DIN within HP**	**DIN within LP**	**DIN within HA**	**DIN within LA**	**DIN within UF**
+N+P vs.	Diff of means	0.460	0.564	0.231	0.441	0.589
-N-P	q	8.349	10.220	4.185	7.997	10.685
	P	**<0.001**	**<0.001**	**0.012**	**<0.001**	**<0.001**
+N+P vs.	Diff of means	0.509	0.500	0.324	0.168	0.594
+N-P	q	7.989	7.843	5.086	2.644	9.332
	P	**<0.001**	**<0.001**	**0.002**	0.156	**<0.001**
-N-P vs.	Diff of means	0.0483	0.0642	0.0931	0.273	0.00501
+N-P	q	0.876	1.163	1.688	4.943	0.0908
	P	0.810	0.691	0.461	**0.003**	0.998

Table A3.11| Results of Tukey's test for multiple pairwise comparisons following a two-way ANOVA on polyp tissue cover, with the two factors being dissolved inorganic nutrient availability (DIN) and feeding treatment.

Comparison		**Feeding within +N+P**	**Feeding within -N-P**	**Feeding within +N-P**
HA vs. LP	Diff of means	0.317	6.341	5.604
	q	0.651	10.357	7.473
	P	0.991	**<0.001**	**<0.001**
HA vs. HP	Diff of means	0.652	2.908	4.687
	q	1.406	4.750	6.251
	P	0.587	**0.010**	**<0.001**
HA vs. LA	Diff of means	0.826	4.069	1.521
	q	1.901	6.646	2.028
	P	0.665	**<0.001**	0.608
HA vs. UF	Diff of means	1.320	10.926	7.188
	q	2.678	17.845	9.585
	P	0.329	**<0.001**	**<0.001**
UF vs. LP	Diff of means	0.351	4.585	1.583
	q	0.681	7.489	2.111
	P	0.989	**<0.001**	0.570
UF vs. HP	Diff of means	0.668	8.018	2.500
	q	1.328	13.095	3.334
	P	0.881	**<0.001**	0.137
UF vs. LA	Diff of means	2.145	6.857	5.667
	q	4.502	11.200	7.557
	P	**0.017**	**<0.001**	**<0.001**
LA vs. LP	Diff of means	1.795	2.272	4.083
	q	3.903	3.711	5.445
	P	0.054	0.075	**0.002**
LA vs. HP	Diff of means	1.477	1.161	3.167
	q	3.312	1.896	4.223
	P	0.142	0.667	**0.030**
HP vs. LP	Diff of means	0.317	3.433	0.917
	q	0.651	5.607	1.222
	P	0.991	**0.002**	0.909

Comparison		**DIN within HP**	**DIN within LP**	**DIN within HA**	**DIN within LA**	**DIN within UF**
+N+P vs.	Diff of means	1.607	1.509	3.864	1.031	5.743
-N-P	q	2.934	2.699	7.178	1.970	10.027
	P	0.101	0.142	**<0.001**	0.349	**<0.001**
+N+P vs.	Diff of means	2.303	2.902	1.733	0.613	4.135
+N-P	q	3.670	4.554	2.799	1.011	6.367
	P	**0.030**	**0.005**	0.124	0.755	**<0.001**
-N-P vs.	Diff of means	3.910	1.393	2.130	0.418	1.608
+N-P	q	5.711	2.035	3.112	0.610	2.350
	P	**<0.001**	0.326	0.077	0.903	0.226

Table A3.12| Significant effects of feeding and dissolved inorganic nutrient availability (DIN) on the rate of Fv/Fm decline following exposure to 30°C determined non-parametric Scheirer-Ray-Hare test.

Parameter	Factor	df	SS/MS_{total}	P
Slope of decline in Fv/Fm	DIN	1	28.387	**<0.001**
	Feeding	4	9.550	**0.049**
	DIN x feeding	4	3.110	**0.540**
	Total	39		

Table A3.13| Significant effects of feeding and dissolved inorganic nutrient availability (DIN) on the rate of polyp skeletal tissue cover decline following exposure to 30°C determined by two-way ANOVA.

Parameter	Factor	df	F	P
Slope of decline in tissue cover	DIN	1	22.099	**<0.001**
	Feeding	4	17.802	**<0.001**
	DIN x feeding	4	4.078	**0.009**
	Total	39		

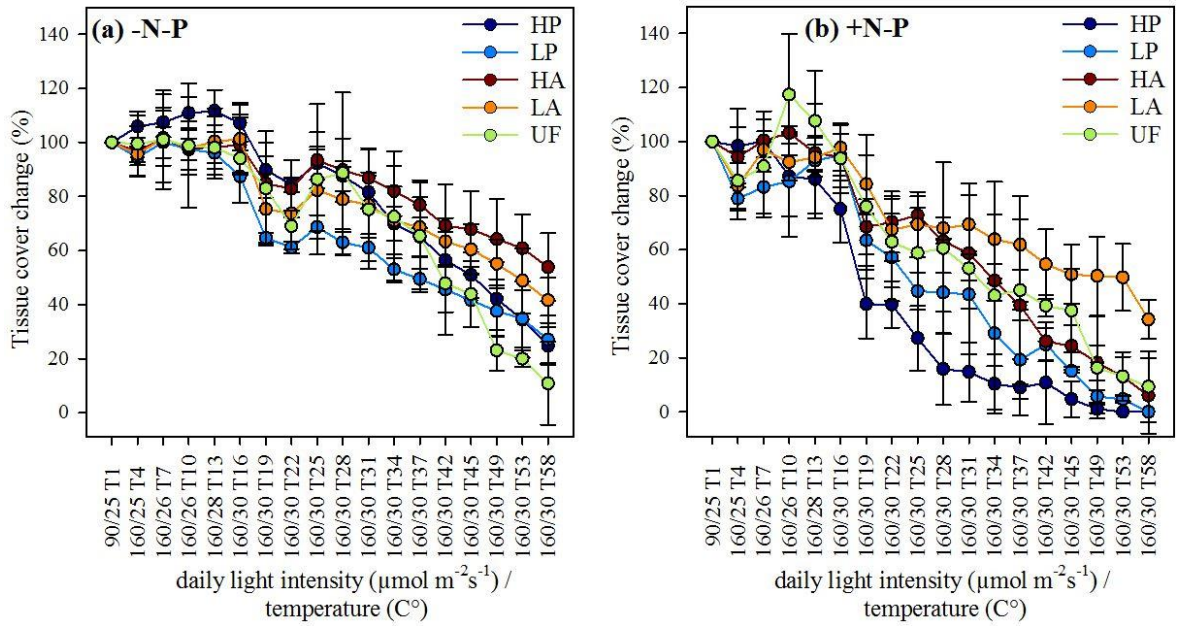

Figure A3.2| Rate of decline in polyp skeletal tissue cover shown as percentage change from length measured prior to onset of stress treatment. **(a)** Nutrient limited system. **(b)** Nutrient imbalanced system.

Table A3.14| Significant differences in rate of decline in polyp skeletal tissue cover following exposure to 30°C. Multiple pairwise comparisons by Tukey's post hoc test.

Comparison		**Feeding within -N-P**	**Feeding within +N-P**
LP vs. HA	Diff of means	0.551	0.0233
	q	1.798	0.0555
	P	0.403	0.956
LP vs. LA	Diff of means	0.434	1.005
	q	1.413	2.712
	P	0.601	0.084
LP vs. UF	Diff of means	0.225	0.444
	q	0.690	1.198
	P	0.871	0.561
LP vs. HP	Diff of means	0.273	0.811
	q	0.891	2.365
	P	0.852	0.161
HP vs. HA	Diff of means	0.825	0.835
	q	2.688	1.987
	P	0.110	0.251
HP vs. LA	Diff of means	0.707	1.816
	q	2.304	4.902
	P	0.205	**<0.001**
HP vs. UF	Diff of means	0.0486	1.255
	q	0.149	3.388
	P	0.882	**0.018**
UF vs. HA	Diff of means	0.776	0.421
	q	2.385	0.950
	P	0.193	0.577
UF vs. LA	Diff of means	0.658	0.561
	q	2.023	1.416
	P	0.312	0.519
LA vs. HA	Diff of means	0.118	0.982
	q	0.384	2.217
	P	0.912	0.189

Comparison		**DIN within HP**	**DIN within LP**	**DIN within HA**	**DIN within LA**	**DIN within UF**
-N-P vs.	Diff of means	1.465	0.927	1.455	0.356	0.258
+N-P	q	4.502	2.849	3.585	1.004	0.697
	P	**<0.001**	**0.008**	**0.001**	0.323	0.491

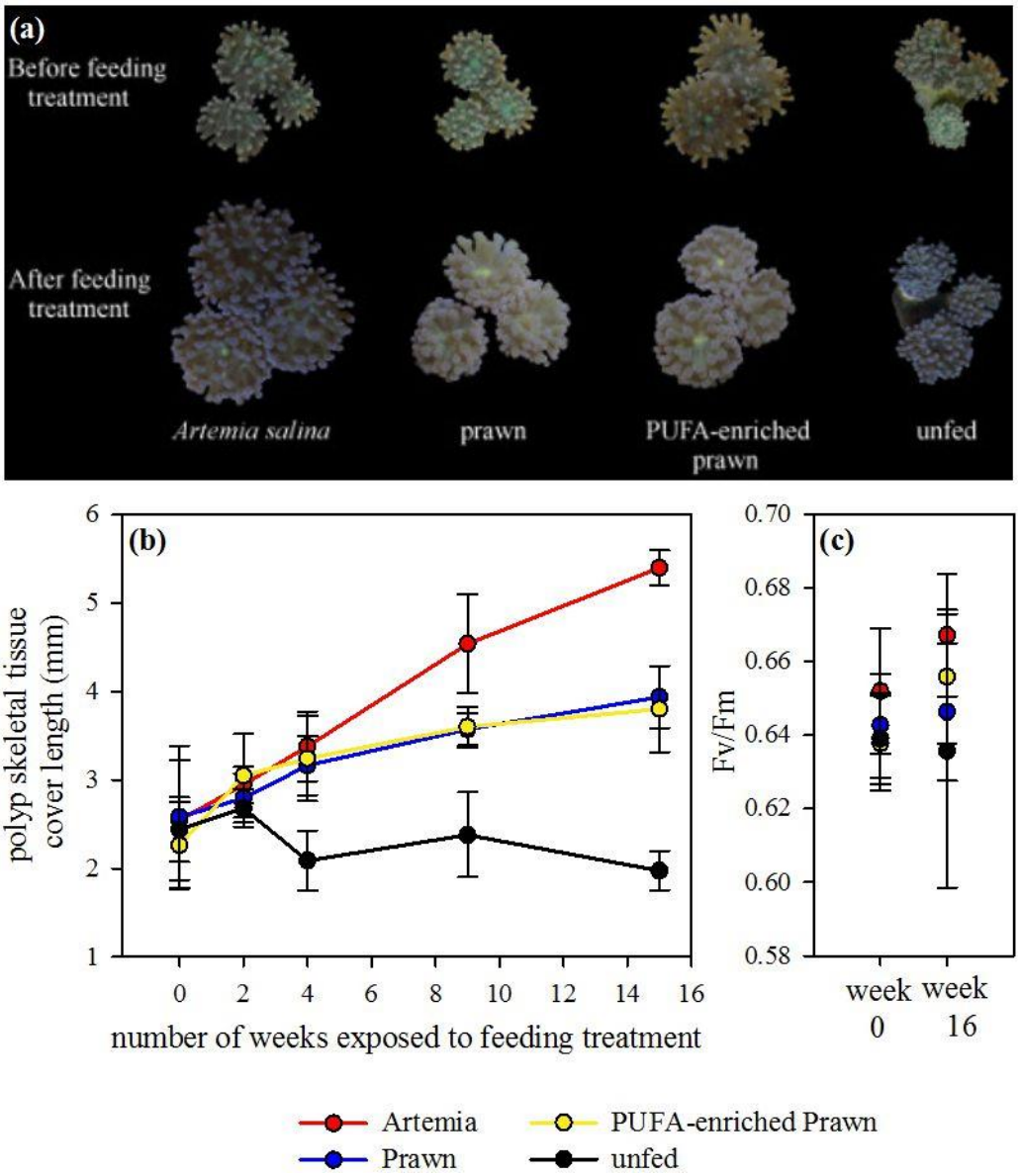

Figure A3.3| Food quality control experiment: effect of PUFA enrichment. Polyps within the -N-P treatment which had been unfed for over one year were fed for 16 weeks with Artemia, prawn, prawn enriched with polyunsaturated fatty acids (PUFA), or remained unfed. **(a)** Changes to polyp biomass were monitored photographically. **(b)** The length of the skeletal tissue cover was monitored. **(c)** Fv/Fm was measured before and after the feeding treatment. PUFA enrichment had no significant effect on polyp biomass or colouration in respect to polyps fed with unenriched prawn, supporting that it is the difference in the N:P ratio of the food that causes the significant differences observed between Artemia and prawn fed polyps.

A4: Appendix for chapter 5

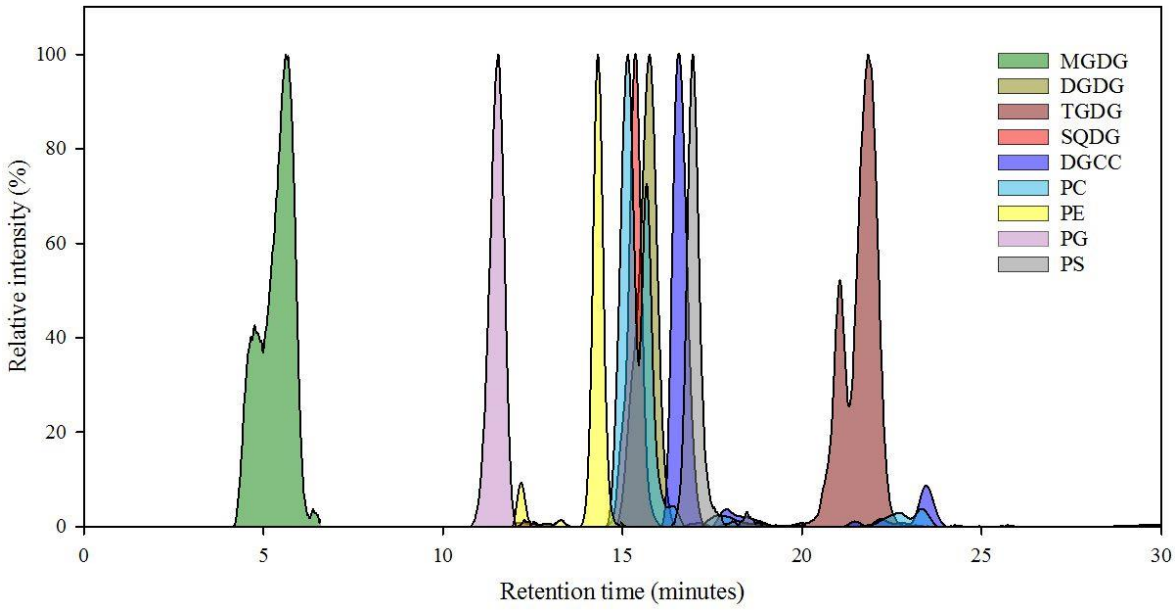

Figure A4.1| Separation of analysed lipid classes by liquid chromatography method. The chromatogram of each lipid class is measured by the use of neutral loss or precursor scans specific to headgroup fragments.

Table A4.1| Mean signal intensity of each investigated lipid class. Statistical significant differences in the abundance of each lipid class are determined by one-way analysis of variance. A pairwise comparison of the two clade C samples and of the purple morph clade C with clade D samples was conducted using Tukey's post hoc test.

Lipid class	CA	CB	D	ANOVA p-value	CA vs CB (Tukey's p-value)	CB vs D (Tukey's p-value)
PC total	665781536	653146921	1127627224	**<0.001**	0.964	**<0.001**
PC diacyl	243669860	242366955	137395395	**0.003**	0.996	**0.005**
PC alkyl	422111676	410779966	990231829	**<0.001**	0.978	**<0.001**
Lyso-PC	33329153	49296264	53801998	0.064	n.a	n.a.
PE	605981	708653	90191	**0.014**	0.789	0.016
Cer PE	9558764	8279586	12115185	0.417	n.a	n.a
PG	7144751	7376158	1573520	**<0.001**	0.751	**<0.001**
PS	3003461	3821806	9063400	0.072	n.a	n.a
PI	28118	31378	145147	0.071*	n.a	n.a
DGCC	1049717007	1096970937	228905104	**<0.001**	0.355	**<0.001**
Lyso-DGCC	110415368	114638762	389539385	**<0.001**	0.979	**<0.001**
MGDG NL179	1186008	1449041	994493	**0.032**	0.178	**0.028**
MGDG P243	14471641	16391589	8101501	**<0.001**	0.303	**0.001**
DGDG NL341	26855744	28993139	26963372	0.209	n.a	n.a
DGDG P243	10315732	12886421	11031645	0.511	n.a	n.a
TGDG	7059171	7018514	2289472	**0.002**	0.997	**0.004**
SQDG	16075946	16330905	13338184	0.175	n.a	n.a
910 P104	80366543	86778093	3057536	**<0.001**	0.579	**<0.001**
P241 ES+	5692204	5805338	8418046	**0.003**	0.974	**0.006**

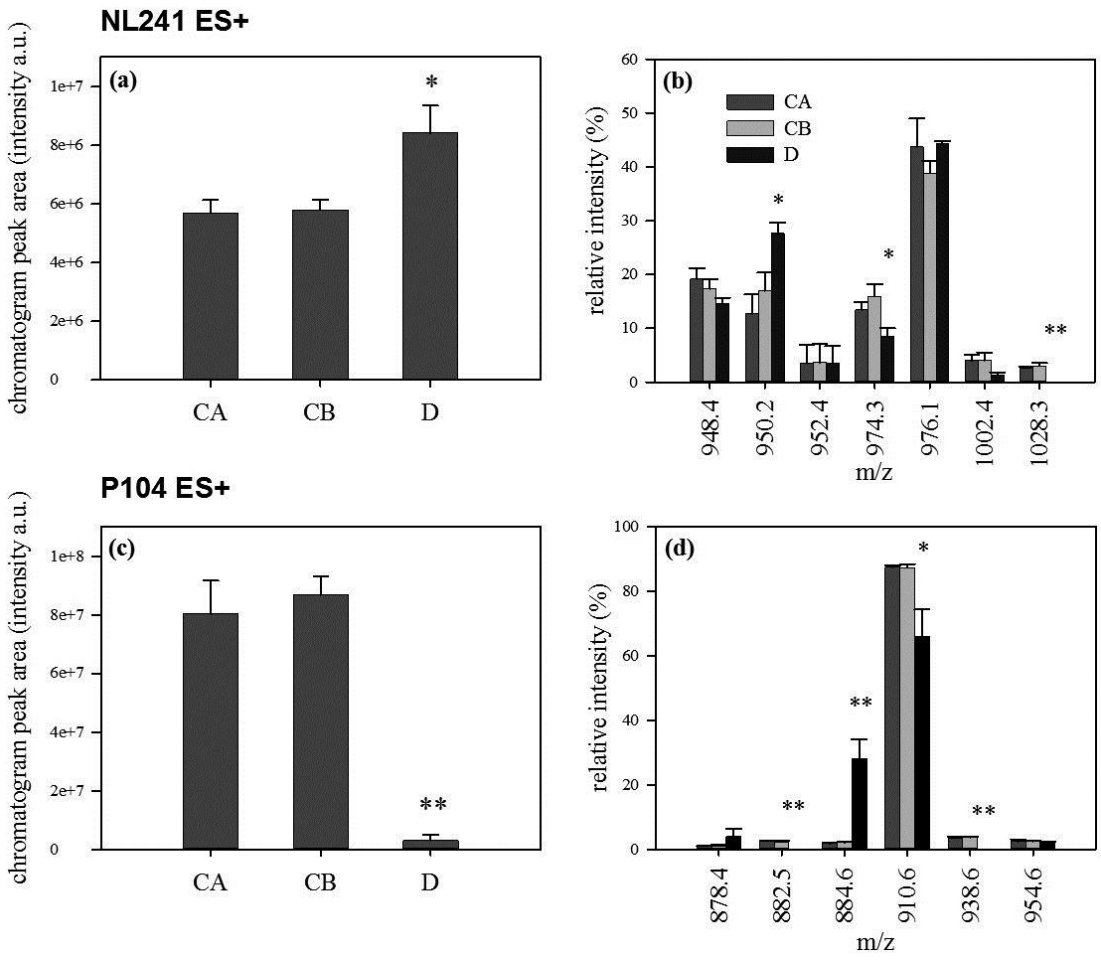

Figure A4.2| Abundance and composition of two unknown lipid classes. Total abundance measured as signal intensity of integrated chromatogram peak area for (a) peaks identified with a neutral loss scan 241 in positive ionisation mode and (c) peaks identified with precursor scan 104 in positive ionisation mode. (b) and (d) respective relative composition of lipid species measured as percent contribution to total lipid class. CA = *Symbiodinium* clade C isolated from brown *A. valida* colour morph, CB = *Symbiodinium* clade C isolated from purple *A. valida* colour morph, D = *Symbiodinium* clade C isolated from purple *A. valida* colour morph. Significant differences between samples CB and D are indicated by the use of asterisk. * = $p<0.05$, ** = $p<0.001$.

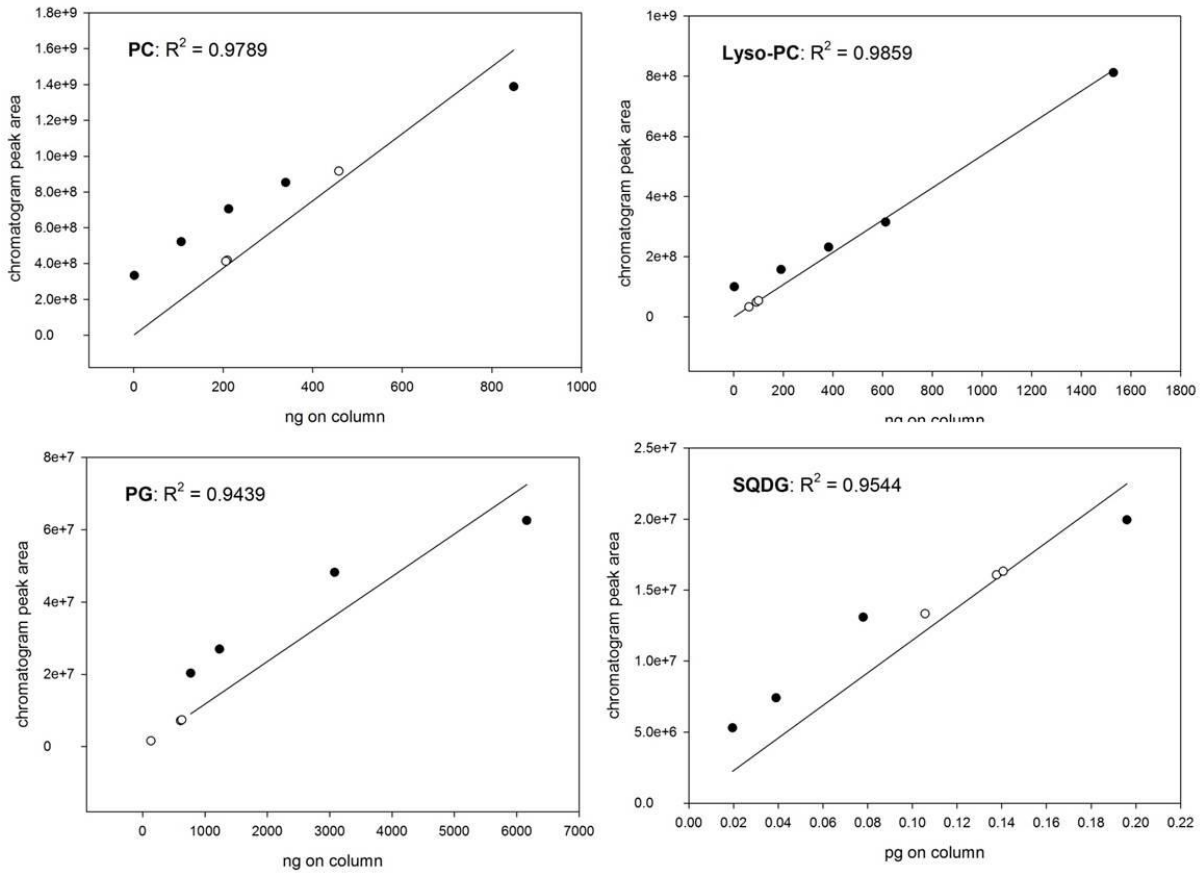

Figure A4.3| Standard curves. Standard curves were generated by measuring the chromatogram peak areas of lipid standards for PC, lyso-PC, PG, and SQDG at different concentrations.

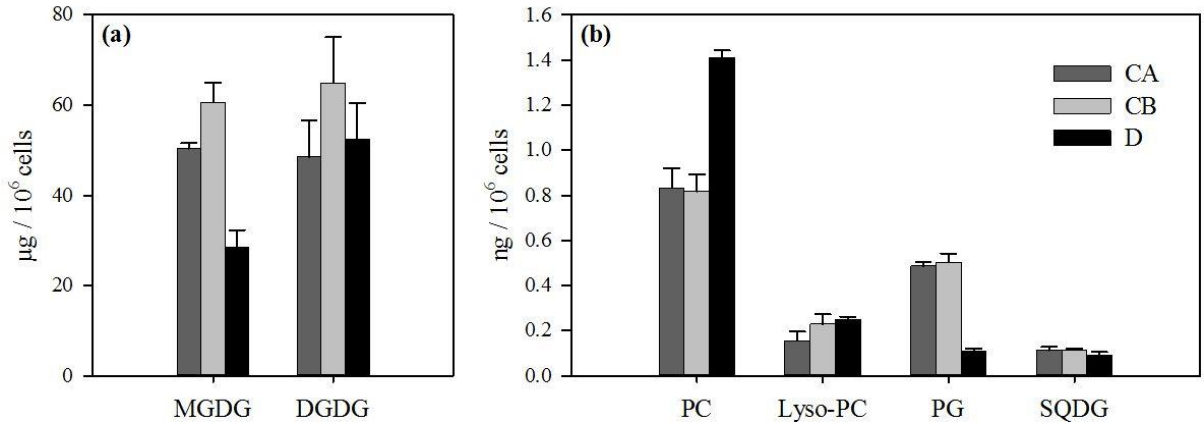

Figure A4.4| Quantification of lipid classes. The quantity of six lipid classes within the total lipid extracted from one million cells were estimated (a) Glycolipid abundance was extrapolated by comparison to internal standards within spectra using a scan of P243 ES+ . (b) PC, lyso-PC, PG, and SQGD abundances were extrapolated from standard curves generated by measuring the chromatogram peak areas of lipid standards at different concentrations.

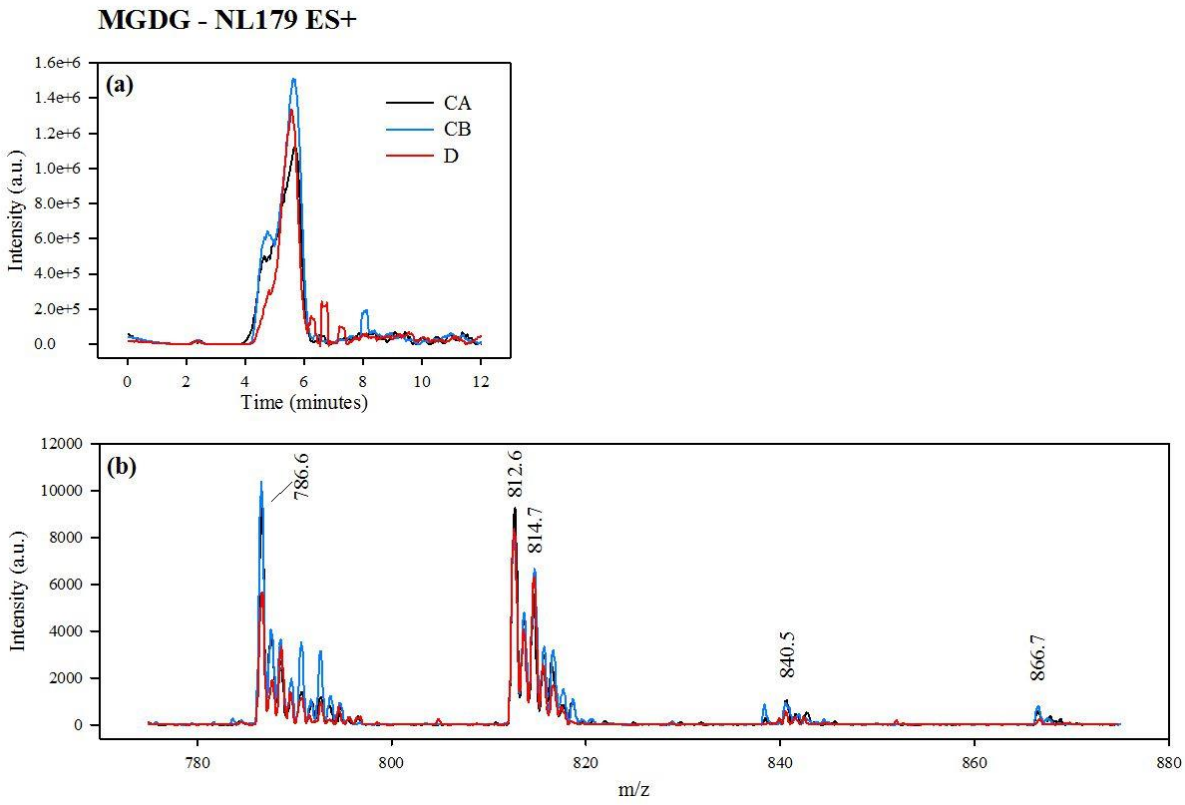

Figure A4.5| Monogalactosyldiacylglycerol measured using a neutral loss scan 179 in positive ionisation mode. (a) Mean chromatogram trace. (b) Mass spectrum. CA = *Symbiodinium* clade C isolated from brown *A. valida* colour morph, CB = *Symbiodinium* clade C isolated from purple *A. valida* colour morph, D = *Symbiodinium* clade C isolated from purple *A. valida* colour morph.

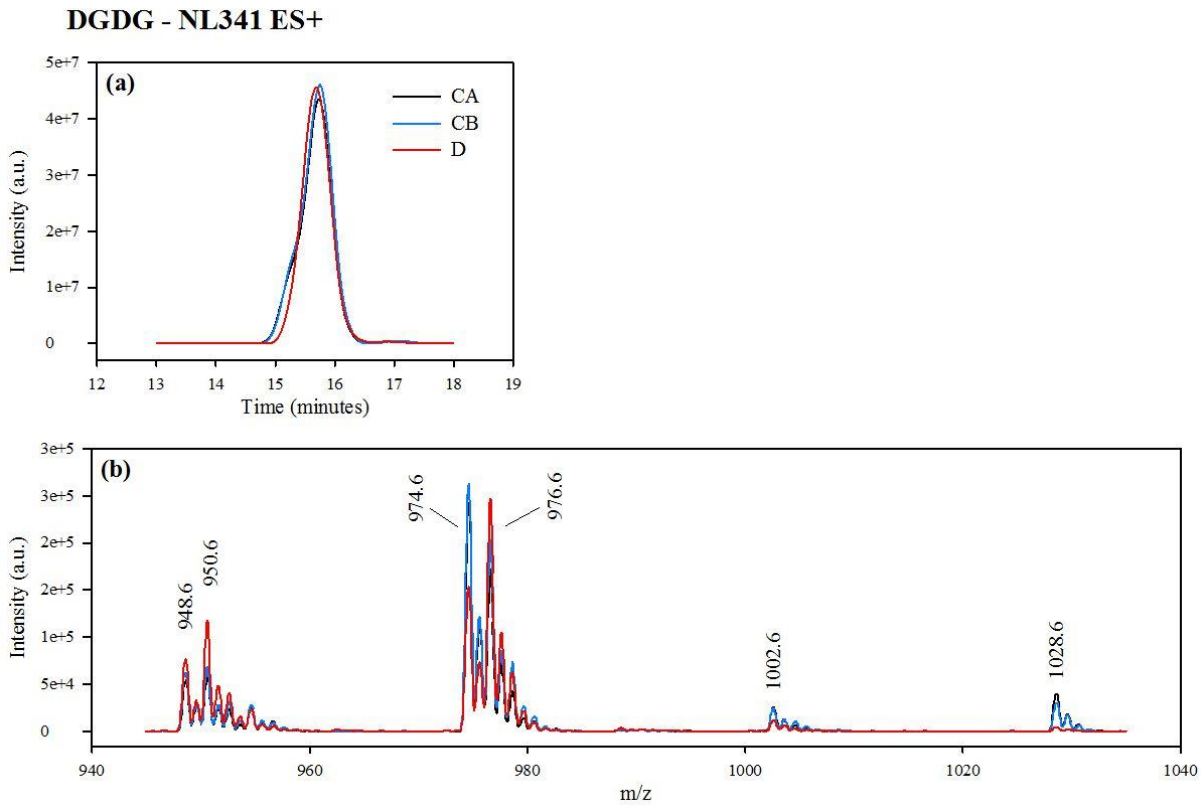

Figure A4.6| Digalactosyldiacylglycerol measured using a neutral loss scan 341 in positive ionisation mode. (a) Mean chromatogram trace. (b) Mass spectrum. CA = *Symbiodinium* clade C isolated from brown *A. valida* colour morph, CB = *Symbiodinium* clade C isolated from purple *A. valida* colour morph, D = *Symbiodinium* clade C isolated from purple *A. valida* colour morph.

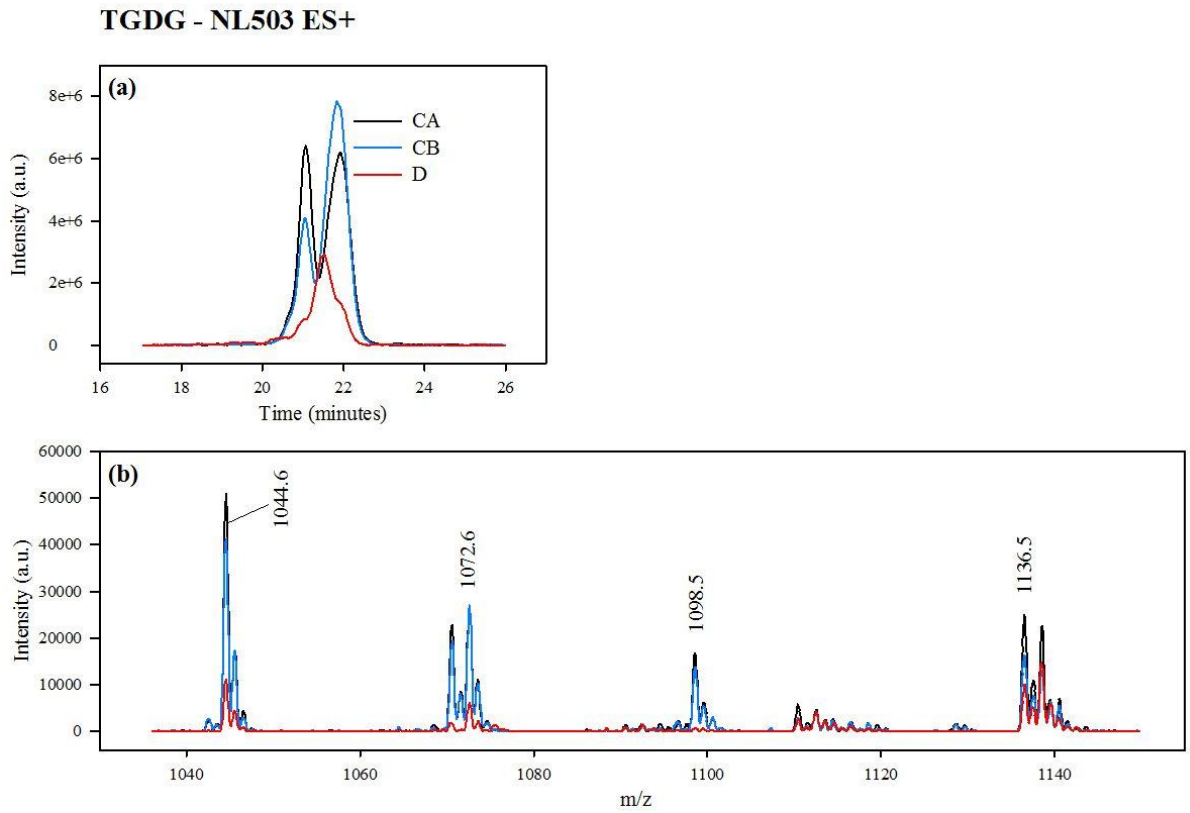

Figure A4.7| Trigalactosyldiacylglycerol measured using a neutral loss scan 503 in positive ionisation mode. (a) Mean chromatogram trace. (b) Mass spectrum. CA = *Symbiodinium* clade C isolated from brown *A. valida* colour morph, CB = *Symbiodinium* clade C isolated from purple *A. valida* colour morph, D = *Symbiodinium* clade C isolated from purple *A. valida* colour morph.

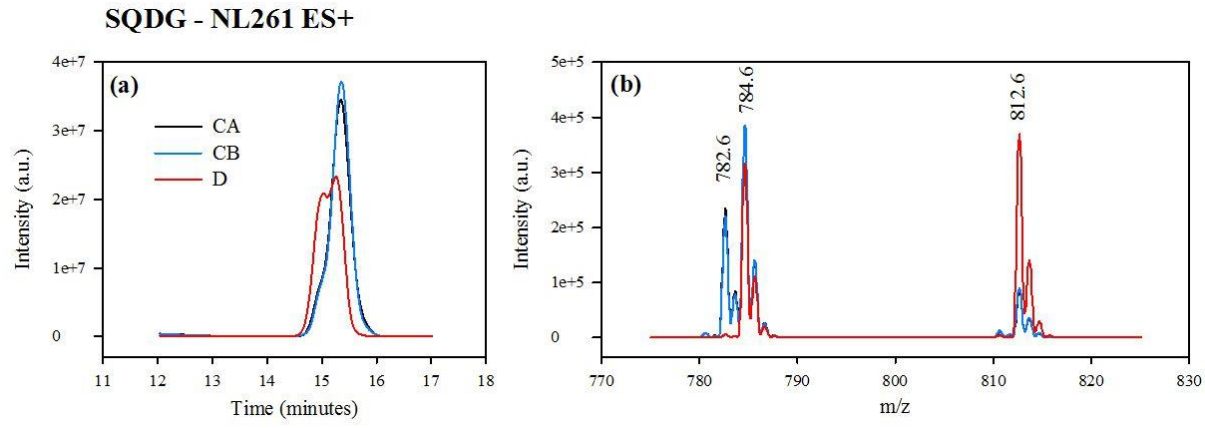

Figure A4.8| Sulfoquinovosyldiacylglycerol measured using a neutral loss scan 261 in positive ionisation mode. (a) Mean chromatogram trace. (b) Mass spectrum. CA = *Symbiodinium* clade C isolated from brown *A. valida* colour morph, CB = *Symbiodinium* clade C isolated from purple *A. valida* colour morph, D = *Symbiodinium* clade C isolated from purple *A. valida* colour morph.

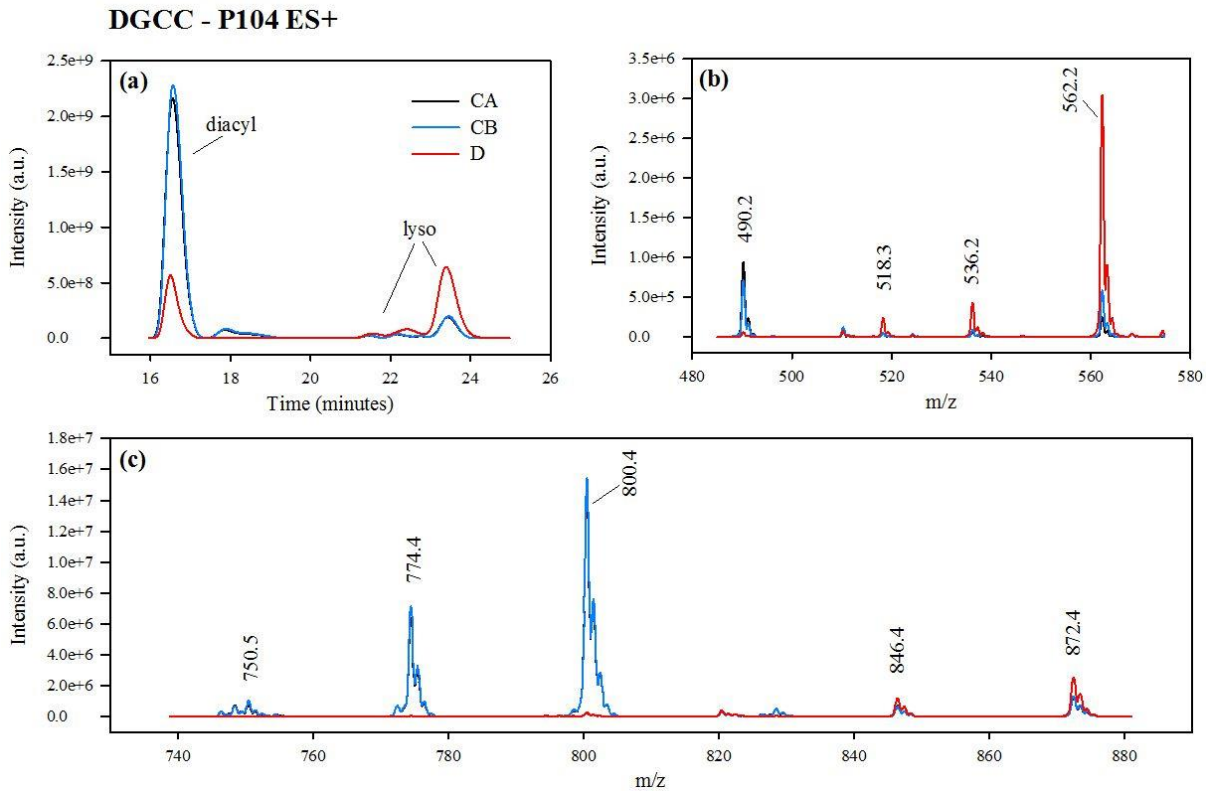

Figure A4.9| Diacylglyceryl carboxyhydroxymethylcholine measured using a precursor scan 104 in positive ionisation mode. (a) Mean chromatogram trace. (b) Mass spectrum of lyso-DGCC. (c) Mass spectrum of diacyl-DGCC. CA = *Symbiodinium* clade C isolated from brown *A. valida* colour morph, CB = *Symbiodinium* clade C isolated from purple *A. valida* colour morph, D = *Symbiodinium* clade C isolated from purple *A. valida* colour morph.

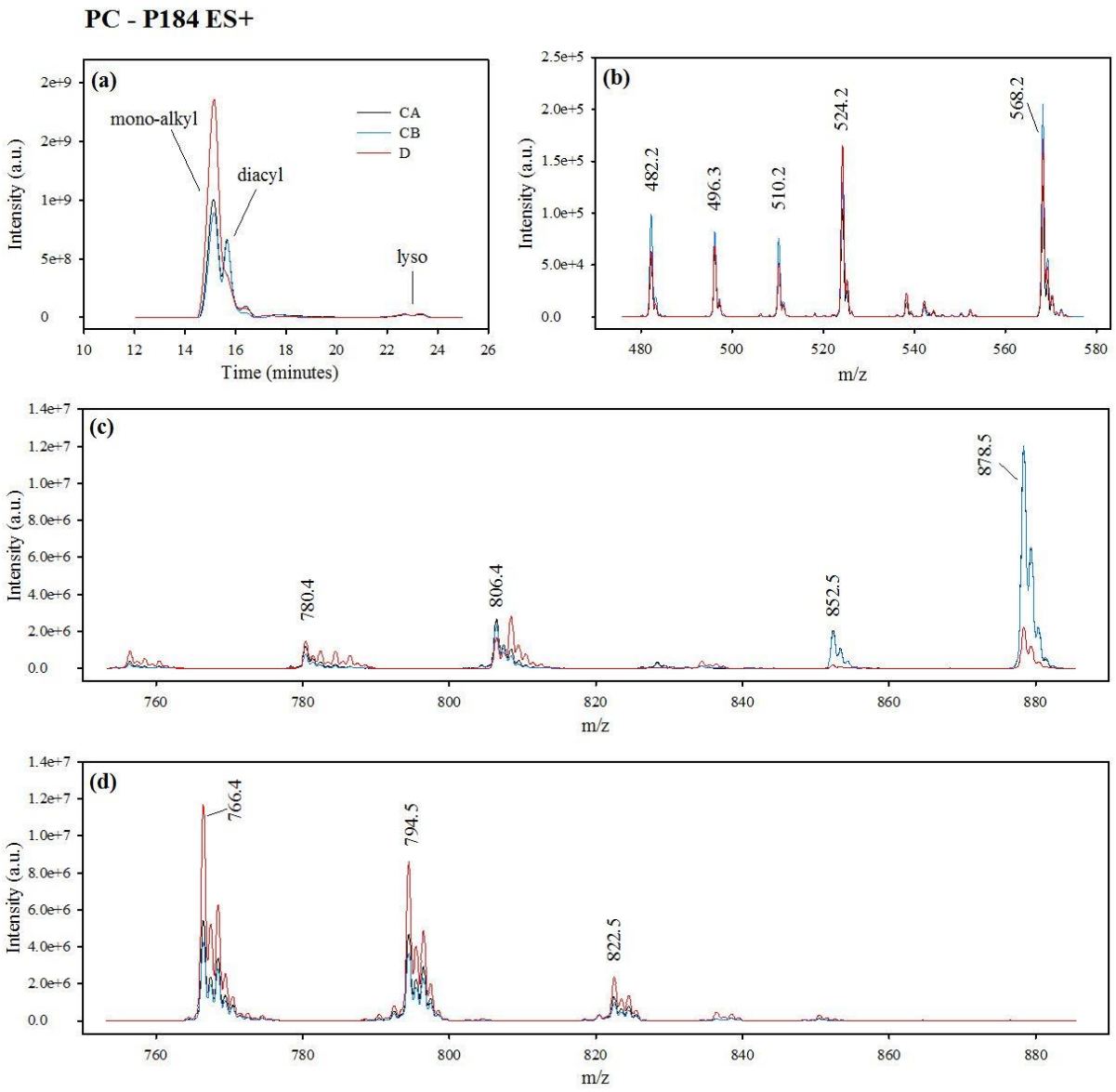

Figure A4.10| Phosphatidylcholine measured using a precursor scan 184 in positive ionisation mode. (a) Mean chromatogram trace. (b) Mass spectrum of lyso-PC. (c) Mass spectrum of diacyl-PC. (d) Mass spectrum of mono-alkyl PC. CA = *Symbiodinium* clade C isolated from brown *A. valida* colour morph, CB = *Symbiodinium* clade C isolated from purple *A. valida* colour morph, D = *Symbiodinium* clade C isolated from purple *A. valida* colour morph.

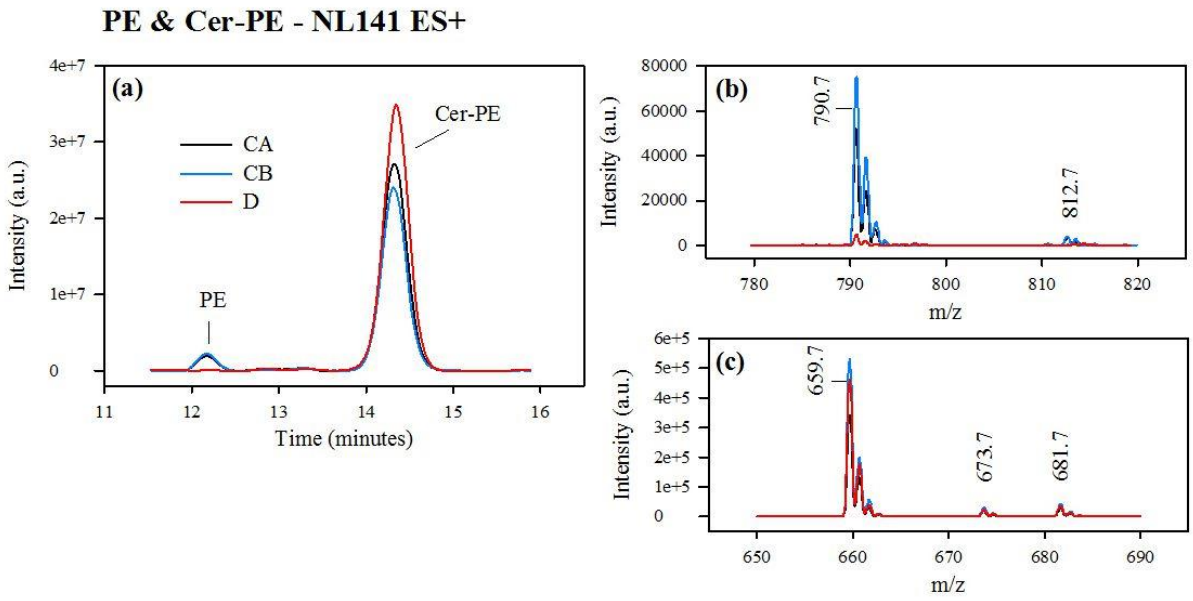

Figure A4.11| Phosphatidylethanolamine and ceramide phosphatidylethanolamine measured using a neutral loss scan 141 in positive ionisation mode. (a) Mean chromatogram trace. (b) Mass spectrum of PE. (c) Mass spectrum of Cer-PE. CA = *Symbiodinium* clade C isolated from brown *A. valida* colour morph, CB = *Symbiodinium* clade C isolated from purple *A. valida* colour morph, D = *Symbiodinium* clade C isolated from purple *A. valida* colour morph.

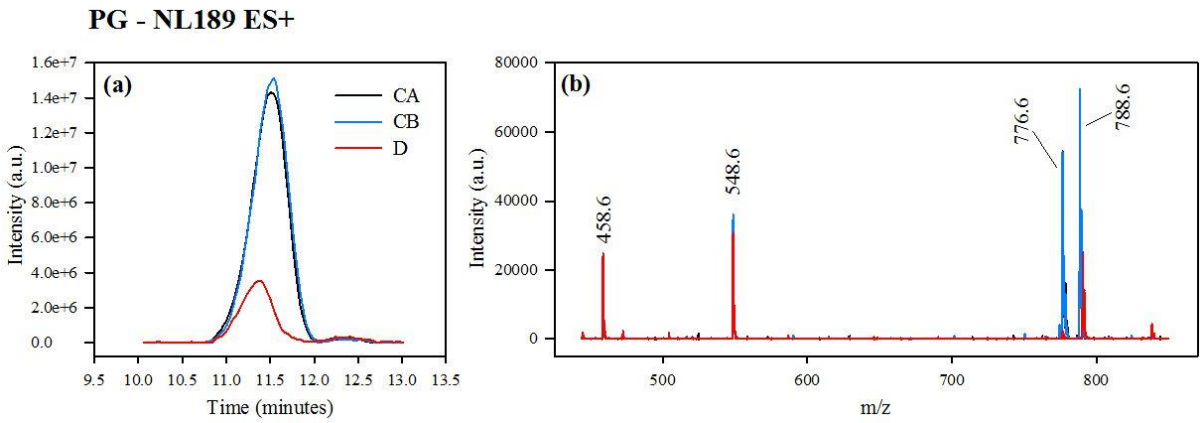

Figure A4.12| Phosphatidylglycerol measured using a neutral loss scan 189 in positive ionisation mode. (a) Mean chromatogram trace. (b) Mass spectrum. CA = *Symbiodinium* clade C isolated from brown *A. valida* colour morph, CB = *Symbiodinium* clade C isolated from purple *A. valida* colour morph, D = *Symbiodinium* clade C isolated from purple *A. valida* colour morph.

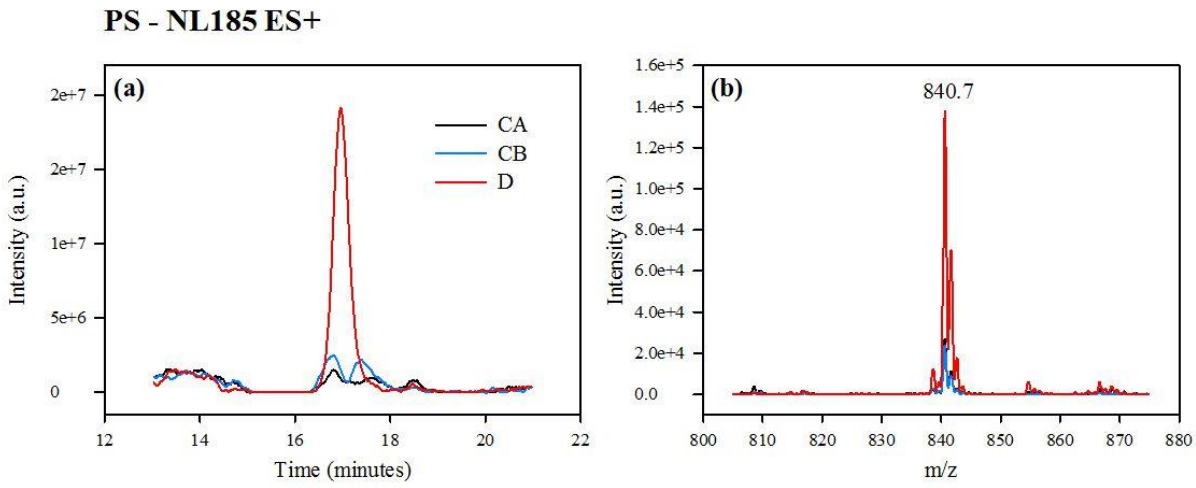

Figure A4.13| Phosphatidylglycerol measured using a neutral loss scan 189 in positive ionisation mode. (a) Mean chromatogram trace. (b) Mass spectrum. CA = *Symbiodinium* clade C isolated from brown *A. valida* colour morph, CB = *Symbiodinium* clade C isolated from purple *A. valida* colour morph, D = *Symbiodinium* clade C isolated from purple *A. valida* colour morph.

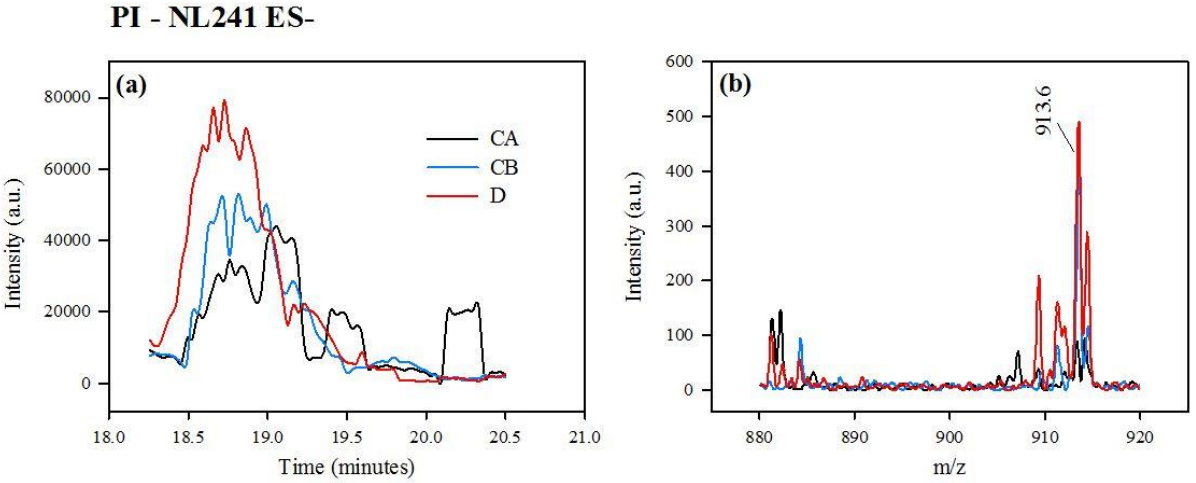

Figure A4.14| Phosphatidylglycerol measured using a neutral loss scan 189 in positive ionisation mode. (a) Mean chromatogram trace. (b) Mass spectrum. CA = *Symbiodinium* clade C isolated from brown *A. valida* colour morph, CB = *Symbiodinium* clade C isolated from purple *A. valida* colour morph, D = *Symbiodinium* clade C isolated from purple *A. valida* colour morph.

Table A4.2| Mean composition of monogalactosyldiacylglycerol. Statistically significant differences in the abundance of each lipid species were determined by one-way analysis of variance and by a Tukey's pairwise comparison between the two clade C samples and between the clade D and the clade C sample originating from the purple *A. valida* colour morph (CB). Asterisk indicated the use of non-parametric Kruskal-Wallis test.

MGDG							
Lipid species		Mean relative abundance (%)			P-value		
diacyl	**m/z**	**CA**	**CB**	**D**	ANOVA	CA vs CB (Tukey's)	CB vs D (Tukey's)
36:9	786.6	23.2 ± 4.2	22.0 ± 4.3	19.2 ± 3.8	0.514	n.a.	n.a.
36:8	788.6	10.3 ± 1.2	8.8 ± 1.5	10.5 ± 1.3	0.322	n.a.	n.a.
36:7	790.6	5.6 ± 1.9	5.5 ± 1.6	4.0 ± 0.6	0.391	n.a.	n.a.
36:6	792.7	4.7 ± 1.4	5.0 ± 2.6	2.5 ± 0.4	0.222	n.a.	n.a.
38:10	812.6	26.1 ± 2.7	30.9 ± 13.0	30.7 ± 2.4	0.707	n.a.	n.a.
38:9	814.7	18.4 ± 2.7	17.3 ± 3.7	24.6 ± 2.3	0.047	0.881	0.052
38:8	816.7	7.3 ± 1.9	6.5 ± 1.5	6.2 ± 2.1	0.511*	n.a.	n.a.
40:10	840.5	2.0 ± 1.1	2.4 ± 0.8	1.8 ± 0.1	0.644	n.a.	n.a.
42:9	866.7	2.3 ± 0.6	1.6 ± 0.4	0.6 ± 0.5	0.016	0.319	0.089

Table A4.3| Mean composition of digalactosyldiacylglycerol. Statistically significant differences in the abundance of each lipid species were determined by one-way analysis of variance and by a Tukey's pairwise comparison between the two clade C samples and between the clade D and the clade C sample originating from the purple *A. valida* colour morph (CB). Asterisk indicated the use of non-parametric Kruskal-Wallis test.

DGDG							
Lipid species		Mean relative abundance (%)			P-value		
diacyl	**m/z**	**CA**	**CB**	**D**	ANOVA	CA vs CB (Tukey's)	CA vs D (Tukey's)
36:9	948.6	7.6 ± 0.1	7.9 ± 0.0	10.0 ± 0.4	**<0.001**	0.420	**<0.001**
36:8	950.6	8.6 ± 0.4	8.8 ± 0.1	15.3 ± 0.2	**<0.001**	0.588	**<0.001**
36:7	952.6	3.4 ± 0.2	3.7 ± 0.1	5.0 ± 0.4	**0.011***	No	No
36:6	954.6	3.7 ± 0.0	3.6 ± 0.2	2.9 ± 0.3	**0.015**	0.992	**0.021**
38:10	974.6	35.3 ± 0.3	33.4 ± 0.5	22.0 ± 0.8	**<0.001**	0.049	**<0.001**
38:9	976.6	25.8 ± 1.2	26.5 ± 0.3	34.1 ± 0.8	**<0.001**	0.614	**<0.001**
38:8	978.6	7.1 ± 1.2	8.6 ± 0.5	8.2 ± 0.5	0.138	n.a.	n.a.
40:10	1002.6	3.5 ± 0.3	3.1 ± 0.1	1.9 ± 0.3	**0.002**	0.237	**0.005**
42:11	1028.6	5.1 ± 1.3	4.4 ± 0.9	0.6 ± 0.0	**0.003**	0.671	**0.005**

Table A4.4| Mean composition of trigalactosyldiacylglycerol. Statistically significant differences in the abundance of each lipid species were determined by one-way analysis of variance and by a Tukey's pairwise comparison between the two clade C samples and between the clade D and the clade C sample originating from the purple *A. valida* colour morph (CB). Asterisk indicated the use of non-parametric Kruskal-Wallis test.

TGDG							
Lipid species		Mean relative abundance (%)			P-value		
diacyl	**m/z**	**CA**	**CB**	**D**	ANOVA	CA vs CB (Tukey's)	CB vs D (Tukey's)
30:0	1044.6	24.2 ± 2.9	28.7 ± 1.8	14.5 ± 2.8	**0.001**	0.155	**0.001**
32:1	1070.6	6.5 ± 5.8	12.6 ± 0.5	3.6 ± 0.2	0.050*	No	No
32:0	1072.6	15.2 ± 1.1	18.6 ± 2.2	9.4 ± 1.6	**0.002**	0.112	**0.001**
34:5	1090.4	0.7 ± 0.3	0.7 ± 0.1	2.2 ± 0.8	**0.017**	1.000	**0.027**
34:4	1092.6	0.8 ± 0.1	0.9 ± 0.1	2.2 ± 0.3	**<0.001**	0.843	**0.001**
34:2	1096.7	0.8 ± 0.3	1.3 ± 0.2	0.8 ± 0.3	0.133	n.a.	n.a.
34:1	1098.5	6.4 ± 2.1	9.0 ± 0.7	1.9 ± 0.7	**0.002**	0.119	**0.002**
36:9	1110.5	3.2 ± 0.4	1.7 ± 0.2	4.0 ± 0.3	**<0.001**	**0.003**	**<0.001**
36:8	1112.6	3.3 ± 0.8	2.2 ± 0.4	7.4 ± 0.5	**<0.001**	0.152	**<0.001**
36:7	1114.5	2.2 ± 0.9	1.3 ± 0.1	3.8 ± 1.0	0.100*	n.a.	n.a.
36:6	1116.5	1.3 ± 0.4	1.1 ± 0.1	2.2 ± 0.6	**0.039**	0.818	**0.041**
36:0	1128.6	0.8 ± 0.2	1.0 ± 0.2	0.0 ± 0.0	**0.001**	0.455	**0.002**
38:10	1136.5	16.0 ± 2.3	10.2 ± 1.4	17.4 ± 1.2	**0.005**	**0.014**	**0.005**
38:9	1138.5	14.2 ± 3.1	8.0 ± 0.6	25.9 ± 2.9	**0.004***	No	**Yes**
38:8	1140.5	4.2 ± 1.8	2.6 ± 0.6	4.8 ± 1.2	0.180	n.a.	n.a.

Table A4.5| Mean composition of sulfoquinovosyldiacylglycerol. Statistically significant differences in the abundance of each lipid species were determined by one-way analysis of variance and by a Tukey's pairwise comparison between the two clade C samples and between the clade D and the clade C sample originating from the purple *A. valida* colour morph (CB). Asterisk indicated the use of non-parametric Kruskal-Wallis test.

SQDG							
Lipid species		Mean relative abundance (%)			P-value		
diacyl	**m/z**	**CA**	**CB**	**D**	ANOVA	CA vs CB (Tukey's)	CB vs D (Tukey's)
30:1	782.6	34.2 ± 2.7	32.7 ± 0.8	1.6 ± 1.1	**<0.001**	0.573	**<0.001**
30:0	784.6	53.0 ± 0.7	54.8 ± 0.4	50.9 ± 7.3	0.552	n.a.	n.a.
32:0	812.7	12.7 ± 2.7	12.4 ± 0.5	47.6 ± 7.7	**<0.001**	0.998	**<0.001**

Table A4.6| Mean composition of diacylglycerol carboxyhydroxymethylcholine. Statistically significant differences in the abundance of each lipid species were determined by one-way analysis of variance and by a Tukey's pairwise comparison between the two clade C samples and between the clade D and the clade C sample originating from the purple *A. valida* colour morph (CB). Asterisk indicated the use of non-parametric Kruskal-Wallis test.

DGCC							
Lipid species		Relative abundance (%)			P-value		
diacyl	**m/z**	**CA**	**CB**	**D**	ANOVA	CA vs CB (Tukey's)	CB vs D (Tukey's)
34:4	748.4	2.9 ± 0.6	2.4 ± 0.1	0.2 ± 0.0	**<0.001**	0.268	**0.001**
34:3	750.5	3.4 ± 0.3	3.7 ± 0.2	0.3 ± 0.0	**<0.001**	0.292	**<0.001**
36:6	772.4	2.6 ± 0.2	2.5 ± 0.1	0.8 ± 0.1	**<0.001**	0.604	**<0.001**
36:5	774.4	21.4 ± 0.9	22.5 ± 0.3	2.5 ± 0.6	**<0.001**	0.155	**<0.001**
36:4	776.4	2.5 ± 0.1	2.7 ± 0.1	0.2 ± 0.2	**<0.001**	0.461	**<0.001**
38:6	800.4	50.8 ± 1.7	50.6 ± 1.1	8.7 ± 1.8	**<0.001**	0.991	**<0.001**
38:5	802.5	8.1 ± 0.3	8.2 ± 0.2	1.5 ± 0.3	**<0.001**	0.987	**<0.001**
40:10	820.4	1.0 ± 0.3	0.9 ± 0.2	6.5 ± 0.1	**<0.001**	0.715	**<0.001**
40:9	822.4	0.4 ± 0.1	0.4 ± 0.0	3.2 ± 0.3	**<0.001**	0.949	**<0.001**
42:11	846.4	1.9 ± 0.4	1.7 ± 0.3	19.9 ± 1.1	**<0.001**	0.912	**<0.001**
42:10	848.5	0.3 ± 0.1	0.3 ± 0.1	2.2 ± 2.0	0.829*	n.a.	n.a.
44:12	872.4	3.9 ± 0.9	3.5 ± 0.8	46.4 ± 0.3	**<0.001**	0.798	**<0.001**
44:11	874.5	0.8 ± 0.2	0.7 ± 0.1	7.6 ± 0.3	**<0.001**	0.940	**<0.001**

Table A4.7| Mean composition of lyso-diacylglycerol carboxyhydroxymethylcholine.
Statistically significant differences in the abundance of each lipid species were determined by one-way analysis of variance and by a Tukey's pairwise comparison between the two clade C samples and between the clade D and the clade C sample originating from the purple *A. valida* colour morph (CB). Asterisk indicated the use of non-parametric Kruskal-Wallis test.

Lyso-DGCC							
Lipid species		Relative abundance (%)			P-value		
acyl	**m/z**	**CA**	**CB**	**D**	ANOVA	CA vs CB (Tukey's)	CB vs D (Tukey's)
(16:0) -H	490.2	63.0 ± 6.0	57.7 ± 9.8	2.4 ± 0.5	**<0.001**	0.626	**<0.001**
(18:0) -H	518.3	4.7 ± 0.5	4.8 ± 0.4	7.6 ±0.6	**<0.001**	0.986	**<0.001**
(20:5) -H	536.2	4.9 ± 0.4	5.2 ± 0.6	9.7 ± 1.1	**<0.001**	0.864	**<0.001**
(22:6) -H	562.2	26.2 ± 6.3	31.1 ± 1.2	78.3 ± 1.8	**<0.001**	0.673	**<0.001**
(22:0) -H	574.3	1.2 ± 0.2	0.2 ± 1.2	2.0 ± 0.3	**0.007**	0.998	**0.012**

Table A4.8| Mean composition of diacyl-phosphatidylcholine. Statistically significant differences in the abundance of each lipid species were determined by one-way analysis of variance and by a Tukey's pairwise comparison between the two clade C samples and between the clade D and the clade C sample originating from the purple *A. valida* colour morph (CB). Asterisk indicated the use of non-parametric Kruskal-Wallis test.

PC - diacyl							
Lipid species		Mean relative abundance (%)			P-value		
Species	**m/z**	**CA**	**CB**	**D**	ANOVA	CA vs CB (Tukey's)	CB vs D (Tukey's)
34:3	756.4	1.3 ± 0.2	1.5 ± 0.3	6.5 ± 0.4	**<0.001**	0.883	**<0.001**
34:2	758.4	0.4 ± 0.1	0.4 ± 0.1	3.8 ± 0.1	**<0.001**	0.981	**<0.001**
34:1	760.5	0.4 ± 0.1	0.5 ± 0.2	2.6 ± 0.3	**<0.001**	0.810	**<0.001**
36:5	780.4	4.6 ± 0.3	4.1 ± 0.7	9.9 ± 1.7	0.121*	n.a.	n.a.
36:4	782.5	1.2 ± 0.3	1.1 ± 0.4	6.7 ± 0.6	**<0.001**	0.996	**<0.001**
36:3	784.5	0.7 ± 0.1	0.7 ± 0.3	6.3 ± 0.1	**<0.001**	0.962	**<0.001**
36:2	786.5	0.5 ± 0.1	0.4 ± 0.1	4.8 ± 0.4	**<0.001**	0.976	**<0.001**
38:6	806.4	13.2 ± 1.7	11.5 ± 0.9	11.0 ± 1.2	0.425*	n.a.	n.a.
38:5	808.5	4.4 ± 0.0	3.8 ± 1.2	20.7 ± 1.4	**<0.001**	0.738	**<0.001**
38:4	810.4	0.8 ± 0.2	0.7 ± 0.1	4.1 ± 0.4	**<0.001**	0.985	**<0.001**
40:9	828.3	1.7 ± 0.4	1.6 ± 0.2	0.6 ± 0.3	**0.014**	0.865	**0.024**
40:6	834.4	1.3 ± 0.8	0.8 ± 0.5	1.7 ± 0.0	0.324	n.a.	n.a.
42:11	852.4	8.3 ± 0.1	8.7 ± 0.0	1.3 ± 0.1	**0.011***	NO	**YES**
44:12	878.4	54.2 ± 4.2	54.0 ± 2.6	17.4	**<0.001**	0.998	**<0.001**
44:11	880.4	7.2 ± 6.2	10.3 ± 2.0	2.7 ± 0.2	0.232	n.a.	n.a.

Table A4.9| Mean composition of mono-alkyl-phosphatidylcholine. Statistically significant differences in the abundance of each lipid species were determined by one-way analysis of variance and by a Tukey's pairwise comparison between the two clade C samples and between the clade D and the clade C sample originating from the purple *A. valida* colour morph (CB). Asterisk indicated the use of non-parametric Kruskal-Wallis test.

PC – mono-alkyl							
Lipid species		Relative abundance (%)			P-value		
Species	**m/z**	**CA**	**CB**	**D**	ANOVA	CA vs CB (Tukey's)	CB vs D (Tukey's)
34:0	748.5	2.7 ± 0.6	3.7 ± 1.1	0.2 ± 0.0	**0.013**	0.315	**0.011**
36:5	766.4	28.6 ± 1.4	26.0 ± 0.6	28.6 ± 1.8	0.157	n.a.	n.a.
36:4	768.5	17.7 ± 2.2	17.1 ± 0.3	17.5 ± 1.3	0.892	n.a.	n.a.
36:3	770.5	3.9 ± 0.2	4.2 ± 0.3	3.5 ± 0.1	**0.039**	0.238	**0.033**
38:6	792.4	2.8 ± 0.1	2.8 ± 0.8	2.6 ± 0.1	0.924	n.a.	n.a.
38:5	794.5	23.3 ± 1.2	22.5 ± 1.2	22.6 ± 1.0	0.707	n.a.	n.a.
38:4	796.5	13.7 ± 0.9	13.6 ± 0.8	14.4 ± 1.6	0.706	n.a.	n.a.
40:5	822.4	6.1 ± 1.2	6.7 ± 0.1	6.4 ± 0.5	0.615	n.a.	n.a.
40:4	824.5	3.2 ± 0.6	3.4 ± 0.3	4.2 ± 0.4	0.150	n.a.	n.a.

Table A4.10| Mean composition of lyso-phosphatidylcholine. Statistically significant differences in the abundance of each lipid species were determined by one-way analysis of variance and by a Tukey's pairwise comparison between the two clade C samples and between the clade D and the clade C sample originating from the purple *A. valida* colour morph (CB). Asterisk indicated the use of non-parametric Kruskal-Wallis test.

Lyso-PC								
Lipid species			Relative abundance (%)			P-value		
acyl	**alkyl**	**m/z**	**CA**	**CB**	**D**	ANOVA	CA vs CB (Tukey's)	CB vs D (Tukey's)
(14:0) -H		468.2	2.0 ± 2.2	0.0 ± 0.0	0.0 ± 0.0	0.075*	n.a.	n.a.
	(O- 16:0) -H	482.2	10.7 ± 2.4	9.1 ± 6.6	10.2 ± 0.9	0.911	n.a.	n.a.
(16:0) -H		496.2	12.9 ± 1.7	12.8 ± 1.0	10.5 ± 1.7	0.235		n.a.
	(O- 18:0) -H	510.3	13.7 ± 3.9	10.4 ± 0.9	9.2 ± 0.8	0.220	n.a.	n.a.
(18:0) -H		524.3	18.9 ± 4.9	18.9 ± 1.5	26.5 ± 2.0	0.095	n.a.	n.a.
	(O- 20:0) -H	538.4	2.8 ± 0.4	3.0 ± 0.6	3.7 ± 0.3	0.169	n.a.	n.a.
(20:5)-H		542.2	2.3 ± 0.1	2.4 ± 0.5	2.7 ± 0.0	0.541	n.a.	n.a.
(22:6)-H		568.3	33.3 ± 7.6	38.5 ± 7.5	32.1 ± 4.3	0.573	n.a.	n.a.
(22:5) -H		570.3	2.4 ± 2.1	3.6 ± 0.9	3.4 ± 0.4	0.557	n.a.	n.a.
		580.3	1.1 ± 0.9	1.3 ± 0.3	1.6 ± 0.1	0.688	n.a.	n.a.

Table A4.11| Mean composition of phosphatidylethanolamine. Statistically significant differences in the abundance of each lipid species were determined by one-way analysis of variance and by a Tukey's pairwise comparison between the two clade C samples and between the clade D and the clade C sample originating from the purple *A. valida* colour morph (CB). Asterisk indicated the use of non-parametric Kruskal-Wallis test.

PE									
Lipid species				Relative abundance (%)			P-value		
diacyl	**alkyl**	**alkenyl**	**m/z**	**CA**	**CB**	**D**	ANOVA	CA vs CB (Tukey's)	CB vs D (Tukey's)
40:7	40:0		790.7	83.7 ± 1.5	80.7 ± 2.7	87.8 ± 6.6	0.199	n.a.	n.a.
40:6	40:1	40:0	792.7	10.6 ± 2.5	11.9 ± 3.3	3.8 ± 6.5	0.296*	n.a.	n.a.
42:10	42:3	42:2	812.7	5.8 ± 1.2	7.3 ± 0.6	8.5 ± 2.4	0.201	n.a.	n.a.

Table A4.12| Mean composition of ceramide phosphatidylethanolamine. Statistically significant differences in the abundance of each lipid species were determined by one-way analysis of variance and by a Tukey's pairwise comparison between the two clade C samples and between the clade D and the clade C sample originating from the purple *A. valida* colour morph (CB). Asterisk indicated the use of non-parametric Kruskal-Wallis test.

Ceramide PE									
Lipid species				Relative abundance (%)			P-value		
diacyl	**alkyl**	**alkenyl**	**m/z**	**CA**	**CB**	**D**	ANOVA	CA vs CB (Tukey's)	CB vs D (Tukey's)
34:2	36:9	36:8	659.7	76.9 ± 2.4	77.3 ± 0.3	78.1 ± 1.8	0.709	n.a.	n.a.
34:1	36:8	36:7	661.7	7.2 ± 0.6	7.0 ± 0.5	7.2 ± 0.4	0.868	n.a.	n.a.
	36:2	36:1	673.7	4.3 ± 0.4	3.3 ± 2.5	4.1 ± 0.3	0.672	n.a.	n.a.
36:3			681.6	11.5 ± 1.5	12.4 ± 1.7	10.5 ± 2.2	0.512	n.a.	n.a.

Table A4.13| Mean composition of phosphatidylglycerol. Statistically significant differences in the abundance of each lipid species were determined by one-way analysis of variance and by a Tukey's pairwise comparison between the two clade C samples and between the clade D and the clade C sample originating from the purple *A. valida* colour morph (CB). Asterisk indicated the use of non-parametric Kruskal-Wallis test.

PG

Lipid species		Relative abundance (%)			P-value		
diacyl	**m/z**	**CA**	**CB**	**D**	ANOVA	CA vs CB (Tukey's)	CB vs D (Tukey's)
lyso(14:0) OH-	458.6	7.4 ± 0.4	8.1 ± 0.4	23.5 ± 1.7	**<0.001**	0.942	**0.002**
lyso(20:5) H-	548.6	9.5 ± 1.8	10.1 ± 1.1	29.5 ± 0.4	**<0.001**	0.876	**<0.001**
36:11	774.7	2.5 ± 0.5	0.8 ± 1.3	0.2 ± 0.2	**<0.001**	0.375	**<0.001**
36:10	776.6	28.9 ± 0.3	29.4 ± 1.0	3.5 ± 0.6	**<0.001**	0.679	**<0.001**
36:9	778.6	7.4 ± 0.5	6.7 ± 0.3	0.3 ± 0.3	**<0.001**	0.984	**<0.001**
36:4	788.6	38.1 ± 0.3	39.5 ± 1.5	0.4 ± 0.3	**<0.001**	0.625	**<0.001**
36:3	790.6	5.1 ± 0.4	4.6 ± 0.3	36.4 ± 2.8	**<0.001**	0.677	**<0.001**
40:7	838.6	1.0 ± 0.3	0.9 ± 0.2	6.2 ± 1.5	**<0.001**	1.000	**<0.001**

Table A.14| Mean composition of phosphatidylserine. Statistically significant differences in the abundance of each lipid species were determined by one-way analysis of variance and by a Tukey's pairwise comparison between the two clade C samples and between the clade D and the clade C sample originating from the purple *A. valida* colour morph (CB). Asterisk indicated the use of non-parametric Kruskal-Wallis test.

PS								
Lipid species			Relative abundance (%)			P-value		
diacyl	**mono-alkyl**	**m/z**	**CA**	**CB**	**D**	ANOVA	CA vs CB (Tukey's)	CB vs D (Tukey's)
38:6		808.5	6.8 ± 1.3	6.3 ± 1.1	0.2 ± 0.2	**<0.001**	0.885	**<0.001**
40:7	40:0	834.6	3.7 ± 1.1	1.9 ± 0.3	0.7 ± 0.7	**0.008**	0.060	0.221
40:5		838.6	8.6 ± 1.0	7.7 ± 1.7	6.4 ± 0.2	0.164	n.a.	n.a.
40:4		840.6	62.0 ± 3.9	64.7 ± 7.0	76.4 ± 2.4	**0.022**	0.641	0.068
40:3		842.7	7.2 ± 1.4	7.4 ± 0.9	8.6 ± 0.4	0.215	n.a.	n.a.
42:10		856.6	3.4 ± 0.8	3.6 ± 1.6	2.5 ± 0.6	0.442	n.a.	n.a.
42:5	44:12	866.6	3.8 ± 2.2	3.8 ± 1.9	3.1 ± 0.6	0.840	n.a.	n.a.
42:4	44:11	868.7	4.6 ± 0.3	4.6 ± 3.1	2.3 ± 0.5	0.300	n.a.	n.a.

Table A4.15| Mean composition of phosphatidylinositol. Statistically significant differences in the abundance of each lipid species were determined by one-way analysis of variance and by a Tukey's pairwise comparison between the two clade C samples and between the clade D and the clade C sample originating from the purple *A. valida* colour morph (CB). Asterisk indicated the use of non-parametric Kruskal-Wallis test.

PI							
Lipid species		Mean relative abundance (%)			P-value		
diacyl	**m/z**	**CA**	**CB**	**D**	ANOVA	CA vs CB (Tukey's)	CB vs D (Tukey's)
32:4	881.2	25.3 ± 24.2	33.3 ± 57.7	3.2 ± 5.5	0.623	n.a.	n.a.
32:3	909.3	7.4 ± 12.9	0.0 ± 0.0	16.5 ± 15.1	0.568	n.a.	n.a.
32:2	911.4	5.5 ± 9.6	0.0 ± 0.0	26.8 ± 5.9	**0.004**	0.924	**0.006**
32:1	913.5	61.8 ± 34.3	66.7 ± 57.7	53.5 ± 14.7	0.929*	n.a.	n.a.

Table A4.16| Mean composition of a unknown lipid class identified by a neutral loss scan 241 ES+. Statistically significant differences in the abundance of each lipid species were determined by one-way analysis of variance and by a Tukey's pairwise comparison between the two clade C samples and between the clade D and the clade C sample originating from the purple *A. valida* colour morph (CB). Asterisk indicated the use of non-parametric Kruskal-Wallis test.

NL241 ES+						
Lipid species	Mean relative abundance (%)			P-value		
m/z	**CA**	**CB**	**D**	ANOVA	CA vs CB (Tukey's)	CB vs D (Tukey's)
948.4	19.3 ± 2.0	17.3 ± 1.7	14.6 ± 1.1	**0.035**	0.368	0.187
950.2	12.8 ± 3.5	17.0 ± 3.3	27.7 ± 2.0	**0.002**	0.275	**0.012**
952.4	3.6 ± 3.5	3.7 ± 3.4	3.5 ± 3.2	0.997	n.a.	n.a.
974.3	13.5 ± 1.3	15.9 ± 2.3	8.5 ± 1.5	**0.006**	0.297	**0.005**
976.1	44.1 ± 5.5	38.9 ± 2.3	44.3 ± 0.5	0.179	n.a.	n.a.
1002.4	4.1 ± 1.1	4.1 ± 1.5	1.4 ± 0.5	**0.038**	1.000	0.056
1028.3	2.7 ± 0.2	3.1 ± 0.6	0.0 ± 0.0	**<0.001**	0.475	**<0.001**

Table A4.17| Mean composition of a unknown lipid class identified by a precursor scan 104 ES+. Statistically significant differences in the abundance of each lipid species were determined by one-way analysis of variance and by a Tukey's pairwise comparison between the two clade C samples and between the clade D and the clade C sample originating from the purple *A. valida* colour morph (CB). Asterisk indicated the use of non-parametric Kruskal-Wallis test.

910 (P104)						
Lipid species	Mean relative abundance (%)			P-value		
m/z	**CA**	**CB**	**D**	ANOVA	CA vs CB (Tukey's)	CB vs D (Tukey's)
878.5	1.1 ± 0.1	1.1 ± 0.2	4.0 ± 2.4	0.074	n.a.	n.a.
882.5	2.6 ± 0.2	2.4 ± 0.4	0.0 ± 0.0	**<0.001**	0.623	**<0.001**
884.6	1.9 ± 0.2	2.1 ± 0.3	28.1 ± 6.0	**<0.001**	0.996	**<0.001**
910.6	88.3 ± 0.3	88.1 ± 0.9	66.0 ± 8.4	**0.002**	0.998	**0.004**
938.6	3.6 ± 0.3	3.8 ± 0.3	0.0 ± 0.0	**<0.001**	0.616	**<0.001**
954.6	2.5 ± 0.6	2.4 ± 0.4	1.9 ± 0.5	0.370	n.a.	n.a.

References

Allgeier, J. E., Layman, C. A., Mumby, P. J., and Rosemond, A. D. (2014). Consistent nutrient storage and supply mediated by diverse fish communities in coral reef ecosystems. *Glob. Chang. Biol.* 20, 2459–2472.

Al-Moghrabi, S., Allemand, D., and Jaubert, J. (1993). Valine uptake by the scleractinian coral Galaxea fascicularis: characterization and effect of light and nutritional status. *J. Comp. Physiol. B*, 355–362.

Anthony, K. (2000). Enhanced particle-feeding capacity of corals on turbid reefs (Great Barrier Reef, Australia). *Coral reefs* 19, 59–67.

Anthony, K., and Fabricius, K. (2000). Shifting roles of heterotrophy and autotrophy in coral energetics under varying turbidity. *J. Exp. Mar. Bio. Ecol.* 252, 221–253.

Aswani, S., Mumby, P. J., Baker, A. C., Christie, P., McCook, L. J., Steneck, R. S., and Richmond, R. H. (2015). Scientific frontiers in the management of coral reefs. *Front. Mar. Sci.* 2, 1–13.

Bachar, A., Achituv, Y., Pasternak, Z., and Dubinsky, Z. (2007). Autotrophy versus heterotrophy: The origin of carbon determines its fate in a symbiotic sea anemone. *J. Exp. Mar. Bio. Ecol.* 349, 295–298.

Bachok, Z., Mfilinge, P., and Tsuchiya, M. (2006). Characterization of fatty acid composition in healthy and bleached corals from Okinawa, Japan. *Coral Reefs* 25, 545–554.

Baghdasarian, G., and Muscatine, L. (2000). Preferential expulsion of dividing algal cells as a mechanism for regulating algal-cnidarian symbiosis. *Biol. Bull.* 199, 278–86. A

Bak, R., Joenje, M., de Jong, I., Lambrechts, D., and Nieuwland, G. (1998). Bacterial suspension feeding by coral reef benthic organisms. *Mar. Ecol. Prog. Ser.* 175, 285–288.

Baker, A. C. (2001). Reef corals bleach to survive change. *Nature* 411, 765–766.

Baker, A. C., Glynn, P. W., and Riegl, B. (2008). Climate change and coral reef bleaching: An ecological assessment of long-term impacts, recovery trends and future outlook. *Estuar. Coast. Shelf Sci.* 80, 435–471.

Baker, D. M., Andras, J. P., Jordán-Garza, A. G., and Fogel, M. L. (2013). Nitrate competition in a coral symbiosis varies with temperature among Symbiodinium clades. *ISME J.* 7, 1248–51.

Bakun, a., Black, B. a., Bograd, S. J., García-Reyes, M., Miller, a. J., Rykaczewski, R. R., and Sydeman, W. J. (2015). Anticipated Effects of Climate Change on Coastal Upwelling Ecosystems. *Curr. Clim. Chang. Reports*, 85–93.

Barshis, D. J., Ladner, J. T., Oliver, T. A., and Palumbi, S. R. (2014). Lineage-specific transcriptional profiles of Symbiodinium spp. Unaltered by heat stress in a coral host. *Mol. Biol. Evol.* 31, 1343–1352.

Barshis, D. J., Ladner, J. T., Oliver, T. a., Seneca, F. O., Traylor-Knowles, N., and Palumbi, S. R. (2013). Genomic basis for coral resilience to climate change. *Proc. Natl. Acad. Sci.* 2012.

Bay, R. a, and Palumbi, S. R. (2015). Rapid Acclimation Ability Mediated by Transcriptome Changes in Reef-Building Corals. *Genome Biol. Evol.* 7, 1602–12.

Behrenfeld, M. J., O'Malley, R. T., Siegel, D. a, McClain, C. R., Sarmiento, J. L., Feldman, G. C., Milligan, A. J., Falkowski, P. G., Letelier, R. M., and Boss, E. S. (2006). Climate-driven trends in contemporary ocean productivity. *Nature* 444, 752–5.

Bellantuono, A. J., Hoegh-Guldberg, O., and Rodriguez-Lanetty, M. (2012). Resistance to thermal stress in corals without changes in symbiont composition. *Proc. Biol. Sci.* 279, 1100–7.

Bellwood, D. R., and Hughes, T. P. (2001). Regional-Scale Assembly Rules and Biodiversty of Coral Reefs. *Science (80-.).* 292, 1532–1534.

Béraud, E., Gevaert, F., Rottier, C., and Ferrier-Pagès, C. (2013). The response of the scleractinian coral Turbinaria reniformis to thermal stress depends on the nitrogen status of the coral holobiont. *J. Exp. Biol.* 216, 2665–74.

Berkelmans, R., and van Oppen, M. J. H. (2006). The role of zooxanthellae in the thermal tolerance of corals: a "nugget of hope" for coral reefs in an era of climate change. *Proc. Biol. Sci.* 273, 2305–12.

Berner, T., Baghdasarian, G., and Muscatine, L. (1993). Repopulation of sea anemone with symbiotic dinoflagellates: analysis by in vivo fluorescence. *J. Exp. Mar. Bio. Ecol.* 170, 145–158.

Berner, T., and Izhaki, I. (1994). Effect of exogenous nitrogen levels on ultrastructure of zooxanthellae from the hermatypic coral Pocillopora damicornis. *Pacific Sci.* 48, 254–262.

Biel, K. Y., Gates, R. D., and Muscatine, L. (2007). Effects of free amino acids on the photosynthetic carbon metabolism of symbiotic dinoflagellates. *Russ. J. Plant Physiol.* 54, 171–183.

Bligh, E. G., and Dyer, W. J. (1959). A rapid method of total lipid extraction and purification. *Can. J. Biochem. Physiol.* 37, 911–917.

Bongiorni, L., Shafir, S., Angel, D., and Rinkevich, B. (2003). Survival, growth and gonad development of two hermatypic corals subjected to in situ fish-farm nutrient enrichment. *Mar. Ecol. Prog. Ser.* 253, 137–144.

Borell, E. M., and Bischof, K. (2008). Feeding sustains photosynthetic quantum yield of a scleractinian coral during thermal stress. *Oecologia* 157, 593–601.

Brander, L. M., Beukering, P., and Cesar, H. S. J. (2006). The recreational value of coral reefs: a metaanalysis. *IVM Work. Pap.*

Brodie, J. E., Devlin, M., Haynes, D., and Waterhouse, J. (2010). Assessment of the eutrophication status of the Great Barrier Reef lagoon (Australia). *Biogeochemistry* 106, 281–302.

Brodie, J. E., Kroon, F. J., Schaffelke, B., Wolanski, E. C., Lewis, S. E., Devlin, M. J., Bohnet, I. C., Bainbridge, Z. T., Waterhouse, J., and Davis, A. M. (2012). Terrestrial pollutant runoff to the Great Barrier Reef: An update of issues, priorities and management responses. *Mar. Pollut. Bull.* 65, 81–100.

Brodie, J., Fabricius, K., De'ath, G., and Okaji, K. (2005). Are increased nutrient inputs responsible for more outbreaks of crown-of-thorns starfish? An appraisal of the evidence. *Mar. Pollut. Bull.* 51, 266–78.

Brown, B. (1997). Coral bleaching: causes and consequences. *Coral reefs* 16, 129–138.

Bruno, J. F., Petes, L. E., Drew Harvell, C., and Hettinger, A. (2003). Nutrient enrichment can increase the severity of coral diseases. *Ecol. Lett.* 6, 1056–1061.

Chavez, F., Strutton, P., and Friederich, G. (1999). Biological and chemical response of the equatorial Pacific Ocean to the 1997-98 El Niño. *Science (80-.).*, 2126–2132.

Chen, H.-K., Song, S.-N., Wang, L.-H., Mayfield, A. B., Chen, Y.-J., Chen, W.-N. U., and Chen, C.-S. (2015). A compartmental comparison of major lipid species in a coral-symbiodinium endosymbiosis: evidence that the coral host regulates lipogenesis of its cytosolic lipid Bodies. *PLoS One* 10, e0132519.

Chen, J., Burke, J. J., Xin, Z., Xu, C., and Velten, J. (2006). Characterization of the Arabidopsis thermosensitive mutant atts02 reveals an important role for galactolipids in thermotolerance. *Plant, Cell Environ.* 29, 1437–1448.

Chen, M.-C., Hong, M.-C., Huang, Y.-S., Liu, M.-C., Cheng, Y.-M., and Fang, L.-S. (2005). ApRab11, a cnidarian homologue of the recycling regulatory protein Rab11, is involved in the establishment and maintenance of the Aiptasia-Symbiodinium endosymbiosis. *Biochem. Biophys. Res. Commun.* 338, 1607–16.

Chen, W.-N. U., Kang, H.-J., Weis, V. M., Mayfield, a. B., Jiang, P.-L., Fang, L.-S., and Chen, C.-S. (2011). Diel rhythmicity of lipid-body formation in a coral-Symbiodinium endosymbiosis. *Coral Reefs* 31, 521–534.

Chust, G., Allen, J. I., Bopp, L., Schrum, C., Holt, J., Tsiaras, K., Zavatarelli, M., Chifflet, M., Cannaby, H., Dadou, I., et al. (2014). Biomass changes and trophic amplification of plankton in a warmer ocean. *Glob. Chang. Biol.* 20, 2124–39.

Clode, P. L., Saunders, M., Maker, G., Ludwig, M., and Atkins, C. A. (2009). Uric acid deposits in symbiotic marine algae. *Plant. Cell Environ.* 32, 170–177.

Conley, D., Paerl, H., Howarth, R., Boesch, D., Seitzinger, S., Havens, K., Lancelot, C., and Likens, G. (2009). Controlling eutrophication: nitrogen and phosphorus. *Science (80-.).* 323, 1014–15.

Connolly, S. R., Lopez-Yglesias, M. A., and Anthony, K. R. N. (2012). Food availability promotes rapid recovery from thermal stress in a scleractinian coral. *Coral Reefs* 31, 951–960.

Cook, C. B., D'Elia, C. F., and Muller-Parker, G. (1988). Host feeding and nutrient sufficiency for zooxanthellae in the sea anemone Aiptasia pallida. *Mar. Biol.* 262, 253–262.

Cooper, T. F., Gilmour, J. P., and Fabricius, K. E. (2009). Bioindicators of changes in water quality on coral reefs: Review and recommendations for monitoring programmes. *Coral Reefs* 28, 589–606.

Costa, O. S., Leao, Z., Nimmo, M., and Attrill, M. (2000). Nutrification impacts on coral reefs from northern Bahia, Brazil. *Hydrobiologia* 440, 307–315.

Crossland, C., and Barnes, D. (1977). Nitrate assimilation enzymes from two hard corals, Acropora acuminata and Goniastrea australensis. *Comp. Biochem.* 57, 151–157.

Crossland, C., Hatcher, B., Atkinson, M., and Smtih, S. (1984). Dissolved nutrients of a high-latitude coral reef, Houtman Abrolhos Islands, Western Australia. *Mar. Ecol. Prog. Ser.* 14, 159–163.

Crossland, C. J. (1987). Coral Reefs In situ release of mucus and DOC-lipid from the corals Acropora variabilis and Stylophora pistillata in different light regimes. *Coral Reefs* 6, 35–42.

Cunning, R., and Baker, A. C. (2012). Excess algal symbionts increase the susceptibility of reef corals to bleaching. *Nat. Clim. Chang.* 3, 259–262.

Cunning, R., and Baker, A. C. (2013). Excess algal symbionts increase the susceptibility of reef corals to bleaching. *Nat. Clim. Chang.* 3, 259–262.

Cunning, R., Silverstein, R. N., and Baker, a. C. (2015). Investigating the causes and consequences of symbiont shuffling in a multi-partner reef coral symbiosis under environmental change. *Proc. R. Soc. B Biol. Sci.* 282, 20141725–20141725.

D'Angelo, C., Denzel, a, Vogt, a, Matz, M., Oswald, F., Salih, a, Nienhaus, G., and Wiedenmann, J. (2008). Blue light regulation of host pigment in reef-building corals. *Mar. Ecol. Prog. Ser.* 364, 97–106.

D'Angelo, C., Hume, B. C. C., Burt, J., Smith, E. G., Achterberg, E. P., and Wiedenmann, J. (2015). Local adaptation constrains the distribution potential of heat-tolerant Symbiodinium from the Persian/Arabian Gulf. *ISME J.*, 1–10.

D'Angelo, C., and Wiedenmann, J. (2012). An experimental mesocosm for long-term studies of reef corals. *J. Mar. Biol. Assoc. United Kingdom* 92, 769–775.

D'Angelo, C., and Wiedenmann, J. (2014). Impacts of nutrient enrichment on coral reefs: new perspectives and implications for coastal management and reef survival. *Curr. Opin. Environ. Sustain.* 7, 82–93.

D'Elia, C. F., and Webb, K. L. (1977). The dissolved nitrogen flux of reef corals. *Proc. 3rd int. Coral Reef Symp. Vol. 1*, 325–331.

Davy, S. K., Allemand, D., and Weis, V. M. (2012). Cell biology of cnidarian-dinoflagellate symbiosis. *Microbiol. Mol. Biol. Rev.* 76, 229–61.

Dembitsky, V. M. (1996). Betaine ether-linked glycerolipids: chemistry and biology. *Prog. Lipid Res.* 35, 1–51.

Díaz-Almeyda, E., Thomé, P. E., El Hafidi, M., and Iglesias-Prieto, R. (2010). Differential stability of photosynthetic membranes and fatty acid composition at elevated temperature in Symbiodinium. *Coral Reefs* 30, 217–225.

Donner, S. D., Skirving, W. J., Little, C. M., Oppenheimer, M., and Hoegh-Guldberg, O. (2005). Global assessment of coral bleaching and required rates of adaptation under climate change. *Glob. Chang. Biol.* 11, 2251–2265.

Downs, C. a, Fauth, J. E., Halas, J. C., Dustan, P., Bemiss, J., and Woodley, C. M. (2002). Oxidative stress and seasonal coral bleaching. *Free Radic. Biol. Med.* 33, 533–43.

Downs, C. A., Kramarsky-winter, E., Martinez, J., Kushmaro, A., Woodley, C. M., and Loya, Y. (2009). Symbiophagy as a cellular mechanism for coral bleaching. *Autophagy* 5, 1–6.

Dubinsky, Z., and Berman-Frank, I. (2001). Uncoupling primary production from population growth in photosynthesizing organisms in aquatic ecosystems. *Aquat. Sci.* 63, 4–17.

Dubinsky, Z., and Jokiel, P. L. (1994). Ratio of energy and nutrient fluxes regulates symbiosis between zooxanthellae and corals. *Pacific Sci.* 48, 313–324.

Dubinsky, Z., Stambler, N., Ben-Zion, M., Mccloskey, L. R., Muscatine, L., and Falkowski, P. G. (1990). The effect of external nutrient resources on the optical properties and photosynthetic efficiency of Stylophora pistillata. *Proc. R. Soc. B Biol. Sci.* 239, 231–246.

Dunn, J. G., Sammarco, P. W., and LaFleur, G. (2012). Effects of phosphate on growth and skeletal density in the scleractinian coral Acropora muricata: A controlled experimental approach. *J. Exp. Mar. Bio. Ecol.* 411, 34–44.

Ezzat, L., Towle, E., Irisson, J. O., Langdon, C., and Ferrier-Pagès, C. (2015). The relationship between heterotrophic feeding and inorganic nutrient availability in the scleractinian coral T. reniformis under a short-term temperature increase. *Limnol. Oceanogr.*, 89–102.

Fabricius, K. E. (2006). Effects of irradiance, flow, and colony pigmentation on the temperature microenvironment around corals: Implications for coral bleaching? *Limnol. Oceanogr.* 51, 30–37.

Fabricius, K. E. (2005). Effects of terrestrial runoff on the ecology of corals and coral reefs: review and synthesis. *Mar. Pollut. Bull.* 50, 125–46.

Fabricius, K. E., Cooper, T. F., Humphrey, C., Uthicke, S., De'ath, G., Davidson, J., LeGrand, H., Thompson, A., and Schaffelke, B. (2012). A bioindicator system for water quality on inshore coral reefs of the Great Barrier Reef. *Mar. Pollut. Bull.* 65, 320–32.

Fabricius, K. E., Cséke, S., Humphrey, C., and De'ath, G. (2013). Does trophic status enhance or reduce the thermal tolerance of scleractinian corals? A review, experiment and conceptual framework. *PLoS One* 8, e54399.

Falcone, D. L., Ogas, J. P., and Somerville, C. R. (2004). Regulation of membrane fatty acid composition by temperature in mutants of Arabidopsis with alterations in membrane lipid composition. *BMC Plant Biol.* 4, 17.

Falkowski, P., Dubinsky, Z., Muscatine, L., and Porter, J. W. (1984). Light and the bioenergetics of a symbiotic coral. *Bioscience* 34, 705–709.

Falkowski, P. G., Dubinsky, Z., Muscatine, L., and McCloskey, L. (1993). Population Control in Symbiotic Corals. *Bioscience* 43, 606–611.

Ferrier-Pagès, C., Gattuso, J., Dallot, S., and Jaubert, J. (2000). Effect of nutrient enrichment on growth and photosynthesis of the zooxanthellate coral Stylophora pistillata. *Coral Reefs* 19, 103–113.

Ferrier-Pagès, C., Rottier, C., Beraud, E., and Levy, O. (2010). Experimental assessment of the feeding effort of three scleractinian coral species during a thermal stress: Effect on the rates of photosynthesis. *J. Exp. Mar. Bio. Ecol.* 390, 118–124.

Ferrier-Pagès, C., Schoelzke, V., Jaubert, J., Muscatine, L., and Hoegh-Guldberg, O. (2001). Response of a scleractinian coral, Stylophora pistillata, to iron and nitrate enrichment. *J. Exp. Mar. Bio. Ecol.* 259, 249–261.

Ferrier-Pagès, C., Witting, J., Tambutte, E., and Sebens, K. P. (2003). Effect of natural zooplankton feeding on the tissue and skeletal growth of the scleractinian coral Stylophora pistillata. *Coral Reefs* 22, 229–240.

Fitt, W. K., and Cook, C. B. (2001). The effects of feeding or addition of dissolved inorganic nutrients in maintaining the symbiosis between dinoflagellates and a tropical marine cnidarian. *Mar. Biol.* 139, 507–517.

Fowler, D., Coyle, M., Skiba, U., Sutton, M. A., Cape, J. N., Reis, S., Sheppard, L. J., Jenkins, A., Grizzetti, B., Galloway, N., et al. (2013). The global nitrogen cycle in the twentyfirst century. *Philos. Trans. R. Soc. Lond. B. Biol. Sci.* 368.

Frentzen, M. (2004). Phosphatidylglycerol and sulfoquinovosyldiacylglycerol: anionic membrane lipids and phosphate regulation. *Curr. Opin. Plant Biol.* 7, 270–6.

Furla, P., Allemand, D., and Orsenigo, M. N. (2000). Involvement of H(+)-ATPase and carbonic anhydrase in inorganic carbon uptake for endosymbiont photosynthesis. *Am. J. Physiol. Regul. Integr. Comp. Physiol.* 278, R870–R881.

Furnas, M., Mitchell, A., and Skuza, M. (1995). *Nitrogen and phosphorus budgets for the central Great Barrier Reef shelf*. Research P. Great Barrier Reef Marine Park Authority

Furnas, M., Mitchell, A., Skuza, M., and Brodie, J. (2005). In the other 90%: phytoplankton responses to enhanced nutrient availability in the Great Barrier Reef Lagoon. *Mar. Pollut. Bull.* 51, 253–65.

Garrett, T. a., Schmeitzel, J. L., Klein, J. a., Hwang, J. J., and Schwarz, J. a. (2013). Comparative Lipid Profiling of the Cnidarian Aiptasia pallida and Its Dinoflagellate Symbiont. *PLoS One* 8, e57975.

Gates, R. D., and Edmunds, P. (1999). The physiological mechanisms of acclimatization in tropical reef corals. *Am. Zool.* 39, 30–43.

Gates, R. D., Hoegh-Guldberg, O., McFall-Ngai, M. J., Bil, K. Y., and Muscatine, L. (1995). Free amino acids exhibit anthozoan "host factor" activity: they induce the release of photosynthate from symbiotic dinoflagellates in vitro. *Proc. Natl. Acad. Sci. USA* 92, 7430–4.

Gaude, N., Bréhélin, C., Tischendorf, G., Kessler, F., and Dörmann, P. (2007). Nitrogen deficiency in Arabidopsis affects galactolipid composition and gene expression and results in accumulation of fatty acid phytyl esters. *Plant J.* 49, 729–39.

Gil, M. (2013). Unity through nonlinearity: A unimodal coral-nutrient interaction. *Ecology* 94, 1871–1877.

Gittins, J. R., D'Angelo, C., Oswald, F., Edwards, R. J., and Wiedenmann, J. (2015). Fluorescent protein-mediated colour polymorphism in reef corals: multicopy genes extend the adaptation/acclimatization potential to variable light environments. *Mol. Ecol.* 24, 453–65.

Glynn, P. W. (1993). Coral reef bleaching: ecological perspectives. *Coral Reefs* 12, 1–17.

Godinot, C., Ferrier-Pagès, C., and Grover, R. (2009). Control of phosphate uptake by zooxanthellae and host cells in the scleractinian coral Stylophora pistillata. *Limnol. Oceanogr.* 54, 1627–1633.

Godinot, C., Ferrier-Pagès, C., Montagna, P., and Grover, R. (2011a). Tissue and skeletal changes in the scleractinian coral Stylophora pistillata Esper 1797 under phosphate enrichment. *J. Exp. Mar. Bio. Ecol.* 409, 200–207.

Godinot, C., Grover, R., Allemand, D., and Ferrier-Pagès, C. (2011b). High phosphate uptake requirements of the scleractinian coral Stylophora pistillata. *J. Exp. Biol.* 214, 2749–54.

Goreau, T., and Hayes, R. (1994). Coral bleaching and ocean" hot spots." *Ambio-Journal Hum. Environ.*, 176–180.

Goulet, T. L. (2006). Most corals may not change their symbionts. *Mar. Ecol. Prog. Ser.* 321, 1–7.

Grant, A. J., Trautman, D. A., Menz, I., and Hinde, R. (2006). Separation of two cell signalling molecules from a symbiotic sponge that modify algal carbon metabolism. *Biochem. Biophys. Res. Commun.* 348, 92–98.

Grant, A., People, J., Remond, M., Frankland, S., and Hinde, R. (2013). How a host cell signalling molecule modifies carbon metabolism in symbionts of the coral Plesiastrea versipora. *FEBS J.* 280, 2085–2096.

Gray, C. G., Lasiter, A. D., and Leblond, J. D. (2009a). Mono- and digalactosyldiacylglycerol composition of dinoflagellates. III. Four cold-adapted, peridinin-containing taxa and the presence of trigalactosyldiacylglycerol as an additional glycolipid. *Eur. J. Phycol.* 44, 439–445.

Gray, C. G., Lasiter, A. D., Li, C., and Leblond, J. D. (2009b). Mono- and digalactosyldiacylglycerol composition of dinoflagellates. I. Peridinin-containing taxa. *Eur. J. Phycol.* 44, 191–197.

Greenspan, P., Mayer, E. P., and Fowler, S. D. (1985). Nile red: a selective fluorescent stain for intracellular lipid droplets. *J. Cell Biol.* 100, 965–73.

Grottoli, A. G., Rodrigues, L. J., and Palardy, J. E. (2006). Heterotrophic plasticity and resilience in bleached corals. *Nature* 440, 1186–9.

Grover, R., Maguer, J., Allemand, D., and Ferrier-Pagès, C. (2003). Nitrate uptake in the scleractinian coral Stylophora pistillata. *Limnol. Oceanogr.* 48, 2266–2274.

Grover, R., Maguer, J.-F., Allemand, D., and Ferrier-Pagès, C. (2008). Uptake of dissolved free amino acids by the scleractinian coral Stylophora pistillata. *J. Exp. Biol.* 211, 860–5.

Grover, R., Maguer, J.-F., Allemand, D., and Ferrier-Pagès, C. (2006). Urea uptake by the scleractinian coral Stylophora pistillata. *J. Exp. Mar. Bio. Ecol.* 332, 216–225.

Grover, R., Reynaud-vaganay, S., and Ferrier-Pagès, C. (2002). Uptake of ammonium by the scleractinian coral Stylophora pistillata : Effect of feeding , light , and ammonium concentrations. *Limnol. Oceanogr.* 47, 782–790.

Han, X., and Gross, R. W. (2005). Shotgun lipidomics: electrospray ionization mass spectrometric analysis and quantitation of cellular lipidomes directly from crude extracts of biological samples. *Mass Spectrom. Rev.* 24, 367–412.

Härtel, H., Dörmann, P., and Benning, C. (2000). DGD1-independent biosynthesis of extraplastidic galactolipids after phosphate deprivation in Arabidopsis. *Proc. Natl. Acad. Sci.* 97, 10649–10654.

Hartmann, M.-A. (1998). Plant sterols and the membrane environment. *Trends Plant Sci.* 3, 170–175.

Heaton, T. H. E. (1986). Isotopic Studies of Nitrogen Pollution in the Hydrosphere and Atmosphere : a Review. *Chem. Geol.* 59, 87–102.

Heidelberg, K. B., Sebens, K. P., and Purcell, J. E. (2004). Composition and sources of near reef zooplankton on a Jamaican forereef along with implications for coral feeding. *Coral Reefs* 23, 263–276.

Hemme, D., Veyel, D., Mühlhaus, T., Sommer, F., Jüppner, J., Unger, A.-K., Sandmann, M., Fehrle, I., Schönfelder, S., Steup, M., et al. (2014). Systems-wide analysis of acclimation responses to long-term heat stress and recovery in the photosynthetic model organism Chlamydomonas reinhardtii. *Plant Cell* 26, 4270–97.

Higashi, Y., Okazaki, Y., Myouga, F., Shinozaki, K., and Saito, K. (2015). Landscape of the lipidome and transcriptome under heat stress in Arabidopsis thaliana. *Sci. Rep.* 5, 1–11.

Hoegh-Guldberg, O. (1999). Climate change, coral bleaching and the future of the world's coral reefs. *Mar. Freshw. Res.* 50, 839–866.

Hoegh-Guldberg, O. (1996). Nutrient enrichment and the ultrastructure of zooxanthellae from the giant clam Tridacna maxima. *Mar. Biol.* 125, 359–363.

Hoegh-Guldberg, O. (1994). Population dynamics of symbiotic zooxanthellae in the coral Pocillopora damicornis exposed to elevated ammonium ((NH-4)-2SO-4) concentrations. *Pacific Sci.* 48, 263–272.

Hoegh-Guldberg, O., Mumby, P. J., Hooten, a J., Steneck, R. S., Greenfield, P., Gomez, E., Harvell, C. D., Sale, P. F., Edwards, a J., Caldeira, K., et al. (2007). Coral reefs under rapid climate change and ocean acidification. *Science* 318, 1737–42.

Hoogenboom, M. O., Campbell, D. a, Beraud, E., Dezeeuw, K., and Ferrier-Pagès, C. (2012). Effects of light, food availability and temperature stress on the function of photosystem II and photosystem I of coral symbionts. *PLoS One* 7, e30167.

Hoogenboom, M., Rodolfo-Metalpa, R., and Ferrier-Pagès, C. (2010). Co-variation between autotrophy and heterotrophy in the Mediterranean coral Cladocora caespitosa. *J. Exp. Biol.* 213, 2399–409.

van Hooidonk, R., Maynard, J. a., and Planes, S. (2013). Temporary refugia for coral reefs in a warming world. *Nat. Clim. Chang.* 3, 508–511.

Horváth, I., Glatz, A., Nakamoto, H., Mishkind, M. L., Munnik, T., Saidi, Y., Goloubinoff, P., Harwood, J. L., and Vigh, L. (2012). Heat shock response in photosynthetic organisms: membrane and lipid connections. *Prog. Lipid Res.* 51, 208–20.

Horváth, I., Glatz, A., Varvasovszki, V., Török, Z., Páli, T., Balogh, G., Kovács, E., Nádasdi, L., Benkö, S., Joó, F., et al. (1998). Membrane physical state controls the signaling mechanism of the heat shock response in Synechocystis PCC 6803: Identification of hsp17 as a "fluidity gene. *Proc. Natl. Acad. Sci. U. S. A.* 95, 3513–3518.

Houlbrèque, F., and Ferrier-Pagès, C. (2009). Heterotrophy in tropical scleractinian corals. *Biol. Rev. Camb. Philos. Soc.* 84, 1–17.

Houlbrèque, F., Tambutté, E., Allemand, D., and Ferrier-Pagès, C. (2004). Interactions between zooplankton feeding, photosynthesis and skeletal growth in the scleractinian coral Stylophora pistillata. *J. Exp. Biol.* 207, 1461–1469.

Houlbrèque, F., Tambutté, E., and Ferrier-Pagès, C. (2003). Effect of zooplankton availability on the rates of photosynthesis, and tissue and skeletal growth in the scleractinian coral Stylophora pistillata. *J. Exp. Mar. Bio. Ecol.* 296, 145–166.

Hu, Q., Sommerfeld, M., Jarvis, E., Ghirardi, M., Posewitz, M., Seibert, M., and Darzins, A. (2008). Microalgal triacylglycerols as feedstocks for biofuel production: perspectives and advances. *Plant J.* 54, 621–39.

Hughes, A. D., and Grottoli, A. G. (2013). Heterotrophic Compensation: A Possible Mechanism for Resilience of Coral Reefs to Global Warming or a Sign of Prolonged Stress? *PLoS One* 8, e81172.

Hughes, A., Grottoli, A., Pease, T., and Matsui, Y. (2010). Acquisition and assimilation of carbon in non-bleached and bleached corals. *Mar. Ecol. Prog. Ser.* 420, 91–101.

Hughes, T. P. (1994). Catastrophes, phase shifts, and large-scale degradation of a Caribbean coral reef. *Science (80-.).* 265, 1547–1551.

Hughes, T. P., Baird, A. H., Bellwood, D. R., Card, M., Connolly, S. R., Folke, C., Grosberg, R., Hoegh-Guldberg, O., Jackson, J. B. C., Kleypas, J., et al. (2003). Climate change, human impacts, and the resilience of coral reefs. *Science (80-.).* 301, 929–33.

Hughes, T. P., Rodrigues, M. J., Bellwood, D. R., Ceccarelli, D., Hoegh-Guldberg, O., McCook, L., Moltschaniwskyj, N., Pratchett, M. S., Steneck, R. S., and Willis, B. (2007). Phase shifts, herbivory, and the resilience of coral reefs to climate change. *Curr. Biol.* 17, 360–365.

Hume, B. C. C., D'Angelo, C., Smith, E. G., Stevens, J. R., Burt, J., and Wiedenmann, J. (2015). Symbiodinium thermophilum sp. nov., a thermotolerant symbiotic alga prevalent in corals of the world's hottest sea, the Persian/Arabian Gulf. *Sci. Rep.* 5, 8562.

Hume, B., D'Angelo, C., Burt, J., Baker, a C., Riegl, B., and Wiedenmann, J. (2013). Corals from the Persian/Arabian Gulf as models for thermotolerant reef-builders: Prevalence of clade C3 Symbiodinium, host fluorescence and ex situ temperature tolerance. *Mar. Pollut. Bull.* 72, 313–22.

Imbs, A. B., Yakovleva, I. M., Dautova, T. N., Bui, L. H., and Jones, P. (2014). Diversity of fatty acid composition of symbiotic dinoflagellates in corals: Evidence for the transfer of host PUFAs to the symbionts. *Phytochemistry* 101, 76–82.

Irwin, A. J., Finkel, Z. V, Müller-Karger, F. E., and Troccoli Ghinaglia, L. (2015). Phytoplankton adapt to changing ocean environments. *Proc. Natl. Acad. Sci. U. S. A.*, 1–5.

Jackson, A. E., Miller, D. J., and Yellowlees, D. (1989). Metabolism in the Coral-Zooxanthellae Symbiosis: Characterization and Possible Roles of Two Acid Phosphatases in the Algal Symbiont Symbiodinium sp. *Proc. R. Soc. London Ser. BBiological Sci.* 238, 193–202.

Jiang, P.-L., Pasaribu, B., and Chen, C.-S. (2014). Nitrogen-deprivation elevates lipid levels in symbiodinium spp. by lipid droplet accumulation: morphological and compositional analyses. *PLoS One* 9, e87416.

Johannes, R. E., Coles, S. L., and Kuenzel, N. T. (1970). The Role of Zooplankton in the Nutrition of Some Scleractinian Corals1. *Limnol. Oceanogr.* 15, 579–586.

Jokiel, P. L., and Coles, S. L. (1990). Response of Hawaiian and other Indopacific reef corals to elevated temperature. *Coral Reefs* 8, 155–162.

Jones, a M., Berkelmans, R., van Oppen, M. J. H., Mieog, J. C., and Sinclair, W. (2008). A community change in the algal endosymbionts of a scleractinian coral following a natural bleaching event: field evidence of acclimatization. *Proc. Biol. Sci.* 275, 1359–65.

Jones, A., and Berkelmans, R. (2010). Potential costs of acclimatization to a warmer climate: growth of a reef coral with heat tolerant vs. sensitive symbiont types. *PLoS One* 5, e10437.

Jones, A. M., and Berkelmans, R. (2011). Tradeoffs to Thermal Acclimation: Energetics and Reproduction of a Reef Coral with Heat Tolerant *Symbiodinium* Type-D. *J. Mar. Biol.* 2011, 1–12.

Jones, R. J., Larkum, a. W. D., Schreiber, U., and Hoegh-Guldberg, O. (1998). Temperature-induced bleaching of corals begins with impairment of the CO2 fixation mechanism in zooxanthellae. *Plant, Cell Environ.* 21, 1219–1230.

Jones, R. J., and Yellowlees, D. (1997). Regulation and control of intracellular algae (= zooxanthellae) in hard corals. *Philos. Trans. R. Soc. Lond. B. Biol. Sci.* 352, 457–468.

Kato, M., Sakai, M., Adachi, K., Ikemoto, H., and Sano, H. (1996). Distribution of betaine lipids in marine algae. *Phytochemistry* 42, 1341–1345.

Kneeland, J., Hughen, K., Cervino, J., Hauff, B., and Eglinton, T. (2013). Lipid biomarkers in Symbiodinium dinoflagellates: new indicators of thermal stress. *Coral Reefs* 32, 923–934.

Koop, K., Booth, D., Broadbent, a, Brodie, J., Bucher, D., Capone, D., Coll, J., Dennison, W., Erdmann, M., Harrison, P., et al. (2001). ENCORE: the effect of nutrient enrichment on coral reefs. Synthesis of results and conclusions. *Mar. Pollut. Bull.* 42, 91–120.

Kopp, C., Pernice, M., Domart-Coulon, I., Djedat, C., Spangenberg, J., Alexander, D., Hignette, M., and Meziane, T. (2013). Highly dynamic cellular-level response of symbiotic coral to a sudden increase in environmental nitrogen. *MBio* 4, e00052–13.

Kou, Z., Bei, S., Sun, J., and Pan, J. (2013). Fluorescent measurement of lipid content in the model organism Chlamydomonas reinhardtii. *J. Appl. Phycol.* 25, 1633–1641.

Kroon, F. J., Schaffelke, B., and Bartley, R. (2014). Informing policy to protect coastal coral reefs: insight from a global review of reducing agricultural pollution to coastal ecosystems. *Mar. Pollut. Bull.* 85, 33–41.

Ladner, J. T., Barshis, D. J., and Palumbi, S. R. (2012). Protein evolution in two co-occurring types of Symbiodinium: an exploration into the genetic basis of thermal tolerance in Symbiodinium clade D. *BMC Evol. Biol.* 12, 217.

LaJeunesse, T. C. (2001). Investigating the biodiversity, ecology, and phylogeny of endosymbiotic dinoflagellates in the genus Symbiodinium using the ITS region: in search of a "species" level marker. *J. Phycol.* 37, 866–880.

Lapointe, B. (1997). Nutrient thresholds for bottom-up control of macroalgal blooms on coral reefs in Jamaica and southeast Florida. *Limnol. Oceanogr.* 42.

Lapointe, B. E., Langton, R., Bedford, B. J., Potts, A. C., Day, O., and Hu, C. (2010). Land-based nutrient enrichment of the Buccoo Reef Complex and fringing coral reefs of Tobago, West Indies. *Mar. Pollut. Bull.* 60, 334–343.

Latasa, M., and Berdalet, E. (1994). Effect of nitrogen or phosphorus starvation on pigment composition of cultured Heterocapsa sp. *J. Plankton Res.* 16, 83–94.

Leal, M. C., Hoadley, K., Pettay, D. T., Grajales, A., Calado, R., and Warner, M. E. (2015). Symbiont type influences trophic plasticity of a model cnidarian-dinoflagellate symbiosis. *J. Exp. Biol.* 218, 858–63.

Leal, M. C., Puga, J., Serôdio, J., Gomes, N. C. M., and Calado, R. (2012). Trends in the discovery of new marine natural products from invertebrates over the last two decades--where and what are we bioprospecting? *PLoS One* 7, e30580.

Leblond, J. D., Khadka, M., Duong, L., and Dahmen, J. L. (2015). Squishy lipids: Temperature effects on the betaine and galactolipid profiles of a C 18 /C 18 peridinin-containing dinoflagellate, Symbiodinium microadriaticum (Dinophyceae), isolated from the mangrove jellyfish, Cassiopea xamachana. *Phycol. Res.* 63, 219–230.

Lee, A. G. (2004). How lipids affect the activities of integral membrane proteins. *Biochim. Biophys. Acta - Biomembr.* 1666, 62–87.

Légeret, B., Schulz-Raffelt, M., Nguyen, H. M., Auroy, P., Beisson, F., Peltier, G., Blanc, G., and Li-Beisson, Y. (2015). Lipidomic and transcriptomic analyses of Chlamydomonas reinhardtii under heat stress unveil a direct route for the conversion of membrane lipids into storage lipids. *Plant. Cell Environ.*

Lema, K. a, Willis, B. L., and Bourne, D. G. (2012). Corals form characteristic associations with symbiotic nitrogen-fixing bacteria. *Appl. Environ. Microbiol.* 78, 3136–44.

Lema, K. A., Bourne, D. G., and Willis, B. L. (2014). Onset and establishment of diazotrophs and other bacterial associates in the early life history stages of the coral Acropora millepora. *Mol. Ecol.* 23, 4682–4695.

Lesser, M., Falcón, L., Rodríguez-Román, A., Enríquez, S., Hoegh-Guldberg, O., and Iglesias-Prieto, R. (2007). Nitrogen fixation by symbiotic cyanobacteria provides a source of nitrogen for the scleractinian coral Montastraea cavernosa. *Mar. Ecol. Prog. Ser.* 346, 143–152.

Lesser, M. P. (1997). Oxidative stress causes coral bleaching during exposure to elevated temperatures. *Coral Reefs* 16, 187–192.

Lesser, M. P. (2006). Oxidative stress in marine environments: biochemistry and physiological ecology. *Annu. Rev. Physiol.* 68, 253–78.

Li, Y., Horsman, M., Wang, B., Wu, N., and Lan, C. Q. (2008). Effects of nitrogen sources on cell growth and lipid accumulation of green alga Neochloris oleoabundans. *Appl. Microbiol. Biotechnol.* 81, 629–36.

Littler, M. M., Littler, D. S., and Brooks, B. L. (2010). The effects of nitrogen and phosphorus enrichment on algal community development: Artificial mini-reefs on the Belize Barrier Reef sedimentary lagoon. *Harmful Algae* 9, 255–263.

Logan, C. a, Dunne, J. P., Eakin, C. M., and Donner, S. D. (2014). Incorporating adaptive responses into future projections of coral bleaching. *Glob. Chang. Biol.* 20, 125–39.

Di Lorenzo, E. (2015). Climate science: The future of coastal ocean upwelling. *Nature* 518, 310–311.

Los, D. a, Mironov, K. S., and Allakhverdiev, S. I. (2013). Regulatory role of membrane fluidity in gene expression and physiological functions. *Photosynth. Res.*

Luo, Y.-J., Wang, L.-H., Chen, W.-N. U., Peng, S.-E., Tzen, J. T.-C., Hsiao, Y.-Y., Huang, H.-J., Fang, L.-S., and Chen, C.-S. (2009). Ratiometric imaging of gastrodermal lipid bodies in coral–dinoflagellate endosymbiosis. *Coral Reefs* 28, 289–301.

Martin, P., Van Mooy, B. a S., Heithoff, A., and Dyhrman, S. T. (2011). Phosphorus supply drives rapid turnover of membrane phospholipids in the diatom Thalassiosira pseudonana. *ISME J.* 5, 1057–60.

Marubini, F., and Davies, P. (1996). Nitrate increases zooxanthellae population density and reduces skeletogenesis in corals. *Mar. Biol.* 127, 319–328.

McAuley, P. J., and Cook, C. B. (1994). Effects of host feeding and dissolved ammonium on cell division and nitrogen status of zooxantheUae in the hydroid Myrionema amboinense. *Mar. Biol.*, 343–348.

Mellors, J., Waycott, M., and Marsh, H. (2005). Variation in biogeochemical parameters across intertidal seagrass meadows in the central Great Barrier Reef region. *Mar. Pollut. Bull.* 51, 335–342.

Mizusawa, N., Sakata, S., Sakurai, I., Sato, N., and Wada, H. (2009). Involvement of digalactosyldiacylglycerol in cellular thermotolerance in Synechocystis sp. PCC 6803. *Arch. Microbiol.* 191, 595–601.

Mizusawa, N., and Wada, H. (2012). The role of lipids in photosystem II. *Biochim. Biophys. Acta* 1817, 194–208.

Moberg, F., and Folke, C. (1999). Ecological goods and services of coral reef ecosystems. *Ecol. Econ.* 29, 215–233.

Moellering, E. R., and Benning, C. (2011). Galactoglycerolipid metabolism under stress: a time for remodeling. *Trends Plant Sci.* 16, 98–107.

Moellering, E. R., Muthan, B., and Benning, C. (2010). Freezing tolerance in plants requires lipid remodeling at the outer chloroplast membrane. *Science (80-.).* 330, 226–8.

Van Mooy, B. S., Fredricks, H. F., Pedler, B. E., Dyhrman, S. T., Karl, D. M., Koblízek, M., Lomas, M. W., Mincer, T. J., Moore, L. R., Moutin, T., et al. (2009). Phytoplankton in the ocean use non-phosphorus lipids in response to phosphorus scarcity. *Nature* 458, 69–72.

Msanne, J., Xu, D., Konda, A. R., Casas-Mollano, J. A., Awada, T., Cahoon, E. B., and Cerutti, H. (2012). Metabolic and gene expression changes triggered by nitrogen deprivation in the photoautotrophically grown microalgae Chlamydomonas reinhardtii and Coccomyxa sp. C-169. *Phytochemistry* 75, 50–9.

Muller-Parker, G., Cook, C. B., and D'Elia, C. F. (1994a). Elemental composition of the coral Pocillopora damicornis exposed to elevated seawater ammonium. *Pacific* 48, 234–246.

Muller-Parker, G., Lee, K. W., and Cook, C. B. (1996). Changes in the ultrastructure of symbiotic zooxanthellae in fed and starved sea anemones maintained under high and low light. *J. Phycol.* 32, 987–994.

Muller-Parker, G., McCloskey, L. R., Hoegh-Guldberg, O., and McAuley, P. J. (1994b). Effect of ammonium enrichment on animal and algal biomass of the coral Pocillopora damicornis. *Pac* 48, 273–283.

Mumby, P. J., Dahlgren, C. P., Harborne, A. R., Kappel, C. V, Micheli, F., Brumbaugh, D. R., Holmes, K. E., Mendes, J. M., Broad, K., Sanchirico, J. N., et al. (2006). Fishing, trophic cascades, and the process of grazing on coral reefs. *Science (80-.).* 311, 98–101.

Muscatine, L. (1967). Glycerol excretion by symbiotic algae from corals and tridacna and its control by the host. *Science (80-.).* 156, 515–519.

Muscatine, L. (1965). Symbiosis of hydra and algae. III. Extracellular products of the algae. *Comp. Biochem. Physiol.* 16, 77–92.

Muscatine, L. (1990). The role of symbiotic algae in carbon and energy flux in reef corals. *Coral Reefs* 25, 75–87.

Muscatine, L., and D'Elia, C. F. (1978). The uptake, retention and release of ammonium by reef corals. *Limnol. Oceanogr.* 23, 725–734.

Muscatine, L., Falkowski, P., Dubinsky, Z., Cook, C. B., and McKloskey, L. R. (1989a). The effect of external nutrient resources on the population dynamics of zooxanthellae in a reef coral. *Proc R Soc Lond, B* 236, 311–324.

Muscatine, L., Falkowski, P. G., Dubinsky, Z., Cook, P. A., and McCloskey, L. R. (1989b). The effect of external nutrient resources on the population dynamics of zooxanthellae in a reef coral. *Proc. R. Soc. B Biol. Sci.* 236, 311–324. d

Muscatine, L., Pool, R., and Cernichiari, E. (1972). Some factors influencing selective release of soluble organic material by zooxanthellae from reef corals. *Mar. Biol.* 308, 298–308.

Muscatine, L., and Porter, J. W. (1977). Reef Corals: Mutualistic Symbioses Adapted to Nutrient-Poor Environments. *Bioscience* 27, 454–460.

Nordemar, I., Nyström, M., and Dizon, R. (2003). Effects of elevated seawater temperature and nitrate enrichment on the branching coral Porites cylindrica in the absence of particulate food. *Mar. Biol.* 142, 669–677.

Oakley, C. A., Ameismeier, M. F., Peng, L., Weis, V. M., Grossman, A. R., and Davy, S. K. (2015). Symbiosis induces widespread changes in the proteome of the model cnidarian Aiptasia. *Cell. Microbiol.*

van Oppen, M. J. H., Oliver, J. K., Putnam, H. M., and Gates, R. D. (2015). Building coral reef resilience through assisted evolution. *Proc. Natl. Acad. Sci. U. S. A.* 112, 2307–13.

Palardy, J., Rodrigues, L., and Grottoli, A. (2008). The importance of zooplankton to the daily metabolic carbon requirements of healthy and bleached corals at two depths. *J. Exp. Mar. …* 367, 180–188

Papina, M., Meziane, T., and Woesik, R. Van (2003). Symbiotic zooxanthellae provide the host-coral Montipora digitata with polyunsaturated fatty acids. *Phytochemistry* 135, 533–537.

Peñuelas, J., Poulter, B., Sardans, J., Ciais, P., van der Velde, M., Bopp, L., Boucher, O., Godderis, Y., Hinsinger, P., Llusia, J., et al. (2013). Human-induced nitrogen-phosphorus imbalances alter natural and managed ecosystems across the globe. *Nat. Commun.* 4, 2934.

Pernice, M., Meibom, A., Van Den Heuvel, A., Kopp, C., Domart-Coulon, I., Hoegh-Guldberg, O., and Dove, S. (2012). A single-cell view of ammonium assimilation in coral-dinoflagellate symbiosis. *ISME J.* 6, 1314–24. doi:10.1038/ismej.2011.196.

Piniak, G., Lipschultz, F., and McClelland, J. (2003). Assimilation and partitioning of prey nitrogen within two anthozoans and their endosymbiotic zooxanthellae. *Mar. Ecol. Prog. Ser.* 262, 125–136.

Poirier, Y., Thoma, S., Somerville, C., and Schiefelbein, J. (1991). Mutant of Arabidopsis deficient in xylem loading of phosphate. *Plant Physiol.* 97, 1087–1093.

Popendorf, K. J., Fredricks, H. F., and Van Mooy, B. a S. (2013). Molecular Ion-Independent Quantification of Polar Glycerolipid Classes in Marine Plankton Using Triple Quadrupole MS. *Lipids* 48, 185–95.

Quinn, P. J. (1988). Effects of temperature on cell membranes. 237–258.

Rädecker, N., Pogoreutz, C., Voolstra, C. R., Wiedenmann, J., and Wild, C. (2015). Nitrogen cycling in corals: the key to understanding holobiont functioning? *Trends Microbiol.*

Rahav, O., Dubinsky, Z., Achituv, Y., and Falkowski, P. (1989). Ammonium metabolism in the zooxanthellate coral, Stylophora pistillata. *Proc. R. Soc. Lond. B* 236, 325–337.

Rands, M. L., Loughman, B. C., and Douglas, A. E. (1993). The Symbiotic Interface in an Alga-Invertebrate Symbiosis. *Proc. R. Soc. London B Biol. Sci.* 253, 161–165.

Redfield, A. C. (1958). The biological control of chemical factors in the environment. *Am. Sci.* 46, 205–221.

Rees, and Ellard, F. M. (1989). Nitrogen conservation and the green hydra symbiosis. *Proc. R. Soc. Lond. B* 236, 203–212.

Riegl, B., Bruckner, A., Coles, S. L., Renaud, P., and Dodge, R. E. (2009). Coral reefs: threats and conservation in an era of global change. *Ann. N. Y. Acad. Sci.* 1162, 136–86.

Riegl, B., Glynn, P. W., Wieters, E., Purkis, S., d'Angelo, C., and Wiedenmann, J. (2015). Water column productivity and temperature predict coral reef regeneration across the Indo-Pacific. *Sci. Rep.* 5, 8273.

Risk, M. J., Heikoop, J. M., Edinger, E. N., and Erdmann, M. V. (2001). The assessment "toolbox": Community-based reef evaluation methods coupled with geochemical techniques to identify sources of stress. *Bull. Mar. Sci.* 69, 443–458.

Roberts, J. M., Davies, P. S., Fixter, L. M., and Preston, T. (1999). Primary site and initial products of ammonium assimilation in the symbiotic sea anemone Anemonia viridis. *Mar. Biol.* 135, 223–236.

Roberts, J. M., Fixter, L. M., and Davies, P. S. (2001). Ammonium metabolism in the symbiotic sea anemone Anemonia viridis. *Hydrobiologia* 461, 25–35.

Rodrigues, L. J., and Grottoli, A. G. (2007). Energy reserves and metabolism as indicators of coral recovery from bleaching. *Limnol. Oceanogr.* 52, 1874–1882.

Rodrigues, L. J., Grottoli, A. G., and Pease, T. K. (2008). Lipid class composition of bleached and recovering Porites compressa Dana, 1846 and Montipora capitata Dana, 1846 corals from Hawaii. *J. Exp. Mar. Bio. Ecol.* 358, 136–143.

Roemmich, D., and McGowan, J. (1995). Climatic warming and the decline of zooplankton in the California Current. *Science (80-.).*

Rosset, S., D'Angelo, C., and Wiedenmann, J. (2015). Ultrastructural Biomarkers in Symbiotic Algae Reflect the Availability of Dissolved Inorganic Nutrients and Particulate Food to the Reef Coral Holobiont. *Front. Mar. Sci.* 2, 1–10.

Rowan, R. (2004). Coral bleaching - Thermal adaptation in reef coral symbionts. *Nature* 430, 2004.

Rowan, R., Whitney, S. M., Fowler, A., and Yellowlees, D. (1996). Rubisco in marine symbiotic dinoflagellates: form II enzymes in eukaryotic oxygenic phototrophs encoded by a nuclear multigene family. *Plant Cell* 8, 539–53.

Ryu, S. B. (2004). Phospholipid-derived signaling mediated by phospholipase A in plants. *Trends Plant Sci.* 9, 229–235.

Saidi, Y., Finka, A., and Goloubinoff, P. (2011). Heat perception and signalling in plants: a tortuous path to thermotolerance. *New Phytol.* 190, 556–65.

Salih, a, Larkum, a, Cox, G., Kühl, M., and Hoegh-Guldberg, O. (2000). Fluorescent pigments in corals are photoprotective. *Nature* 408, 850–853.

Sampayo, E. M., Ridgway, T., Bongaerts, P., and Hoegh-Guldberg, O. (2008). Bleaching susceptibility and mortality of corals are determined by fine-scale differences in symbiont type. *Proc. Natl. Acad. Sci. U. S. A.* 105, 10444–9.

Sato, N., Sonoike, K., Kawaguchi, A., and Tsuzuki, M. (1996). Contribution of lowered unsaturation levels of chloroplast lipids to high temperature tolerance of photosynthesis in Chlamydomonas reinhardtii. *J. Photochem. Photobiol. B Biol.* 36, 333–337.

Schindelin, J., Arganda-Carreras, I., Frise, E., Kaynig, V., Longair, M., Pietzsch, T., Preibisch, S., Rueden, C., Saalfeld, S., Schmid, B., et al. (2012). Fiji: an open-source platform for biological-image analysis. *Nat. Methods* 9, 676–82.

Schoepf, V., Stat, M., Falter, J. L., and McCulloch, M. T. (2015). Limits to the thermal tolerance of corals adapted to a highly fluctuating, naturally extreme temperature environment. *Sci. Rep.* 5, 17639.

Shantz, A., and Burkepile, D. (2014). Context-dependent effects of nutrient loading on the coral-algal mutualism. *Ecology* 95, 1995–2005.

Sheppard, C. (2003). Predicted recurrences of mass coral mortality in the Indian Ocean. *Nature* 275, 272–275.

Silverstein, R. N., Correa, A. M. S., and Baker, A. C. (2012). Specificity is rarely absolute in coral-algal symbiosis: implications for coral response to climate change. *Proc. Biol. Sci.* 279, 2609–18.

Silverstein, R. N., Cunning, R., and Baker, A. C. (2015). Change in algal symbiont communities after bleaching, not prior heat exposure, increases heat tolerance of reef corals. *Glob. Chang. Biol.* 21, 236–249.

Simidjiev, I., Stoylova, S., Amenitsch, H., Javorfi, T., Mustardy, L., Laggner, P., Holzenburg, A., and Garab, G. (2000). Self-assembly of large , ordered lamellae from non-bilayer lipids and integral membrane proteins in vitro. *PNAS* 97, 1473–1476.

Smith, D., Suggett, D., and Baker, N. (2005). Is photoinhibition of zooxanthellae photosynthesis the primary cause of thermal bleaching in corals? *Glob. Chang. Biol.*, 1–11.

Smith, G., and Muscatine, L. (1999). Cell cycle of symbiotic dinoflagellates: variation in G1 phase-duration with anemone nutritional status and macronutrient supply in the Aiptasia pulchella–. *Mar. Biol.* 134, 405–418.

Smith, S. V, Kimmerer, W. J., Laws, E. A., Brock, R. E., and Walsh, T. E. D. W. (1981). Kaneohe Bay sewage diversion experiment : Perspectives on ecosystem responses to nutritional perturbation l. *Pacific Sci.* 35, 279–395.

Stambler, N., Popper, N., Dubinsky, Z., and Stimson, J. (1991). Effects of nutrient enrichment and water motion on the coral Pocillopora damicornis. *Pacific Sci.* 45, 299–307.

Stat, M., and Gates, R. D. (2011). Clade D Symbiodinium in Scleractinian Corals: A "Nugget" of Hope, a Selfish Opportunist, an Ominous Sign, or All of the Above? *J. Mar. Biol.* 2011, 1–9.

Stuhldreier, I., Sánchez-Noguera, C., Roth, F., Cortés, J., Rixen, T., and Wild, C. (2015). Upwelling Increases Net Primary Production of Corals and Reef-Wide Gross Primary Production Along the Pacific Coast of Costa Rica. *Front. Mar. Sci.* 2.

Suggett, D. J., Warner, M. E., Smith, D. J., Davey, P., Hennige, S., and Baker, N. R. (2008). Photosynthesis and production of hydrogen peroxide by Symbiodinium (Pyrrhophyta) phylotypes with different thermal tolerances. *J. Phycol.* 44, 948–956.

Summons, R. E., and Osmond, C. B. (1981). Nitrogen assimilation in the symbiotic marine alga Gymnodinium microadriaticum: direct analysis of 15N incorporation by gc-ms methods. *Phytochemistry* 20, 575–578.

Sutton, D. C., and Hoegh-Guldberg, O. (1990). Host-Zooxanthella Interactions in Four Temperate Marine Invertebrate Symbioses : Assessment of Effect of Host Extracts on Symbionts. *Biol. Bull.* 178, 175–186.

Szmant, A. (2002). Nutrient enrichment on coral reefs : Is it a major cause of coral reef decline? *Estuaries* 25, 743–766.

Tanaka, Y., Miyajima, T., Koike, I., Hayashibara, T., and Ogawa, H. (2006). Translocation and conservation of organic nitrogen within the coral-zooxanthella symbiotic system of Acropora pulchra, as demonstrated by dual isotope-labeling techniques. *J. Exp. Mar. Bio. Ecol.* 336, 110–119.

Taylor, D. L. (1968). In situ studies on the cytochemistry and ultrastructure of a symbiotic marine dinoflagellate. *J. Mar. Biol. Assoc. United Kingdom* 48, 349.

Tchernov, D., Gorbunov, M. Y., Vargas, C. De, Yadav, S. N., Milligan, A. J., Ha, M., and Falkowski, P. G. (2004). Membrane lipids of symbiotic algae are diagnostic of sensitivity to thermal bleaching in corals. *PNAS* 101, 13531–13535.

Tchernov, D., Kvitt, H., Haramaty, L., Bibby, T. S., Gorbunov, M. Y., Rosenfeld, H., and Falkowski, P. G. (2011). Apoptosis and the selective survival of host animals following thermal bleaching in zooxanthellate corals. *Proc. Natl. Acad. Sci. U. S. A.* 108, 9905–9.

Titlyanov, E. A., Titlyanova, T. V., Leletkin, V. A., Tsukahara, J., van Woesik, R., and Yamazato, K. (1996). Degradation of zooxanthellae and regulation of their density in hermatypic corals. *Mar. Ecol. Prog. Ser.* 139, 167–178.

Titlyanov, E. a., Titlyanova, T. V., Yakovleva, I. M., and Kalita, T. L. (2006). Rhythmical changes in the division and degradation of symbiotic algae in hermatypic corals. *Russ. J. Mar. Biol.* 32, 12–19.

Titlyanov, E., Bil, K., Fomina, I., Titlyanova, T., Leletkin, V., Eden, N., Malkin, A., and Dubinsky, Z. (2000). Effects of dissolved ammonium addition and host feeding with Artemia salina on photoacclimation of the hermatypic coral Stylophora pistillata. *Mar. Biol.* 137, 463–472.

Tolosa, I., Treignier, C., Grover, R., and Ferrier-Pagès, C. (2011). Impact of feeding and short-term temperature stress on the content and isotopic signature of fatty acids, sterols, and alcohols in the scleractinian coral Turbinaria reniformis. *Coral Reefs* 30, 763–774.

Treignier, C., and Grover, R. (2008). Effect of light and feeding on the fatty acid and sterol composition of zooxanthellae and host tissue isolated from the scleractinian coral Turbinaria reniformis. *At. Energy* 53, 2702–2710.

Tremblay, P., Grover, R., Maguer, J. F., Hoogenboom, M., and Ferrier-Pagès, C. (2014). Carbon translocation from symbiont to host depends on irradiance and food availability in the tropical coral Stylophora pistillata. *Coral Reefs* 33, 1–13.

Tremblay, P., Maguer, J. F., Grover, R., and Ferrier-Pagès, C. (2015). Trophic dynamics of scleractinian corals: stable isotope evidence. *J. Exp. Biol.* 218, 1223–34.

Trench, R. K. (1971). Physiology and biochemistry of zooxanthellae symbiotic with marine coelenterates. II. Liberation of fixed C14 by zooxanthellae in vitro. *Proc. R. Soc. Lond. B* 177, 237–250.

Vaulot, D., Olson, R. J., and Merkel, S. (1987). Cell-cycle response to nutrient starvation in two phytoplankton species, Thalassiosira weissflogii and Hymenomonas carterae *. *Mar. Biol.* 630, 625–630.

Vega Thurber, R. L., Burkepile, D. E., Fuchs, C., Shantz, A. a, McMinds, R., and Zaneveld, J. R. (2014). Chronic nutrient enrichment increases prevalence and severity of coral disease and bleaching. *Glob. Chang. Biol.* 20, 544–54.

Venn, a a, Loram, J. E., and Douglas, a E. (2008). Photosynthetic symbioses in animals. *J. Exp. Bot.* 59, 1069–80.

Vítová, M., Bišová, K., Kawano, S., and Zachleder, V. (2015). Accumulation of energy reserves in algae: From cell cycles to biotechnological applications. *Biotechnol. Adv.* 33, 1204–1218.

Voss, M., Bange, H. W., Dippner, J. W., Middelburg, J. J., Montoya, J. P., B, P. T. R. S., and Ward, B. (2013). The marine nitrogen cycle : recent discoveries , uncertainties and the potential relevance of climate change The marine nitrogen cycle : recent discoveries , uncertainties and the potential relevance of climate change. *Philos. Trans. R. Soc. Lond. B. Biol. Sci.* 368.

Wada, H., Gombos, Z., and Murata, N. (1994). Contribution of membrane lipids to the ability of the photosynthetic machinery to tolerate temperature stress. *Proc. Natl. Acad. Sci. U. S. A.* 91, 4273–7.

Wagner, D., Kramer, P., and van Woesik, R. (2010). Species composition, habitat, and water quality influence coral bleaching in southern Florida. *Mar. Ecol. Prog. Ser.* 408, 65–78.

Wakefield, T. S., Farmer, M. a, and Kempf, S. C. (2000). Revised description of the fine structure of in situ "zooxanthellae" genus Symbiodinium. *Biol. Bull.* 199, 76–84.

Walther, G., Post, E., Convey, P., Menzel, A., Parmesan, C., Beebee, T. J. C., Fromentin, J., Hoegh-guldberg, O., and Bairlein, F. (2002). Ecological responses to recent climate change. *Nature* 416, 389–395.

Wang, J., and Douglas, A. (1998). Nitrogen recycling or nitrogen conservation in an alga-invertebrate symbiosis? *J. Exp. Biol.* 201, 2445–53.

Wang, J., and Douglas, A. E. (1997). Nutrients , Signals , and Photosynthate Release by Symbiotic Algae '. 631–636.

Wang, J. T., and Douglas, A. E. (1999). Essential amino acid synthesis and nitrogen recycling in an alga–invertebrate symbiosis. *Mar. Biol.* 135, 219–222.

Wang, L. H., Liu, Y.-H., Ju, Y.-M., Hsiao, Y.-Y., Fang, L.-S., and Chen, C.-S. (2008). Cell cycle propagation is driven by light–dark stimulation in a cultured symbiotic dinoflagellate isolated from corals. *Coral Reefs* 27, 823–835.

Wang, Z. T., Ullrich, N., Joo, S., Waffenschmidt, S., and Goodenough, U. (2009). Algal lipid bodies: stress induction, purification, and biochemical characterization in wild-type and starchless Chlamydomonas reinhardtii. *Eukaryot. Cell* 8, 1856–68.

Warner, M. E., Fitt, W. K., and Schmidt, G. W. (1999). Damage to photosystem II in symbiotic dinoflagellates: a determinant of coral bleaching. *Proc. Natl. Acad. Sci. U. S. A.* 96, 8007–12.

Weis, V. M. (2008). Cellular mechanisms of Cnidarian bleaching: stress causes the collapse of symbiosis. *J. Exp. Biol.* 211, 3059–66.

Weis, V. M., Smith, G. J., and Muscatine, L. (1989). A "CO2 supply" mechanisms in zooxanthellate cnidarians: role of carbonic anhydrase. *Mar. Biol.* 100, 195–202.

Wellington, G. M., and Glynn, P. W. (1983). Environmental influences on skeletal banding in eastern Pacific (Panama) corals. *Coral Reefs* 1, 215–222.

Welti, R., Li, W., Li, M., Sang, Y., Biesiada, H., Zhou, H.-E., Rajashekar, C. B., Williams, T. D., and Wang, X. (2002). Profiling membrane lipids in plant stress responses. Role of phospholipase D alpha in freezing-induced lipid changes in Arabidopsis. *J. Biol. Chem.* 277, 31994–2002.

Welti, R., Shah, J., Li, W., Li, M., Chen, J., Burke, J., Fauconnier, M., Chapman, K., Chye, M., and Wang, X. (2007). Plant lipidomics: Discerning biological function by profiling plant complex lipids using mass spectrometry. *Front. Biosci.* 12, 2494–2506.

Welti, R., Wang, X., and Williams, T. D. (2003). Electrospray ionization tandem mass spectrometry scan modes for plant chloroplast lipids. *Anal. Biochem.* 314, 149–152.

Weng, L.-C., Pasaribu, B., -Ping Lin, I., Tsai, C.-H., Chen, C.-S., and Jiang, P.-L. (2014). Nitrogen deprivation induces lipid droplet accumulation and alters fatty acid metabolism in symbiotic dinoflagellates isolated from Aiptasia pulchella. *Sci. Rep.* 4, 1–8.

Wiedenmann, J., D'Angelo, C., Smith, E. G., Hunt, A. N., Legiret, F., Postle, A. D., and Achterberg, E. P. (2013). Nutrient enrichment can increase the susceptibility of reef corals to bleaching. *Nat. Clim. Chang.* 2, 1–5.

Wild, C., Hoegh-Guldberg, O., Naumann, M. S., Colombo-Pallotta, M. F., Ateweberhan, M., Fitt, W. K., Ortiz, J., Loya, Y., and van Woesik, R. (2011). Climate change impedes reef ecosystem engineers. *Mar. Freshw. Res.* 62, 205–215.

Wild, C., Huettel, M., Klueter, A., and Kremb, S. G. (2004). Coral mucus functions as an energy carrier and particle trap in the reef ecosystem. 66–70.

Wild, C., Woyt, H., and Huettel, M. (2005). Influence of coral mucus on nutrient fluxes in carbonate sands. *Mar. Ecol. Prog. Ser.* 287, 87–98.

Wilkinson, C. (2008). Status of coral reefs of the worls: 2008. Townsville, Australia.

Wooldridge, S. a (2009). Water quality and coral bleaching thresholds: formalising the linkage for the inshore reefs of the Great Barrier Reef, Australia. *Mar. Pollut. Bull.* 58, 745–51.

Xu, C., Fan, J., and Riekhof, W. (2003). A permease-like protein involved in ER to thylakoid lipid transfer in Arabidopsis. *EMBO J.* 22, 2370–2379.

Yahel, R., Yahel, G., and Genin, A. (2005). Near- bottom depletion of zooplankton over coral reefs: I: diurnal dynamics and size distribution. *Coral Reefs* 24, 75–85.

Yellowlees, D., Rees, T. A. V, and Leggat, W. (2008). Metabolic interactions between algal symbionts and invertebrate hosts. *Plant. Cell Environ.* 31, 679–94.

Yonge, C. M. (1930). Studies on the physiology of corals. I. Feeding mechanisms and food. *Sci. Rep. Gt. Barrier Reef Exped* 1, 13–57.

Zhao, Y., Yang, X., Lu, W., Liao, H., and Liao, F. (2008). Uricase based methods for determination of uric acid in serum. *Microchim. Acta* 164, 1–6.

Zheng, G., Tian, B., Zhang, F., Tao, F., and Li, W. (2011). Plant adaptation to frequent alterations between high and low temperatures: remodelling of membrane lipids and maintenance of unsaturation levels. *Plant. Cell Environ.* 34, 1431–42.

Zhukova, N. V, and Aizdaicher, N. A. (1995). Fatty acid composition of 15 species of marine microalgae. *Phytochemistry* 39, 351–356.